Relationships between Synoptic Circulation Patterns and Freezing Rain in Churchill, Manitoba (1953-2009)

by

Ryan Smith

A Thesis submitted to the Faculty of Graduate Studies of

The University of Manitoba

in partial fulfilment of the requirements of the degree of

MASTER OF SCIENCE

Department of Environment and Geography

University of Manitoba

Winnipeg

Abstract

Freezing rain is an especially hazardous type of adverse weather and is frequently observed in Churchill, Manitoba. The goals of this study were to assess the climatology of freezing rain in Churchill, assess the synoptic climatology of the Hudson Bay region using a multi-level synoptic classification scheme, assess the relationships between the synoptic climate and freezing rain events, and assess the trends in synoptic types and to discuss the implications of climate change in relation to the expected changes in freezing rain. For the years 1953 thru 2009, freezing rain was observed during 796 hours, an average of approximately 15 hours per year. A 34-type multi-level synoptic classification consisting of five NCEP/NCAR reanalysis datasets was constructed. Type-20 was associated with a majority of the freezing rain cases. More research is needed to understand how climate change may impact the timing, frequency and intensity of freezing rain in Churchill.

Acknowledgements

The completion of my thesis is an accomplishment that would not have been possible without the guidance, support, expertise and patience of many people.

First, I would like to express my sincere gratitude for the assistance Dr. Danny Blair has provided me with. He has been a mentor and friend for the majority of my university career and it is with his support that this project has come to fruition. His passion for climate research, focus towards producing meaningful results, and his proficient attention to detail have both inspired and motivated me. I feel very lucky to have had the opportunity to learn with him.

I would like to thank Dr. Robert Dahni, the original creator of the Synoptic Typer program, for his continued involvement in and enthusiasm for synoptic research. Knowing that the changes to Synoptic Typer Tools have been instrumental in the research he conducts has been a motivating factor in completing this work. His feedback was very meaningful to me and instrumental to the growth and evolution of STT.

I would like to thank my supervisor, Dr. John Hanesiak, for helping fund my program and for taking the time to analyze and form suggestions to improve my writing and research. I have appreciated his critiques and insistence on producing top quality research and clear, concise writing technique. Similarly, I would like to thank my thesis committee member Dr. Ronald Stewart for his helpful suggestions.

There are, of course, many personal friends, family and colleagues whose presence over the last two and a half years has been both a support and welcome distraction as I worked towards completion. Special thanks to the Geo crew at the University of Winnipeg, my fellow UofM storm chasing movie stars, and the University of Winnipeg Geography Department Staff. Thanks to my Mom and Dad for their willingness to learn obscure science terminology in order to help me edit my work, and to Annie, for everything.

Table of Contents

List of Figures

List of Tables

Chapter 1

Introduction

The climate of the Arctic is warming faster than any on Earth. This so called 'polar amplification', initiated by increases in anthropogenic greenhouse gas emissions, is amplified due to positive feedback systems at the Arctic surface (Screen and Simmonds, 2010). Specifically, changes to the Arctic surface initiated by warmer temperatures are reducing surface albedo, which in turn is causing further warming. The Fourth Assessment Report on Climate Change predicted that a warming of the Arctic would have enormous and far-reaching impacts on the region's terrestrial and marine ecosystems and on human activities (Anisimov et al., 2007). Many researchers now believe that the Arctic is quickly approaching a tipping point, a permanent and irreversible shift in the way the climate behaves, away from natural climate variability and towards anthropogenic warming (Lindsay and Zhang, 2005).

Hudson Bay, a large, northern inland sea and sub-arctic region, is especially sensitive to climate change, mainly because of its relatively shallow depth and the fact that there is relatively little mixing between the Bay and other major oceans (Saucier et al., 2004; Gagnon and Gough, 2005; Joly et al., 2011 Hochheim et al., 2011). The bay is also important because it has far-reaching impacts on the surrounding local and regional climates (Rouse, 1991). The bay and its surrounding coastal lowlands are also home to an impressive array of Arctic fauna and the region is home to many native and non-native peoples who are reliant on transportation and natural resources for survival. To this end, Hudson Bay is a region of increasing importance and concern as amplified Arctic climate change disturbs many of these sensitive climatic, ecological and human systems.

The loss of sea ice is related to changes in energy flux at the surface, particularly increased latent heat flux at the boundary between sea ice and open water (Simmonds and Keay, 2009). Similarly, moisture flux between the surface and the atmosphere is enhanced in an ice-free regime (Sortberg and Walsh, 2008), and evidence of this enhanced moisture flux can be observed in changes to cloud cover, precipitation and storm frequency and intensity (Deser et al., 2000; Vavrus et al., 2010). In general, it is believed that a warmer, reduced-ice Arctic and sub-arctic will result in an increase in the severity of storms and possibly several types of adverse weather (Anisimov et al., 2007).

Adverse weather throughout Canada is often associated with mid and high-latitude cyclones (Stewart et al., 1995). These are important mechanisms of energy and moisture advection into the Arctic from more southern latitudes (Sorteberg and Walsh, 2008) and cyclones are part of a positive feedback loop in which melting ice increases heat and moisture flux from the surface to the atmosphere which in turn produces more

intense cyclones that have the potential to further reduce sea ice through wave action and the advection of ice into warmer waters (Serreze, 1994; Deser et al., 2000; Bengtsson et al., 2004; Simmonds and Keay, 2009). The extent of the influence that surface climate changes have on cyclone development and intensification remains largely speculative, and while most researchers agree that changes to sea ice extent and concentration should influence cyclone storm tracks, frequencies and intensities, relatively little research has been done to assess these relationships.

Since cyclones are important drivers of adverse weather at the surface, changes in cyclone storm track, frequency and intensity may be evident in changes to adverse weather frequencies observed at the surface. Climatologies of several adverse weather types in the Canadian Arctic were compiled by Hanesiak and Wang (2005) and by Hanesiak et al. (2003), using Environment Canada hourly weather data. Prior to Hanesiak et al. (2003), little research related to the daily, monthly and annual frequencies of adverse weather types in the Arctic had been compiled. Previous studies include these by Stuart and Isaac (1999) and Cortinas et al. (2004), who studied freezing precipitation events across Canada, and Stewart et al. (1995) who studied winter storms.

The position of a cyclone relative to a location at the surface often dictates the type of adverse weather witnessed at the surface. For example, the occurrence of freezing rain is often associated with the passing of a warm front aloft (Cheng et al., 2004). Although cold fronts can produce freezing rain, the duration and intensity of freezing rain events are generally much smaller than with warm fronts due to the cold front's faster motion and smaller horizontal extent of the inversion region aloft that is responsible for such events (Bernstein, 2000). Therefore, the position of the cyclone with

respect to the surface is an important variable in forecasting freezing rain. Stuart and Isaac (1999) noted that the frequency of freezing rain events seemed to be influenced by the presence of sea ice over Hudson Bay, yet were unable to quantify this relationship. In particular, the fact that Hudson Bay is largely frozen during spring (when freezing rain is most commonly observed) seemed counterintuitive, as the Bay's heat and moisture content is effectively cut off from the atmosphere during this time of year. Therefore, a study of cyclones and their position relative to Hudson Bay during periods of heavy and light sea ice may reveal previously unknown mechanisms of sea ice forcing on atmospheric circulation and adverse weather, specifically on the development and intensification of freezing rain.

Freezing rain can be a particularly hazardous type of adverse weather for humans and other animal populations. One of the most notable freezing rain events took place in the province of Quebec during the month of January in 1998. During this six daylong event, freezing rain coated electrical transmission wires, resulting in wide spread power loss and loss of life (Lecomte et al., 1998). Freezing rain also impacts ground and air transportation, agriculture and can even increase rates of animal mortality (Stuart 1994; Cortinas et al., 2004; Hanesiak and Wang, 2005). Approximately 15 hours of freezing rain are observed each year in Churchill, and most of this freezing rain is observed during the spring months (Stuart and Isaac, 1999; Hanesiak et al., 2003; Hanesiak and Wang, 2005)

Analyzing the synoptic climatology of a region can provide insights into how the large-scale upper-air and surface circulation correlates with adverse weather, such as freezing rain, observed at the surface. The goal of synoptic climatology is to explain

surface climates using synoptic scale circulation patterns (Barry and Perry, 1973). By definition, synoptic scale patterns are approximately 1000 km in horizontal extent, or the scale at which operational weather maps are typically drawn, labeled with terms such as troughs, ridges, cyclones and anticyclones.

Synoptic classifications are often utilized to help summarize synoptic scale data. A synoptic classification is a set of synoptic circulation patterns chosen to summarize and illustrate the important modes of variability within the chosen study region. In other words, classifications are used to characterize and simplify a synoptic climate by reducing the complexity within the synoptic realm into a manageable number of representative synoptic types. Typically, these synoptic types (also referred to as circulation types) are first identified and subsequently referenced against surface processes (so-called circulation-to-environment processes). However, researchers can also define synoptic types using the opposite approach, in which types are the composite patterns present during known surface events (so-called environment-to-circulation processes) (Yarnal, 1993; Yarnal and Draves, 1993).

Techniques for generating classifications vary between studies. Techniques can be categorized as either subjective (manual) or objective (automated) depending on whether synoptic pattern identification and map sorting is done by eye or by algorithm. Typically, automated techniques are preferred because they are faster, can be applied to a broader range of climates and generally result in less user bias. One disadvantage of automated techniques is that they often require computer programming, mathematical and statistical knowledge that can be challenging to learn and difficult to implement (Yarnal, 1993).

In summary, there is a need for more research related to linkages between climate variability, sea ice, cyclones and adverse weather in the Arctic and sub-arctic using historical data and climate model projections as temperatures rise and the timing of freeze-up and thaw of Hudson Bay continues to change. We must first examine the large scale (synoptic) relations to adverse weather using historical datasets, which is the main motivation for this thesis. Specifically, an analysis of the synoptic climatology of the Hudson Bay region may provide useful insights into how the synoptic climate relates to adverse weather at the surface and how ice may play a role in adverse weather events, such as freezing rain.

1.1 Scope

This study is an attempt to address some of the above-noted research needs by using new synoptic classification tools to analyze freezing rain events over Hudson Bay and its surrounding coastal region (known as the Hudson Bay Lowlands). Data obtained from Environment Canada for Churchill, Manitoba, are used to produce a climatology of freezing rain. Churchill is highlighted because it is the community with the longest and most complete data record (hourly weather data is available since 1953). Next, a synoptic map classification computer program called Synoptic Typer Tools (STT) is implemented to generate a synoptic classification of gridded National Center for Environmental Prediction and National Center for Atmospheric Research (NCEP/NCAR) reanalysis data from the surrounding Hudson Bay region and to relate these features to freezing rain events.

1.2 Objectives

The objectives of this thesis are to:

(a) assess the climatology of freezing rain events in Churchill, Manitoba;

(b) assess the synoptic climatology of the Hudson Bay region;

(c) assess the relationship between synoptic scale circulation and freezing rain events in Churchill; and

(d) assess the trends in synoptic types and to discuss the implications of climate change in relation to the expected changes in freezing rain frequency and intensity in Churchill.

Chapter 2

Climate Background

Churchill, Manitoba, Canada is situated along the western shore of Hudson Bay, near the boundaries of the Southern Arctic, Taiga Shield and Hudson Bay Plains ecozones (Figure 1), the boreal forest and tundra biomes and the southern limit of continuous permafrost. There are many aspects of the Arctic and sub-arctic climate which need to be discussed in order to understand the unique climate of Churchill and the Hudson Bay region, particularly how sea ice over Hudson Bay and synoptic scale circulation processes relate to the development of freezing rain. It is especially important to understand how these relationships might change under future climate projections.

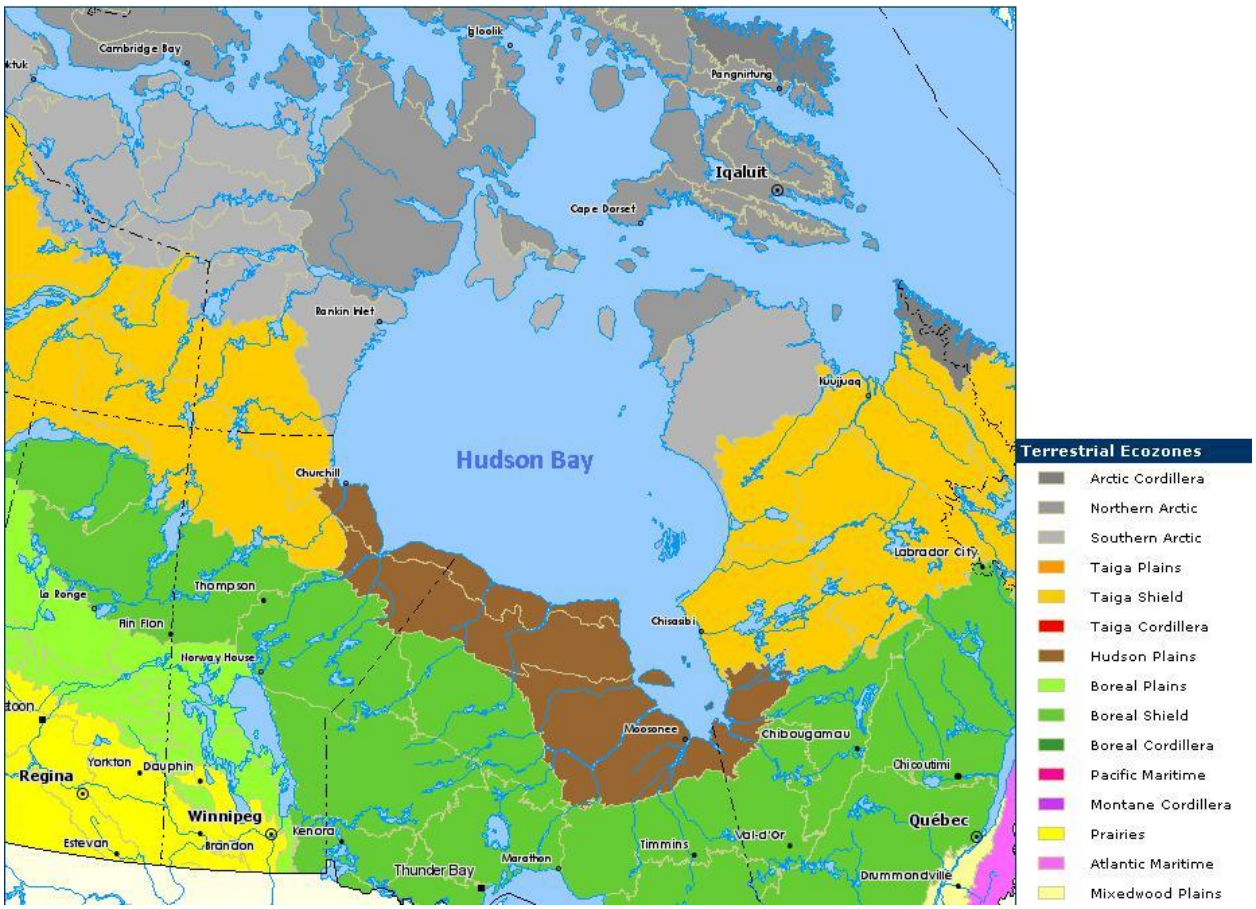

Figure 1: Terrestrial Ecozones, rivers and lakes and major communities of the Hudson Bay region (source: Atlas of Canada online, royalty free imagery. http://atlast.gc.ca).

2.1 Climate of the Arctic and sub-arctic

Throughout most of the year, the Arctic and sub-arctic (including Hudson Bay) is characterized by an energy deficit driven largely by the surface radiation budget. This deficit results in a mean poleward movement of energy from the equatorial and mid-latitude regions. This poleward movement results in the well-known patterns of the general atmospheric circulation and the ocean currents. In the mid-latitudes, the relatively warm and moist extra-tropical air masses migrate northward and meet cold, dry air masses migrating southward. The boundary between these air-masses forms a

circumpolar front that propagates around the world in the form of large planetary waves called Rossby waves. These waves drive the formation of mid-latitude cyclones largely though positive vorticity advection and the promotion of baroclinic zones (regions of large horizontal temperature change over a relatively short distance) (Barry, 1973).

The surface climate of the Arctic and sub-Arctic is dominated by extreme variability in solar radiation. During winter, when parts of the high-Arctic experience long periods of time with no incoming solar radiation (many days with 24 hours of darkness, known as the 'polar night'), the radiation budget is governed exclusively by longwave radiation emission away from the surface and counter radiation from cloud cover and other greenhouse gases in the atmosphere. During the spring, a high surface albedo created by snow and ice restricts the absorption of shortwave radiation at the surface. Furthermore, most of the absorbed radiation is used to melt snow and ice; therefore very little energy is available to heat the air and temperatures remain relatively cool. During the summer, when the Arctic and sub-arctic experiences long hours of daylight, large amounts of energy are absorbed by the ocean, which has a relatively low albedo compared to the land. Then, during fall and early winter, the ocean becomes an important source of energy to the atmosphere (Simmonds and Keay, 2009).

In spring, when Hudson Bay is covered in ice, the bay can strongly influence lower atmosphere temperatures over its western coastline when easterly winds blow inland off of the ice, advecting cold air (Szeto et al., 1999; Prairie and Arctic Storm Prediction Centre, pers. comm., 2011). When warm fronts approach Hudson Bay from the south and advect warm air aloft (possibly above freezing) while at the same time

cooler air is advected at the surface from over the bay, conditions may be favourable for freezing rain production.

2.2 Hudson Bay

Hudson Bay is an inland, Arctic sea that has far reaching impacts on the Canadian climate (Joly et al., 2011). With an area of 1.2 million square kilometers, it is the second largest bay in the world. However, Hudson Bay is unique with regards to other inland seas for many reasons. First, Hudson Bay is relatively large and shallow compared to most seas (Saucier et al., 2004; Stewart and Barber, 2010). Also noteworthy is the fact that the Bay undergoes a complete cryogenic life cycle every year; the Bay is completely frozen during winter and completely thawed during summer (Saucier et al., 2004; Qian et al., 2008). Furthermore, the closed-in nature of the Bay limits mixing with other Arctic bodies of water. Therefore, interannual variability in the bay's sea ice extent and concentration is closely linked with climate variability, annual patterns in atmospheric winds and interannual fluctuations of the North Atlantic Oscillation (NAO) and Arctic Oscillation (AO) (Tivy et al., 2006; Qian et al., 2008; Joly et al., Hochheim and Barber, 2010; 2011; Hochheim et al., 2011). Consequently, many researchers have determined that Hudson Bay is very sensitive to climate change (Saucier et al., 2004; Gagnon and Gough, 2005; Joly et al., 2011; Hochheim et al., 2011). Finally, Hudson Bay is unique because it is surrounded by one of the world's largest peatlands, and the potential for methane emissions in future climate scenarios is therefore very large (Pickett-Heaps et al., 2011).

A total of 42 rivers flow into Hudson Bay and drain a total of 717 cubic kilometers of water per year from the Hudson Bay drainage basin, making the Hudson Bay basin one of the largest in North America (Déry et al., 2005; McClelland et al., 2006; Mundy et al., 2010). The largest estuaries of Hudson Bay are those associated with the Nelson and Churchill rivers.

From an oceanographic point of view, seasonal patterns of fresh water flux from the estuaries of Hudson Bay drive circulation and influence sea ice development and sea surface temperatures (Kuzyk et al., 2007). Specifically, freshwater facilitates water stratification and limits vertical mixing. This allows surface temperatures to increase following large freshwater injections into Hudson Bay, thus influencing further sea ice development (Else et al., 2008).

2.2.1 Hudson Bay Climate

Large variations between summer and winter incoming solar radiation and a general shallow solar altitude give rise to large intra-annual temperature variations and very cold winter temperatures across the Bay and along its coasts (*see* Hochheim et al., 2010). This is apparent in the mean monthly temperature graph for Churchill, Manitoba (Figure 2).

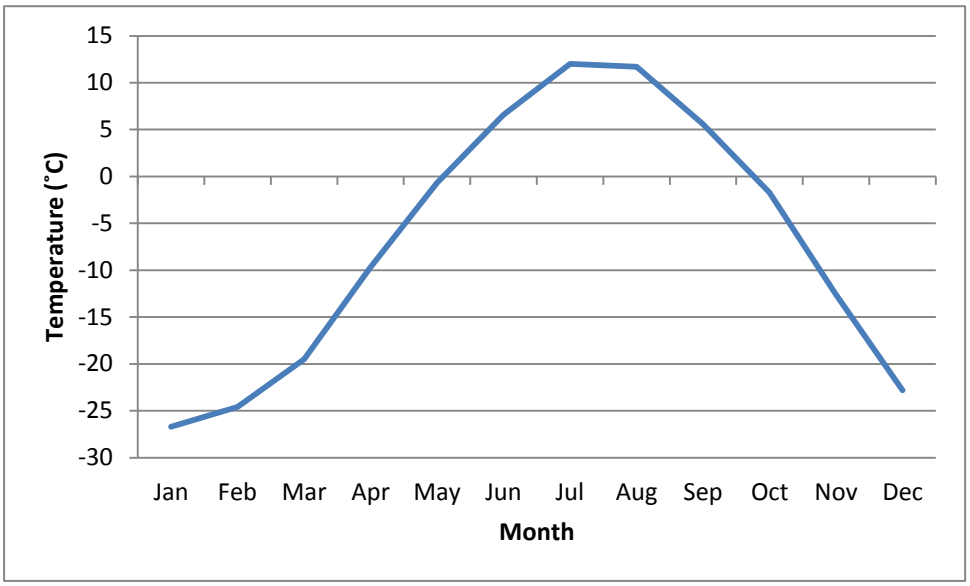

Figure 2: Monthly mean temperature normals (1961-2000) for Churchill, Manitoba (source: Environment Canada, 2011)

Cold winter temperatures increase atmospheric stability which limits winter precipitation. Annual precipitation in Churchill is usually between 500 and 700 mm per year (CCEA, 2007) (Figure 3). In Churchill, most of the precipitation falls as rain during the late summer and early fall months (July to September).

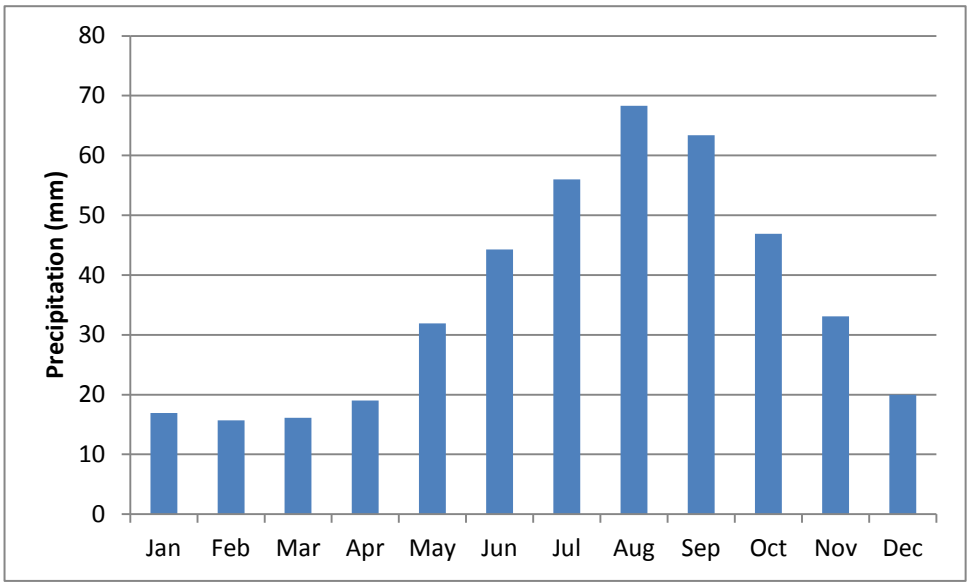

Figure 3: Monthly precipitation normals (1961-2000) for Churchill, Manitoba (source: Environment Canada, 2011)

The effects of Hudson Bay on local, coastal climates are pronounced throughout the year (Rouse, 1991). During winter, sea ice generally covers the entire bay and therefore the climate is very continental (in the past few years, freeze up has been significantly delayed and therefore the continentalization of the climate is much less pronounced). Furthermore, low-level diabatic cooling due to the presence of sea ice increases the frequency of temperature inversions and increases the planetary boundary layer stability (Wu et al., 2004).

Summer over Hudson Bay is characterized by large freshwater inputs from melting sea ice, sharp increases in radiative forcing, and a lag in surface air temperatures as melting sea ice consumes much of the available energy. The latter process describes the 'winterization' effect of Hudson Bay sea ice during the spring and early summer. Rouse (1991) showed that this winterization effect can influence climates as far as 500 km inland. Furthermore, summer isotherms are typically bent to the south along the coast

of Hudson Bay, resulting in temperatures 4 to 5 degrees cooler than similar latitudes further inland (Rouse, 1991).

In the fall, cooling air temperatures and the lack of sea ice facilitate large energy fluxes from the ocean to the atmosphere and it is during this season that temperature feedbacks can be most intense (Simmonds and Keay, 2009). Changes in sea ice cover or in the timing of sea ice formation and thaw therefore act to alter the impact the bay has on local climates throughout the year. Hudson Bay can also impact the frequency and severity of adverse weather events experienced along the coast and for several hundreds of kilometers inland, mainly by supplying moisture to weather systems (Rouse, 1991).

2.2.2 Hudson Bay Sea Ice

Variability and trends in sea ice concentration (SIC) and sea ice extent (SIE) over Hudson Bay can largely be explained by atmospheric processes. This is unlike other large bodies of water in the Arctic, where sea ice processes are largely governed by ocean currents (Wang et al. 1994). Many studies have correlated Hudson Bay sea ice data with teleconnection indices. In particular, the positive phase of the NAO and the negative phase of the Southern Oscillation Index (SOI) have been linked to cooler temperatures and northerly winds over the bay, leading to higher SIC and SIE.

Because Hudson Bay undergoes a full cryogenic cycle each year, all sea ice within the Bay can be classified as first-year ice (with the exception of a small amount of ice that may float in from the north). Hochheim and Barber (2010), who used Canadian Ice Survey data, give a detailed description of mean annual Sea Ice Extent (SIE)

processes over Hudson Bay during freeze-up. First, ice starts to form during week-of-year (WOY) 43 in the northern part of the Bay. Near-shore ice begins to form, expand and consolidate during WOY 44, and by WOY 45 it is likely that sea ice will be fully consolidated in the north. The amount of consolidated ice continues to grow and spread southward, and by WOY 48 ice has developed across all of Hudson Bay and into James Bay.

In a follow-up study, Hochheim et al. (2011) detailed the atmospheric forcing on sea ice during the spring months. Ice begins to breakup over the bay between WOY 18 and WOY 24. Atmospheric forcing, combined with the natural shape of the Bay, results in a steady cyclonic circulation within the Bay throughout the year. This cyclonic circulation results in an accumulation of mobile ice in the eastern portion of the Bay and a faster rate of ice melt in the western portion of the Bay. Landfast ice is the first to melt, and by WOY 30 there is very little consolidated ice left over the bay. Hudson Bay is not completely ice free, however, until mid-August (Hochheim et al., 2011).

2.2.3 Climate Change

Recent analyses of surface air temperature trends over and around Hudson Bay indicate an increase in annual temperatures of 0.2 to 1.8˚C per decade (Hochheim and Barber, 2010). Fall, on average, has witnessed the largest increases in temperature - nearly 1.4˚C per decade (Hochheim and Barber, 2010) - whereas spring trends are slightly lower, 0.26 to 0.3˚C per decade (Hochheim et al., 2011). Smith and Blair (2012) calculated mean daily temperature trends across Canada using Environment Canada's

Archived Homogenized Canadian Climate Data (AHCCD) for the years 1970 to 2011. They, too, found that the largest increases in surface air temperature since 1970 in the Hudson Bay region have occurred during fall and winter (Figure 4).

These temperature trends are expected to continue or accelerate in the future. Environment Canada's current Canadian Global Climate Model (CGCM), the CGCM4/CanESM2 fourth generation model, predicts very large changes (> 3˚C) in the mean annual temperatures of the Hudson Bay region (Figure 5). The model also predicts a slight increase in the amount of precipitation across most of the Arctic over the next century (Figure 6).

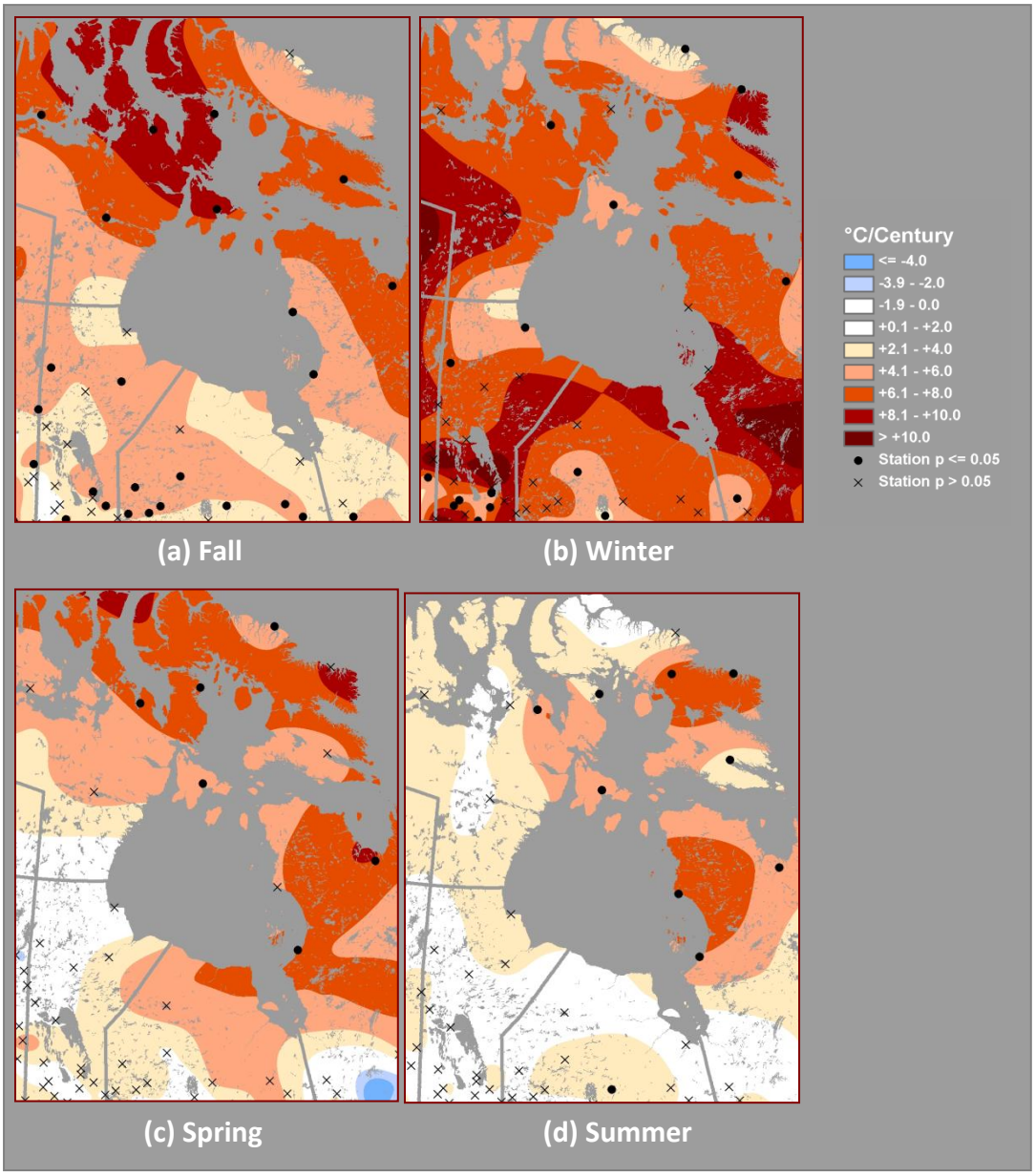

Figure 4: 1970-2010 mean daily temperature trends in the Hudson Bay region for (a) Fall, (b) Winter, (c) Spring and (d) Fall (maps created by Dr. Danny Blair and Ryan Smith, University of Winnipeg Department of Geography, 2012)

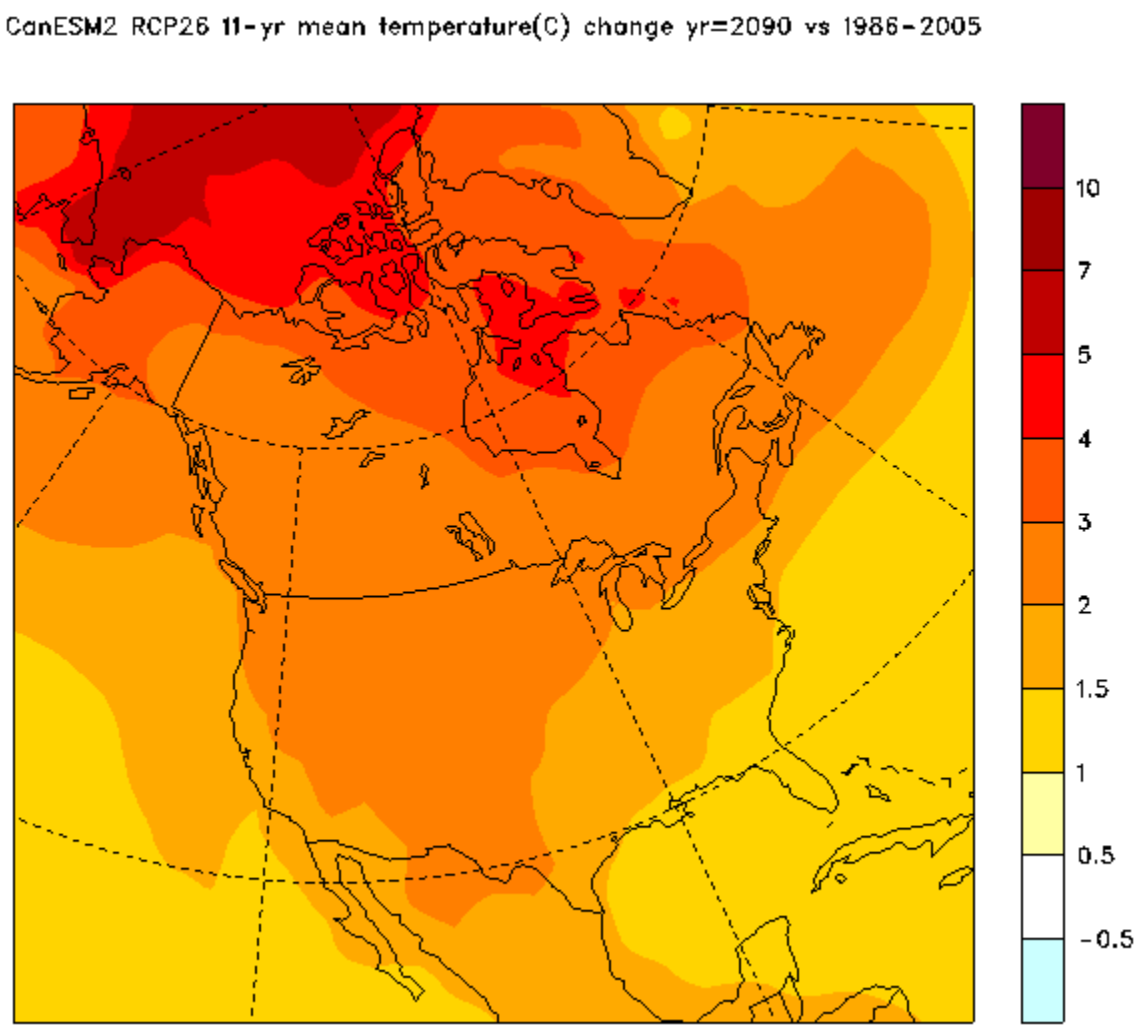

Figure 5: Projected 11-year mean temperature change for the year 2090 over North America using the CGCM4/CanESM2 model (vs. 1986-2005) (source: Environment Canada, 2012)

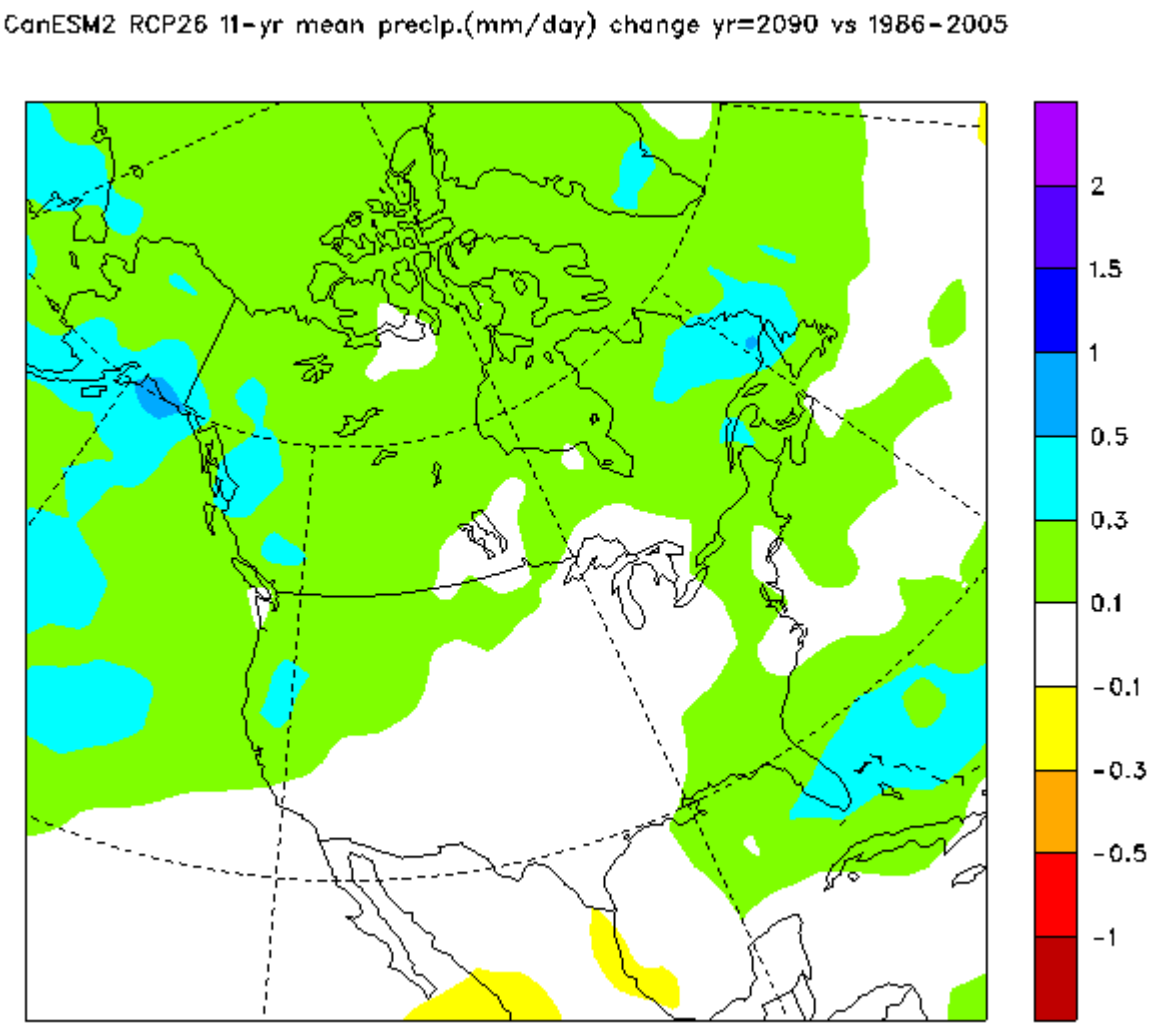

Figure 6: Projected 11-year mean precipitation change (mm) for the year 2090 over North America using the CGCM4/CanESM2 model (vs. 1986-2005) (source: Environment Canada, 2012)

An increase in surface air temperature has a profound impact on sea ice concentration and extent. Hochheim et al. (2011) demonstrated that the largest decreases in sea ice concentration have been occurring along the southwest and northwest coasts of the Bay. Recent calculations of changes in sea ice concentration are between -15.1 to -20.4 percent per decade (Hochheim et al., 2011). Trends are not as extreme in the eastern

portion of the Bay, but this is probably because mobile ice accumulates in the east due to the cyclonic circulation in the bay. Hochheim et al. 2011 showed that wind direction and speed correlates highly with sea ice concentration anomalies.

Prior to 1993, sea ice concentration trends in Hudson Bay were only slightly negative or very near zero. In fact researchers found that some Arctic water bodies (between the 1960s and 1993) were experiencing an increase in sea ice concentration. However, post-1993, trends across the Arctic became negative. In the case of Hudson Bay, these trends have accelerated since the mid-1990s (Hochheim et al., 2010).

2.3 Freezing Precipitation

One of the major focuses of this thesis is freezing rain. In Canada, freezing rain is defined as rain, the "drops of which freeze on impact with the ground or with other objects at or near the Earth's surface", and is defined as being distinct from freezing drizzle (Environment Canada, 1990; Stewart, 1992). Freezing rain can occur during any month of the year, but is most prevalent during spring and fall (Hanesiak and Wang, 2005; Hanesiak et al., 2003). There are, however, many other types of freezing precipitation which can occur frequently throughout the Arctic and sub-arctic.

Freezing precipitation events include freezing rain, freezing drizzle, freezing fog, liquid core pellets, wet snow and sometimes includes ice pellets, although ice pellets are typically defined as frozen precipitation. Freezing precipitation is a relatively infrequent type of adverse weather; however its effects on human operations and on wildlife can be

very severe. For example, freezing precipitation can impact ground transportation, air transportation, electricity transmission, agriculture and cause fauna mortality (Stuart 1994; Cortinas et al., 2004; Hanesiak and Wang, 2005).

Freezing drizzle is the most frequently observed type of freezing precipitation across most of North America (Rauber et al., 2000; Cortinas et al., 2004). The most common mechanism of freezing drizzle production is the so-called 'warm rain' or 'collision–coalescence' mechanism. During warm rain events, cloud temperatures tend to remain greater than -10˚C and therefore ice production within the cloud is limited because of the lack of active ice nuclei. In these situations, water tends to remain in the liquid state (it becomes a super cooled liquid) and will precipitate as freezing drizzle (Bernstein, 2000; Rauber et al., 2000; Cortinas et al., 2004).

Another common mechanism of freezing precipitation production is called the 'melt process' or the 'classical' process. In this case, precipitation first passes through a melting layer (above 0˚C) aloft then a sub-freezing layer (also called the refreezing layer) at or near the surface (Figure 7) (Zerr, 1997; Roberts and Stewart, 2008; Thériault and Stewart, 2010). The melt-process mechanism is more commonly associated with freezing rain production than freezing drizzle (Bernstein, 2000; Cortinas et al., 2004). Several factors influence whether ice crystals falling through a melt-layer and subsequent refreezing layer will cause freezing precipitation at the surface, including size and shape of the ice crystals, number of ice crystals, number of collisions between ice crystals, rate at which the crystals fall, maximum temperature of the melt-layer, thickness of the melt-layer, thickness of the refreezing layer, surface temperature, wind speed and direction, and surface characteristics (*see* Gibson and Stewart, 2007; Roberts and Stewart, 2008;

Thériault and Stewart, 2010). Additionally, if the relative humidity of the air is less than 100 percent then the wet-bulb temperature will be lower than the air temperature and this can affect how quickly falling particles will melt in the melting layer and cool in the freezing layer (Hanesiak and Stewart, 1995). Some of these factors are discussed in more detail below.

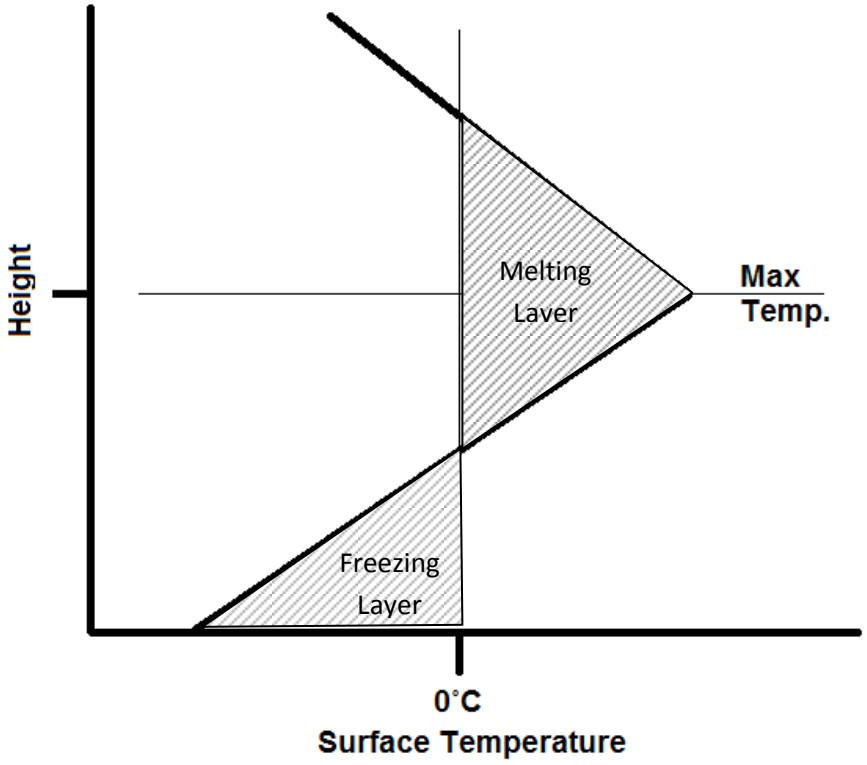

Figure 7: Conceptual illustration of the melt process model for freezing precipitation production. Adapted from Zerr (1997), Robbins and Cortinas (2002) and Thériault and Stewart (2010).

The depth of the freezing layer and melting layer are important in determining what type of freezing precipitation will develop. For example, Bernstein (2000) determined that a warm layer with a depth of up to 2800 m and a maximum temperature of 10˚C over a sub-freezing layer not more than 1400 m thick and with a temperature not

less than -7˚C favoured freezing rain production. However, it is important to note that the freezing drizzle and freezing rain case studies examined by Bernstein (2000) were within the contiguous United States and therefore these same depths may not apply to the sub-Arctic region of Hudson Bay. Zerr (1997) and Roberts and Stewart (2008) both showed that freezing rain occurred more frequently when the maximum temperature and depth of the freezing layer were high, whereas ice pellets and freezing drizzle occurred more frequently when the maximum temperature and the depth of the freezing layer were low.

The role synoptic circulation plays in determining when and what type of freezing precipitation will form has been the focus of many studies. For example, Roberts and Stewart (2008) examined composite maps of synoptic scale sea level pressure, 1000-850 mb thickness, 850 mb temperature, 850 mb geopotential heights, 1000-500 mb thickness, 500 mb geopotential heights and 500 mb vorticity associated with freezing rain and ice pellets in the Eastern Canadian Arctic. Similarly, Robbins and Cortinas (2002) examined various synoptic-scale variables at the 850 mb and 500 mb pressure levels. Cheng et al. (2004) studied many synoptic scale and surface variables, including sea level pressure, geopotential heights at five pressure levels, vorticity, cloud cover and temperature at various vertical levels. This type of synoptic scale research can be defined as 'environment-to-circulation', as only the synoptic maps associated with freezing precipitation events are analyzed (Yarnal, 1993).

This type of research has led to the discovery that freezing precipitation (in particular freezing rain) is sensitive to synoptic scale circulation. Typically, warm fronts or occulded fronts are associated with freezing precipitation because these fronts

facilitate the advection of warm air aloft, fitting the melt process model of freezing rain production. Robbins and Cortinas (2002) found that in most freezing rain cases observed in the United States, surface temperatures increased up to six hours prior to the freezing rain event and this was shown to be consistent with a passing warm front. Cheng et al. (2004) found an association between cyclone tracks and freezing rain, particularly when a cyclone was situated to the south and/or west of a weather station. When a cyclone was in this position, a warm front was likely to be observed. Roberts and Stewart (2008) noted that 87 percent of the freezing precipitation cases studied in the Eastern Arctic were associated with warm fronts. A further five percent was found to be associated with on-shore winds, and this echoed a similar observation made by Stuart and Isaac (1999), who noted the presence of on-shore winds during freezing rain events in the Hudson Bay region. In these cases, on-shore winds helped lower surface temperatures below the freezing point.

Freezing rain is a relatively rare event across most of North America. However, in some locations topography, surface feature and synoptic and meso-scale circulation can combine to form regional maxima as high as 50 hours or more per year (Cortinas et al., 2004). The east coast of Canada usually receives the most freezing rain mainly due to the availability of water (Atlantic Ocean) and frequent cyclonic storms. Similarly, regions around the Great Lakes often experience relatively large amounts of freezing rain because of the cyclonic storms that frequently track through the region (Bernstein, 2000; Cheng et al., 2004). Stuart and Isaac (1999) demonstrated that Hudson Bay can also enhance freezing rain production along its western shore and for several hundreds of kilometers inland. Bernstein (2000) demonstrated that even relatively small topographic

features and bodies of water can greatly impact the amount of freezing precipitation in a region. Finally, Bernstein (2000) also showed that air cleanliness (pollution) can impact freezing rain development by increasing the number of condensation nuclei.

In the United States, freezing precipitation is most commonly observed during the winter (December through February) whereas in Canada freezing precipitation is often associated with spring and fall. In the far north and along the north-west coast, freezing precipitation is more common during fall compared to spring (NAV CANADA, 2011). However, the opposite is true for the east coast (Cortinas et al., 2004). Hanesiak and Wang (2005) observed similar monthly frequencies across the Canadian Arctic; however they noted that freezing precipitation in Churchill is slightly more common during the spring compared to the fall. Some studies have examined the diurnal aspect of freezing precipitation events. For example, Cortinas et al. (2004) discovered that freezing rain and freezing drizzle events were more commonly observed near sunrise, when surface temperatures are lowest.

Most freezing precipitation events are short-lived. Cortinas et a. (2004) noted that only five percent of freezing rain cases across the United States and Canada lasted longer than four hours. However, freezing rain events that persist for long periods of time and are associated with high rates of precipitation, or occur during strong winds, can pose significant risk to human populations. For example, Roberts and Stewart (2008) noted that ice accretion on power lines is greatly enhanced when strong winds are observed during freezing rain events. On January 4th, 1998, a six day freezing rain event was observed across much of southeastern Ontario and southwestern Quebec, resulting in

over 30 deaths, knocking out power for weeks and causing billions in damage (Lecomte et al., 1998).

Few studies have examined long-term trends in freezing precipitation, including the effects climate change may have on the timing, frequency and duration of these events. The exception is Hanesiak and Wang (2005), who discovered that many areas of the Canadian Arctic have experienced an increase in freezing rain since the 1950s (a decrease in winter freezing rain events but an increase during all other seasons). This analysis was done using normalized Environment Canada hourly weather reports collected by trained surface weather observers (as opposed to automated weather reports generated by computers).

Chapter 3

Synoptic Classification Background

3.1 Overview

Synoptic classifications have a long history of application. In Europe, some of the first classifications were produced by hand (eye) and have since been termed manual classifications. Lamb (1972), for example, developed a 26-type manual classification of the British Isles based on surface pressure maps (and it is still in use). Manual classifications have also been termed subjective classifications, since the delineation between synoptic patterns is not based on mathematical procedures or statistical rules, but rather on the knowledge and expertise of the synoptic climatologist.

Yarnal et al. (2001) identified several disadvantages of these earlier classification attempts. Mainly, these classifications took a long time to produce (as they must be sorted by hand) and an uncontrolled amount of researcher bias is introduced due to the subjective nature of the sorting process.

Lund (1962) was among the first to apply automation to classification. His methodology involved calculating correlation statistics between maps and grouping maps together that shared high correlation values. While Lund's technique made it possible to quickly produce (and reproduce) synoptic classifications, researcher bias (mainly in the determination of cut-off values between types) was still an important issue.

Currently, the most popular automated synoptic classification methods utilize advanced, multidimensional statistics that seek to reduce large (and often noisy or redundant) synoptic weather maps into fewer dimensions. Principal Component Analysis (PCA) is a commonly applied data reduction technique and is often used in conjunction with the nonhierarchical clustering technique called K-means to generate synoptic classifications. PCA combined with K-means cluster analysis is sometimes described as a supervised technique, since key processes require user intervention and interpretation. However, techniques can also be un-supervised, such as the technique known as Self-Organizing Maps (SOMs), also frequently used to construct synoptic classifications. Since the methods applied in this paper concern PCA, the focus hereafter will be on this technique.

3.2 Principal Component Analysis

Principal Component Analysis (PCA) is a multivariate statistical procedure wherein complex datasets are said to be reduced when a subset of the components of the data (called principal components) that describe large proportions of variance are

retained. Each principal component (PC) is uncorrelated and orthogonal (perpendicular in a multidimensional plane) with all other principal components. The first principal component accounts for the largest share of variance in the data and all other components are ordered according to their share of explained variance. Generally, only the first few principal components are required to account for most of the variance in the data (Jolliffe, 2002).

The term PCA is often used synonymously with empirical orthogonal function (EOF). Some additional terms are used interchangeably throughout the literature (for example eigenvector and principal component are often considered synonymous). Inconsistent uses of terminology are a challenge to anyone learning PCA. In this section, the terms and definitions used are the same as in their indicated sources.

The maximum number of principal components (p) in a data matrix of *m-variables* by *n-observations* is equal to (mn), and when all mn principal components are retained the data has been re-projected back to its original state (i.e., before PCA was performed). When fewer PCs are retained ($r<p$), only the most 'important' aspects of the data are retained and the number of dimensions is reduced. If too few PCs are retained, potentially important modes of variability within the dataset may be lost; however if too many PCs are retained these smaller modes may start to remove focus from the larger modes of variability.

PCA is commonly used during the construction of synoptic classifications. When using PCA on environmental variables, a researcher assumes that a region can be described by relatively few components (i.e., much of the variability in the system can be

captured in relatively few modes). This assumption generally holds true due to the underlying physical processes that govern or constrain the atmospheric circulation (i.e., diurnal and seasonal cycles). Prior to performing PCA on environmental variables, however, the researcher must be aware of any regional biases in the data – for these biases may become magnified post PCA (i.e., during cluster analysis). First, if using location-dependent data, the study region size must reflect the desired scope of the analysis (i.e., large enough to encompass influential modes of variability in the local system). Second, if the data are also time-dependant, determining the time of day, months of the year and range of years to be analysed will greatly depend on the project's scope (and on the availability of data). Finally, if the data is gridded by latitude and longitude, grid spacing bias should be addressed. Grid spacing bias exists because lines of longitude converge at the poles and therefore gridded data will be more tightly clustered at the poles than nearer the equator (Araneo and Compagnucci, 2004).

PCA can be a challenging exercise for a researcher not familiar with matrix algebra. However, PCA on small datasets (two or three dimensions, for example) is fairly easy to understand. Smith (2002) offers a simple tutorial on PCA. Following this tutorial, the steps of a simple PCA on a single matrix of *m*-variables by *n*-observations involves:

- Standardizing (normalizing) the dataset (making the mean of the data zero).
- Calculating a covariance (or correlation) matrix.

- Calculating the eigenvectors and eigenvalues of the data. Eigenvectors are vectors that, when multiplied by the covariance or correlation matrix, are elongated but not transformed. The eigenvalue describes the degree of elongation. The eigenvalue is sometimes called the coefficient of the principal component. The eigenvector with the largest coefficient is the first principal component.

- Transforming the original data through a subset of these eigenvectors (fewer than the original number of dimensions). The term used to describe an array of eigenvectors is 'feature array'.

PCA is generally applied to a single matrix of data (i.e., multidimensional array of variables at a single instance of time). Often in atmospheric research, matrices of environmental variables (i.e., maps) can be both spatially dependent and time dependent. In these cases, in which there may be multiple modes of variation in the data (spatial and temporal, in this example), a different PCA mode must be adopted. Jolliffe (2002) summarizes the two PCA modes most commonly used in atmospheric research: S-mode and T-mode. S-mode is the most common form found in the literature. In this mode, the spatially dependent data are the variables (*m*) and the time dependant data are the observations (*n*). In T-mode, the time dependant data are the variables and the spatially dependent data are the observations (Jolliffe, 2002).

Generally, very few principal components are necessary to identify the majority of variation within a series of weather map (whether this is variation in shape, intensity

and for time). However, the number of principal components to retain is very important since the process can be extremely sensitive. In other words, the decision to retain r+1 principal components will produce noticeable changes to the synoptic classification, regardless of whether r+1 component account for 0.01 percent of the total variation or 99.99 percent of the total variation. While the addition of low-ordered components should intuitively have little effect on the reduction of the map, the reality is entirely opposite (*for an example of principal component sensitivity see* Cuell and Bonsal, 2009). Therefore, choosing the number of principal components to retain (sometimes called principal component truncation) is an important issue and a possible weakness of PCA.

Unfortunately, no one method of principal component truncation can be adapted to all scenarios. Jolliffe (2002) describes some of the different methods for selecting the number of principal components to retain. The most commonly used methods (as seen in climatological literature) are listed below:

- Determine a cutoff value when a desired amount of cumulative variance is reached (usually 95 or 99 percent).
- Only retain principal components which have eigenvalues greater than 1 (*originally proposed by* Kaiser, 1960) (in other words, only use components that account for more than one percent of the variance).
- Select the value visually from a scree-plot (plot of total explained variance vs. component number) such that the graphed line is steep to the

left and shallow to the right of the chosen principal component (Cattell, 1966).

In discussing the various methods of principal component truncation (not all are listed above), Jolliffe (2002) notes that all methods are based on subjective decisions made by the researcher. Wilks (2006) offers a very similar list of selection criteria and a similar opinion of the inherent subjectivity within PCA. However, Wilks notes that not all selection criteria have to be based on statistical rules or on the amount of variance explained by each component. For example, he notes that pertinent principal components of datasets that contain time-dependence (such as seasonality) should also display similar time-dependence. Using this logic, principal components that do not show time-dependence should be eliminated.

However the subset of principal components is reached, additional decisions must be made throughout the PCA process. In particular, a researcher must determine if rotation of the eigenvectors is appropriate. Rotation involves the transformation of the eigenvectors and tends to spread variance amongst the first few principal components (Jolliffe, 2002). The need for rotation arises when performing PCA on geographical data, such as climatological and meteorological maps. In these cases, the requirement that all principal components must be orthogonal to all other principal components introduces unnatural constraints on the data (the real-world does not constrain itself orthogonally). Wilks (2006) notes that the tendency in un-rotated PCA of geographic data is for natural modes to be split (defined) between two or more principal components.

Similarly, un-rotated components are prone to so-called Buell patterns: statistical artifacts of PCA that have characteristic (predictable) shapes (Buell, 1979). These patterns can also be attributed to the orthogonal constraints PCA places on geographical data. In cases where principal component maps are attributed to real-world phenomenon (such as the definition of the Arctic Oscillation as the leading principal component of sea level pressure) these Buell patterns can lead to inappropriate results.

Rotated Principal Component Analysis (RPCA) can be achieved by using orthogonal or oblique transformations, but the most popular form of rotation in climatological analysis is the orthogonal rotation developed by Kaiser (1958) called VARIMAX. Regardless of the rotation method applied, Wilks (2006) reminds meteorologists and climatologists that orthogonal rotation is very sensitive to the initial scaling of the eigenvectors. A good example of this sensitivity is when RPCA output is compared between a 64-bit and 32-bit computer. Here, the extra floating-point precision of the 64-bit machine can drastically alter the shapes and amounts of variation explained by each of the rotated principal components. Finally, it would appear that many researchers often misinterpret the effects of rotation on PCA – particularly by claiming that rotated principal components are both orthogonal and uncorrelated, which can never be true (Wilks, 2006).

Another major decision that a researcher must make during PCA and RPCA is whether to calculate eigenvectors using a correlation or a covariance matrix. Wilks (2006) notes that covariance matrices tend to align with the largest variances while correlation matrices will not. With weather maps, the effect is for covariance-based PCA to highlight intensities and for correlation-based PCA to highlight shapes. In the

literature related to synoptic classification, correlation-based PCA is applied more frequently than covariance-based PCA. However the reasons why correlation or covariance was selected over the other are usually not stated or clear.

3.3 Cluster Analysis

Cluster analysis is the process by which data are grouped according to some measure of similarity. Cluster analysis is (generally) based on the Euclidean straight-line distances between data points on a plane. Data points belong to a cluster if the distance between each data point and its assigned cluster's centroid are smaller than the distance between each data point and all other cluster centroids (Wilks, 2006).

Cluster analysis is commonly used post PCA to produce synoptic classifications. When data is reduced in a PCA, features of atmospheric circulation are often much better defined and therefore clusters tend to exhibit much lower within-type variability and much higher between-type variability than if maps were clustered without first utilizing PCA.

Clustering can be done using hierarchical or non-hierarchical methods. The most popular form of hierarchical clustering is called agglomerative. This procedure begins by assigning a unique cluster to all data points. Next, these clusters are merged repeatedly until there is only one cluster (to which all the data now belong). The researcher must then decide how many clusters produced an optimal result, usually from statistics summarizing within-type and between-type goodness-of-fit (Wilks, 2006). Conversely,

nonhierarchical clustering begins with the number of desired clusters predetermined and uses an iterative method to determine where the cluster boundaries should be placed.

The most popular clustering method in climate research is the nonhierarchical clustering method known as K-means. During K-means clustering, data are first clustered arbitrarily (generally initiated by a seed value). Then the distance between each data point and its arbitrarily assigned cluster's centroid is calculated. If any cluster member is found to be closer to the centroid of a cluster to which it was not assigned, the cluster boundaries are redefined. This process is repeated until all data points are closest to the cluster centroids to which they were assigned (Wilks, 2006).

Choosing an appropriate number of clusters for a dataset is, in some ways, analogous to choosing the number of principal components to retain during PCA. In both cases, the decision is often subjective and generally based on the desired resolution of the resulting classification. When producing a synoptic classification, too few or too many clusters may place unnatural constraints on the data. Furthermore, a finer scaled classification (more clusters) may reveal small scale features not otherwise captured in a more coarse classification. Methods for selecting the number of clusters to keep when using non-hierarchical clustering vary greatly between studies. In the end, the researcher must decide how many clusters are appropriate for the study at hand.

3.4 Multi-level classifications

It is often desirable to analyze multiple data types from multiple atmospheric levels (e.g., pressure, heights, temperature, vorticity, humidity and wind at the 1000mb, 925mb, 850mb, 700mb, 500mb and 250mb pressure levels, as well as surface measurements) because most atmospheric processes depend on the three-dimensional structure of the atmosphere. Three distinct methods have been observed in the literature for producing synoptic classifications for multiple variables and/or levels.

In the first case, the researcher enters all of the variables into a massive matrix that is subsequently passed through PCA (see Frank et al., 2008a; Cheng et al., 2004). Here, the leading principal components will be defined by those variables which account for the largest share of variance in the data. For example, Cheng et al. (2004) loaded 240 atmospheric variables into the PCA and the first principal component was found to be defined by thermodynamic variables, whereas the low-ordered components tended to account for diurnal variation in non-thermodynamic variables. Therefore, this type of analysis reveals the important variables in the dataset, from a climatological point of view.

A second method for analyzing multiple variables and/or levels involves performing PCA on two or more variables individually and then combining a subset of the PCA loadings (i.e., reduced maps) into a single cluster analysis (see Martínez et al., 2008). Here, the goal is not to identify which variables are the most 'important' but rather to 'clean' each variable individually (passing it through PCA and retaining a subset of the principal components) and then treating each member in the clustering processes as a multi-layered map. Typically, many clusters are needed to satisfy all of the permutations and combinations that the system may exhibit. For example, high surface

pressure may exist under a range of upper-air temperatures and heights, and in order to avoid a mistype one must expand the number of available classes to accommodate the fact that one layer may remain the same while another layer may change.

A third type of analysis involves generating two or more classifications completely independently from one another (*see* Bettolli et al., 2010). In these cases, researchers hope to find co-varying trends in type frequencies between classifications and between surface phenomena. For example, Bettolli et al. (2010) generated two classifications using 1000mb and 850mb geopotential heights and compared both of them to heavy rainfall events to evaluate the role of thickness between these two heights.

3.5 Self-Organizing Maps (SOMs)

Unlike PCA, which requires the user to pre-determine key parameters of the analysis (such as the number of principal components to retain), SOM is an unsupervised technique that seeks to find an optimal solution. Because of this, some researchers have identified the SOM technique as an improvement upon PCA.

SOM techniques seek to reduce multidimensional data into a two-dimensional space called a map using unsupervised learning (Kohonen, 1991). SOMs can be described as the opposite of cluster analysis: where cluster analysis seeks to 'lump' patterns into distinct, non-continuous classes, SOMs are built to encompass the entire range of patterns on a continuum (Reusch and Alley, 2007). Some researchers have noted that PCA (especially un-rotated PCA) can result in artificial modes of variation (due to the orthogonal constraint of the procedure) whereas SOM techniques tend to

better identify natural, non-orthogonal modes (Iseri et al., 2009). However, rotated PCA alleviates the amount of orthogonal constraint during PCA and therefore may still produce an adequate solution. SOM techniques are growing in popularity and may one day replace PCA as the preferred method for generating synoptic classifications.

3.6 Examples of Classifications

In almost all cases, synoptic classifications are used to find relationships between synoptic type frequencies and surface weather and climate variables. These relationships may be derived to improve weather forecasting, model long-term climate change scenarios or simply to better understand the spatial-temporal characteristics of the synoptic climate. In this section, the scope and nature of classification methodologies and applications in recent literature are highlighted. The scope of the reviewed content is restricted to recent publications that used some form of multivariate statistic or cluster analysis, or both, to produce the synoptic classification.

Cheng et al. (2004) developed a synoptic classification from sea level pressure (SLP) data using PCA and agglomerative clustering to determine the synoptic types most often associated with freezing rain events in Ottawa, Canada. This research aimed to improve freezing rain modeling and prediction. Only principal components with eigenvalues greater than 1.0 were retained post PCA, and this resulted in 18 principal components being saved. The number of clusters (13) was determined using a 'minimum within-type' vs. 'maximum between-type' calculation. An analysis of which meteorological variables favored freezing rain resulted in a model of freezing rain likelihood based on surface and upper-air parameters. Next, the averages and standard

deviations of each of the model's parameters were calculated for days associated with each synoptic type. Ideally, forecasters would be able to forecast atmospheric conditions using knowledge of the current and forecasted synoptic types and then use this knowledge to model freezing rain event probability.

Bettolli et al. (2010) generated two synoptic classifications using geopotential height anomalies at the 1000 and 500mb levels to analyze rainfall patterns in Argentina. Unlike the previously study by Cheng et al. (2004), this study's goal was to characterize annual and intra-annual variations in 'rainy' synoptic types rather than to improve short-term forecasting. Rotated PCA (using VARIMAX) was used to reduce the data to six principal components; however, it is unclear which principal component truncation method was used. Following rotated PCA, K-means clustering was done with the number of clusters ranging from 2 to 20. The number of clusters to retain in the two classifications was based on a method similar to that in Cheng et al. (2004) and seven and five types were chosen for the 1000mb and 500mb classifications, respectfully. The purpose of using two atmospheric layers was to identify the role that vertical structure plays in rainfall.

Asplin et al. (2009) produced a classification of mean sea level pressure (MSLP) gridded data for the Canadian Arctic for the purpose of relating synoptic circulation patterns with sea-ice movement. The results showed that anomalous cyclonic pressure patterns can help explain vorticity anomalies in the Beaufort Gyre. Six principal components were retained during PCA, and rotation was not used. Furthermore, the grids were not standardized (normalized) prior to PCA (as is common), and the authors maintained that this was done to preserve seasonality in the data. The reduced data was

then clustered using K-means and this processes was repeated using 9 to 16 clusters. In the end, Asplin et al. (2009) retained 12 clusters based partly on the desired classification resolution and partly on the interpretation of a graph that displayed mean cluster differences (a measure of cluster homogeneity) from the 9 to 16 type classifications. On this graph, inflection points were interpreted as suitable break points for the number of clusters to retain.

Sheridan et al. (2008) generated a nine type synoptic classification from 850mb geopotential heights over the contiguous United States for the purpose of identifying flow patterns associated with boundary layer aerosol characteristics (to aid climate model parameterization of aerosol radiative forcing). S-mode PCA was used on a grid of standardized data, and all principal components with eigenvalues greater than one were retained (actual number components truncated not given). Nine clusters were produced using Ward's cluster method (Ward, 1963). These authors were able to associate synoptic types with aerosol characteristics, and this association was greatest during the summer months.

Martínez et al. (2008) produced a classification using three gridded variables: 1000mb and 500mb geopotential heights and 850mb temperatures, for the purpose of correlating heavy rainfall days with synoptic patterns over the Mediterranean. T-mode PCA was used on the three datasets and principal component truncation was invoked once 90 percent of the variance was reached. This resulted in six principal components for the height classifications and five principal components for the temperature classification. Once the three variables were reduced, their combined daily values were clustered using K-means. Here, the choice for the number of clusters was made when the

mean within-type sums-of-squares value (which is a value that decreases with increasing clusters) did not change significantly when additional clusters were computed. This method resulted in 8 types (each type is made up of a 1000mb and 500mb height pattern and a 850mb temperatures pattern).

A paper by Skinner et al. (2002) is an example of when variation in terminology within the literature can cause confusion. In this paper, classified monthly averaged 500mb heights were used to identify anomalous mid-tropospheric flows correlated with forest fires across Canada. The classification methodology was poorly described. The authors used RPCA on a correlation matrix (they did not want map intensities to bias the result) of the 500mb grids. It then appears that the authors did not keep a subset of principal components to retain, and proceeded directly to cluster analysis (which would mean the data was still in its original, unreduced form). The authors then indicated that a scree-plot was used to determine the number of *clusters* to use during a K-means cluster analysis and not the number of *principal components*. Despite the confusion within their methods section, the authors appear to have successfully identified several atmospheric types associated with large forest fires.

McKendry et al. (2006), using the methods detailed by Stahl et al. (2006), produced a classification of MSLP grids obtained from the NCEP/NCAR re-analysis project (*see* Kalnay et al., 1996). The authors chose to leave their grids un-standardized, citing that standardization removes seasonal information from the data. The objective of this study was to compare monthly and seasonal synoptic type frequencies to those produced from a classification of types in a global climate model (GCM) (i.e., to test how well the GCM could be downscaled for regional climate analysis). It was found that the

GCM data did not always yield realistic type frequencies, which the authors suggested was the result of regional parameterization problems in the GCM.

Frank et al. (2008a) investigated whether synoptic patterns of heights, humidity and wind at the 500mb level over North America could account for the propagation of white pine rust, a pathogen. The authors also chose to analyze these four variables at six hourly intervals, resulting in a massive data matrix that was subsequently passed through a RPCA. The authors determined the number of principal components to keep by retaining all components with eigenvalues greater than one (an objective selection criterion). Due to the very large dataset being classified, 87 principal components were retained. A clustering algorithm (not K-means) was then used to sort the data into 16 types. Frank et al. (2008b) assessed how well this classification scheme accounted for white pine rust dispersal.

The methods of generating and applying synoptic classifications vary significantly between studies, and the above samples from recent literature is by no means exhaustive. It is clear that no one method of producing a classification can apply to all scenarios, and the decisions of whether or not to standardize the variables before passing them to PCA, to use S-mode or T-mode, to rotate or not, to use correlation or covariance matrices, and to use hierarchical or non-hierarchical clustering depends greatly on how a researcher interprets the effects these options have upon their data. Because of the complex nature of multivariate analyses such as PCA, it is not surprising to see that many climatologists and meteorologists explain their methodologies poorly. In particular, the use of proper terminology seems to be an issue. In this author's

opinion, misinterpretations arising from this issue propagate quickly through the literature.

Chapter 4

Methodology

4.1 Overview

The core objectives of this thesis are to produce a climatology of freezing rain events in Churchill, Manitoba, produce a synoptic climatology of the Hudson Bay region, analyze the relationship between the synoptic climate system of Hudson Bay and the frequency and timing of freezing rain events in Churchill and, finally, to evaluate how future climates may impact the frequency and timing of freezing rain events. A multi-faceted methodology was developed to address these research goals. First, a climatology of freezing rain events in Churchill was produced using Environment Canada hourly weather records, which extend back to 1953. In order to examine the synoptic climatology of the Hudson Bay region, NCEP/NCAR reanalysis data were processed by a synoptic classification computer program known as Synoptic Typer Tools (STT). The

outputs from STT were then compared to freezing rain events, and used to determine which synoptic map types coincide with freezing rain cases in Churchill. Finally, long-term trends in the synoptic type frequencies were used to hypothesize how the future climate may impact the frequency, intensity and duration of freezing rain events in Churchill.

4.2 Study Region

A large area surrounding Hudson Bay, from 45˚N to 70˚N and from 245˚E to 290˚E, was selected as the study region (Figure 8). This area covers all of Hudson Bay and the Hudson Bay lowlands. This boundary was determined subjectively, and was partially determined by the resolution of the gridded data used to produce the synoptic classification (the NCEP/NCAR reanalysis data grid has a 2.5˚ latitude/longitude resolution; consequently, the study region consists of 19x11 grid points). Due to the convergence of the lines of longitude near the north pole, grid spacing is tighter in the northern portion of the study region compared to the south. This may mean that more smaller-scaled synoptic features will be identified in the north compared to the south. A total of 25 grids points fall within the boundary of Hudson Bay, which means that data are not too coarse to identify the bay as a major feature of the study region. Also, the study area was centred over Churchill, Canada. This study region is larger than the region originally proposed by Smith (2008), and was enlarged to better resolve cyclonic circulation patterns south of Hudson Bay.

4.3 Environment Canada Hourly Weather Data

Hourly weather data was obtained from Environment Canada (2011) for Churchill, Manitoba, for the years 1953 to 2009. The quality of the Environment Canada data is somewhat inconsistent. Many of the weather descriptions made were by trained specialists; however, during periods of low visibility and light, errors can still occur. Also, periodic 'holes' in the data occur, presumably due to equipment malfunctions. Additionally, some of the methods and tools used to measure and observe weather variables have changed since 1953. For example, for many years wind direction was rounded to the nearest 20 degrees of azimuth but more recently has been rounded to the nearest 10 degrees. Additional issues regarding the Environment Canada data are described by Hanesiak and Wang (2005) but are not deemed to have substantially affected the quality of the analysis.

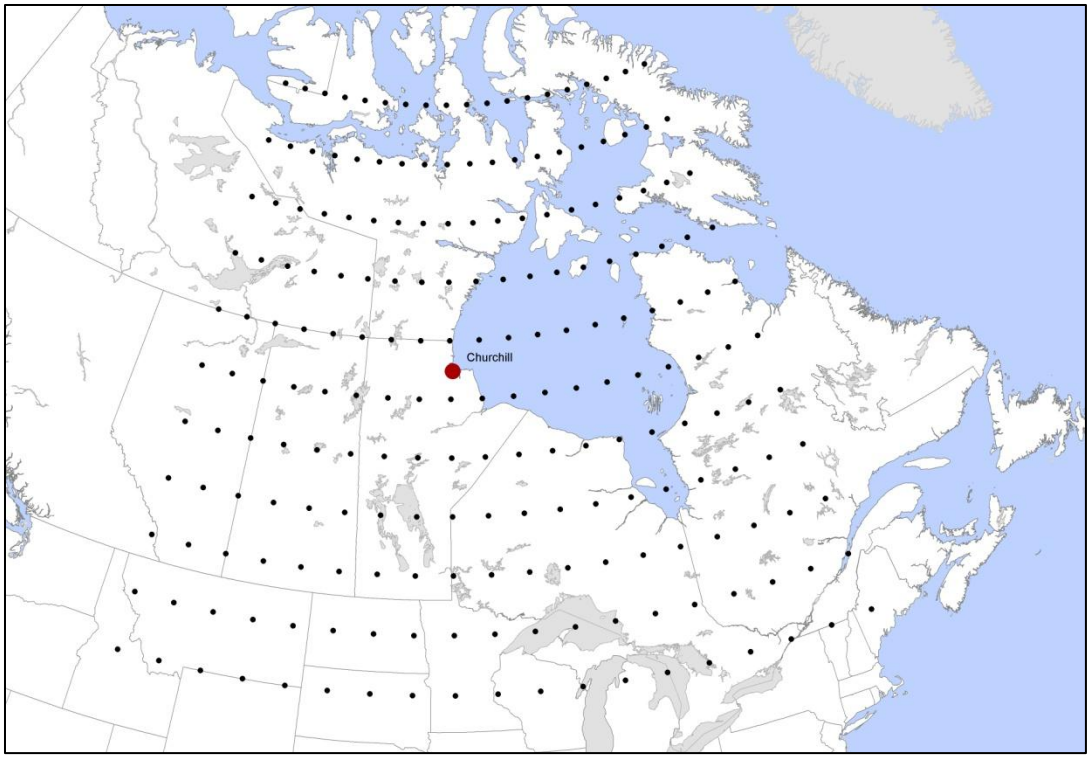

Figure 8: Study area (45˚N to 70˚N, 245˚E to 290˚E). Black dots represent the NCEP/NCAR reanalysis grid points used during analysis.

Environment Canada data are available to the public via their website (http://climate.weatheroffice.gc.ca). The data can be downloaded as comma-delimited text files, and include hourly information on temperature, dew point temperature, wind speed, wind direction, wind chill temperature, barometric pressure and weather descriptions. Interestingly, hourly precipitation totals are not provided.

Weather description variables, such as fog, freezing rain, blowing snow and snow, are listed if at least some of these weather and precipitation types occurred during the previous hour. This creates a challenging situation when analyzing past weather information, because there is no way to determine the actual duration or intensity of these weather events. For example, there is no way to tell from the Environment Canada data

whether freezing rain fell for one minute or one hour during an event. Therefore, determining the actual duration and intensity of these past weather events depends largely on analyzing corresponding wind speed, temperature and visibility data.

All of the hourly data from Environment Canada for Churchill since 1953 was downloaded and a computer program written in Interactive Data Language (IDL) was used to parse these data files and generate statistics on freezing rain. Freezing rain was counted in many different ways. First, a tally of all hours in which freezing rain was reported between the years 1953 and 2009. Next, a tally of all days with freezing rain was generated. Finally, freezing rain events were counted – consecutive hours of freezing rain were counted as one event. Events were ranked according to their durations. Here, the duration was measured as the number of consecutive hours that freezing rain was reported (in other words, it was assumed that freezing rain fell consistently during the entire event). Event durations at or above the 90^{th} percentile were categorized as 'extreme'. The hourly air temperatures, wind speeds, wind directions, dates and times associated with each freezing rain event were extracted.

4.4 Synoptic Scale Data – NCEP/NCAR Reanalysis Data Sets

The synoptic climatology of the Hudson Bay region was analyzed using gridded data from the NCEP/NCAR (National Centers for Environmental Prediction/National Center for Atmospheric Research) Reanalysis I project (Kalnay et al., 1996). These data are available at six hourly intervals since 1948 at 2.5° latitude/longitude resolution and from 90°S to 90°N and 0°E to 357.5°E. The data is in netCDF format, a commonly used binary file format. Each year of global data requires about 500MB of disk space.

Many different atmospheric variables are available from the Reanalysis data project, including surface variables and upper-air variables. It was determined that five Reanalysis variables would be used to construct a synoptic climatology of the Hudson Bay region: mean sea level pressure (SLP), 500 mb geopotential heights, the difference in air temperature between 1000 mb and 925 mb (ΔT), atmospheric thickness between 1000 mb and 925 mb and 925 mb specific humidity. The total volume of data downloaded for the study region was in excess of 150 GB.

SLP data were chosen for inclusion mainly to identify the presence and location of surface cyclones. Since previous research has shown links between cyclonic systems and freezing rain, it was important to verify whether similar synoptic scale controls govern freezing rain in the Hudson Bay region. Five-hundred mb geopotential height data were useful to assess mid-level flow and regions of positive vorticity advection. The change in air temperature between the 1000 mb and 925 mb levels were used to identify low-level temperature inversions, which are generally present during a freezing rain event. The 1000 mb level was used as a proxy for surface temperature. Prior analysis by this author of temperature inversions during freezing rain events indicated that 925 mb was a suitable height to capture the 'nose' of any temperature inversion that may be present. The 1000 mb to 925 mb thickness variable was selected to determine the average temperature within this layer of the atmosphere. Atmospheric thickness is also an important variable for forecasters trying to determine whether precipitation will reach the surface as rain, snow or freezing rain. Finally, the 925 mb specific humidity was used to identify regions where adequate moisture may be present to form freezing rain.

4.4 Synoptic Data Analysis – Synoptic Classification with Synoptic Typer Tools

Synoptic Typer Tools (STT) is an objective, supervised synoptic map pattern classification computer program written in Interactive Data Language (IDL). STT was written under the supervision of Dr. Danny Blair at the University of Winnipeg and is an update to Synoptic Typer, a computer program designed, in part, for NWP forecast guidance by the Australian Bureau of Meteorology (Dahni, 2003; Blair et al., 2011) (Figure 9). The goals of STT are to improve upon the original Synoptic Typer design and to shift the focus of the program from meteorology to climatology (Smith, 2008).

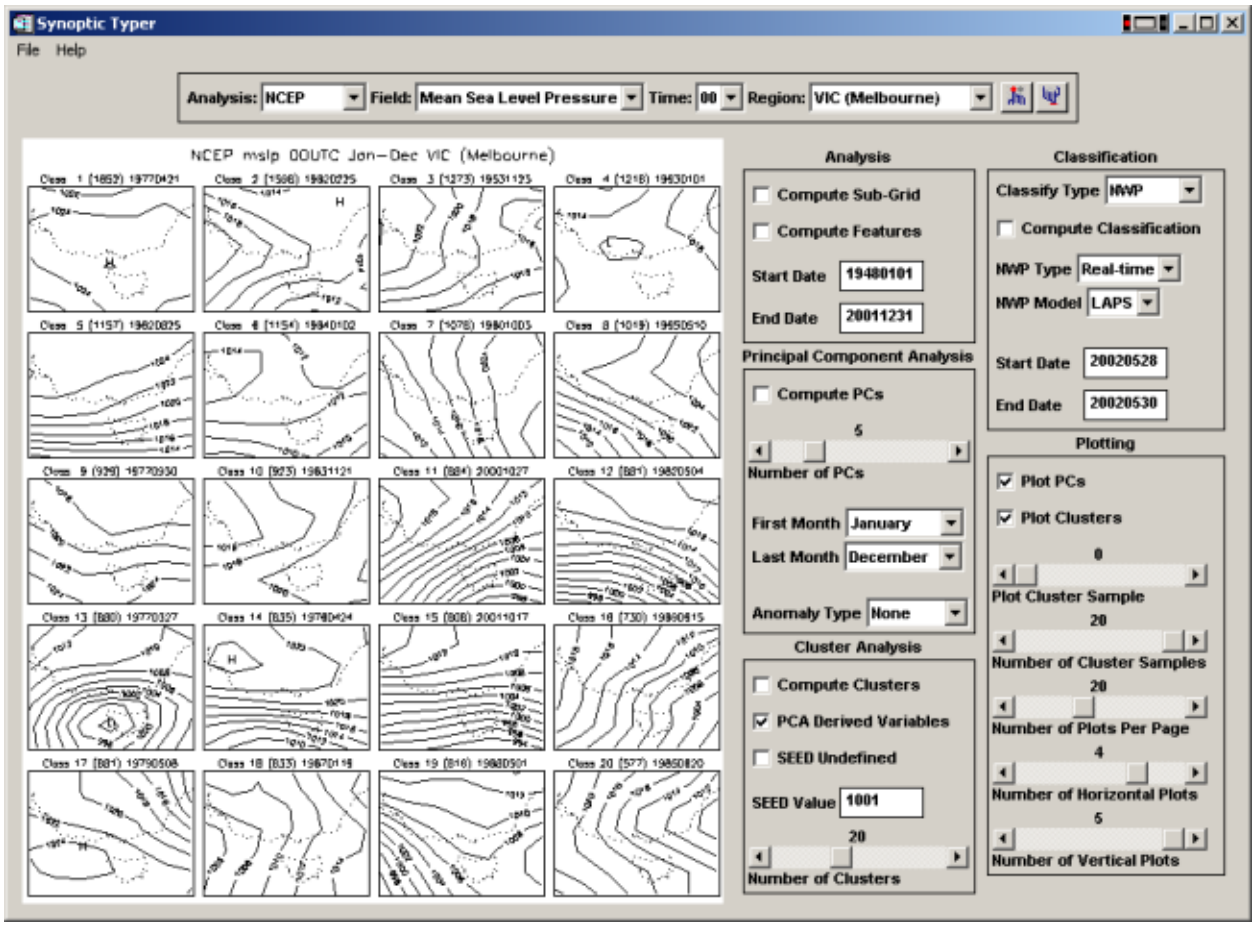

Figure 9: The original Synoptic Typer GUI (c.2002)

In early 2010, Synoptic Typer's original author, Dr. Robert Dahni, became an official co-author of STT, making STT an international collaboration. In late 2010, STT v.2.0.4 was made available to the public on its website, http://stt.uwinnipeg.ca. The author of this thesis is continuing work on additional versions of STT, named v.3.4 (Figure 10).

STT is designed to be a user friendly and relatively simple tool to use and can significantly reduce the amount of time required to generate synoptic classifications. STT classifies NCEP/NCAR Reanalysis I data and 20th Century Reanalysis data, including the

commonly used 4-times daily SLP and four-times daily geopotential height data. Both data sets are available since 1948 at 2.5˚ latitude/longitude resolution. The geopotential height data are available at 17 pressure levels within the Reanalysis data and 24 pressure levels within the 20th Century Reanalysis data, including the commonly analyzed 925 mb, 850 mb, 700 mb, 500 mb and 250 mb levels.

During the STT design process, a large focus was put on the provision of feedback to the user regarding how well their classification described the real-world. There are two main variables that control the classification output: the number of principal components retained post PCA and the number of clusters used during K-means cluster analysis. In both cases, decisions concerning these important parameters are often highly subjective and vary between study regions. In STT, the user can initiate a loop that will generate numerous synoptic classifications with varying numbers of principal components and clusters. STT then compares the classification runs and generates output that can help the user identify optimal classification parameters. Specifically, various cluster score graphs, scree-plots and within-type variance plots are generated.

Improving STT by expanding the types of data it can classify was one of the primary challenges of this thesis. Specifically, a new version of STT was built to produce so-called 'multi-level' classifications (Figure 11). Previously, STT could only analyze SLP and geopotential heights. Three additional variables are now included: relative humidity, specific humidity and air temperature. In addition to these new variables, it is now possible to classify atmospheric thickness data derived from any two geopotential heights and to classify the change in air temperature between any two pressure levels.

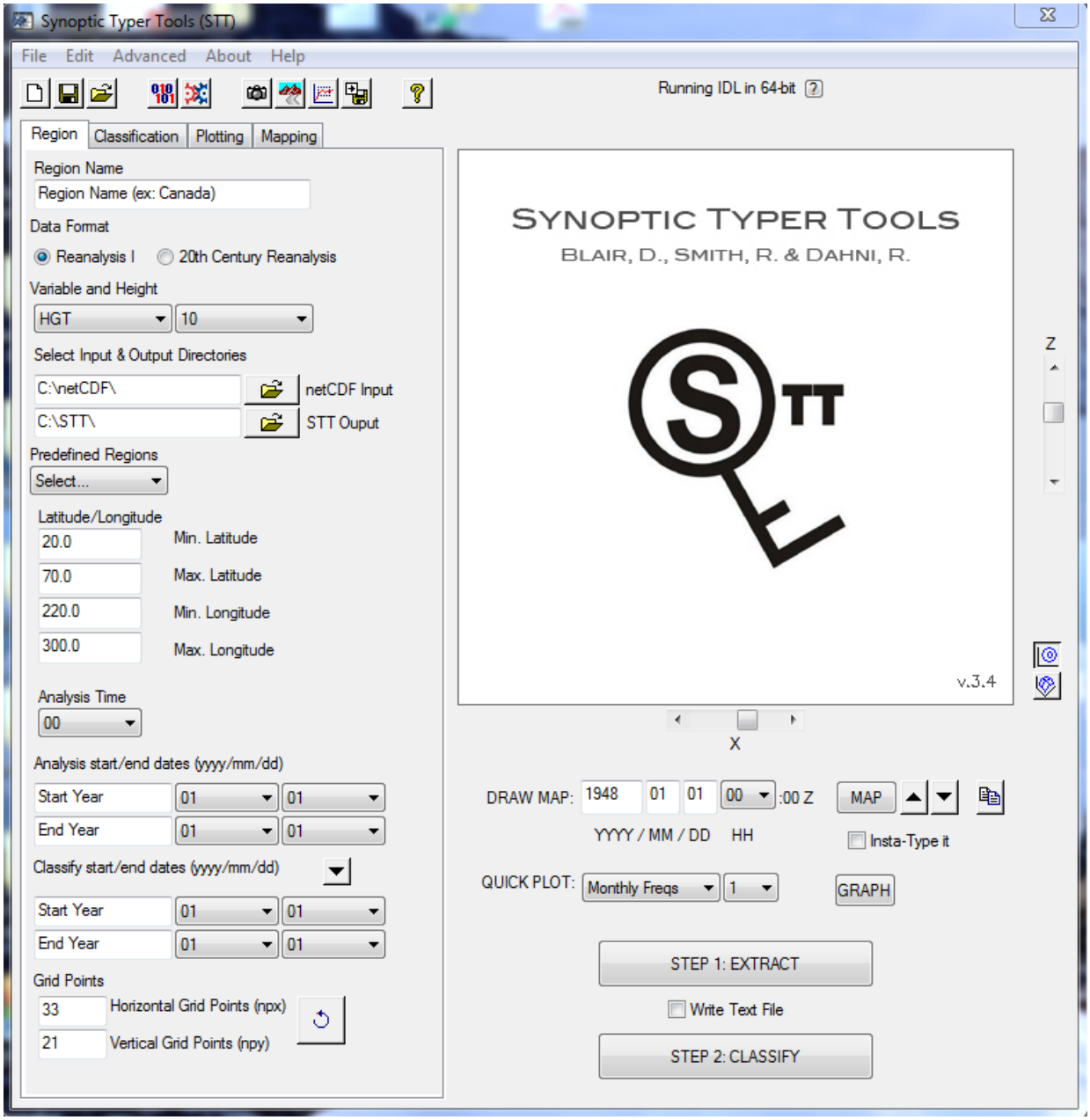

Figure 10: STT v.3.4 Graphic User Interface (GUI) at runtime

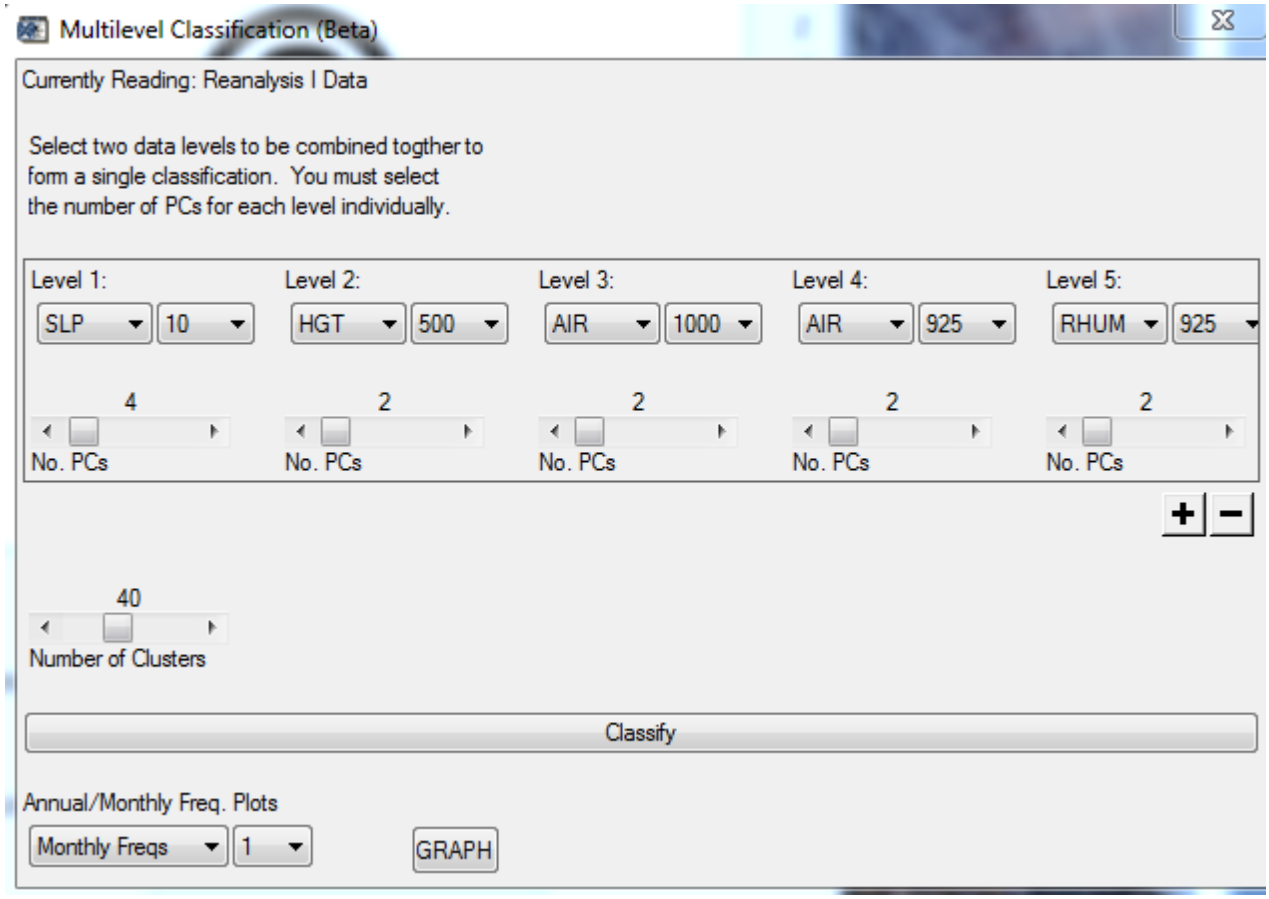

Figure 11: STT v.3.4 multi-level classification GUI demonstrating the classification of five NCEP/NCAR Reanalysis I variables. Note: each variable is first reduced according to its designated principal component value and then subsequently classified together.

4.5 Synoptic Typing Procedure

The five Reanalysis variables selected to assess the synoptic climatology of Hudson Bay (SLP, 500 mb geopotential height, 1000 mb and 925 mb change in air temperature, 1000 mb and 925 mb atmospheric thickness and 925 mb specific humidity) were used to create one, multi-leveled synoptic classification. The type of synoptic classification produced is called 'multi-leveled' because more than one variable from more than one pressure level is considered when determining which synoptic type will be assigned to each day in the analysis period. Furthermore, each synoptic type is actually made up of up to five individual composite maps. A synoptic classification is more typically constructed using just one variable.

The first step in producing the synoptic classification was to read in the very large netCDF data files and to retain only the grid points that fall within the study region boundary. Furthermore, only the 12:00 GMT synoptic grids were retained. The 12:00 GMT (06:00 CST or 07:00 CDT) time was utilized because preliminary analysis showed that freezing rain in Churchill was most common in the early hours of the day.

The next step in producing the synoptic classification involved principal component analysis (PCA). Unrotated, correlation based PCA was used in this case. Unrotated PCA was used because preliminary analysis showed that rotation sometimes resulted in very little data reduction (variance was spread out amongst too many principal components). This was especially true for the specific humidity grids and the 1000-925 mb ΔT grids which, due to higher variability within and between these grids, would have resulted in the retention of more than forty principal components to preserve an adequate

amount of variance in the reduced dataset. In contrast, only two principal components were needed to retain the same amount of variance after unrotated PCA was applied to the specific humidity grids. Each of the five variables were passed through PCA individually, resulting in five reduced datasets.

An important next step was to determine how many principal components ought to be retained following PCA on the five variables. A combination of the scree-plot method and a cut-off value of at least five percent of the total explained variance was used to determine when an adequate number of principal components were reached. The five percent cutoff value means that any principal component that contributes less than five percent of the total explained variance was considered too low and therefore ignored. However, this rule was not followed exclusively, for if there was an obvious break in the line on the scree-plot, separating components that explain a relatively large amount of variance from those which explain relatively little, this point was used to determine the suitable number of components to keep.

In the case of the SLP variable, four principal components were retained (Figure 12). For the 500 mb data, only the first three principal components were kept (Figure 13). Only two principal components were required to retain most of the variance within the 925 mb specific humidity and 1000-925 mb thickness variables (Figure 14 and Figure 15). Finally, five principal components were needed to retain enough variance from the 1000-925 mb ΔT grids (Figure 16Figure 15).

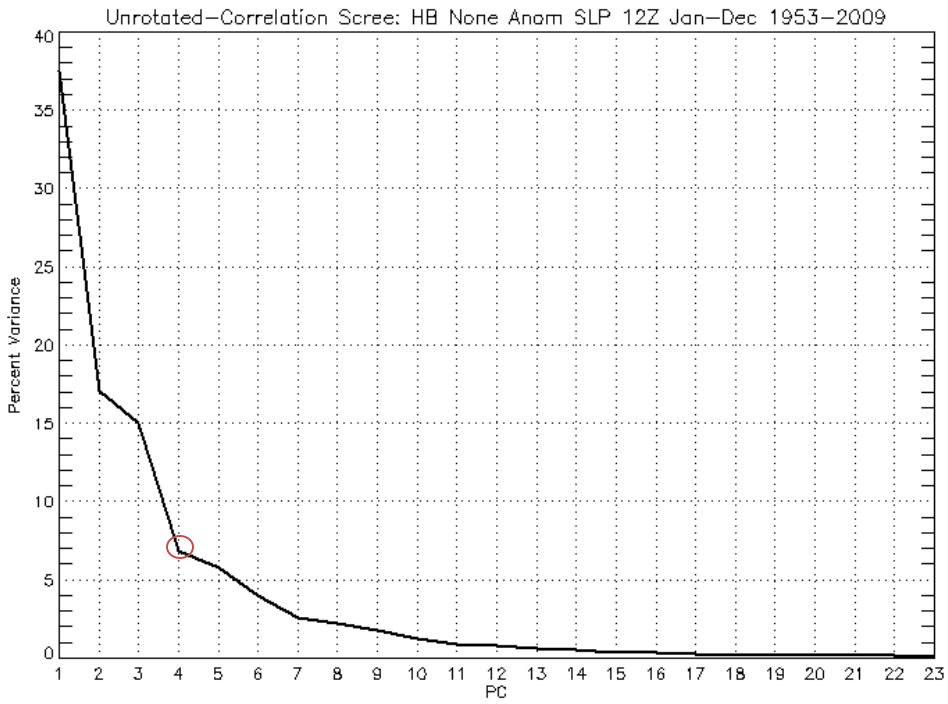

Figure 12: Scree-plot showing the percent variance explained by each principal component in an un-rotated PCA of 12:00 GMT SLP girds (1953-2009)

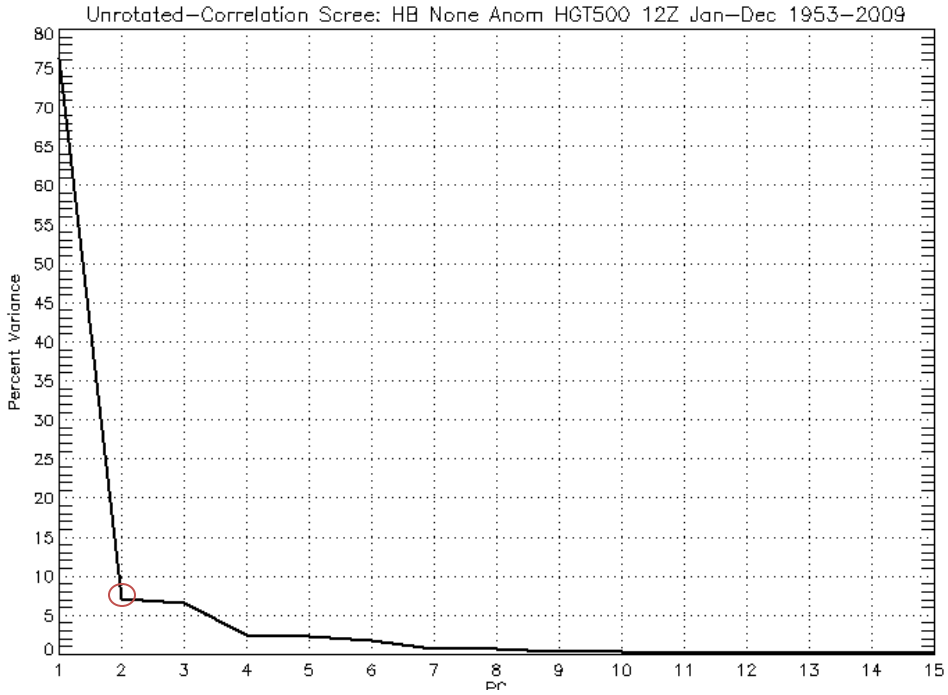

Figure 13: Scree-plot showing the percent variance explained by each principal component in an un-rotated PCA of 12:00 GMT 500 mb geopotential height girds (1953-2009)

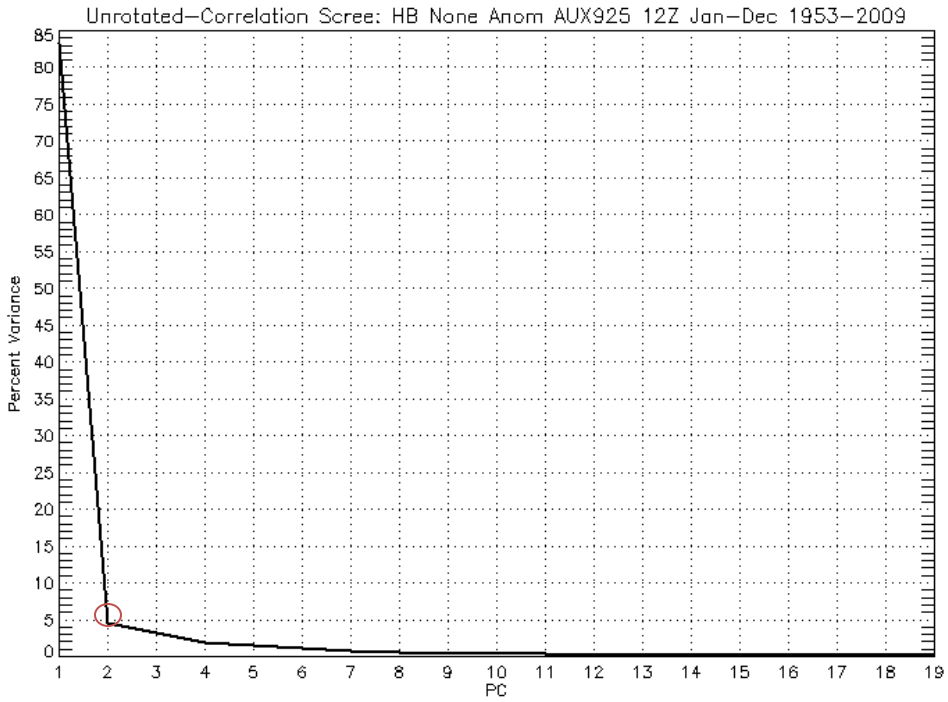

Figure 14: Scree-plot showing the percent variance explained by each principal component in an un-rotated PCA of 12:00 GMT 1000-925 mb thickness girds (1953-2009)

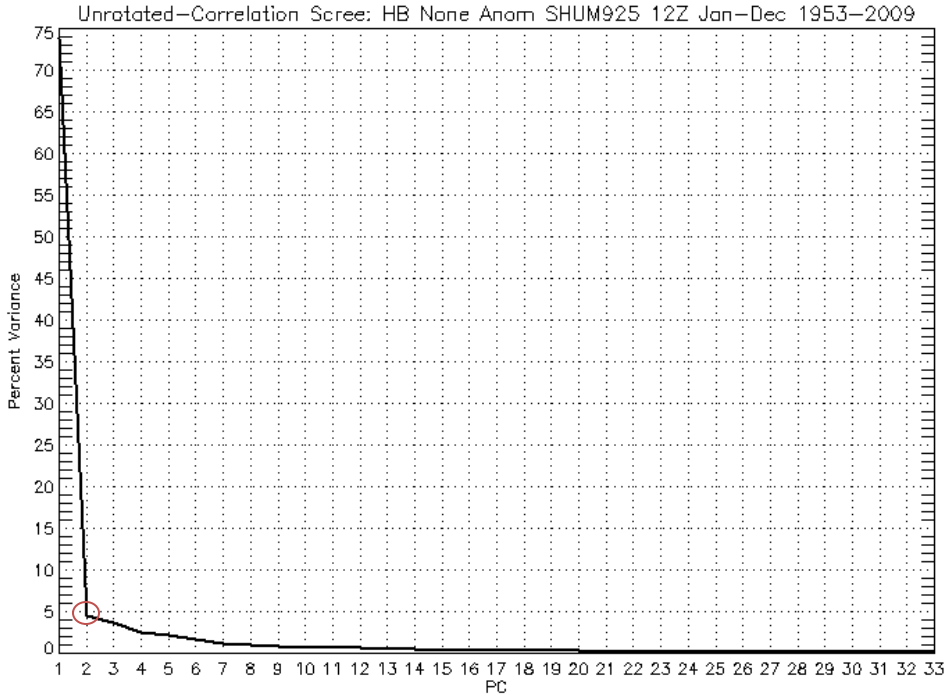

Figure 15: Scree-plot showing the percent variance explained by each principal component in an un-rotated PCA of 12:00 GMT 925 mb specific humidity girds (1953-2009)

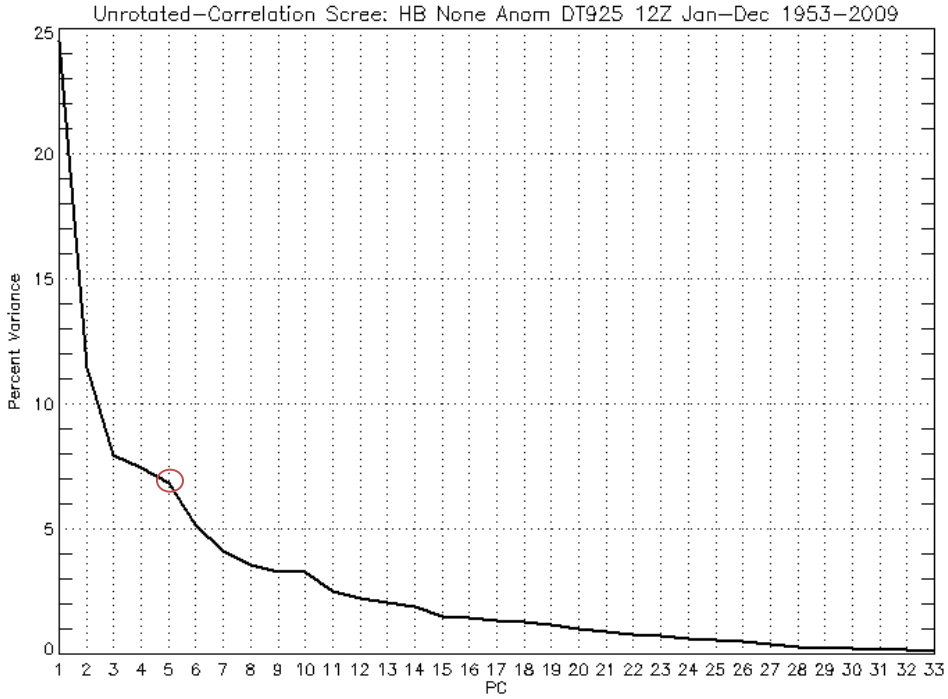

Figure 16: Scree-plot showing the percent variance explained by each principal component in an un-rotated PCA of 12:00 GMT 1000-925 mb change in temperature girds (1953-2009)

Following PCA, K-means cluster analysis was used to sort each grid into one of an arbitrary number of synoptic types. In order to accurately type each grid so that each of the five variables had equal weight in determining the type, each of the five now reduced grids were joined together to form one large matrix per day. This larger set of grids was then fed into the cluster analysis algorithm.

There are no agreed upon methods for determining the correct number of synoptic types to use in a classification. In this case, the overall goal of the classification was to find a relatively small number of types that coincide with freezing rain events in Churchill. In other words, the goal of this analysis is to find a synoptic classification that does a reasonably good job at sorting freezing rain events from non freezing rain events.

A number of classifications were computed using the same five variables but with the number of types ranging from three to seventy. Each classification was then compared individually to the freezing rain catalogue. Two additional calculations were made to objectively judge how well the freezing rain catalogue fit with the synoptic type catalogue: the value of the type with the maximum number of freezing rain events associated with it per classification and the value of the type with the maximum relative percent frequency of freezing rain events associated with it per classification.

The synoptic type with the highest relative percentage of freezing rain events was plotted against the total number of synoptic types in the classification (Figure 17; blue symbols). When few synoptic types were calculated, the relative percent frequency of freezing rain events per synoptic type was very low. As more and more types were calculated, the relative percentage of freezing rain events per type began to increase. Between 30 and 40 types, the relationship between the total number of types and the maximum relative percent frequency of freezing rain events per type became less predictable. Conversely, the maximum number of freezing rain events per type was also plotted against the total number of synoptic types in the classification (Figure 17; red symbols) and when a small number of synoptic types were calculated, the maximum number of freezing rain events per type was relatively high. As expected, increasing the number of synoptic types decreased the number of freezing rain events per type.

The combination of synoptic types that resulted in both a large number of freezing rain events per type and a high relative percent frequency of freezing rain events per type was determined to be the optimal solution. In this case, 34 synoptic types were selected.

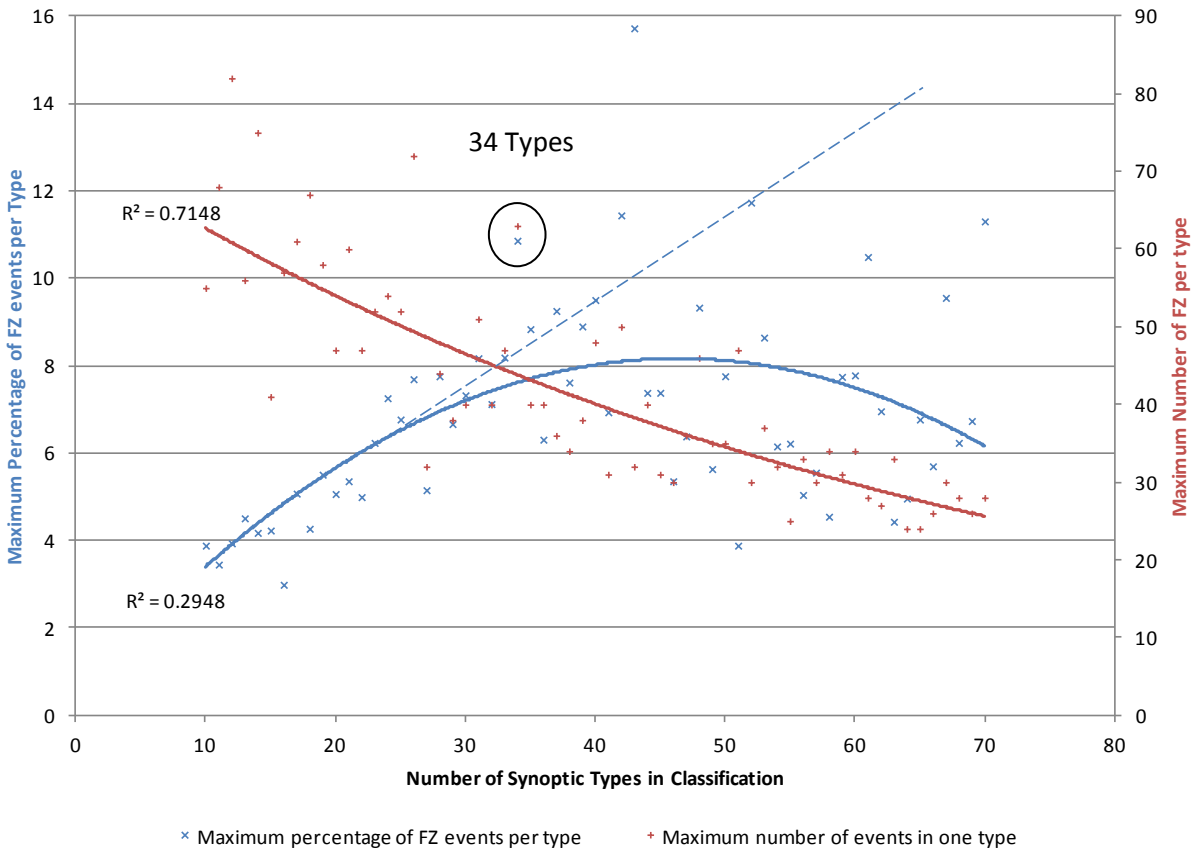

Figure 17: Maximum percentage of freezing rain (FZ) events per number of synoptic types used in classification (blue) and maximum number of freezing rain events per number of synoptic types used in classification (red). The maximum percentage of freezing rain events will eventually reach 100 percent, illustrated by the dashed blue line.

4.6 Synoptic Classification and Surface Temperature Anomalies

A simple procedure was developed to test whether the 34 synoptic types explain temperature anomalies in Churchill. Daily surface temperatures in Churchill from 1953 to 2009 were obtained from Environment Canada. From these data, daily temperature anomalies (departures from the mean daily temperature) were calculated. Finally, the average daily temperature anomaly was calculated for each synoptic type. Types with an average daily temperature anomaly above zero were considered warm types, those with values below zero were considered cold types. Whether a type is expected to be warm or

cool depends on many factors, but arguably one of the most important factors is wind direction. Specifically, a south wind should usually be associated with warmer air and thus higher daily temperature anomalies. Alternatively, a north wind should usually result in cooler air temperatures. Wind direction at various heights can be estimated by the orientation of the height contours (above the surface, winds flow parallel to the height contours due to a balance between the Coriolis Effect and the pressure gradient force). Therefore, if a synoptic type has a pattern that would facilitate a south wind over Churchill and the same type has an above-zero daily temperature anomaly then the type was said to accurately represent the surface climate.

4.7 Synoptic Classification Application

The ultimate goal of producing the multi-level synoptic classification was to determine what synoptic-scale processes are responsible for freezing rain in Churchill. A circulation-to-environment procedure was constructed to relate the synoptic catalogue with the freezing rain catalogue. The synoptic catalogue is simply a list of the synoptic type numbers observed on each day in the classification. Similarly, the freezing rain catalogue is a list of the freezing rain events observed in the Environment Canada data in addition to the date and time of the event. Unlike the synoptic catalogue, there may be more than one event listed per day in the freezing rain catalogue. Finally, the freezing rain catalogue is based on local standard time, which means for nearly half the year the region is in Daylight Savings Time while during the rest of the year it falls in Central Standard Time. The synoptic maps are only based on the 12:00 GMT/UTC synoptic

time-step because, as previously explained, this is the time of day associated with the most freezing rain events.

A simple script was written in Microsoft Visual Basic to count the number of freezing rain events associated with each synoptic circulation type. Some important generalizations were made that will influence the final results. First, freezing rain events were counted during all hours of the day while the synoptic map patterns were based solely on the 12:00 GMT data. Therefore, an event may lag the synoptic map by as much as 18 hours or precede the synoptic map by as much as six hours. Second, the date and time associated with a freezing rain event was based on the event's ending time. As a result, the dates associated with events that spanned over midnight or over multiple days may lag the event's starting date. .

Inevitably, some freezing rain events will be mistyped because of the generalizations in the procedure detailed above. Unfortunately, it is difficult or even impossible to quantify these errors. Therefore, it was necessary to manually inspect a subset of the freezing rain events to verify that events were being associated with the appropriate synoptic types.

Eight freezing rain case studies were produced, one case for the eight synoptic types most frequently associated with freezing rain. In an effort to reduce bias, the most recent example of a freezing rain event coinciding with each of the eight synoptic types was selected. Archived upper-level sounding data recorded in Churchill was accessed for each of the case studies. Additionally, surface observations made in Churchill and Reanalysis data from over the study region were extracted for up to 48 hours prior to each

freezing rain case study. These data were used to assess (a) why freezing rain formed and (b) whether the synoptic type assigned to each freezing rain case study event matched surface and upper-level conditions.

Chapter 5

Results

5.1 Overview

The results are presented in four main sections: analysis of freezing rain events observed in Churchill, Manitoba, the synoptic classification produced for the Hudson Bay region using gridded NCEP/NCAR Reanalysis data, relationships found between the synoptic classification and days with freezing rain and lastly the expected changes in the timing and duration of freezing rain events following an analysis of long-term trends in the synoptic type record.

5.2 Freezing Rain in Churchill, Manitoba

For the years 1953 thru 2009, freezing rain was observed during 796 hours, an average of approximately 15 hours per year. The number of freezing rain hours observed per year varies considerable throughout the study period (Figure 18). The year 1960 experienced the most freezing rain hours (43) and the years 1970 and 1973 both experienced zero freezing rain hours. Although the Environment Canada data was not homogenized, a very small (and insignificant) negative linear trend in the number of freezing rain events per year was calculated (-0.07 hours per year). A total of 286 days with one or more hours of freezing rain were identified, (1.37 percent of all days of 1953-2009). A total of 332 freezing rain events were identified (some days had multiple freezing rain events).

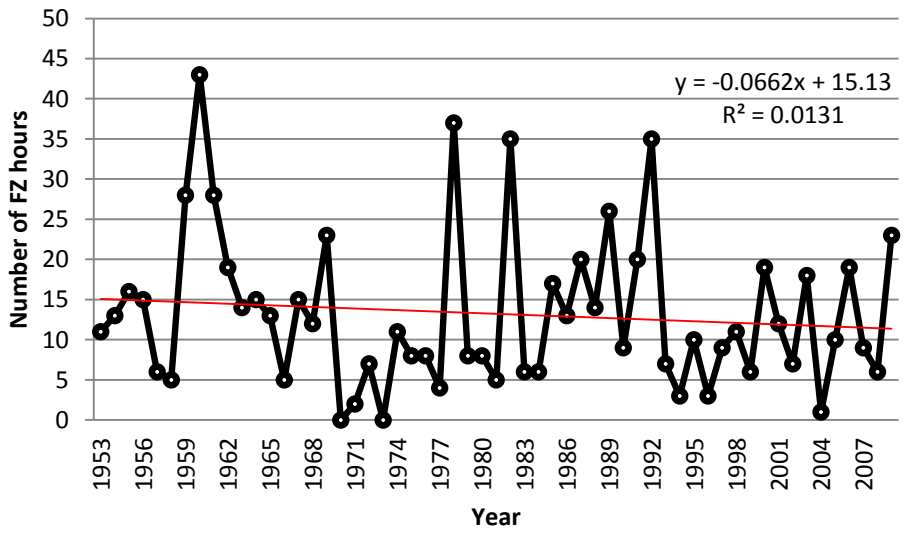

Figure 18: Annual frequency of freezing rain events in Churchill (1953-2009)

The majority of the freezing rain was observed between the morning and the early evening (Figure 19). Again, the reason why the 12:00 GMT synoptic time-scale was used to construct the synoptic classification was because it was the time of day that precedes maximum morning freezing rain events.

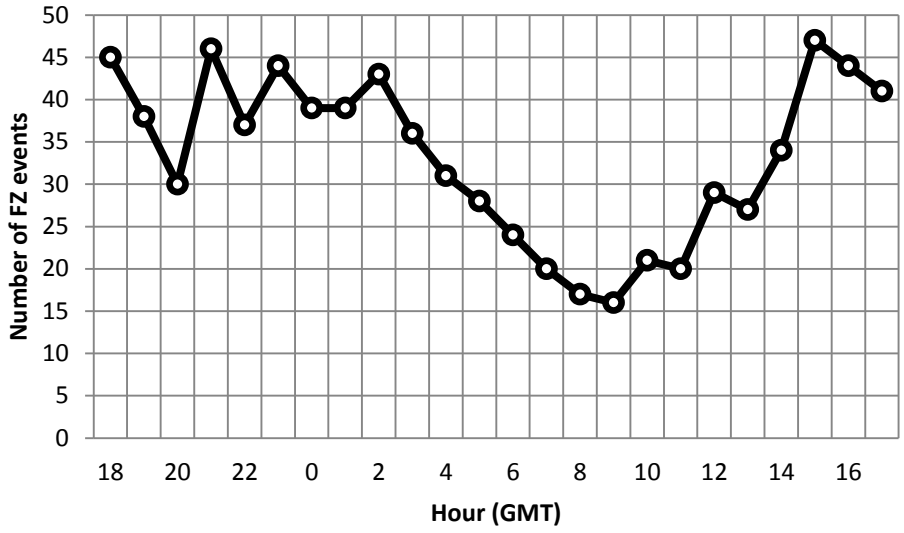

Figure 19: Average hourly frequencies of freezing rain hours in Churchill from 1953-2009

A majority of the 796 freezing rain hours fell in the spring (April-May-June) (Figure 20). A much smaller peak in freezing rain hours occurred in the fall (October-November). Very few freezing rain events occurred in December and January and in July thru September.

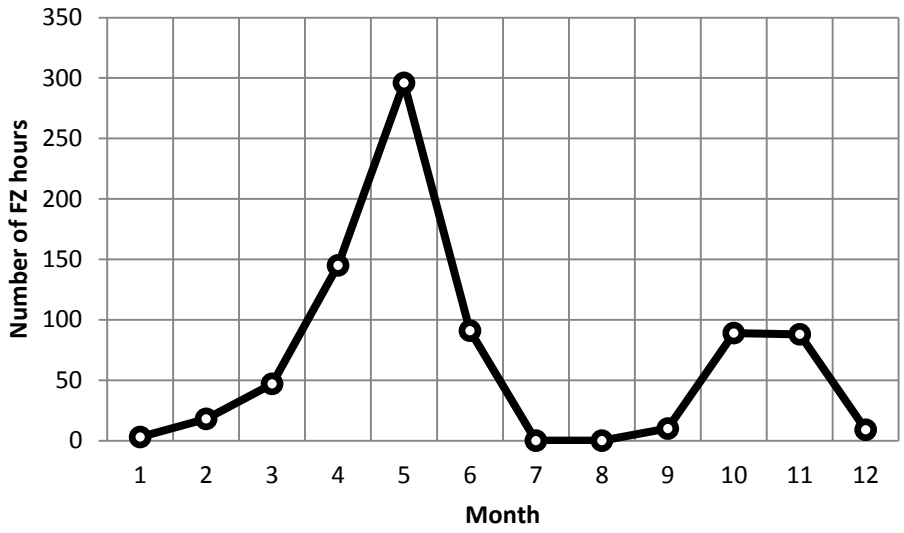

Figure 20: Average monthly frequency of freezing rain hours from 1953-2009

The duration of each freezing rain event was computed by adding up the number of consecutive hours freezing rain was observed (Figure 21). Over ninety percent of all freezing rain events persisted six or fewer hours. Most events were only one hour long, and undoubtedly many of these one hour events were actually less than one full hour in duration. Unfortunately it is impossible to determine the exact duration of each freezing rain event without smaller observation time steps (observations are typically only once an hour). The longest freezing rain event spanned 16 consecutive hours.

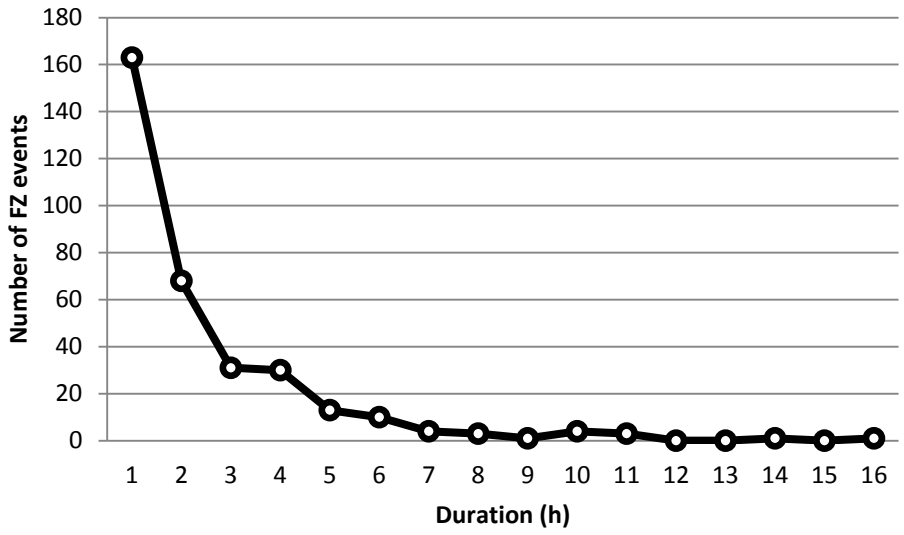

Figure 21: Frequency of freezing rain events by duration in Churchill

The surface temperature in Churchill was identified during each freezing rain hour (Figure 22). Most freezing rain events were associated with surface temperatures at or just below the freezing point. The lowest temperature recorded during a freezing rain event was -12 °C and the warmest temperature recorded during a freezing rain event was 1 °C. Freezing rain reports above 0 °C are obviously suspect given the definition of freezing rain. These potentially erroneous reports may be due to human error (the precipitation was misidentified as freezing rain), instrument error (faulty temperature readings) or be an artifact of the hourly weather data (freezing rain was observed during the first part of the hour, when temperatures were still below zero, but then temperatures quickly rose above zero during the rest of the hour and precipitation fell as rain).

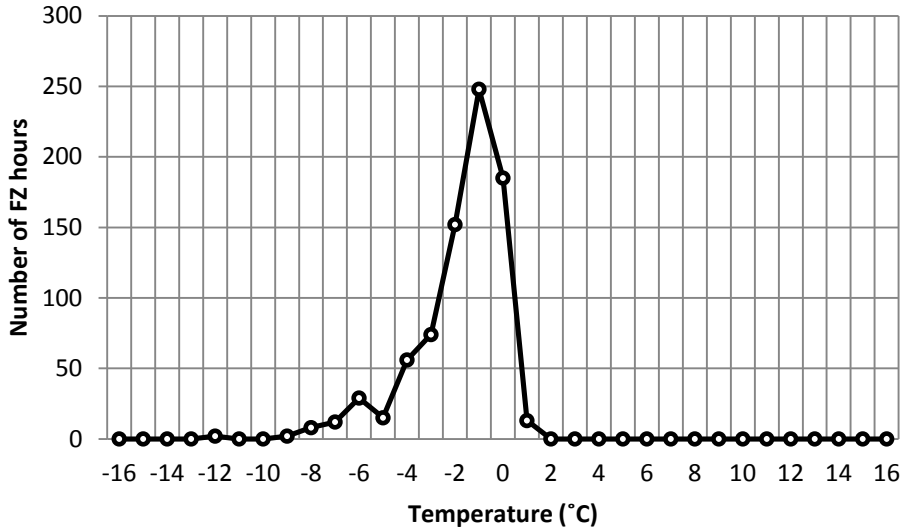

Figure 22: Frequency of freezing rain events by temperature in Churchill

The visibility associated with each freezing rain hour was also analyzed (Figure 23). Many freezing rain hours were not associated with hazardously low visibility (aircraft may still land in ½ mi or 400 m visibility). In fact, many hours had full (24.1 km) visibility associated with them. In some cases, when heavy fog was also present during the freezing rain hour, visibility was much lower.

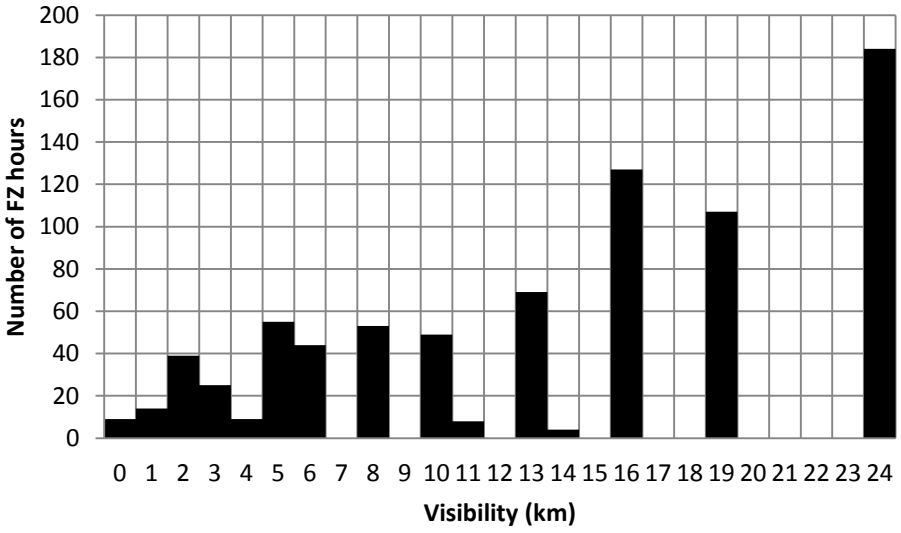

Figure 23: Frequency of freezing rain hours by visibility in Churchill

The 12:00 GMT wind directions recorded at the surface in Churchill during days with freezing rain were also identified. The 12:00 GMT time was used so that the identified wind directions matched the extracted daily synoptic patterns. The surface wind directions were found to vary considerably during freezing rain days; however, the top three modal wind directions were from the northeast, east and south (Figure 24). Winds were seldom out of the west and north during freezing events. In comparison, the wind direction recorded during non-freezing rain events (including all other types of weather) show that a northwest wind is the most frequently observed wind direction in Churchill (Figure 25). Winds from the northeast, east and south are relatively rare in comparison.

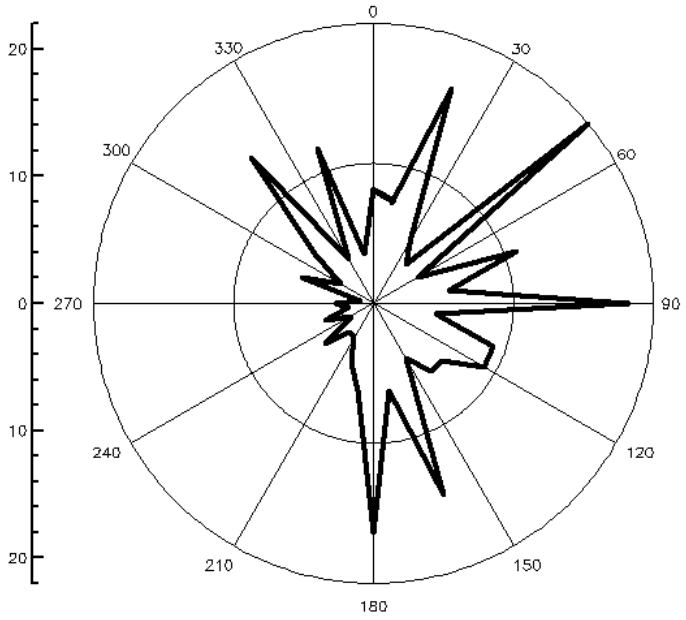

Figure 24: Wind rose diagram displaying the 12:00 GMT wind direction observed in Churchill during all freezing rain days

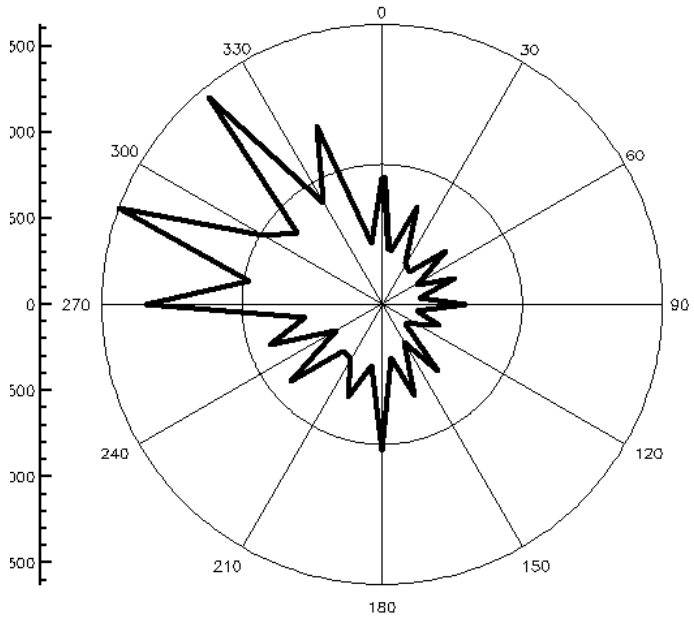

Figure 25: Wind rose diagram displaying the 12:00 GMT wind direction observed in Churchill during all non-freezing rain days

It is important to examine the influence Hudson Bay may have in shaping the climatology of freezing rain in Churchill. One aspect of the freezing rain climatology that stood out as having a potential link with Hudson Bay was its seasonality. Specifically, much more freezing rain was observed during spring, when Hudson Bay is completely covered by sea ice, compared to fall, when much of the bay remains open water. When air temperatures begin to drop during fall, the open water remains relatively warm compared to the air. This might affect surface temperatures in Churchill and, therefore, the potential for freezing rain, by keeping temperatures above the freezing point. Hanesiak and Stewart (1995) tried to quantify sea ice influence on ice pellets in Eastern Canada and found that the presence of sea ice can lead to cooler temperatures at the surface.

For comparison, the number of freezing rain days per month was calculated for seven additional Canadian communities: Thompson, MB, Arviat, NU, Coral Harbour, NU, Iqaluit, NU, Kuujjuarapik, QC, Cartwright, NF and Ottawa, ON (Figure 26). Thompson is a community located to the southwest of Hudson Bay and much further inland compared to Churchill. Arviat is further north than Churchill and also on the west coast of Hudson Bay. Coral Harbour and Iqaluit are both Arctic coastal communities. Coral Harbour is situated along the northern extent of Hudson Bay and Iqaluit between the Hudson Strait and Davies Strait. Kuujjuarapik is community along the east coast of Hudson Bay. Cartwright is a community along the coast of the Labrador Sea. Finally, Ottawa is a city far south of Hudson Bay but its climate is somewhat influenced by the Great Lakes.

For Ottawa, it was found that most freezing rain was reported during the winter and early spring months (November to April). This coincides with the times of year surface temperatures frequently straddle the freezing point. In Cartwright, the freezing rain season is slightly longer than in Ottawa, with the majority of freezing rain cases observed between November and May. In Kuujjuarapik, the community on the east side of Hudson Bay, most of the freezing rain cases were observed during spring and fall, with a maximum number of cases observed during November. Coral Harbour and Iqaluit had similar monthly frequencies. For both of these communities freezing rain was found to be slightly more common in the spring (month of May) compared to the fall. Churchill and Arviat have very similar monthly freezing rain distributions. In both of these communities, freezing rain occurred much more frequently during the spring compared to the fall. Finally, in Thompson, freezing rain occurred mainly during spring and fall, and was found to occur slightly more frequently in the fall (peaked during the month of November).

These results seem to indicate that Hudson Bay may play an important role in determining the timing of freezing rain in Churchill (and Arviat). Specifically, along its west coast, the Bay may be reducing the number of freezing rain events that occur during the fall by increasing the surface temperature, and increasing the number of freezing rain events that occur during spring by decreasing the surface temperature.

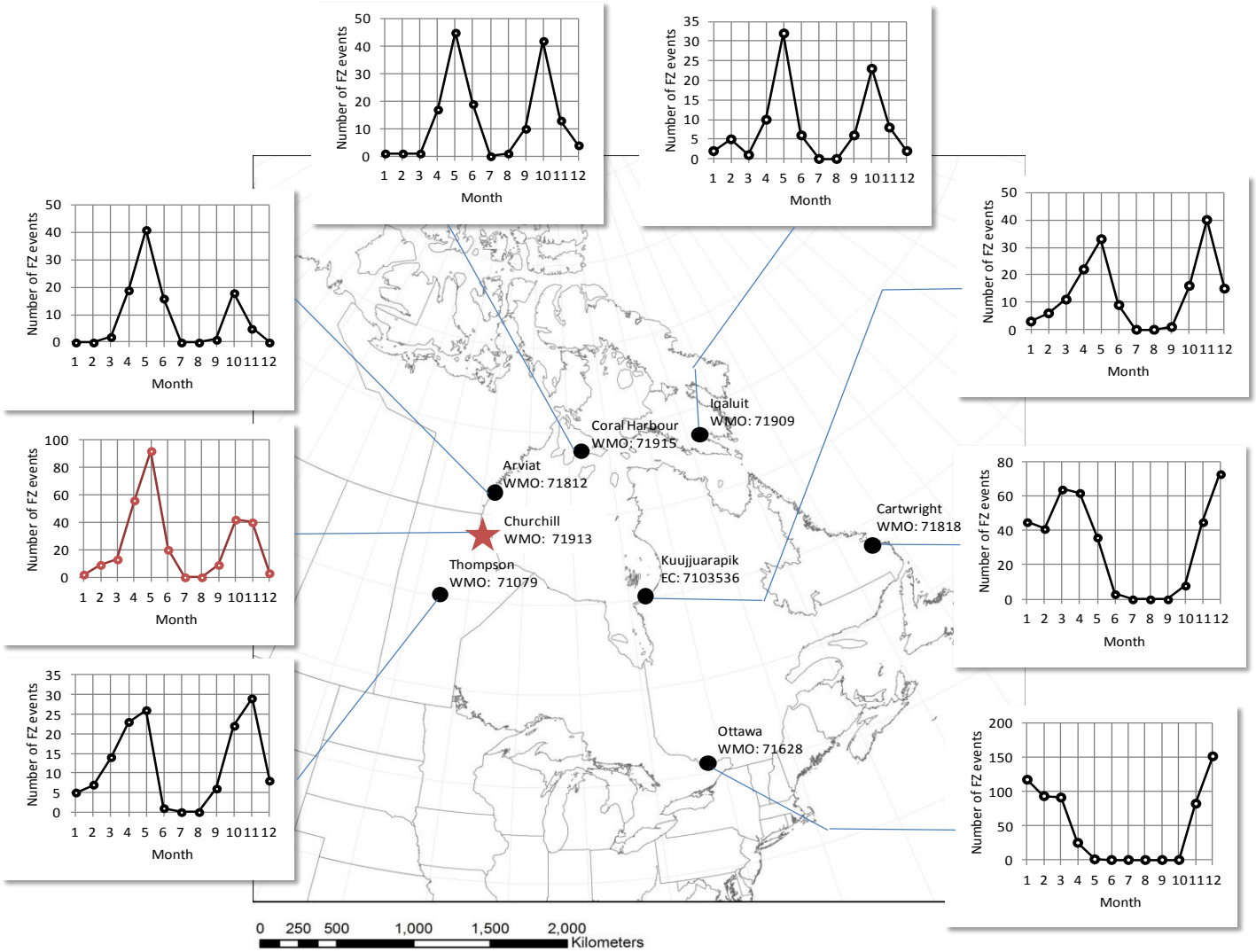

Figure 26: Monthly frequencies of freezing rain days observed in various Canadian communities (source: Environment Canada, 2011)

5.3 Synoptic Data Analysis

The five synoptic scale variables used to describe the synoptic climatology of the Hudson Bay region were: SLP, 1000-925 mb change in temperature (ΔT), 1000-925 mb atmospheric thickness, 925 mb specific humidity and 500 mb geopotential height. The climatology of each of these five variables is described using monthly average maps. For SLP, it was found that higher SLP values tend to be found along the west coast of Hudson Bay and lower SLP values tend to be found in the northeast quadrant of the study region during winter (December-February). During spring (April-June), lower SLP values begin to show up in the southwest quadrant of the study region and higher SLP values tend to exist north of Churchill. By July, the average SLP values over Hudson Bay begin to lower, and this gradual lowering of the SLP values continues until November and remains throughout the winter (Figure 27). This result mirrors previously studied general circulation patterns in the Arctic, specifically the persistence of surface and upper-air low pressure systems over Baffin Island and Northern Hudson Bay throughout the winter months. This low pressure systems form because the sea water remains relatively warm compared to the air and therefore vertical mixing is enhanced (Stewart and Lockhart, 2005).

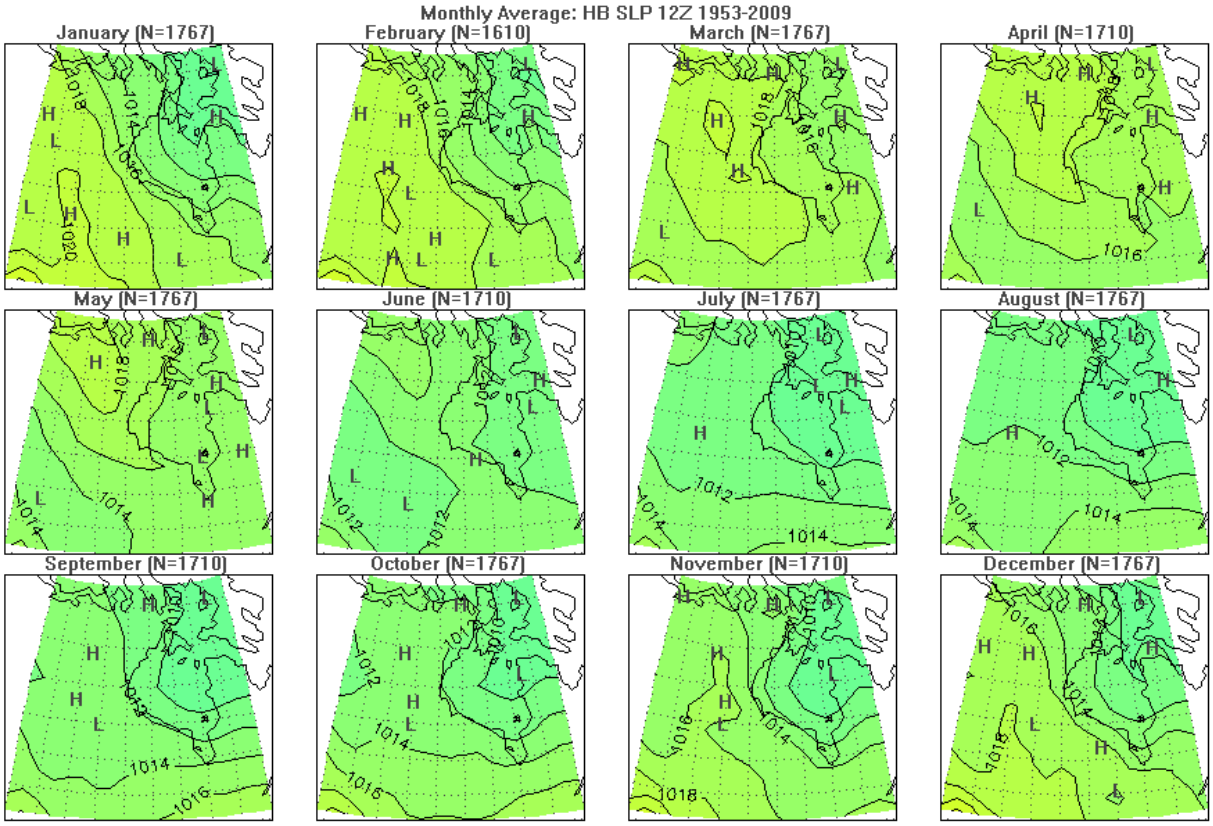

Figure 27: Monthly average SLP maps (1953-2009)

The monthly average 1000-925 mb ΔT maps show the influence Hudson Bay has on the vertical temperature profile. During the months of heavy sea ice cover (December-April), 925 mb temperatures tend to be warmer than 1000 mb temperatures (orange shading denotes warmer temperatures at 925 mb compared to 1000 mb). By September, when air temperatuers begin to fall and Hudson Bay remains completely ice free, temperature lapse rates over Hudson Bay are more frequently negative (blue colors denote cooler temperatures at 925 mb compared to 1000 mb) (Figure 28).

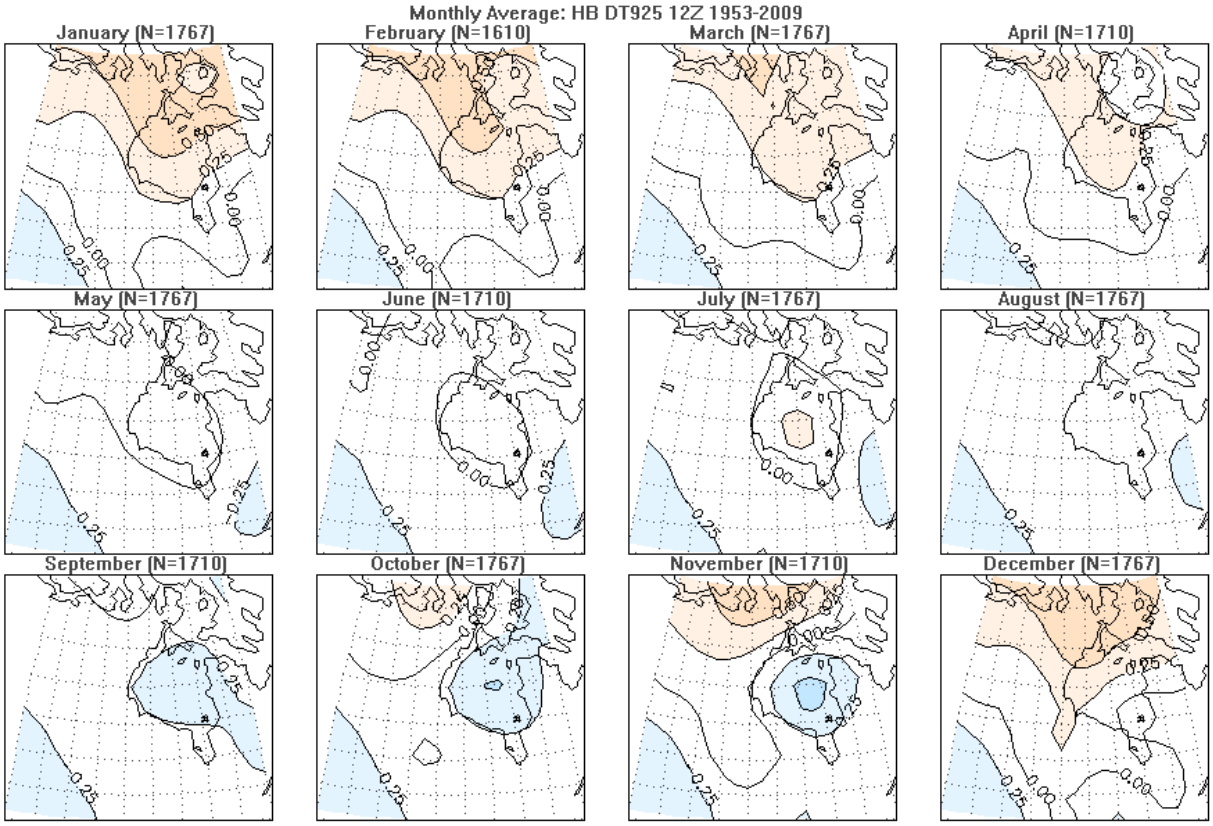

Figure 28: Monthly average 1000-925 mb change in temperature maps (1953-2009). Blue indicates 1000 mb level warmer than 925 mb level; orange indicates 925 mb level warmer than 1000 mb level. Units are in K.

The 1000-925 mb monthly average thickness maps (Figure 29) show that during late winter (January to March), the thickness lines over Hudson Bay are relatively zonal (consistent values across the bay from west to east), indicating that temperatures across Hudson Bay are on average very similar. However, by May (when sea ice is beginning to melt) the isopachs are noticeably depressed towards the south over Hudson Bay, indicating that temperatures within this layer over the bay lag behind temperatures further inland of the Bay. In September, this process reverses, and a ridge in the thickness contours over Hudson Bay is now visible. This ridge indicates that temperatures in the lower part of the atmosphere over Hudson Bay are warmer compared to locations further inland of the bay. The ridge in thickness lines over Hudson Bay is most visible in

November. During the month of November, low SLP over Hudson Bay facilitates northwesterly winds across the west coast of the bay which depresses air temperatures. Meanwhile, temperatures over the bay remain relatively warm as the bay transports stored latent and sensible heat to the overlying air.

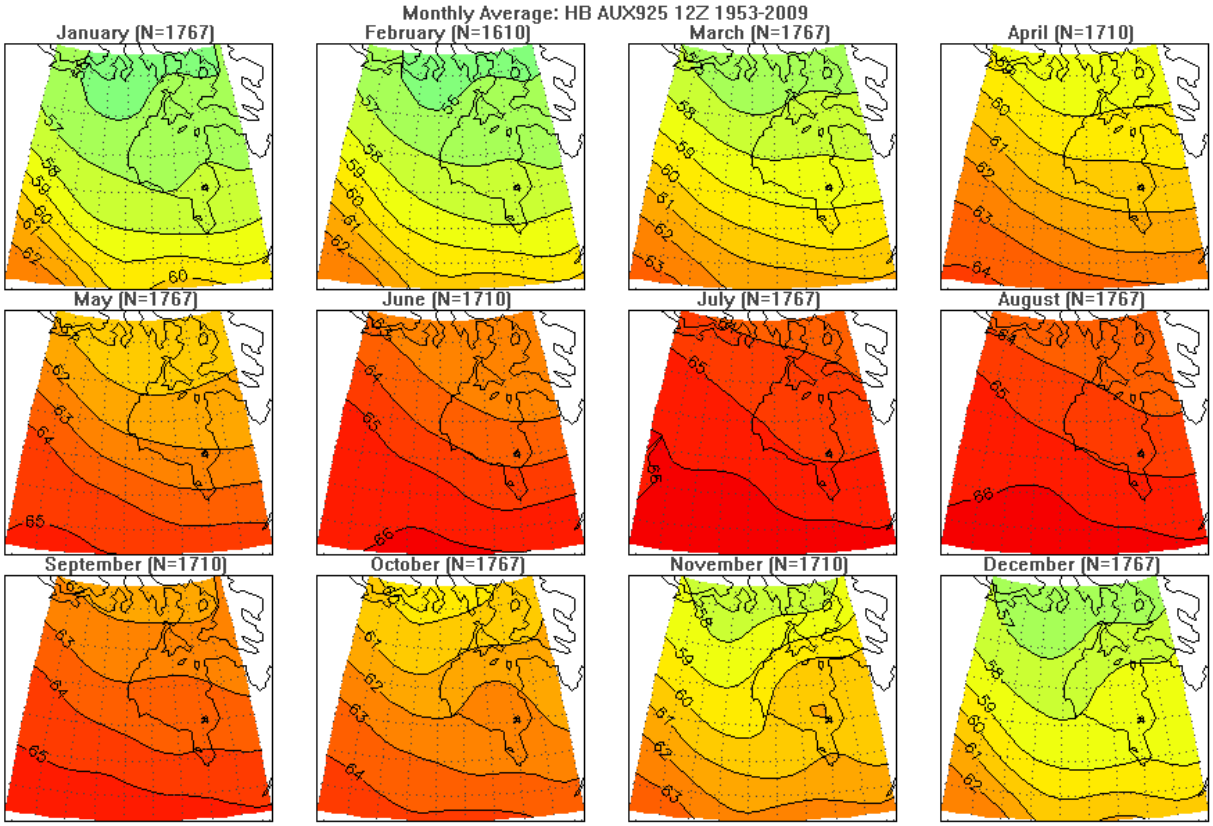

Figure 29: Average monthly 1000-925 mb atmospheric thickness maps (1953-2009)

The monthly average 925 mb specific humidity maps also clearly show the influence that Hudson Bay has on its surroundings (Figure 30). From November to March temperatures are cold enough on average to prevent the atmosphere from holding more than 1.0 g/kg of water vapour. Therefore, these maps exhibit mostly white (white indicates a specific humidity value between 0 and 1 g/kg). As the atmosphere warms through the spring and summer (April to August), the amount of water vapour also

increases. However, average monthly specific humidity values are consistently lower over the relatively cold surface of Hudson Bay, where presumably the melting ice buffers any potential temperature gains from increased radiative heating. The air above Hudson Bay remains relatively dry compared to the air over its east and west coasts.

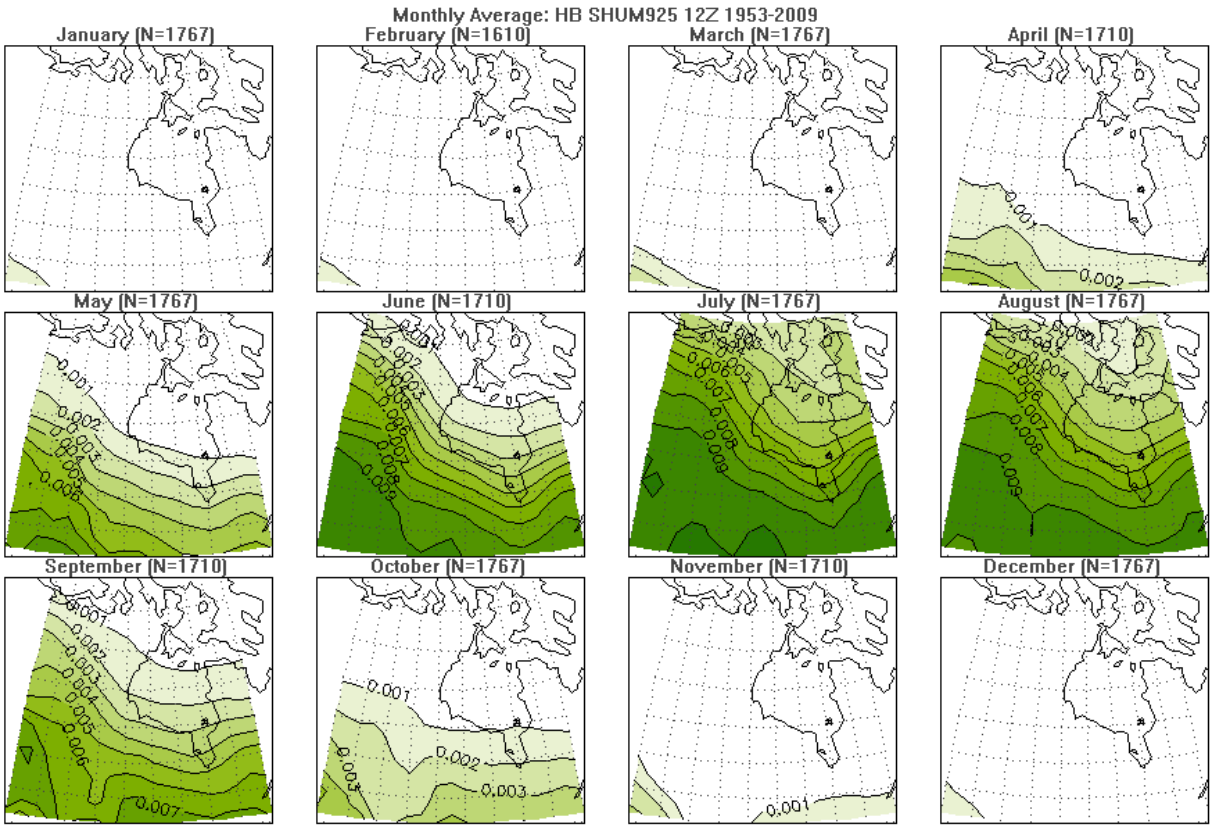

Figure 30: Monthly average 925 mb specific humidity maps (units are in kg/kg) (1953-2009)

The monthly plots of average 500 mb geopotential height (Figure 31) indicate that during the winter, the average 500 mb height in the northern part of the study region is approximately 506 dam, whereas the average height in the southern portion of the region is 580 dam during summer. For most of the year, the average 500 mb isohypse maps show a large trough (the so-called North American trough) across the entire study region.

However, during some of the warmer months some ridging at this height can be seen in the southern portion of the study region. A troughing pattern at 500 mb suggests that cyclones would generally move into the study region from the northwest. These cyclones would be relatively dry and therefore less likely to produce precipitation. The more zonal or ridging patterns seen between April and October allow for warmer and moister air to migrate into the study region. Therefore, this type of pattern would have a higher likelihood of producing precipitation (including freezing rain).

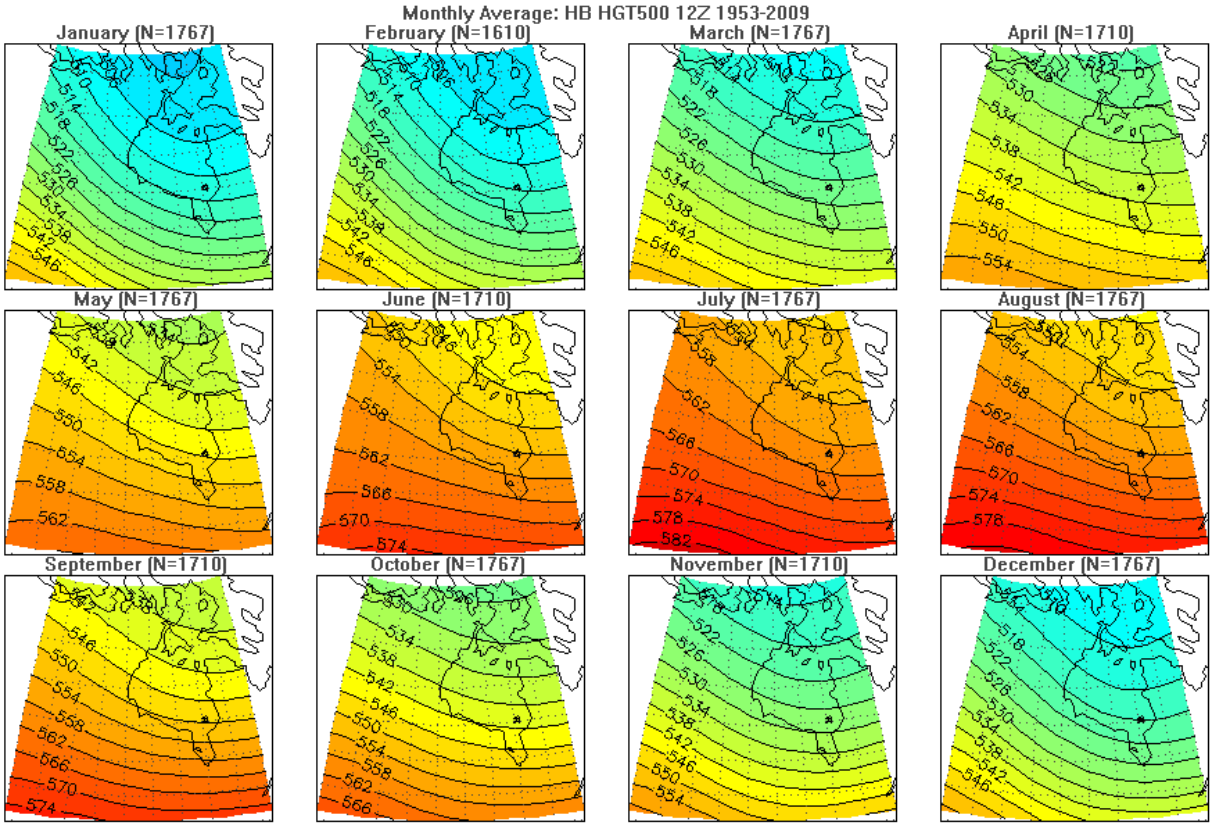

Figure 31: Average monthly 500 mb geopotential height maps (1953-2009)

5.4 Synoptic Classification

The multi-level classification of SLP, 1000-925 mb ΔT, 1000-925 mb thickness, 925 mb specific humidity and 500 mb geopotential height consists of 34 types (Figure 32). Each of the 34 synoptic types are illustrated below as composite maps (averages of all the days classified as that type). The monthly and annual percent frequencies of the synoptic types are presented and a wind rose diagram is constructed for all 34 types from the 12:00 GMT surface winds recorded in Churchill.

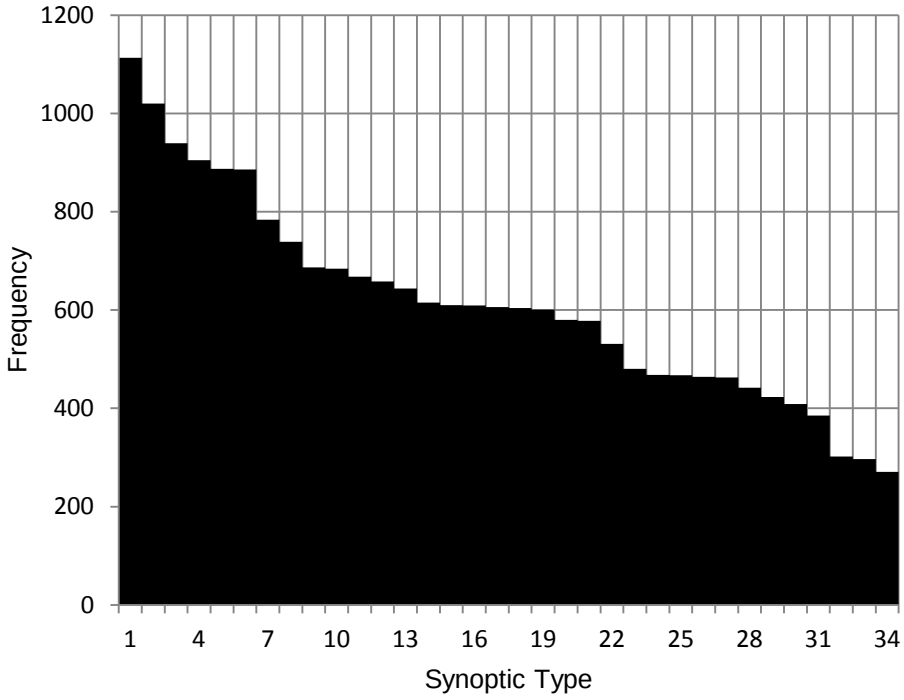

Figure 32: Frequency of the 34 synoptic types (1953-2009)

Synoptic Type 1 (hereafter Type-1) is predominantly a summer synoptic pattern (June to August) (Figure 33). This type is characterized as having lower SLP southwest of Hudson Bay and very warm and moist air over much of the study region. Most of the

temperature lapse rates between 1000 and 925 mb are negative, with positive lapse rates centred over Hudson Bay. A total of 1113 days were classified as Type-1, or an average of 20 days per year.

Type-2 is another mid-summer pattern (Figure 34). Large thickness values and high specific humidity values over the study region indicate that this type is associated with warm and humid conditions. The main differences between Type-2 and Type-1 are in the location of the low SLP relative to Hudson Bay and in the shape of 500 mb contours. Specifically, the western half of the study region tends to experience low SLP while the eastern half, including Hudson Bay, experiences relatively high SLP during a Type-2 event. Surface winds during at Type-2 event are predominantly from the south. At the 500 mb surface there is a very meridianal pattern with strong ridging over most of the region. A total of 1020 days were classified as a Type-2, or an average of 18 days per year.

Type-3 is very strongly a winter and early spring pattern (December to April) (Figure 35). This type is characterized as having lower SLP values to the west of Hudson Bay and high SLP over much of Hudson Bay and to the south. Aside from the southeast quadrant of the study region, 925 mb temperatures are considerably warmer than 1000 mb temperatures. Clearly, thie type is associated with cold, dry Arctic highs producing surface inversion over the bay. This air is also very dry, with most of the region having less than 0.001 kg/kg of water vapour at 925 mb. As was the case for Type-2, which has a similar SLP composite map, winds observed in Churchill during Type-3 days were typically out of the south. A total of 939 days were classified as Type-3, or an average of 16 days per year.

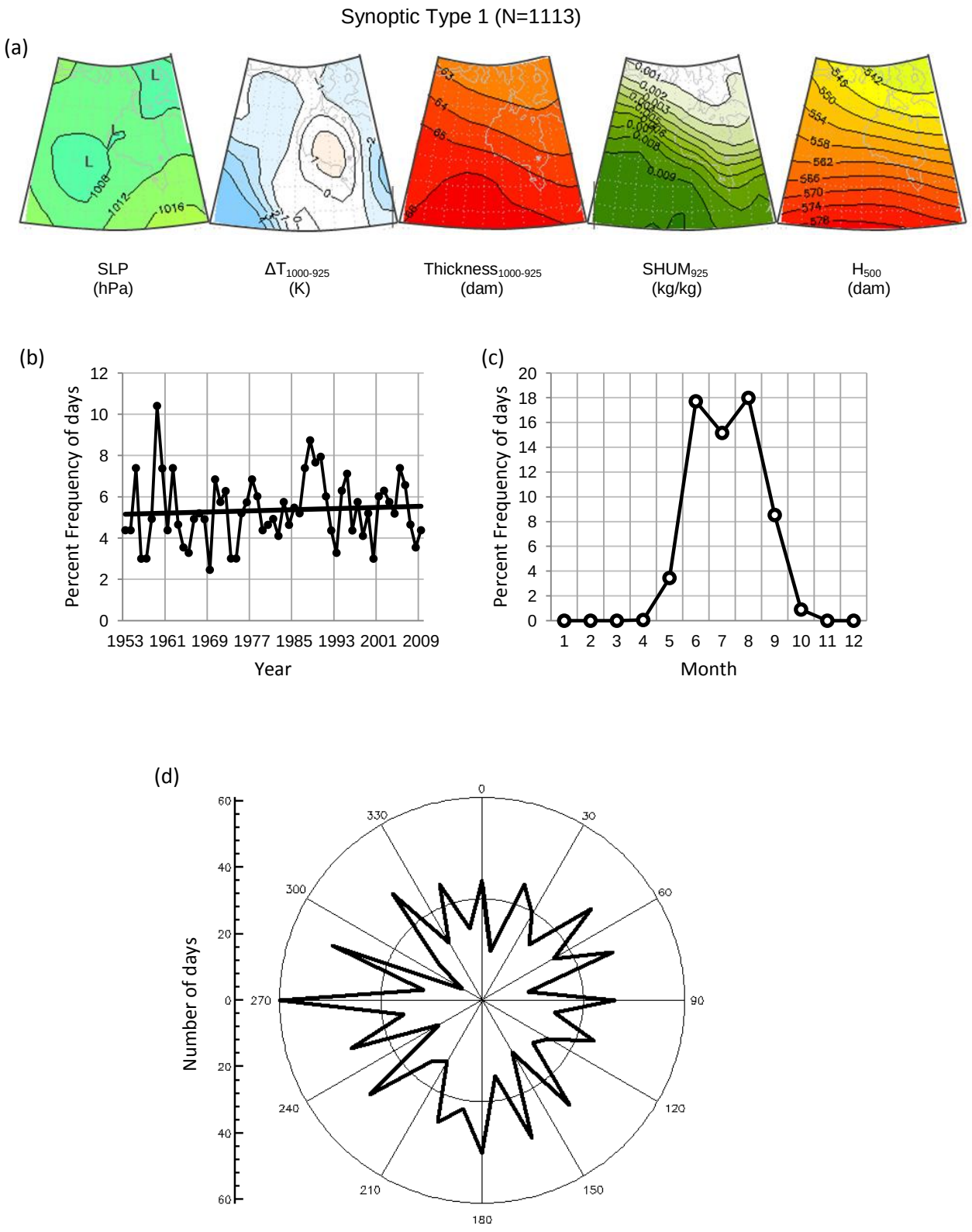

Figure 33: Synoptic Type 1 (a) composite maps, (b) annual percent type frequencies, (c) monthly percent type frequencies and (d) wind rose diagram displaying surface winds observed in Churchill at 12:00 GMT during this synoptic type

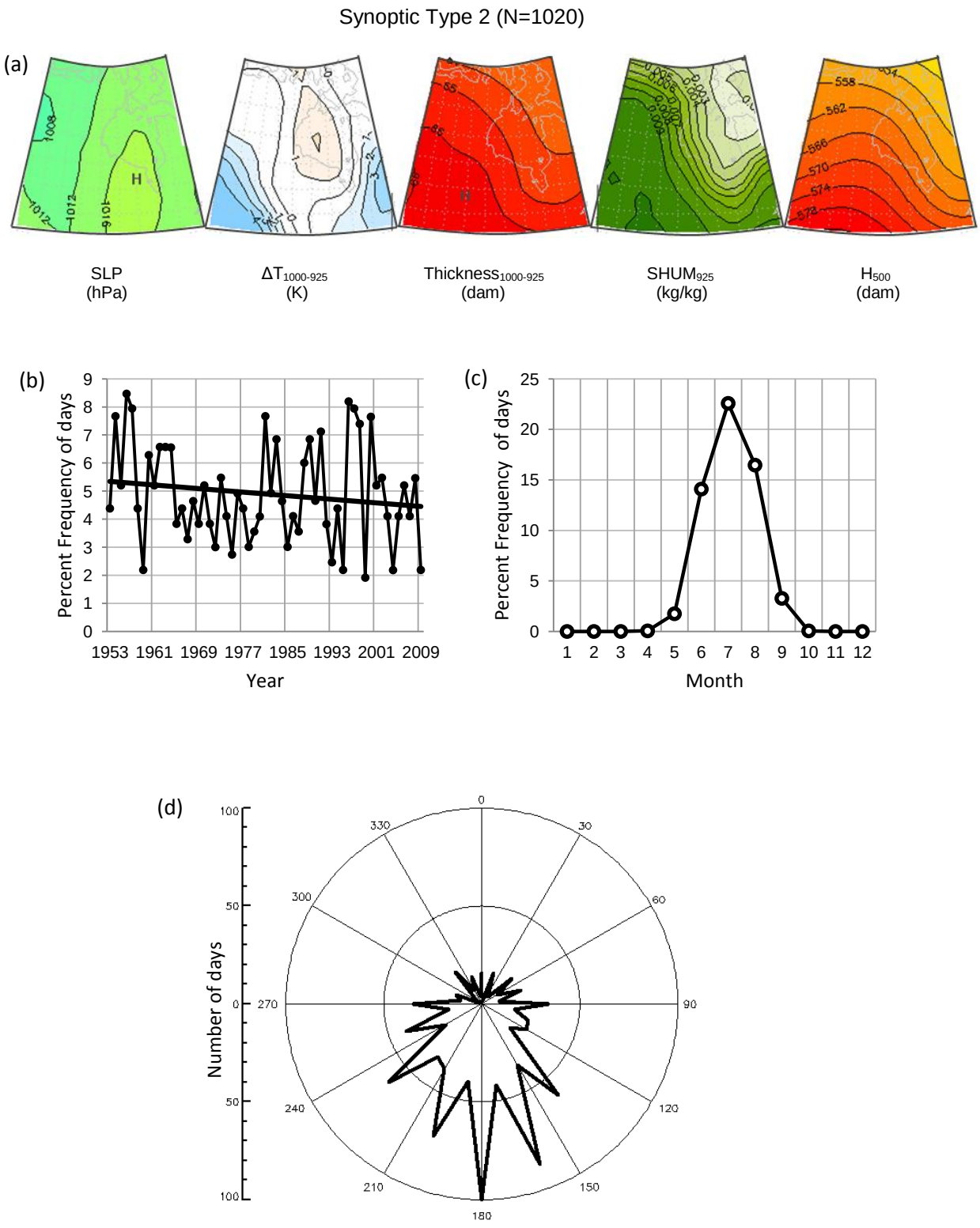

Figure 34: Synoptic Type 2 (a) composite maps, (b) annual percent type frequencies, (c) monthly percent type frequencies and (d) wind rose diagram displaying surface winds observed in Churchill at 12:00 GMT during this synoptic type

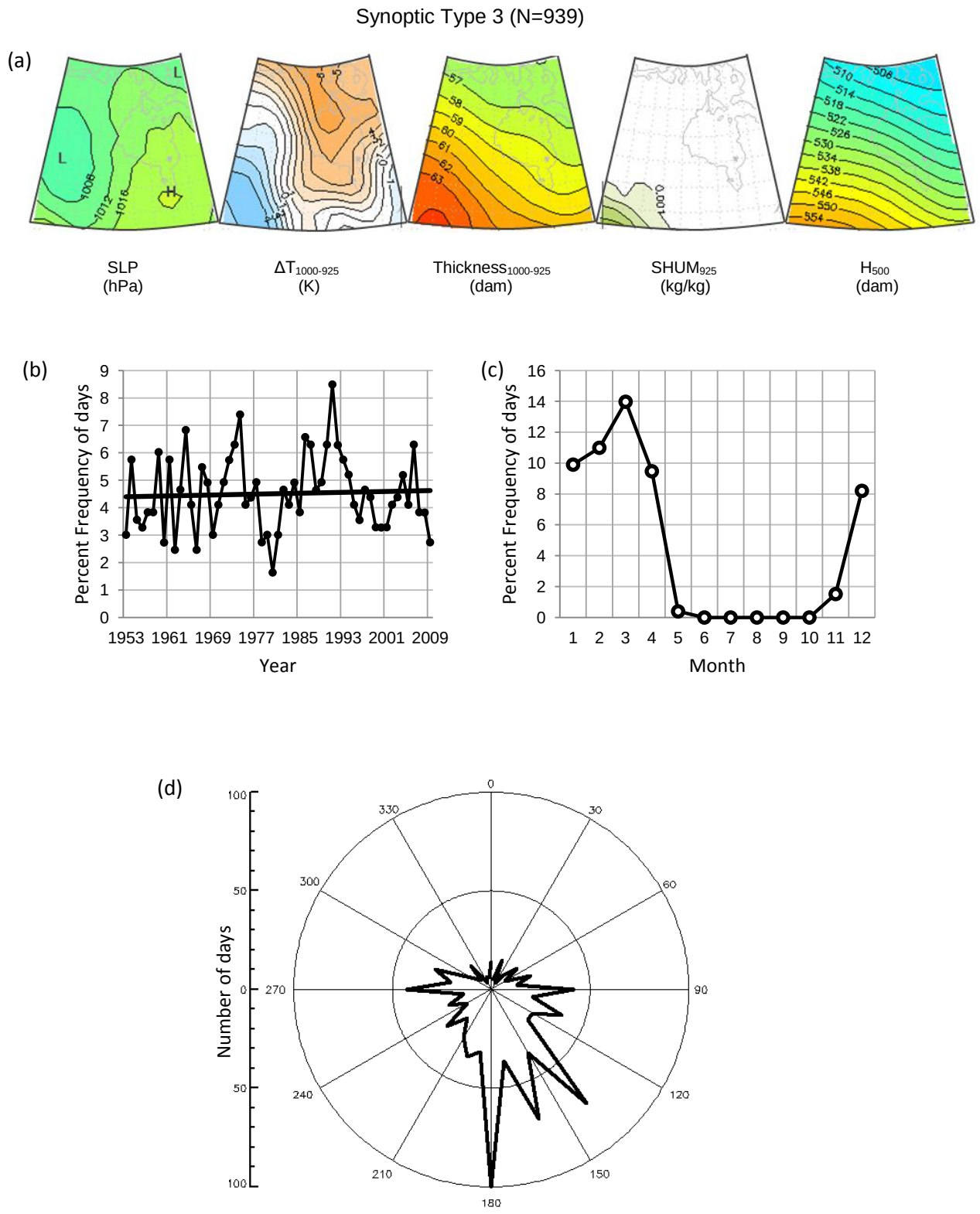

Figure 35: Synoptic Type 3 (a) composite maps, (b) annual percent type frequencies, (c) monthly percent type frequencies and (d) wind rose diagram displaying surface winds observed in Churchill at 12:00 GMT during this synoptic type

Type-4 is very much a summer synoptic type (Figure 36). The Type-4 composite maps are very similar to the Type-1 composite maps. The major differences between these types are that Type-4 events have more positive temperature lapse rates over Hudson Bay and specific humidity values to the north of Hudson Bay are higher. As was the case for Type-1, there is no clear preferred surface wind direction in Churchill during Type-4 events. A total of 905 days were classified as Type-4, or an average of 16 days per year.

Type-5 is a summer type with several of its patterns opposite to those for of a Type-1 and Type-4 (Figure 37). It has high SLP west of the bay, thus, surface winds are more frequently from the northwest quadrant. This more northerly flow brings cooler temperatures into the region. 1000-925 mb thickness values are depressed over Hudson Bay, indicating that the temperature over the bay is much lower than its surrounding lowlands. The normally positive temperature lapse rates between 1000 and 925 mb over Hudson Bay are replaced during a Type-5 event by negative values. A total of 887 days were classified as Type-5, or an average of 15.5 days per year.

Type-6 is another mid-winter to early-spring pattern that peaks in March (Figure 38). This type is characterized by dry air at 925 mb and steep temperature inversions between 1000 and 925 mb. The main differences between Type-6 and Type-3 are the large centre of low SLP values found to the west of Hudson Bay during a Type-3 event are replaced by higher SLP values and a much smaller centre of low pressure exists to the southwest of the bay during a Type-6 event. This results in westerly winds observed in Churchill during a Type-6 event compared to a south wind during a Type-3 event. A total of 886 days were classified as Type-6, or an average of 15.5 days per year.

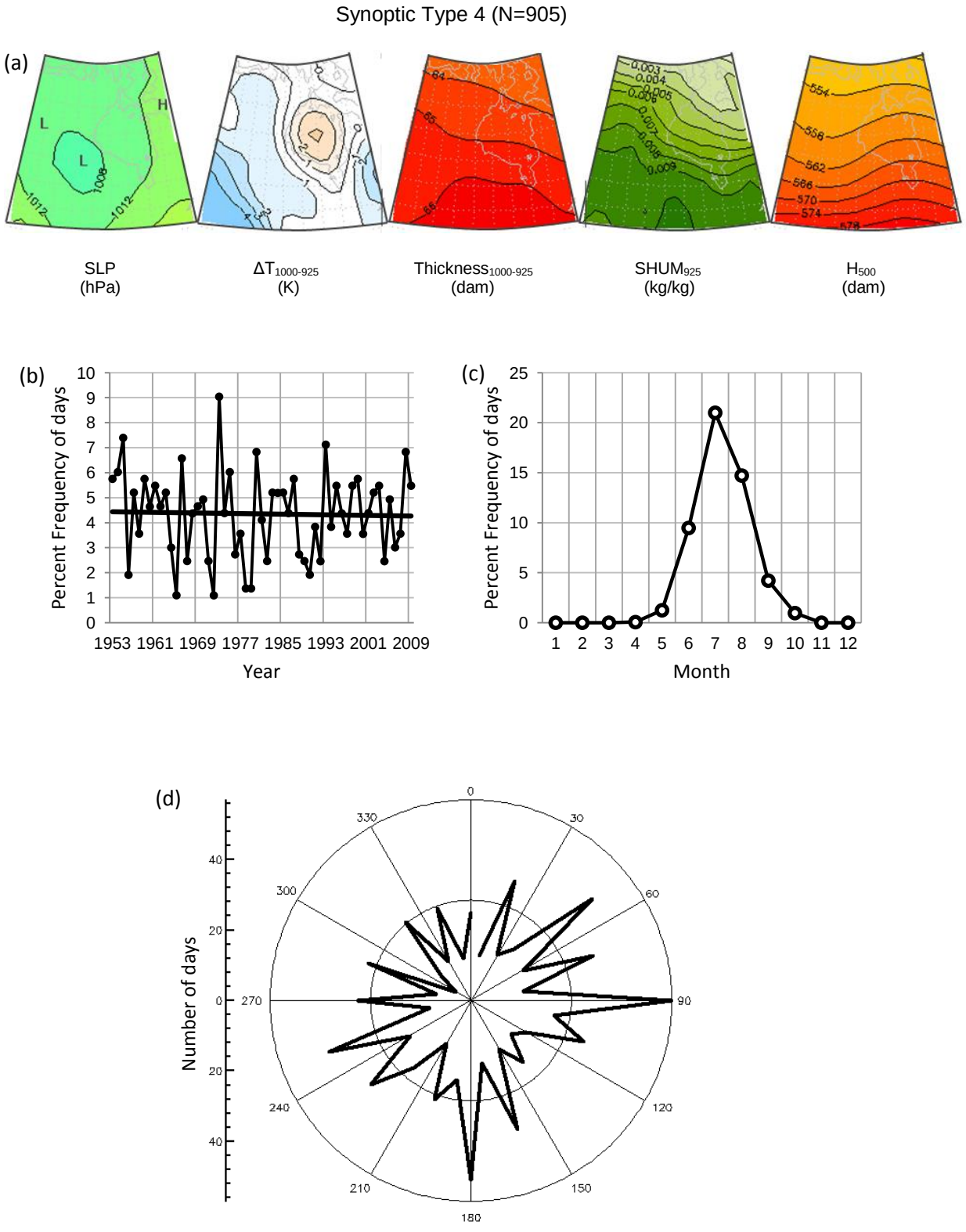

Figure 36: Synoptic Type 4 (a) composite maps, (b) annual percent type frequencies, (c) monthly percent type frequencies and (d) wind rose diagram displaying surface winds observed in Churchill at 12:00 GMT during this synoptic type

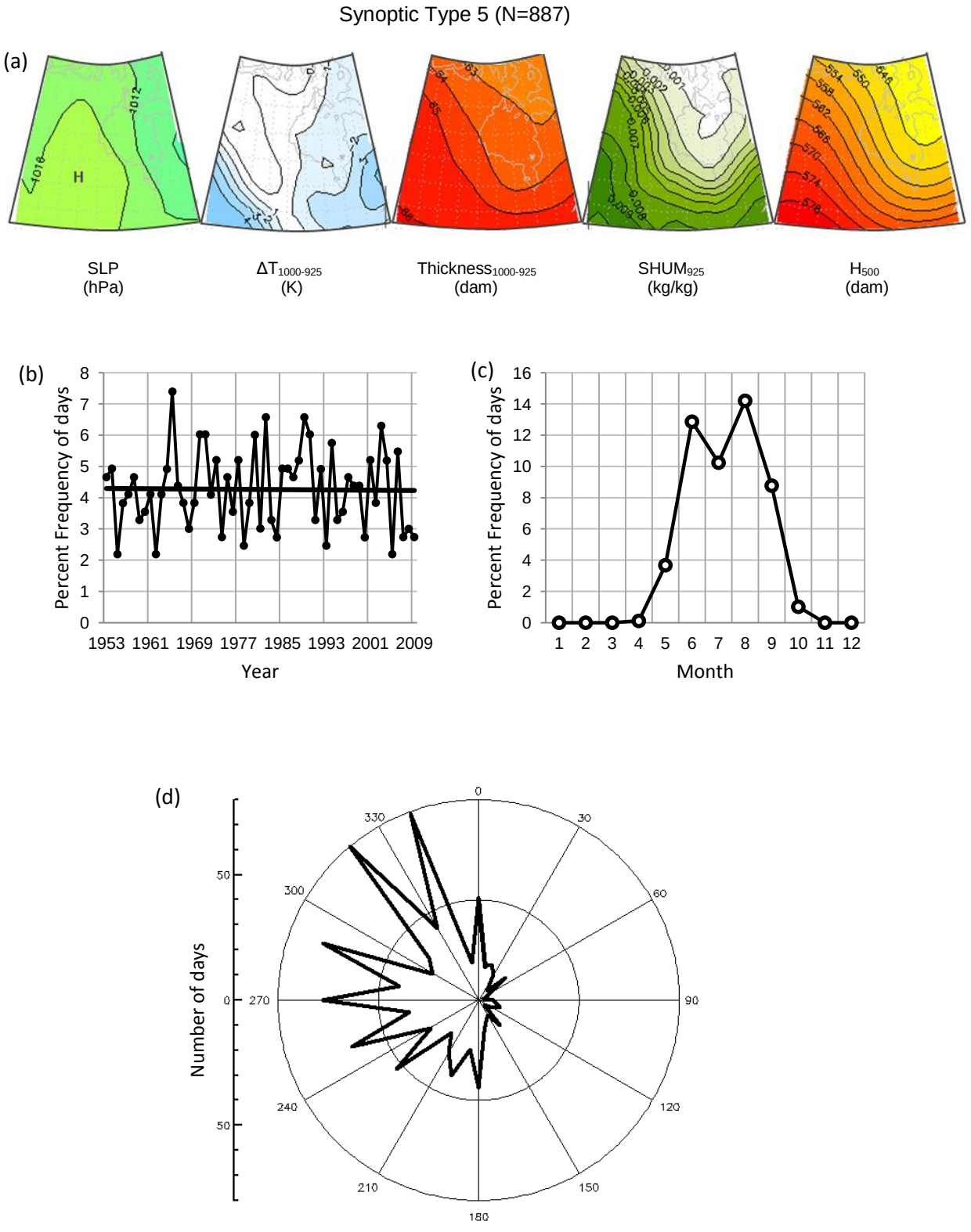

Figure 37: Synoptic Type 5 (a) composite maps, (b) annual percent type frequencies, (c) monthly percent type frequencies and (d) wind rose diagram displaying surface winds observed in Churchill at 12:00 GMT during this synoptic type

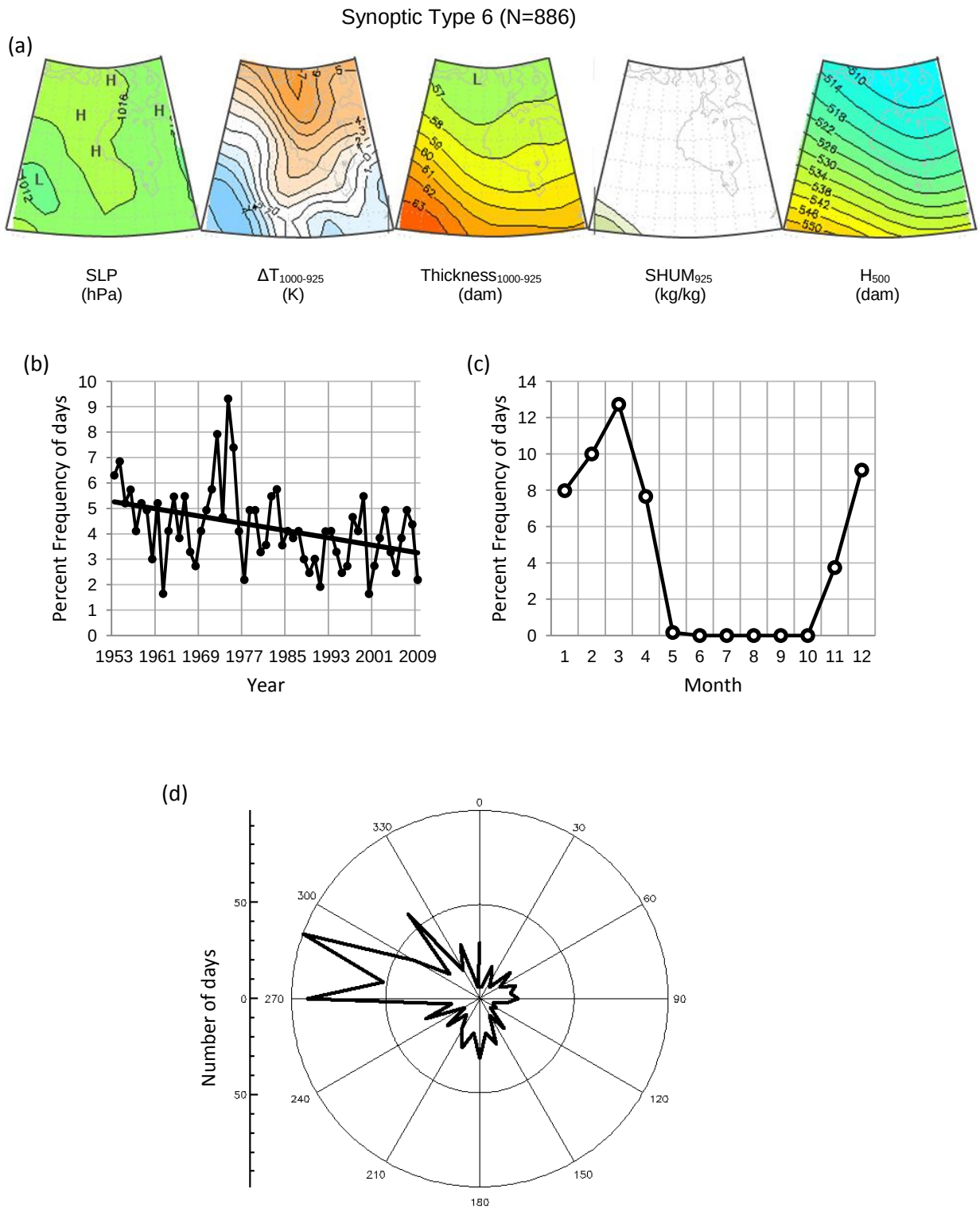

Figure 38: Synoptic Type 6 (a) composite maps, (b) annual percent type frequencies, (c) monthly percent type frequencies and (d) wind rose diagram displaying surface winds observed in Churchill at 12:00 GMT during this synoptic type

Type-7 is a summer pattern, peaking in July (Figure 39). It is characterized by low SLP centered over the southeast portion of Hudson Bay and high humidity values at 925 mb. The position of the low SLP produce surface winds in Churchill out of the northwest. A total of 784 days were classified as Type-7, or an average of 14 days per year.

Type-8 is pattern (November to March) (Figure 40). This type is associated with low SLP in the northeast quadrant of the study region, very low thickness and humidity values, and a very strong gradient across the 500 mb pressure surface, which would result in strong, northwesterly geostrophic flow at 500 mb. Winds in Churchill during a Type-8 event are exclusively out of the northwest. A total of 739 days were classified as Type-8, or an average of 13 days per year.

Type-9 is the first spring (May-June) and fall (August-November) pattern (Figure 41). It is characterized by lower SLP west of Hudson Bay and a high south of the bay and moderately cool and dry air in the northeast quadrant of the study region. Winds in Churchill during a Type-9 event are typically out of the south or southwest. A total of 687 days were classified as Type-9, or an average of 12 days per year.

Type-10 is another winter and early-spring pattern (Figure 42). This type is similar to Type-8 in that low SLP values and low 500 mb heights are present in the northeast quadrant of the study region. This type is associated with westerly or northwesterly winds at the surface in Churchill and with dry air at 925 mb. A total of 684 days were classified as Type-10 (12 days per year).

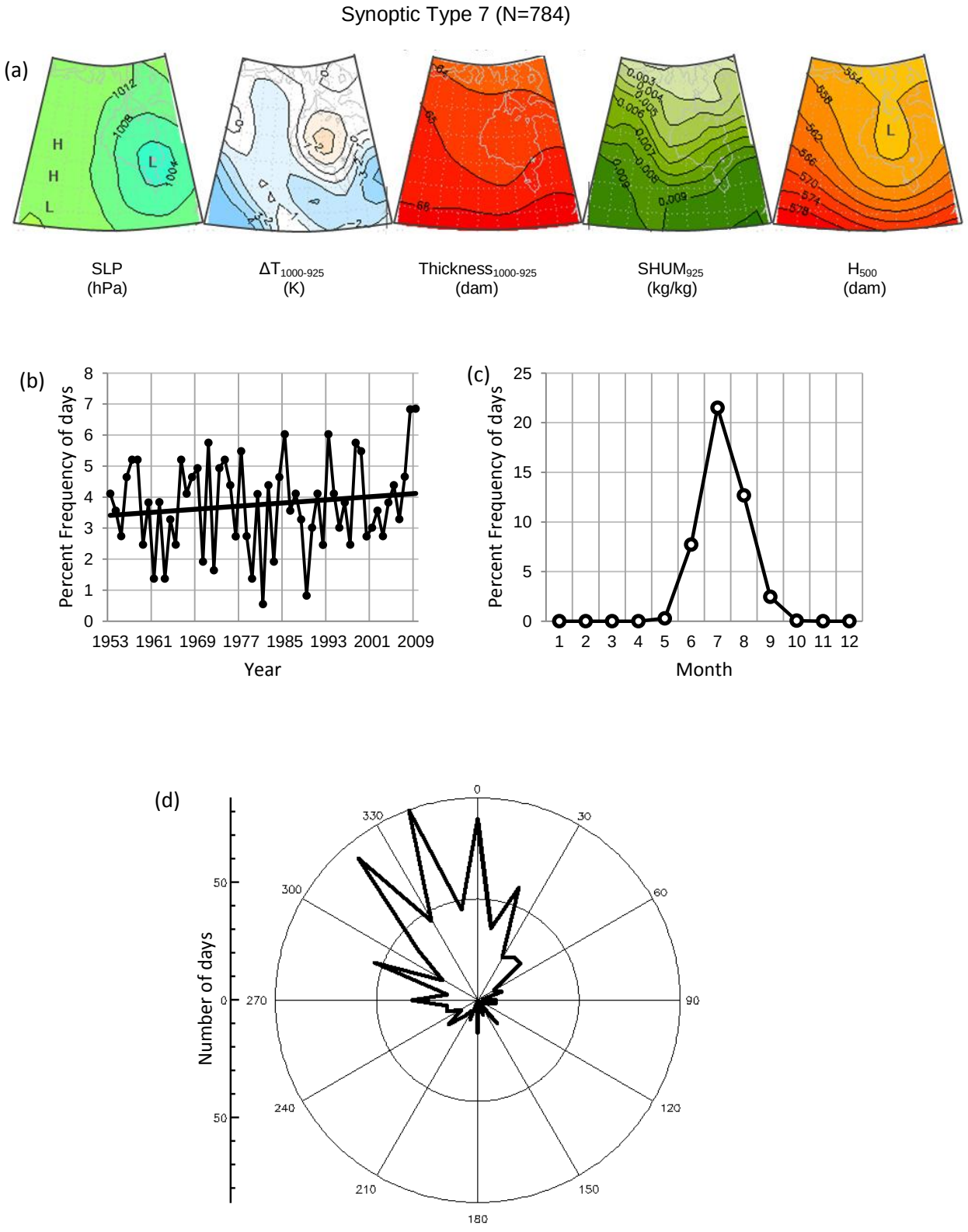

Figure 39: Synoptic Type 7 (a) composite maps, (b) annual percent type frequencies, (c) monthly percent type frequencies and (d) wind rose diagram displaying surface winds observed in Churchill at 12:00 GMT during this synoptic type

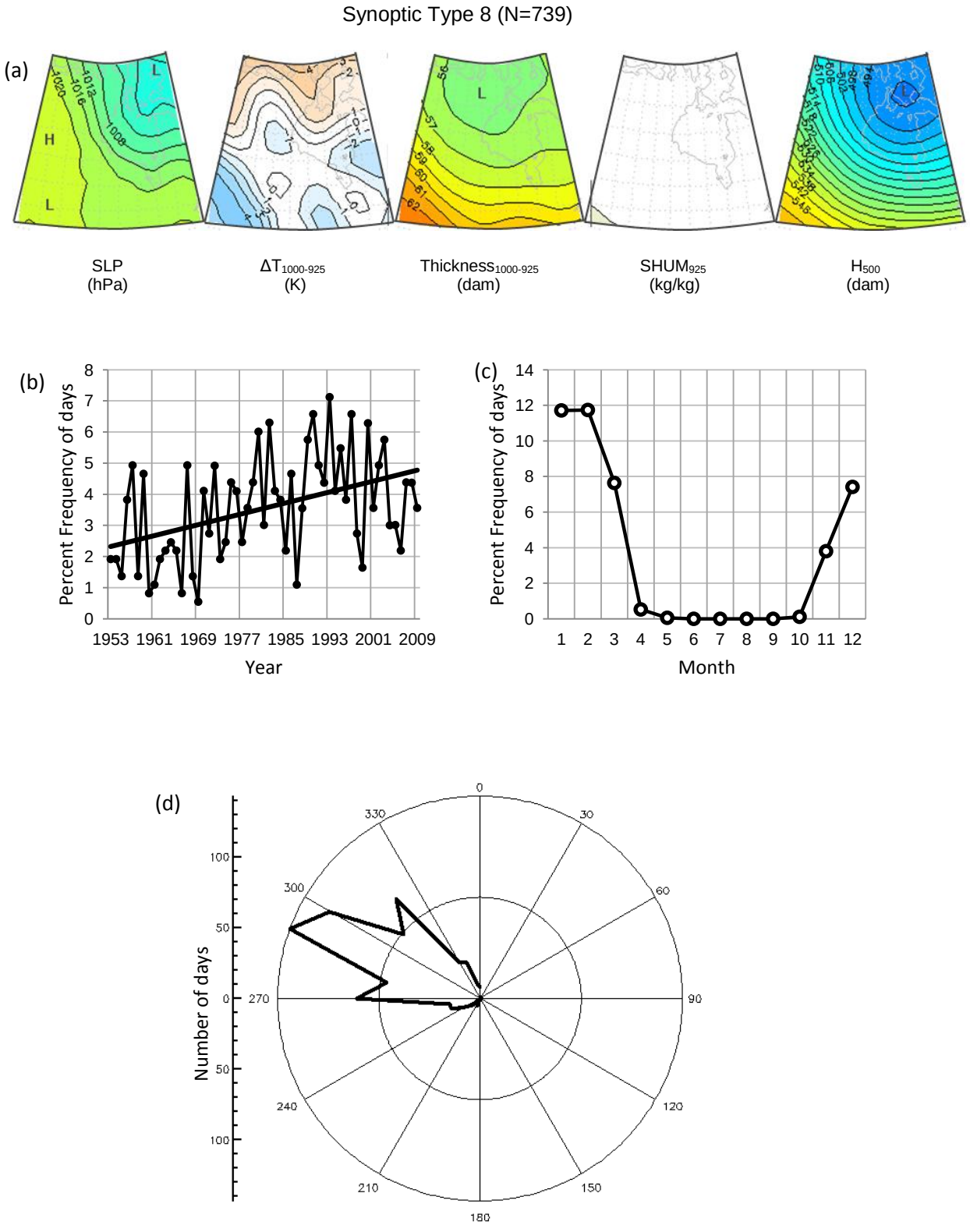

Figure 40: Synoptic Type 8 (a) composite maps, (b) annual percent type frequencies, (c) monthly percent type frequencies and (d) wind rose diagram displaying surface winds observed in Churchill at 12:00 GMT during this synoptic type

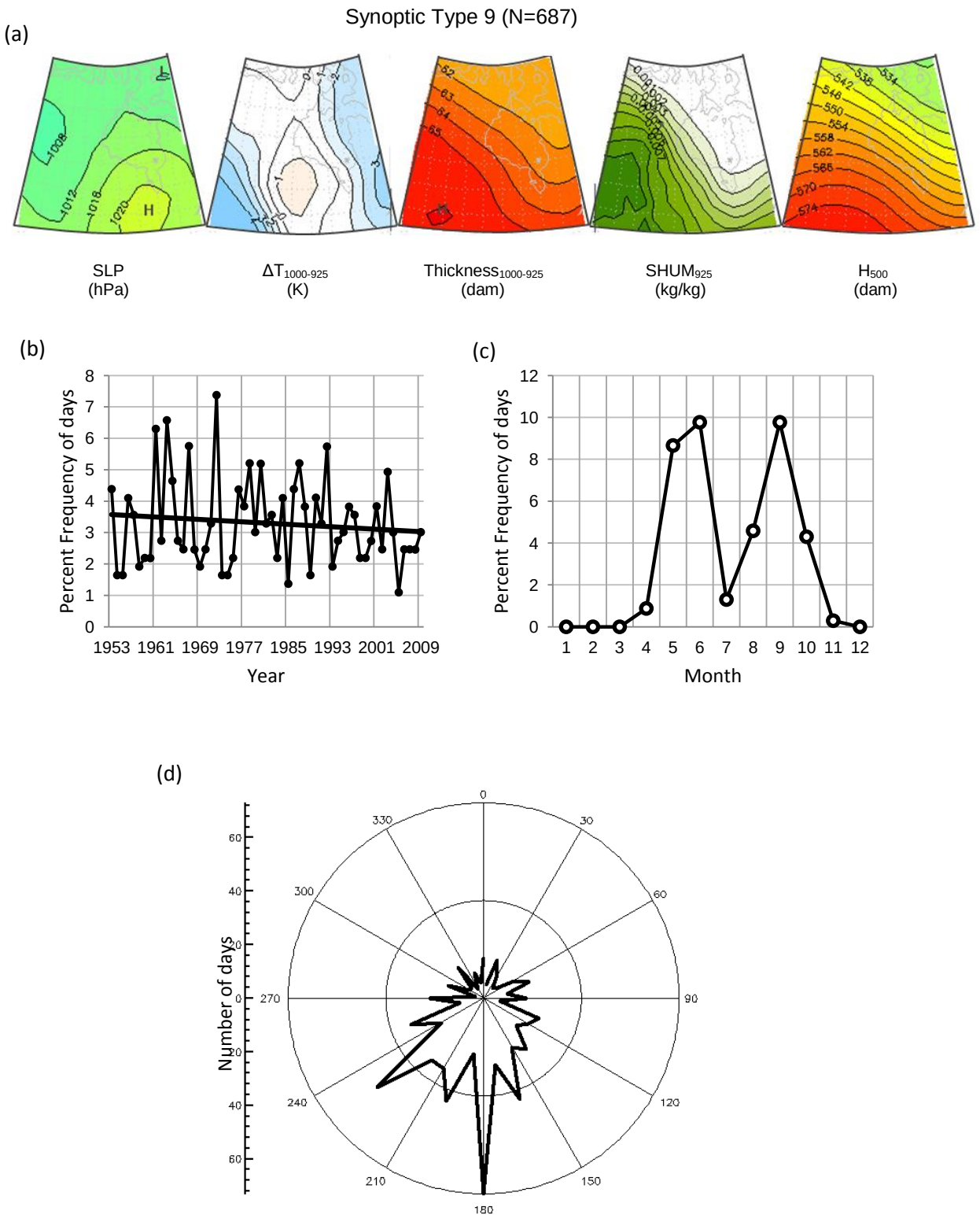

Figure 41: Synoptic Type 9 (a) composite maps, (b) annual percent type frequencies, (c) monthly percent type frequencies and (d) wind rose diagram displaying surface winds observed in Churchill at 12:00 GMT during this synoptic type

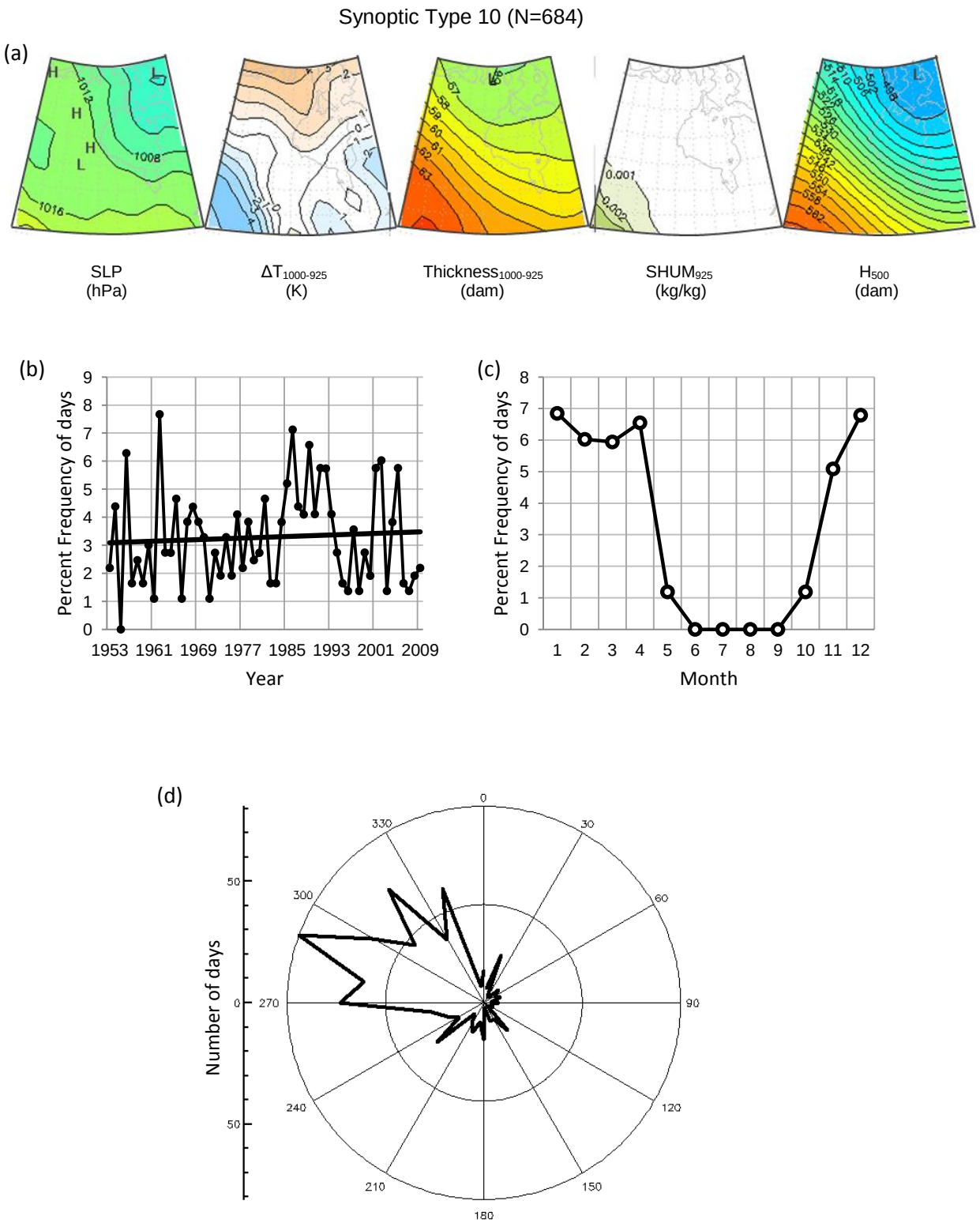

Figure 42: Synoptic Type 10 (a) composite maps, (b) annual percent type frequencies, (c) monthly percent type frequencies and (d) wind rose diagram displaying surface winds observed in Churchill at 12:00 GMT during this synoptic type

Type-11 occurs throughout the winter months and peaks in March (Figure 43). During a Type-11 event, the 1000-925 mb temperature lapse rate is positive across much of the western portion of the study region, across Hudson Bay and south of James Bay. Low SLP is found southwest of the bay, and 500 mb flow is relatively zonal. Winds in Churchill during a Type-11 event are most commonly out of the northeast; however, winds are also frequently from the northwest and the south. A total of 668 days were classified as Type-11, or an average of 12 days per year.

Type-12 most frequently occurs during late summer and less frequently during the spring (Figure 44). This type is similar to Type-9 event, with the exception of the SLP pattern and 1000-925 mb temperature change map. During a Type-12 event, temperature lapse rates are distinctly negative over all of Hudson Bay, whereas during a Type-9 event the negative lapse rates are restricted to the eastern side of the bay. Winds in Churchill during Type-12 events are predominantly out of the northwest. A total of 658 days were classified as Type-12, or an average of 11.5 days per year.

Type-13 is a spring and fall pattern (Figure 45). Unlike Type-9 events, Type-13 events are characterized by high SLP values over most of the study region. Additionally, winds in Churchill are typically out of the west rather than out of the south. Temperature lapse rates between 1000-925 mb over Hudson Bay are negative, while along the west coast of Hudson Bay they are positive. 644 days were classified as Type-13, or an average of 11 days per year.

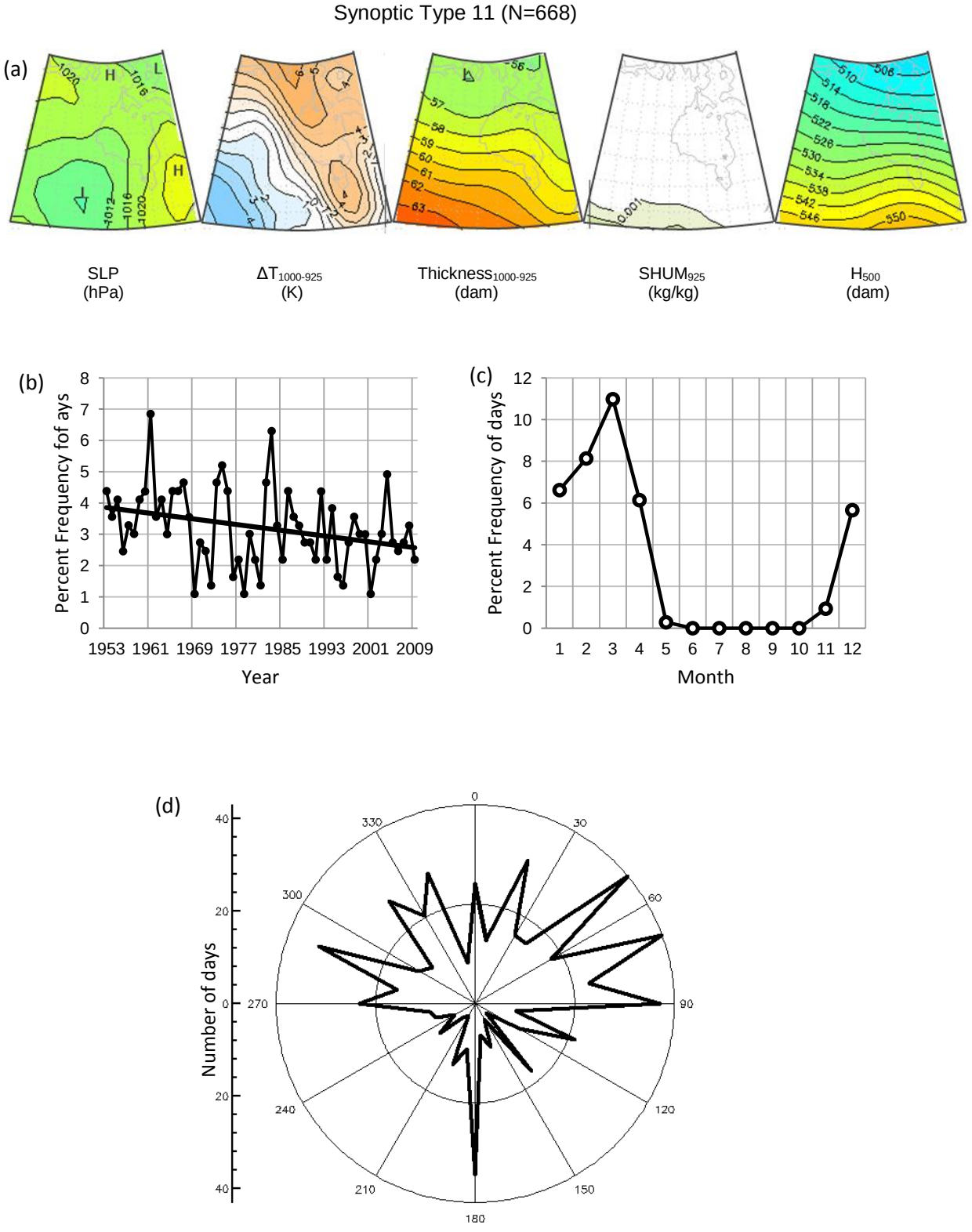

Figure 43: Synoptic Type 11 (a) composite maps, (b) annual percent type frequencies, (c) monthly percent type frequencies and (d) wind rose diagram displaying surface winds observed in Churchill at 12:00 GMT during this synoptic type

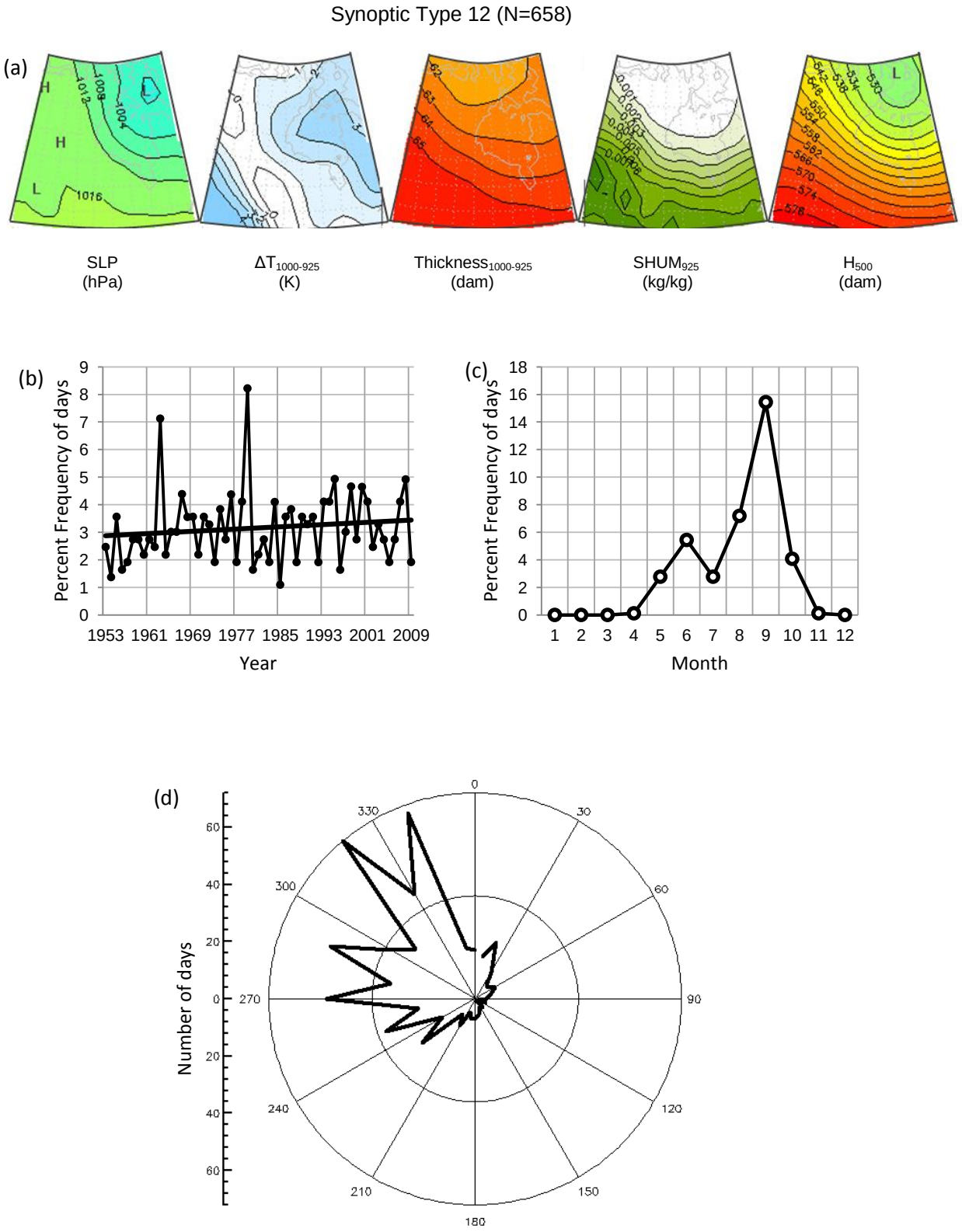

Figure 44: Synoptic Type 12 (a) composite maps, (b) annual percent type frequencies, (c) monthly percent type frequencies and (d) wind rose diagram displaying surface winds observed in Churchill at 12:00 GMT during this synoptic type

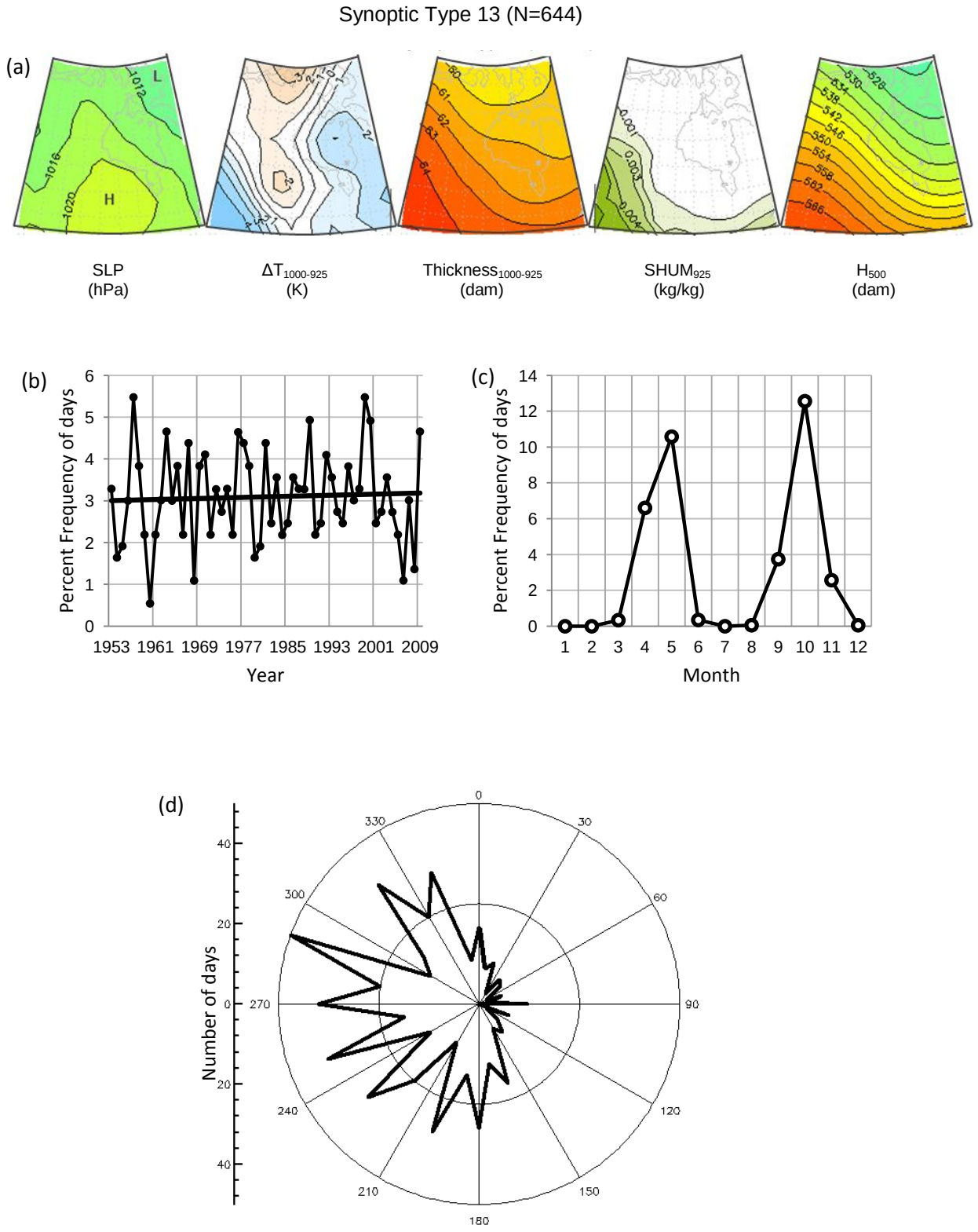

Figure 45: Synoptic Type 13 (a) composite maps, (b) annual percent type frequencies, (c) monthly percent type frequencies and (d) wind rose diagram displaying surface winds observed in Churchill at 12:00 GMT during this synoptic type

Type-14 is a spring and fall pattern (Figure 46). Type-14 is characterized by low SLP over the southeastern portion of Hudson Bay. This type is unique from Types 9 and 13 in that temperature lapse rates between 1000-925 mb are negative across most of the study region. Winds in Churchill during a Type-14 event are typically out of the north or northwest. A total of 615 days were classified as Type-14, or an average of 11 days per year.

Type-15 is predominantly a fall pattern. A comparatively small number of Type-15 events occur during the spring (Figure 47). During a Type-15 event, SLP is low across the central portion of the study region. Over Hudson Bay and in the southwestern portion of the study region, temperature lapse rates are negative. Winds in Churchill during a Type-15 event are often out of the northwest. A total of 610 days were classified as Type-15, or an average of 11 days per year.

Type-16 occurs throughout the summer and peaks during the month of September (Figure 48). This type is characterized mainly by low SLP over Hudson Bay, relatively mild temperatures and negative lapse rates between 1000 and 925 mb. Winds are typically out of the northwest during a Type-16 event. A total of 609 days were classified as Type-16, or an average of 11 days per year.

Type-17 is a colder version of Type-16 (Figure 49). This type frequently occurs during both spring and fall, but is slightly more common in fall (peaks in October) compared to spring. Winds in Churchill during Type-17 events are typically out of the northwest. A total of 606 days were classified as Type-17, or an average of 10.5 days per year.

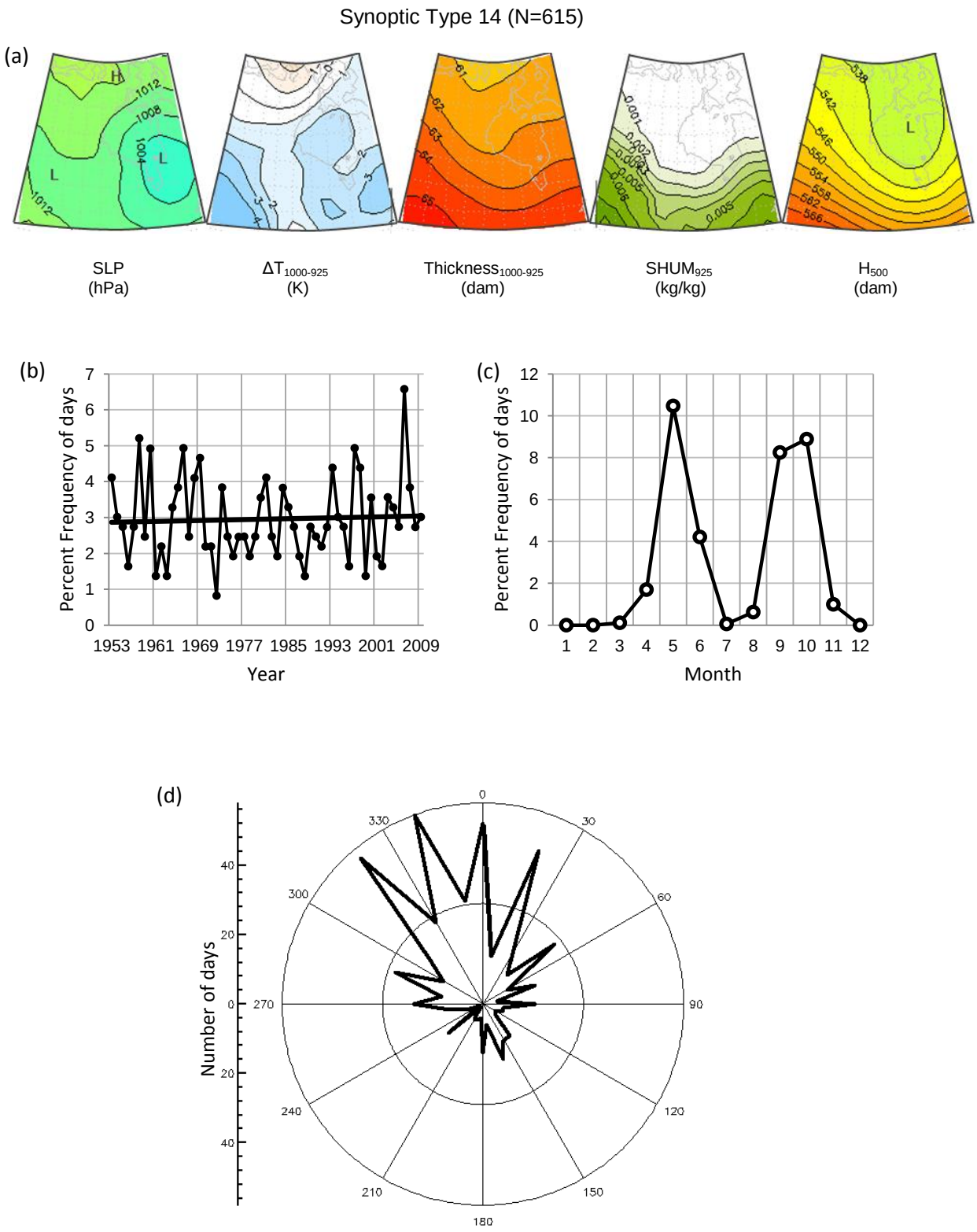

Figure 46: Synoptic Type 14 (a) composite maps, (b) annual percent type frequencies, (c) monthly percent type frequencies and (d) wind rose diagram displaying surface winds observed in Churchill at 12:00 GMT during this synoptic type

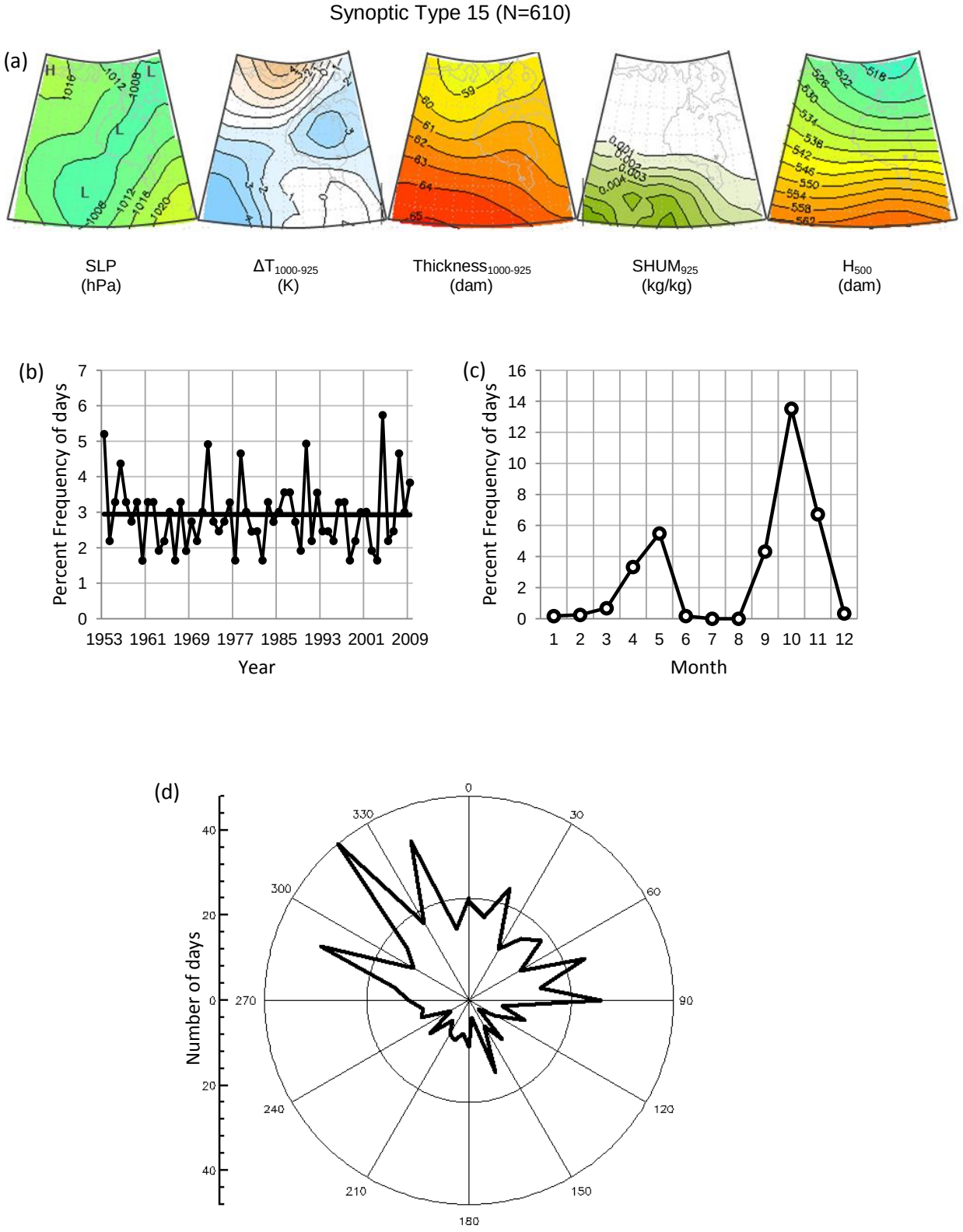

Figure 47: Synoptic Type 15 (a) composite maps, (b) annual percent type frequencies, (c) monthly percent type frequencies and (d) wind rose diagram displaying surface winds observed in Churchill at 12:00 GMT during this synoptic type

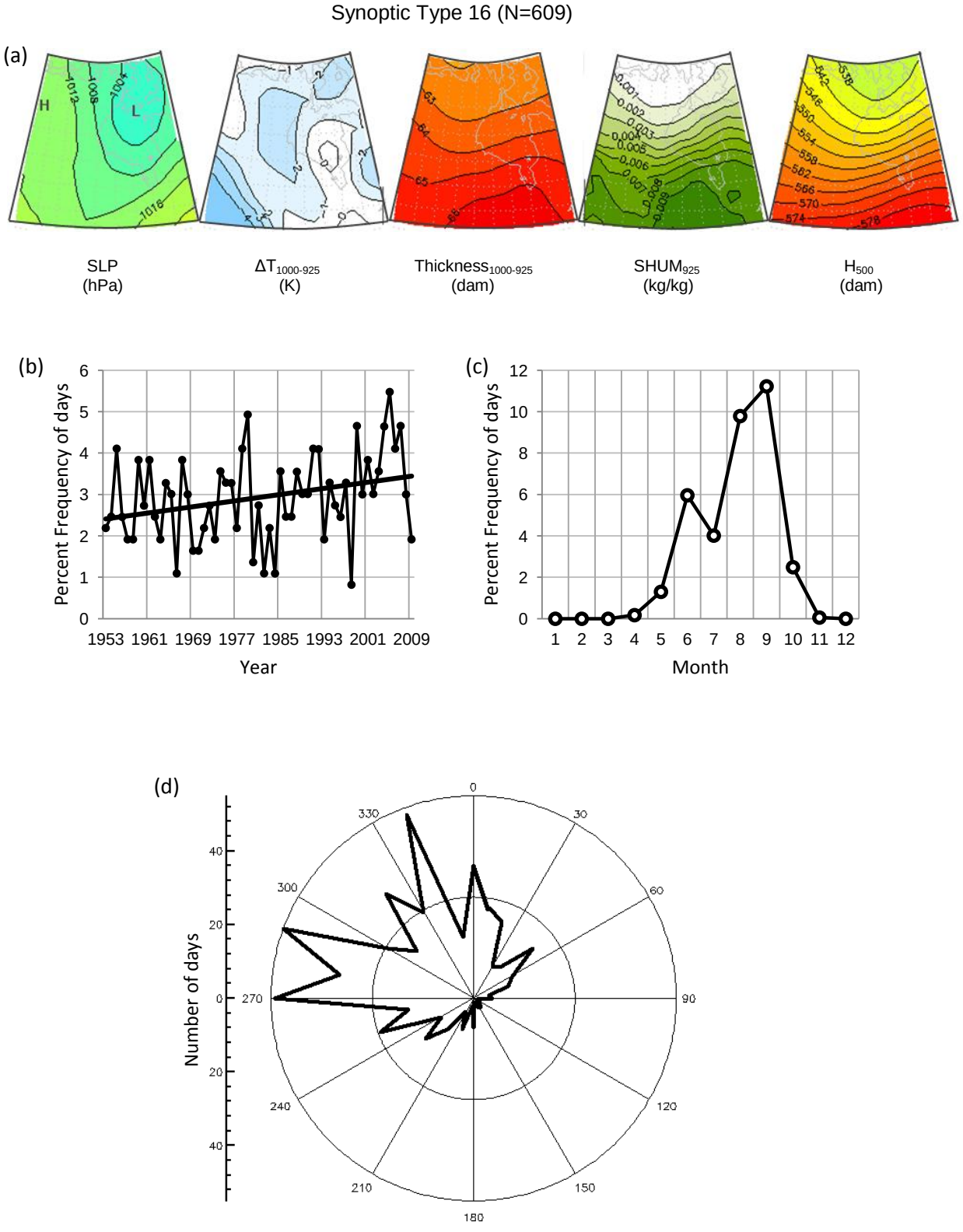

Figure 48: Synoptic Type 16 (a) composite maps, (b) annual percent type frequencies, (c) monthly percent type frequencies and (d) wind rose diagram displaying surface winds observed in Churchill at 12:00 GMT during this synoptic type

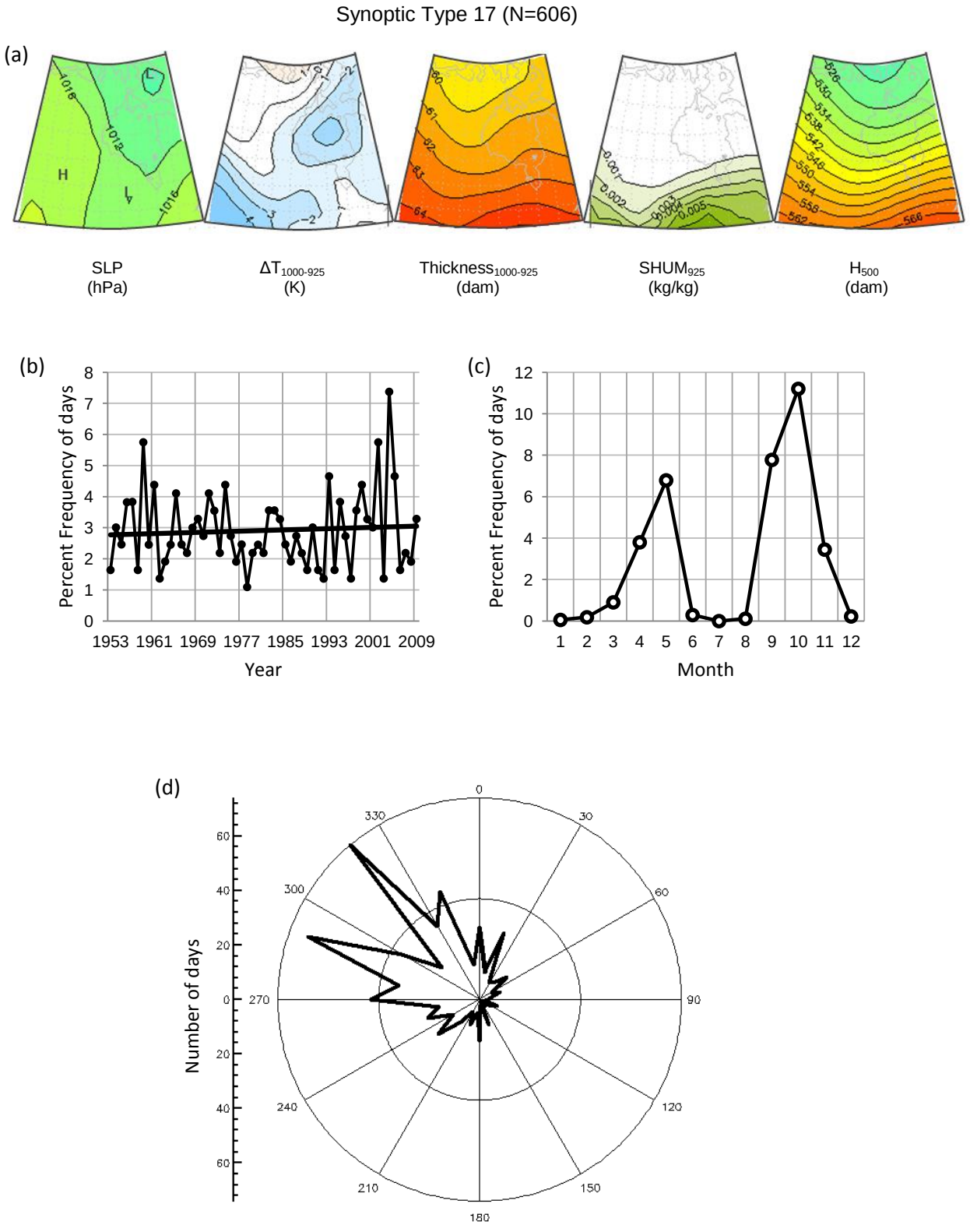

Figure 49: Synoptic Type 17 (a) composite maps, (b) annual percent type frequencies, (c) monthly percent type frequencies and (d) wind rose diagram displaying surface winds observed in Churchill at 12:00 GMT during this synoptic type

Type-18 is a winter synoptic pattern (November to April) (Figure 50). It is characterized by high SLP to the southwest of the Hudson Bay, very steep temperature inversions between 1000 and 925 mb and very cold and dry air. Winds during a Type-18 event are typically from the west. A total of 604 days were classified as Type-18, or an average of 10.5 days per year.

Similarly, Type-19 is another winter pattern associated with very cold and dry low-level air (Figure 51). However, during a Type-19 event low SLP is typically found over Hudson Bay as well as south of Hudson Bay. Winds during a Type-19 event are from the northwest. 601 days were classified as Type-19 (10.5 days per year).

Type-20 is predominantly a spring synoptic pattern (April-May) (Figure 52). This is one of the few synoptic types which are associated with easterly surface winds in Churchill. The cause of this easterly flow is most likely due to the orientation of high SLP over Hudson Bay and low SLP to the southwest of Hudson Bay (generating onshore winds). Temperature lapse rates between 1000 and 925 mb are positive over the bay. This type is also characterized by ridging of the 500 mb contours over the central portion of the study region. A total of 580 days were classified as Type-20, or an average of 10 days per year.

Type-21 is another spring synoptic pattern (Figure 53). However, unlike Type-20, Type-21 is characterized by troughing in the 500 mb contours over the central portion of the study region. Also, low SLP tends to exist to the south of Hudson Bay, generating surface winds that are out of the north and northeast. A total of 578 days were classified as Type-21, or an average of 10 days per year.

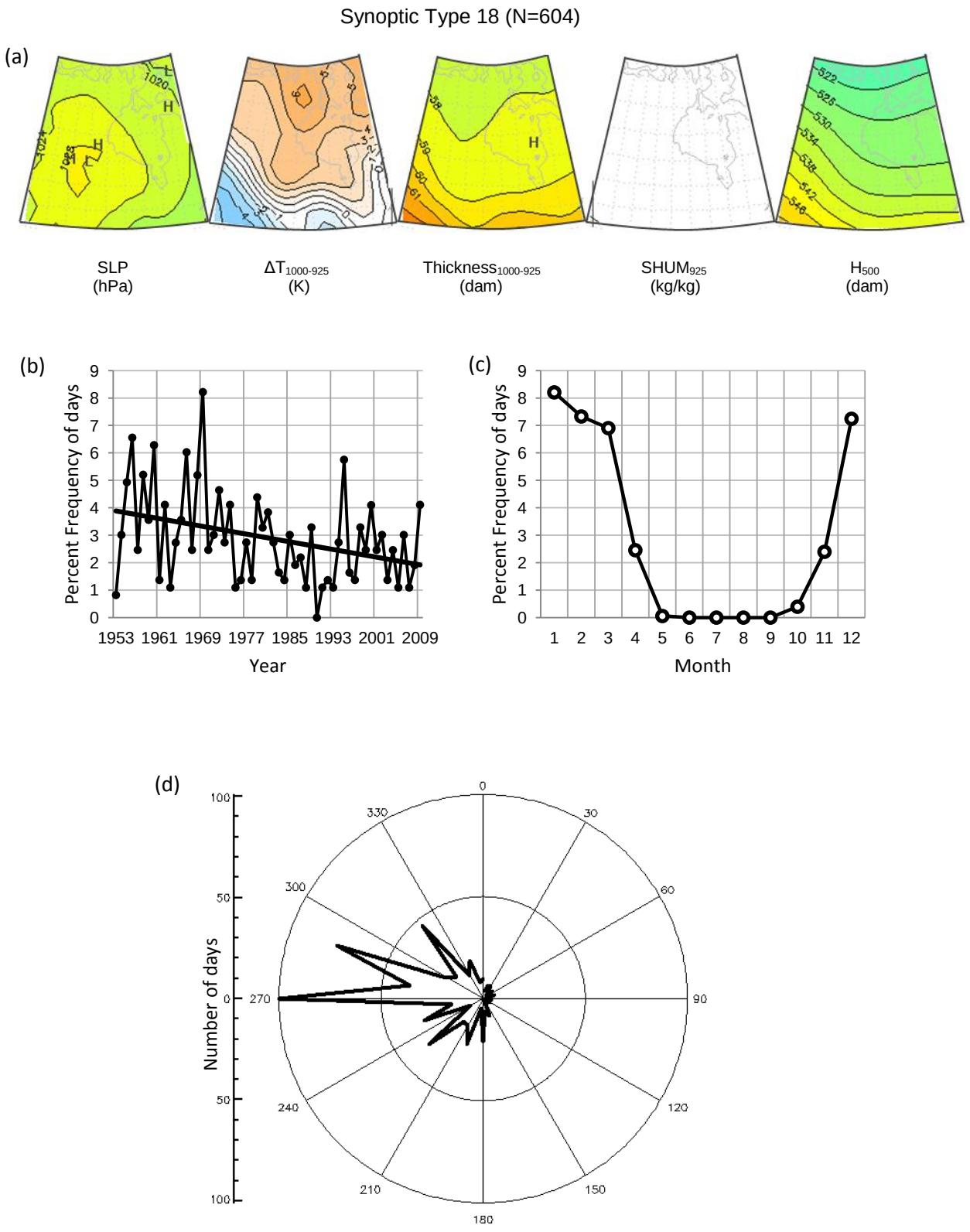

Figure 50: Synoptic Type 18 (a) composite maps, (b) annual percent type frequencies, (c) monthly percent type frequencies and (d) wind rose diagram displaying surface winds observed in Churchill at 12:00 GMT during this synoptic type

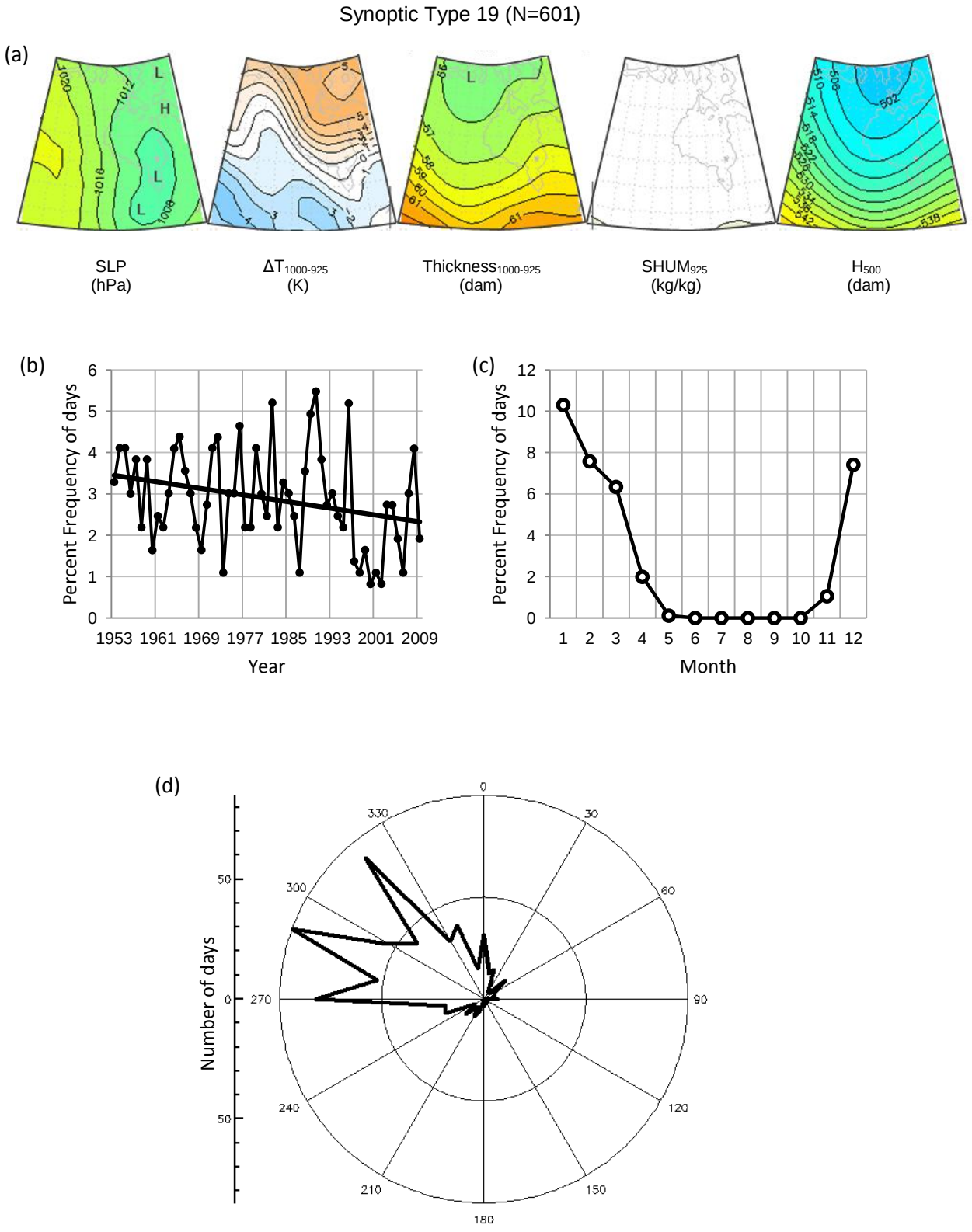

Figure 51: Synoptic Type 19 (a) composite maps, (b) annual percent type frequencies, (c) monthly percent type frequencies and (d) wind rose diagram displaying surface winds observed in Churchill at 12:00 GMT during this synoptic type

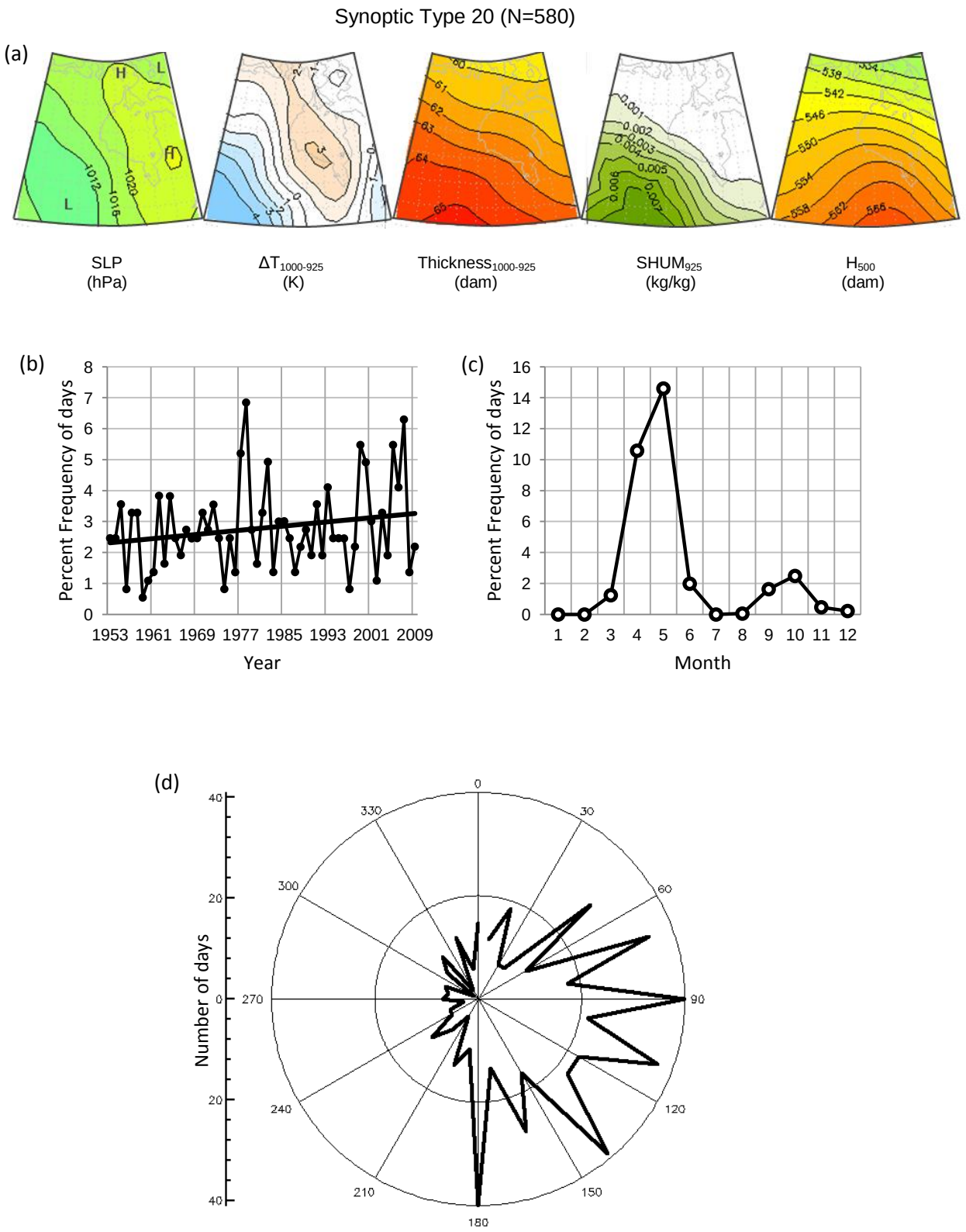

Figure 52: Synoptic Type 20 (a) composite maps, (b) annual percent type frequencies, (c) monthly percent type frequencies and (d) wind rose diagram displaying surface winds observed in Churchill at 12:00 GMT during this synoptic type

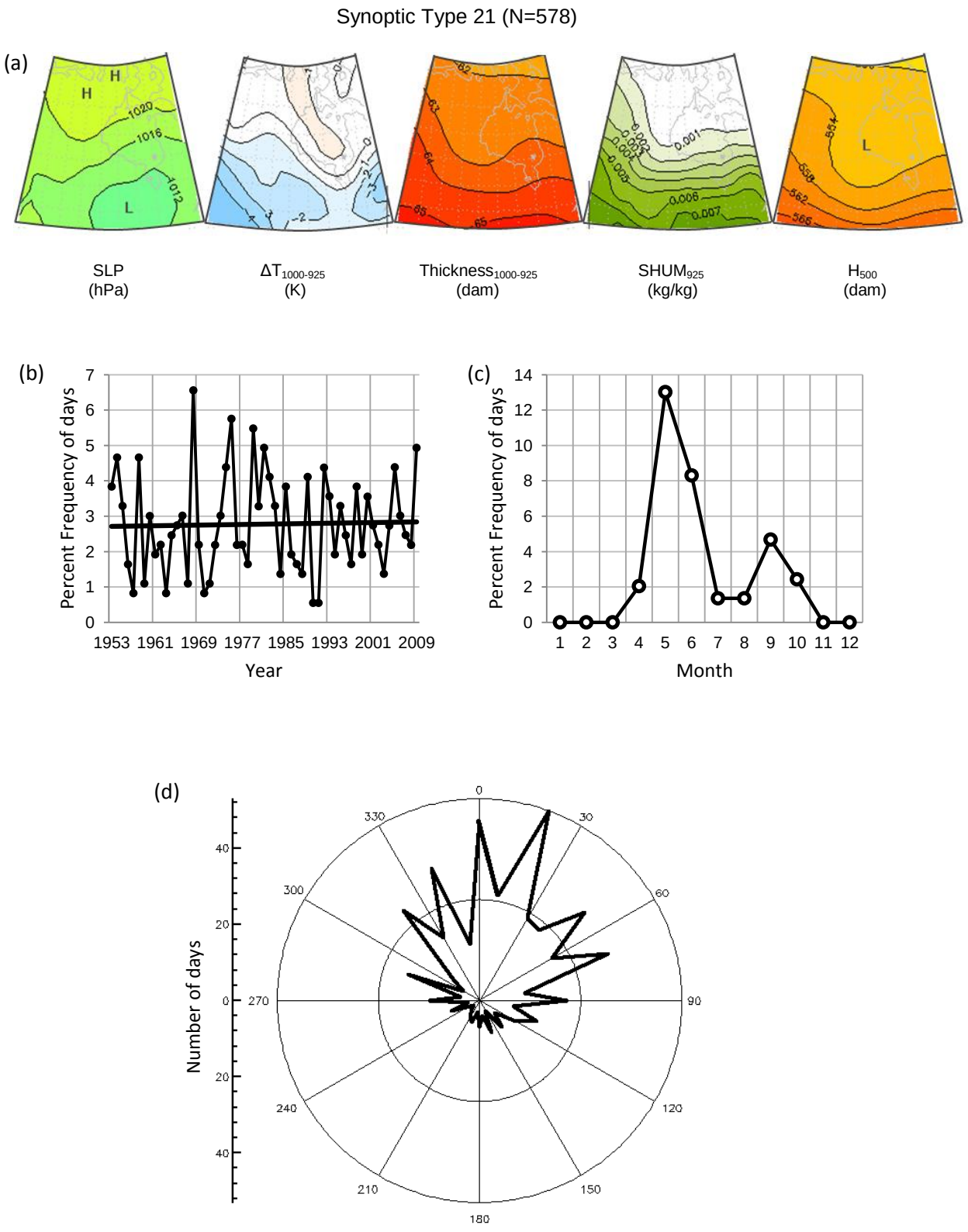

Figure 53: Synoptic Type 21 (a) composite maps, (b) annual percent type frequencies, (c) monthly percent type frequencies and (d) wind rose diagram displaying surface winds observed in Churchill at 12:00 GMT during this synoptic type

Type-22 is a cooler version of Type-21 (Figure 54). This type tends to occur in the early spring (peaks in April). Many of the Type-22 composite maps are very similar to the Type-21 composite maps, with the exception of lower thickness and humidity values. Wind direction in Churchill during a Type-21 event varies between northwest and east. A total of 531 days were classified as Type-22, or an average of 9 days per year.

Type-23 is a winter pattern that is characterized by a ridge of SLP over the south-central portion of the study region, very steep low-level temperature inversions, and very low temperatures (Figure 55). Winds observed in Churchill during a Type-23 event are out of the southwest. A total of 480 days were classified as Type-23, or an average of 8 days per year.

Type-24 is pattern that occurs almost exclusively during the month of November (Figure 56). It is characterized by low SLP to the west of Hudson Bay and negative temperature lapse rates between 1000 and 925 mb over Hudson Bay. A ridge in the 1000-925 mb isohypses over Hudson Bay also characterizes Type-24 events. Winds observed in Churchill during a Type-24 event are typically from the west or southwest. A total of 468 days were classified as Type-24, or an average of 8 days per year.

Type-25 is a late fall to early spring pattern (Figure 57). It is characterized by low SLP across the eastern portion of the study region and high SLP across the west. Temperatures within the 1000 and 925 mb layer are cooler along the west coast of Hudson Bay compared to the east coast. Winds during a Type-24 event in Churchill are from the northwest. A total of 467 days were classified as Type-25, or an average of 8 days per year.

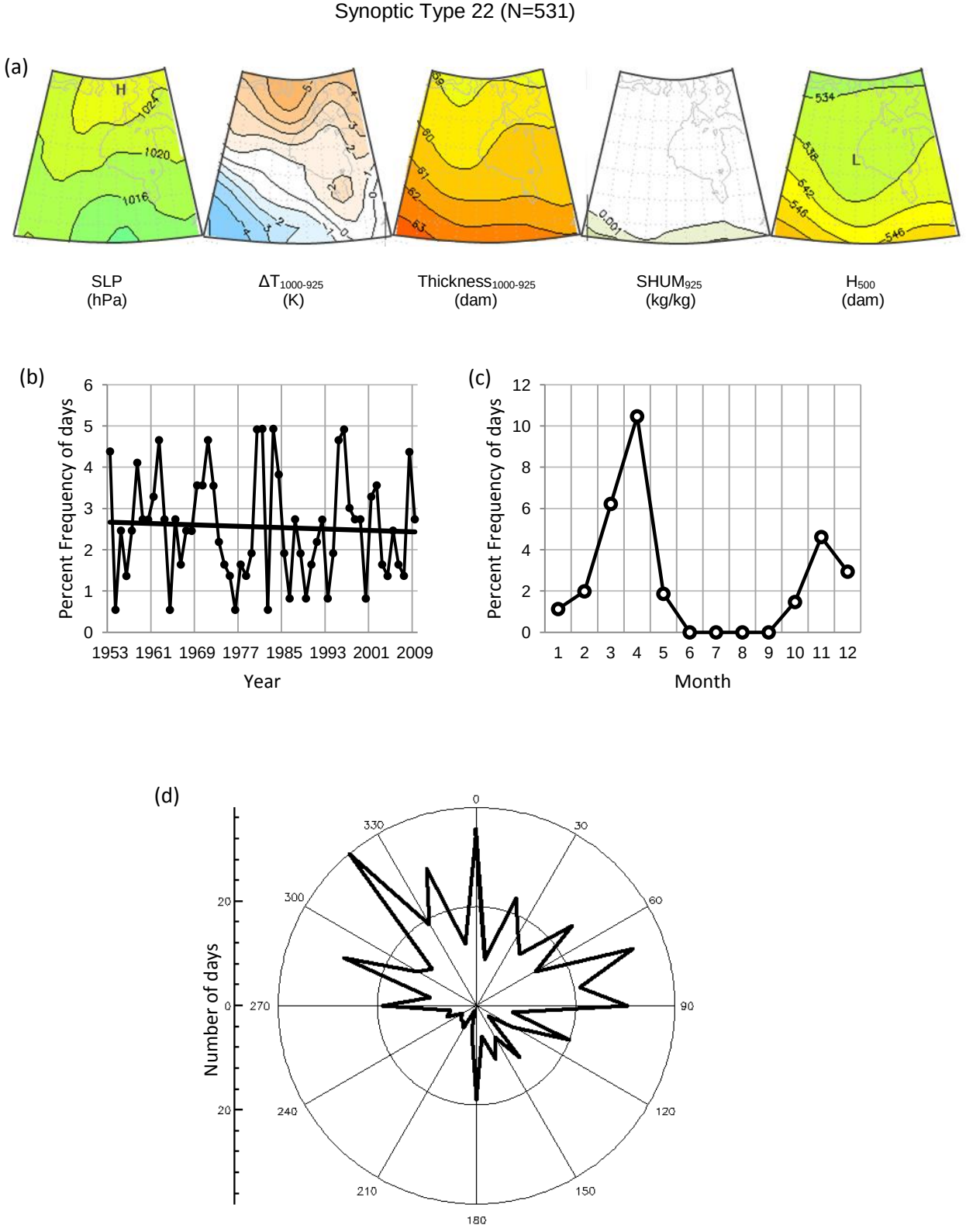

Figure 54: Synoptic Type 22 (a) composite maps, (b) annual percent type frequencies, (c) monthly percent type frequencies and (d) wind rose diagram displaying surface winds observed in Churchill at 12:00 GMT during this synoptic type

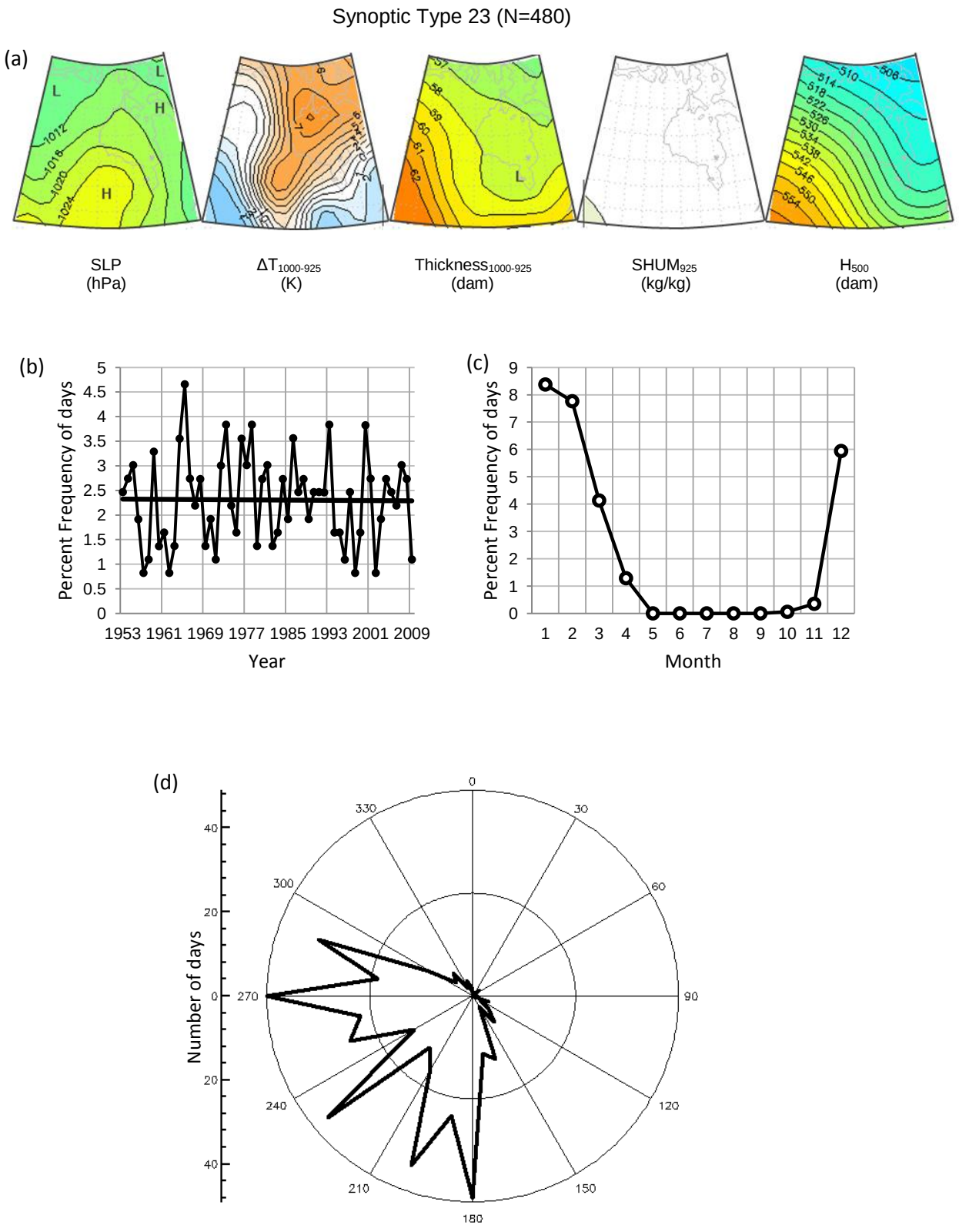

Figure 55: Synoptic Type 23 (a) composite maps, (b) annual percent type frequencies, (c) monthly percent type frequencies and (d) wind rose diagram displaying surface winds observed in Churchill at 12:00 GMT during this synoptic type

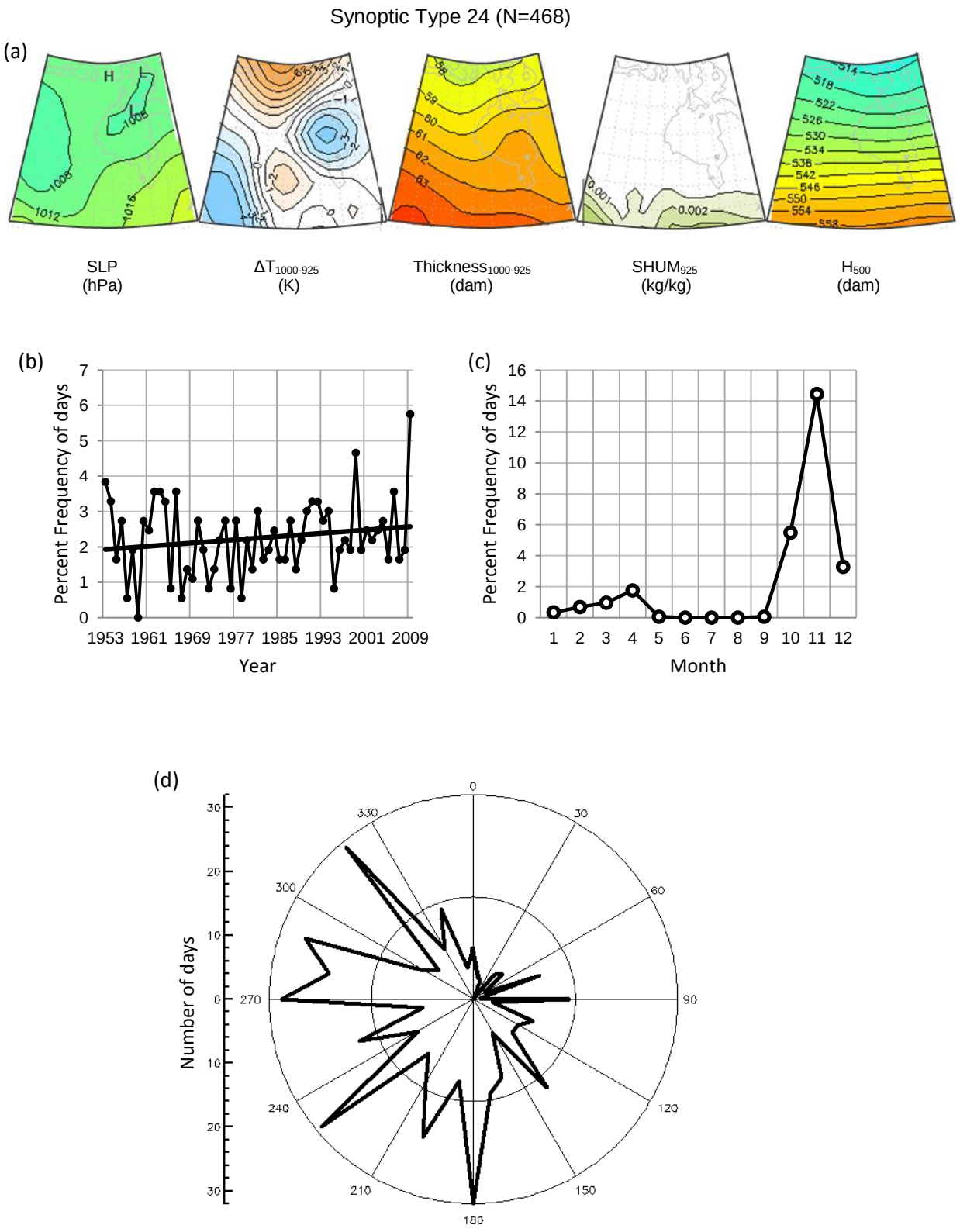

Figure 56: Synoptic Type 24 (a) composite maps, (b) annual percent type frequencies, (c) monthly percent type frequencies and (d) wind rose diagram displaying surface winds observed in Churchill at 12:00 GMT during this synoptic type

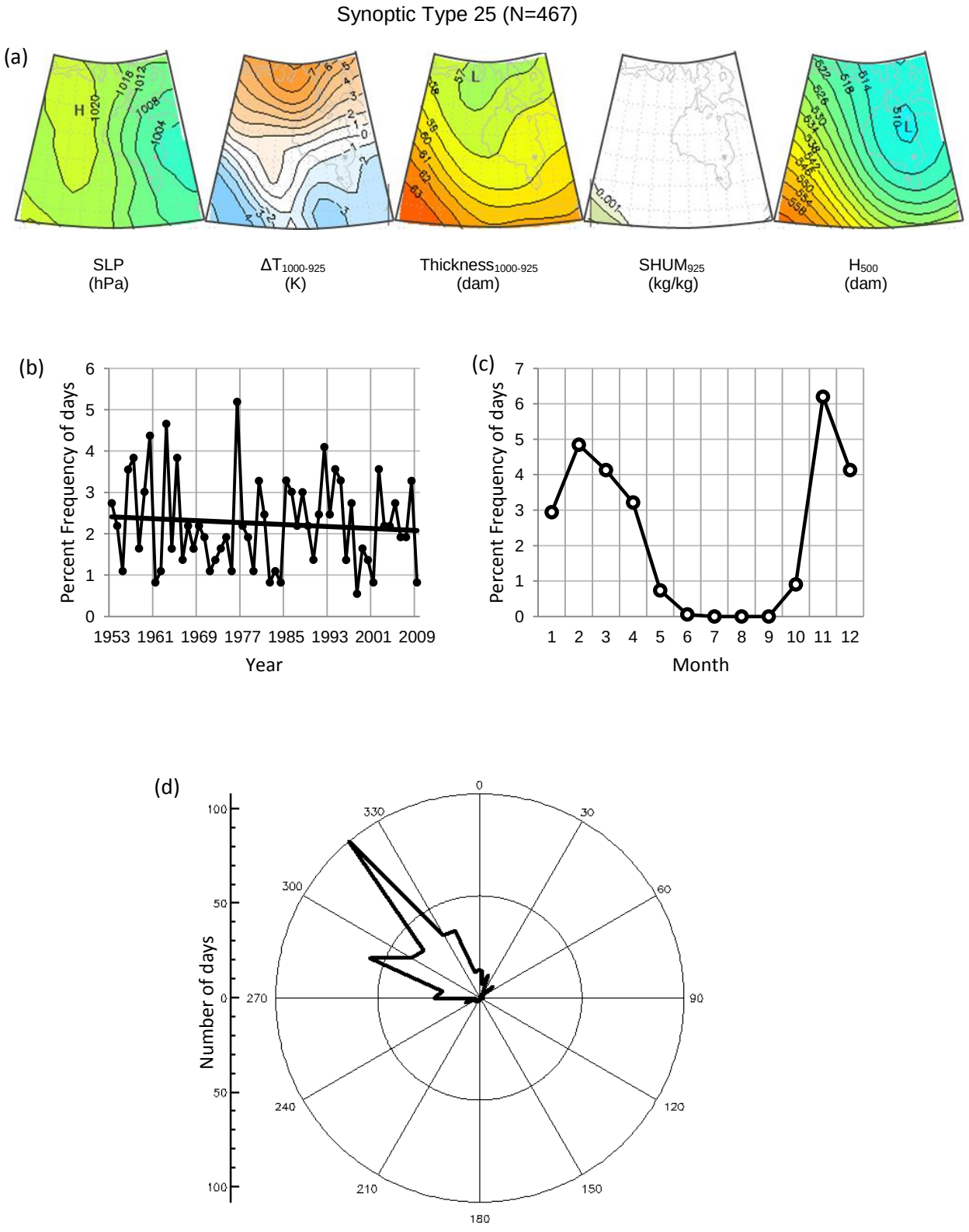

Figure 57: Synoptic Type 25 (a) composite maps, (b) annual percent type frequencies, (c) monthly percent type frequencies and (d) wind rose diagram displaying surface winds observed in Churchill at 12:00 GMT during this synoptic type

Type-26 is another pattern frequently found between the months of November and March (Figure 58). This type is very similar to Type-23 but with more negative isothermal lapse rates between 1000 and 925 mb over Hudson Bay and more positive lapse rates to the southwest of the bay. Winds in Churchill during a Type-26 event are almost exclusively from the west. A total of 464 days were classified as Type-26, or an average of eight days per year.

Type-27 is a fall pattern that is most commonly observed during the month of October (Figure 59). This type has many of the same elements of Type-24, with negative lapse rates over Hudson Bay, a ridge in the 1000-925 mb isohypses over the Bay and troughing of the 500 mb isopachs. Surface winds during a Type-27 event are from the northwest. A total of 463 days were classified as Type-27, or an average of 8 days per year.

Type-28 is a winter pattern (Figure 60). Type-28 is characterized by very low heights at the 500 mb surface over the southern portion of Hudson Bay, thickness values that are much lower over the western side of Hudson Bay compared to the eastern side and low SLP across much of the eastern portion of the study region. Winds in Churchill during a Type-28 event are from the northwest. A total of 442 days were classified as Type-28, or an average of 7.5 days per year.

Type-29 is a spring and fall pattern characterized by high SLP over Hudson Bay and low SLP to the west of the bay (Figure 61). This type of pattern facilitates southerly winds in Churchill, which bring milder and moister air into the region. A total of 423 days were classified as Type-29, or an average of 7.5 days per year.

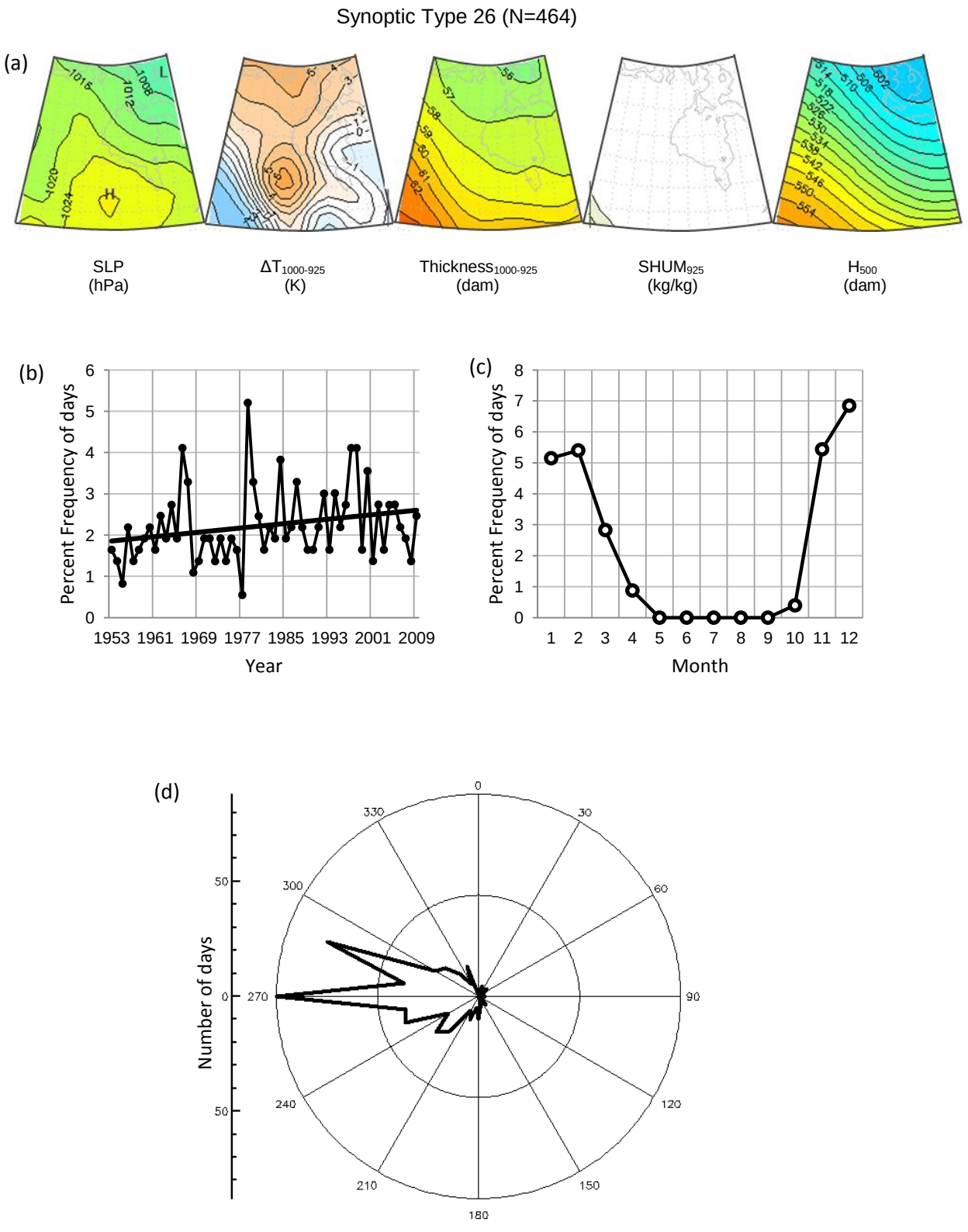

Figure 58: Synoptic Type 26 (a) composite maps, (b) annual percent type frequencies, (c) monthly percent type frequencies and (d) wind rose diagram displaying surface winds observed in Churchill at 12:00 GMT during this synoptic type

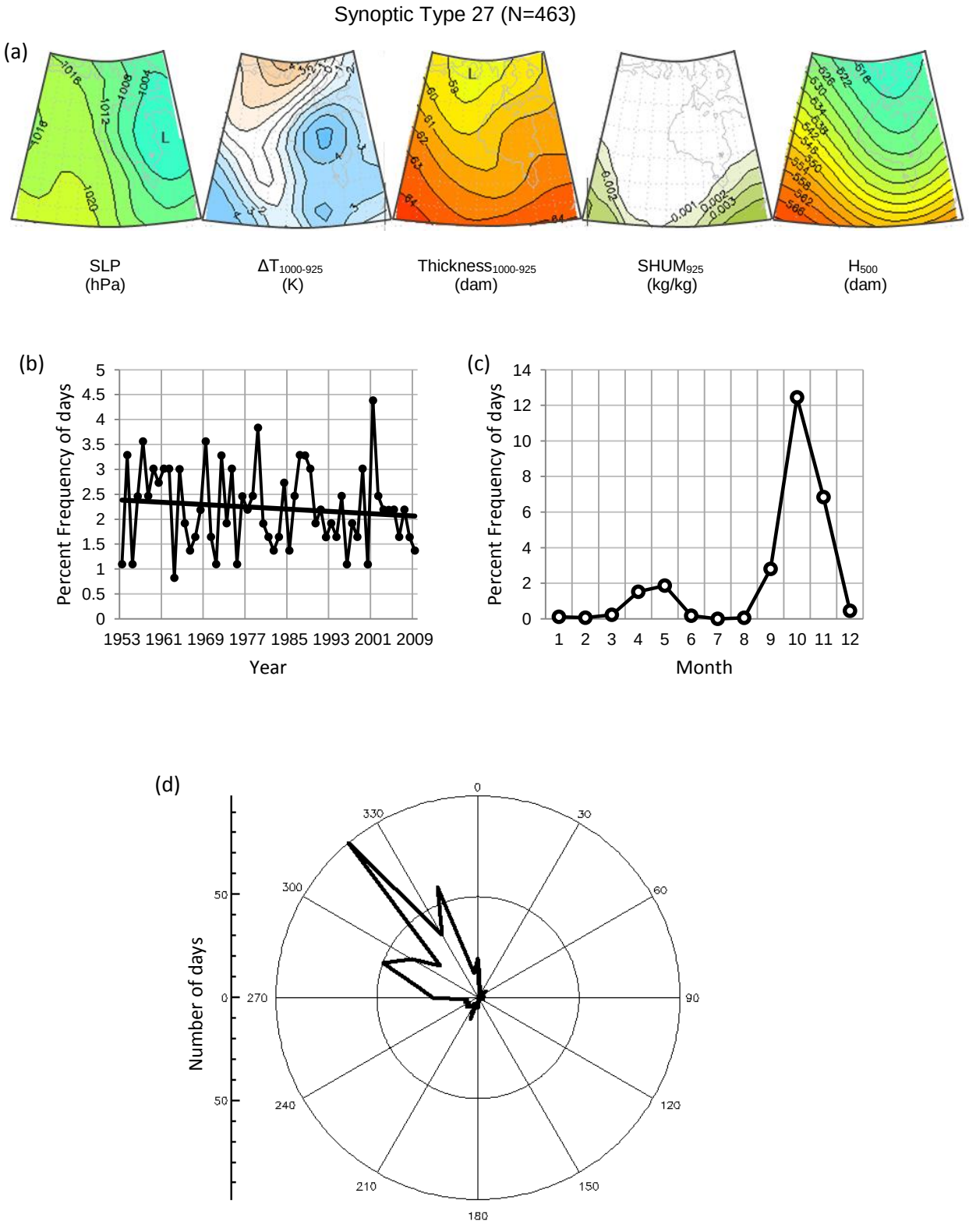

Figure 59: Synoptic Type 27 (a) composite maps, (b) annual percent type frequencies, (c) monthly percent type frequencies and (d) wind rose diagram displaying surface winds observed in Churchill at 12:00 GMT during this synoptic type

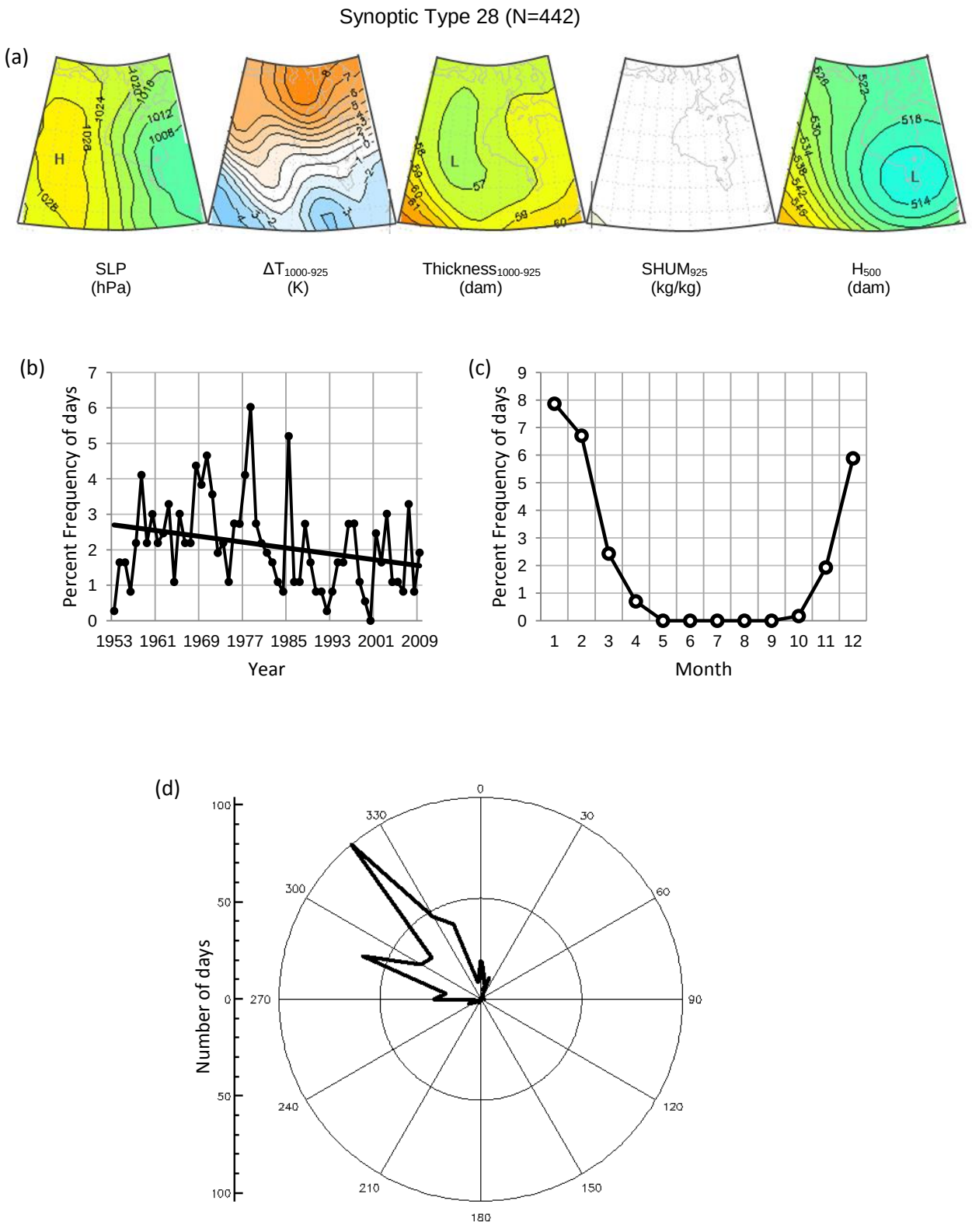

Figure 60: Synoptic Type 28 (a) composite maps, (b) annual percent type frequencies, (c) monthly percent type frequencies and (d) wind rose diagram displaying surface winds observed in Churchill at 12:00 GMT during this synoptic type

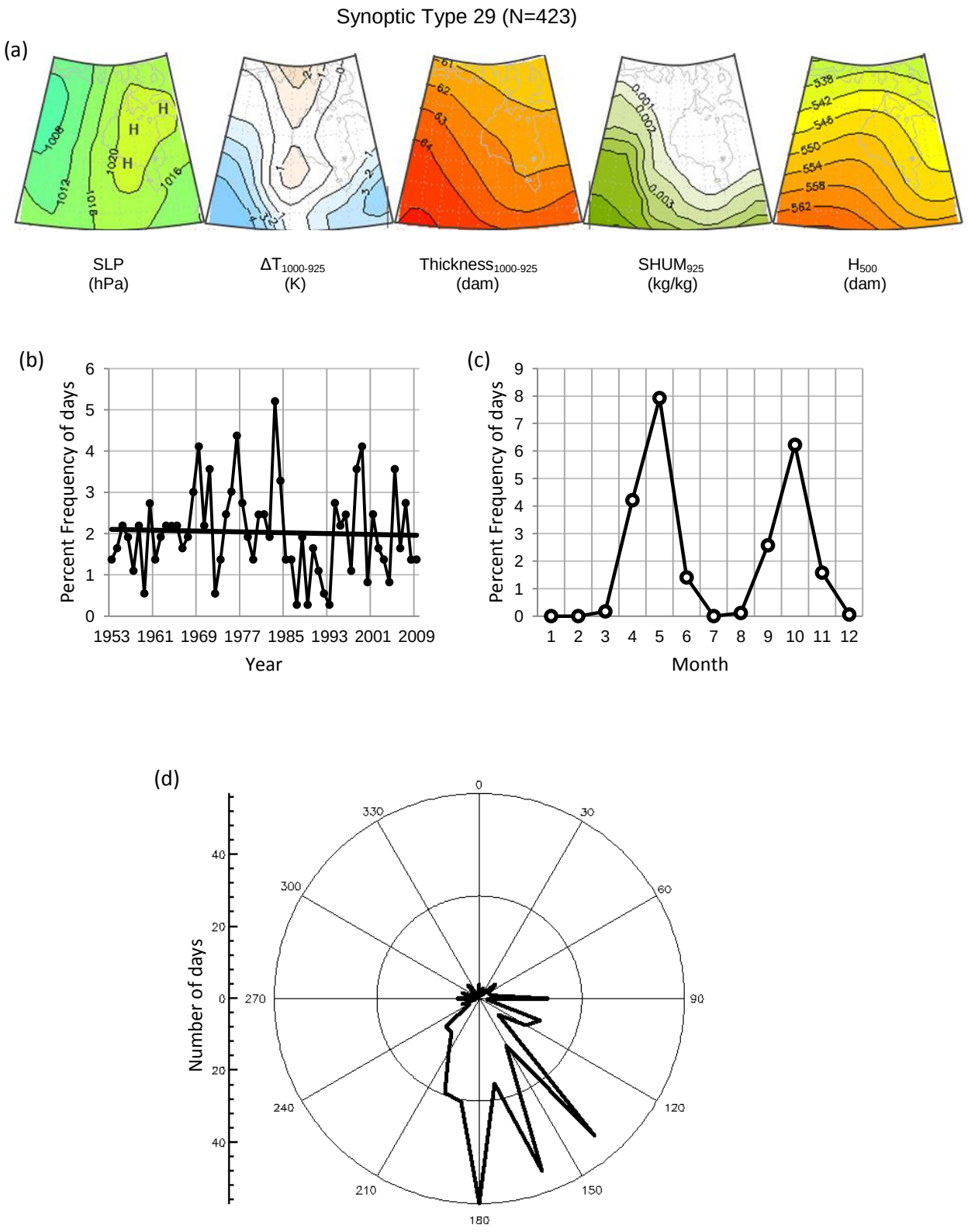

Figure 61: Synoptic Type 29 (a) composite maps, (b) annual percent type frequencies, (c) monthly percent type frequencies and (d) wind rose diagram displaying surface winds observed in Churchill at 12:00 GMT during this synoptic type

Type-30 is a predominantly late fall and early spring pattern (Figure 62). In some ways, this pattern is similar to Type-25, with ridging of the thickness contours over Hudson Bay and very low 500 mb heights across most of the region. However, unlike Type-25, Type-30 is characterized by low SLP values in the southeast quadrant of the study region and relatively high SLP across the rest of the study region. This facilitates more northwesterly surface winds in Churchill. A total of 409 days were classified as Type-30, or an average of 7 days per year.

Type-31 is another type that occurs between October and April (Figure 63). During a Type-31 event, a trough of low SLP extends north over the southern portion of Hudson Bay. Temperature lapse rates are depressed over the bay. Winds observed in Churchill during a Type-31 event are typically from the west or northwest. A total of 385 days were classified as Type-31, or an average of 6.5 days per year.

Type-32 is another pattern that frequently occurs in the late fall (November to December) (Figure 64). Type-32 has some similar elements to Type-27, with negative low-level temperature lapse rates over Hudson Bay, lower thicknesses between 1000 and 925 mb over the west side of Hudson Bay compared to the east, and very low 500 mb heights across much of the study region. During a Type-32 event low SLP is confined to the northeast quadrant of the study region and high SLP values are observed across much of the southwest. Winds in Churchill during a Type-32 event are typically out of the west. A total of 302 days were classified as Type-32, or an average of 5 days per year.

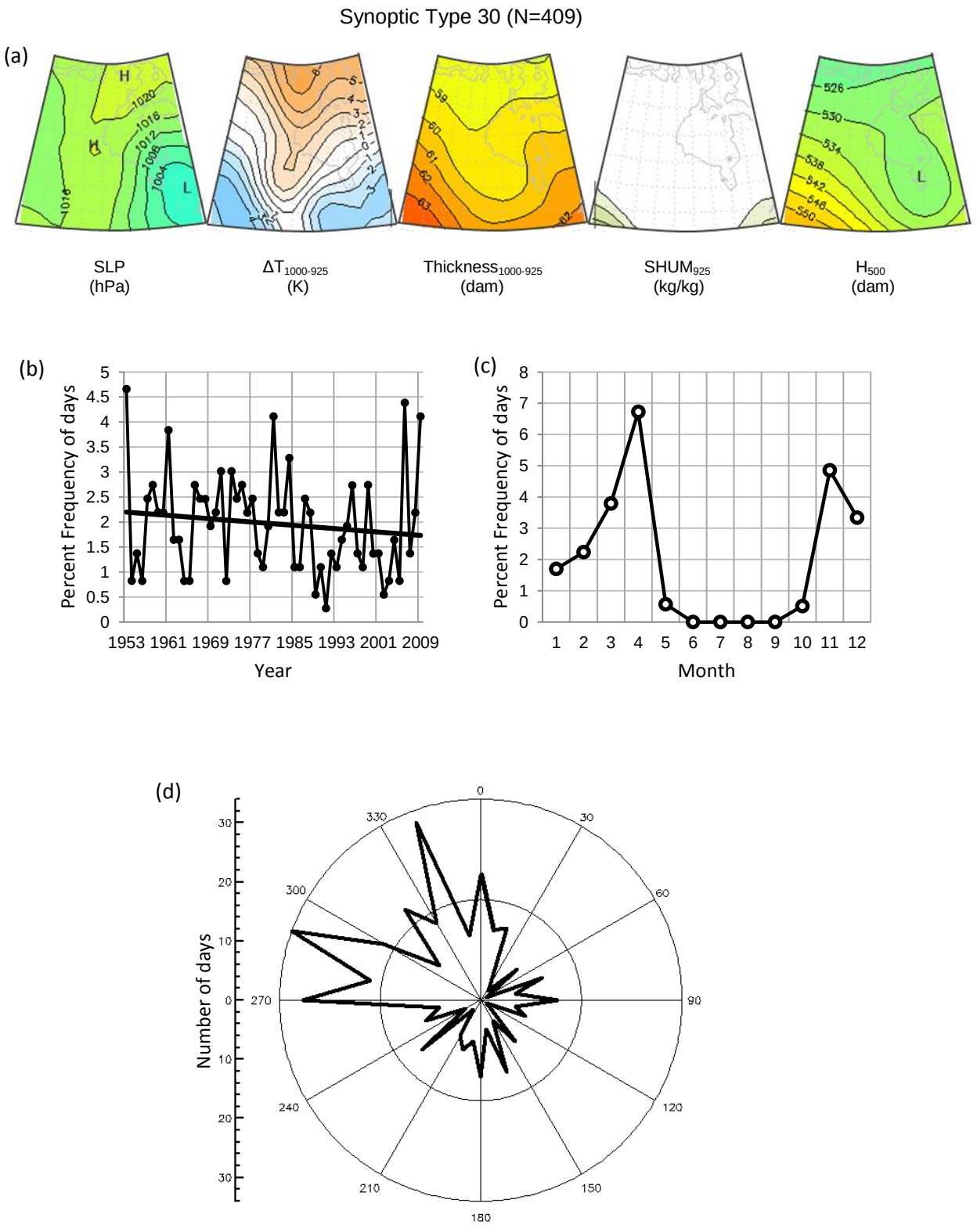

Figure 62: Synoptic Type 30 (a) composite maps, (b) annual percent type frequencies, (c) monthly percent type frequencies and (d) wind rose diagram displaying surface winds observed in Churchill at 12:00 GMT during this synoptic type

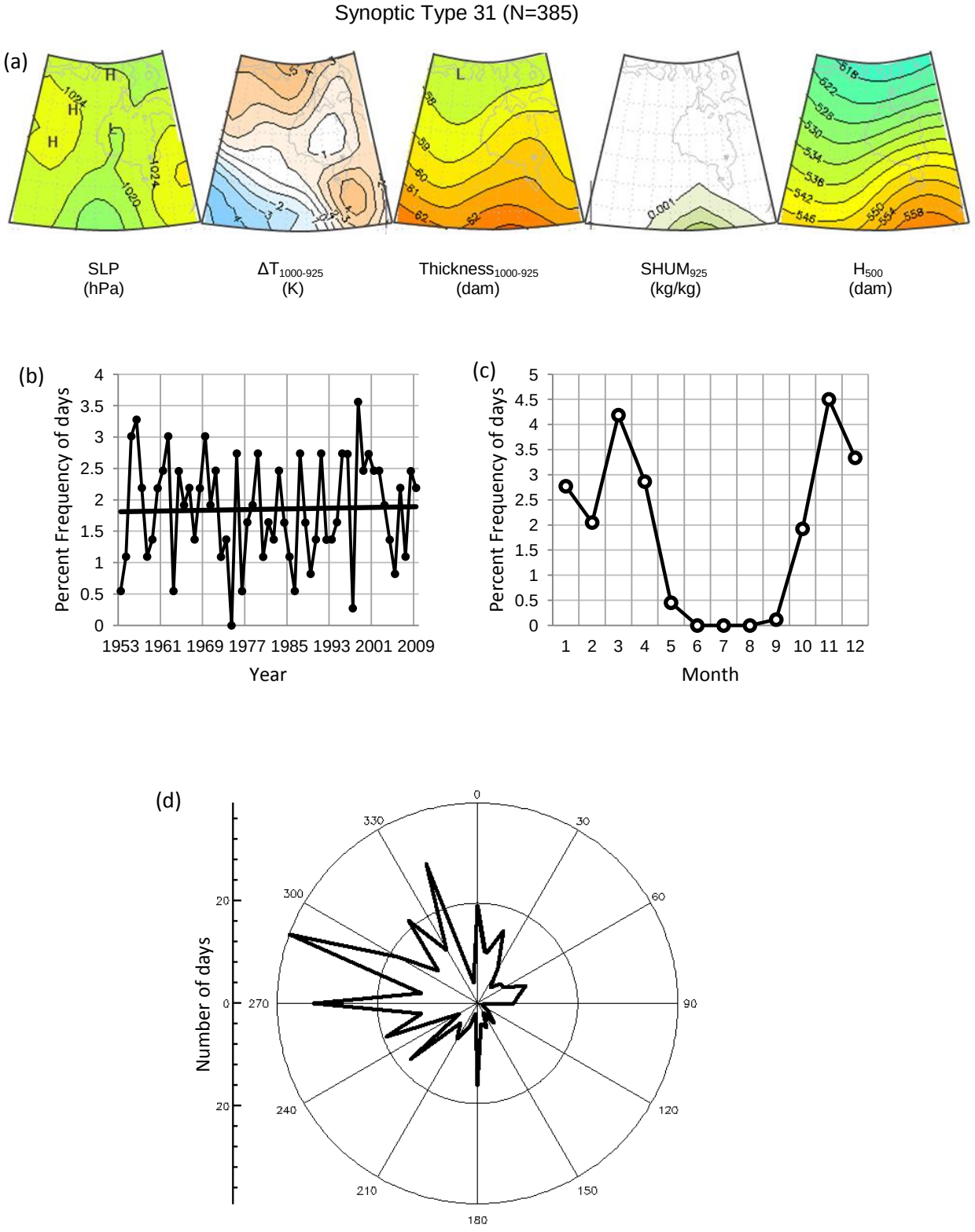

Figure 63: Synoptic Type 31 (a) composite maps, (b) annual percent type frequencies, (c) monthly percent type frequencies and (d) wind rose diagram displaying surface winds observed in Churchill at 12:00 GMT during this synoptic type

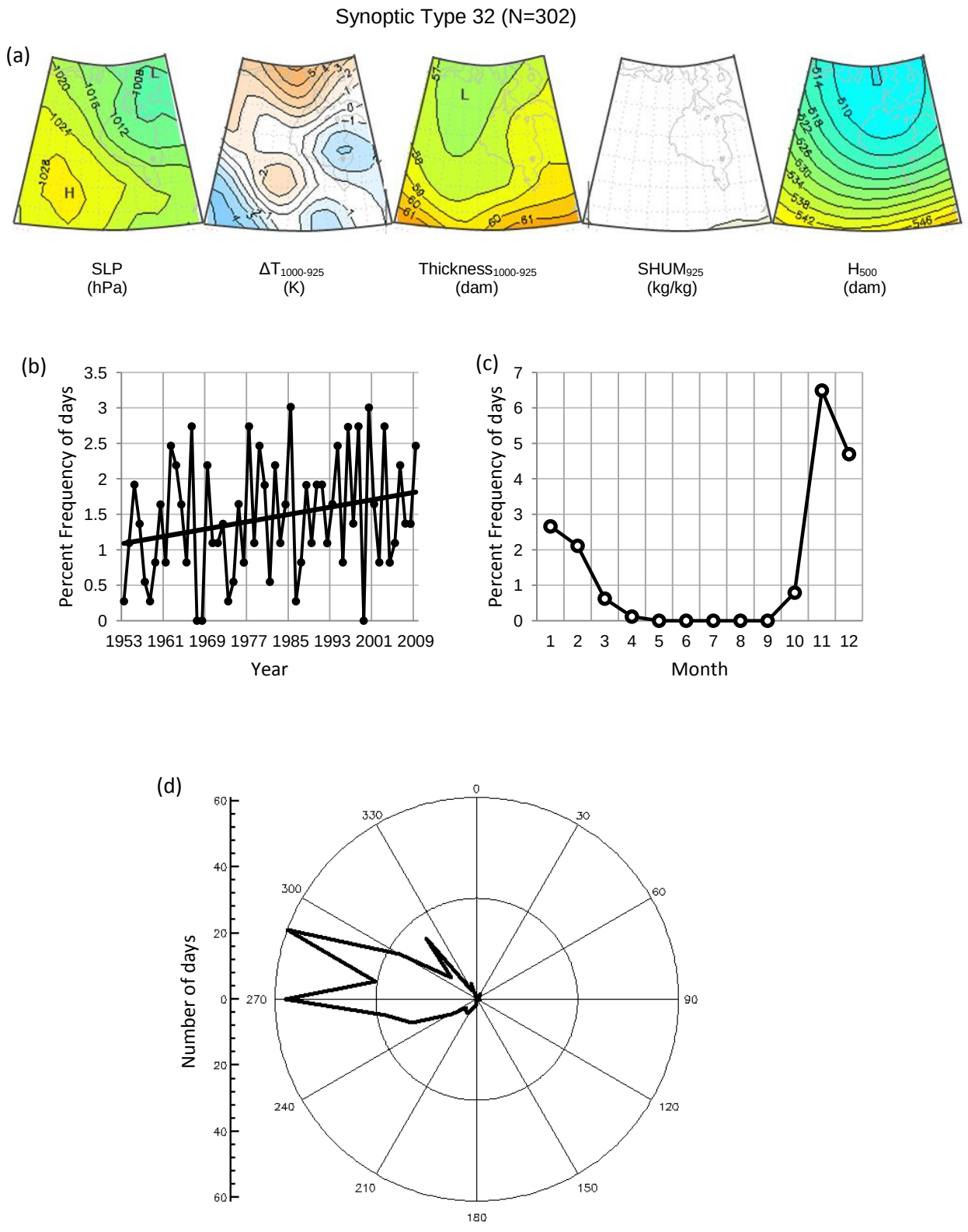

Figure 64: Synoptic Type 32 (a) composite maps, (b) annual percent type frequencies, (c) monthly percent type frequencies and (d) wind rose diagram displaying surface winds observed in Churchill at 12:00 GMT during this synoptic type

Type-33 is another pattern that occurs almost exclusively during the fall (peaks during the month of November) (Figure 65). This type can be described as a more 'extreme' version of Type-27 and Type-32. Low SLP values are centred over Hudson Bay, generating surface winds in Churchill that are from the northwest. A total of 297 days were classified as Type-33, or an average of 5 days per year.

Finally, Type-34 is a winter pattern that peaks during December and January (Figure 66). This pattern is very similar to Type-28; however during a Type-34 event low SLP is observed further northeast of Hudson Bay compared to Type-28. Winds observed in Churchill during a Type-34 event were typically out of the northwest. A total of 271 days were classified as Type-34, or an average of 4.5 days per year.

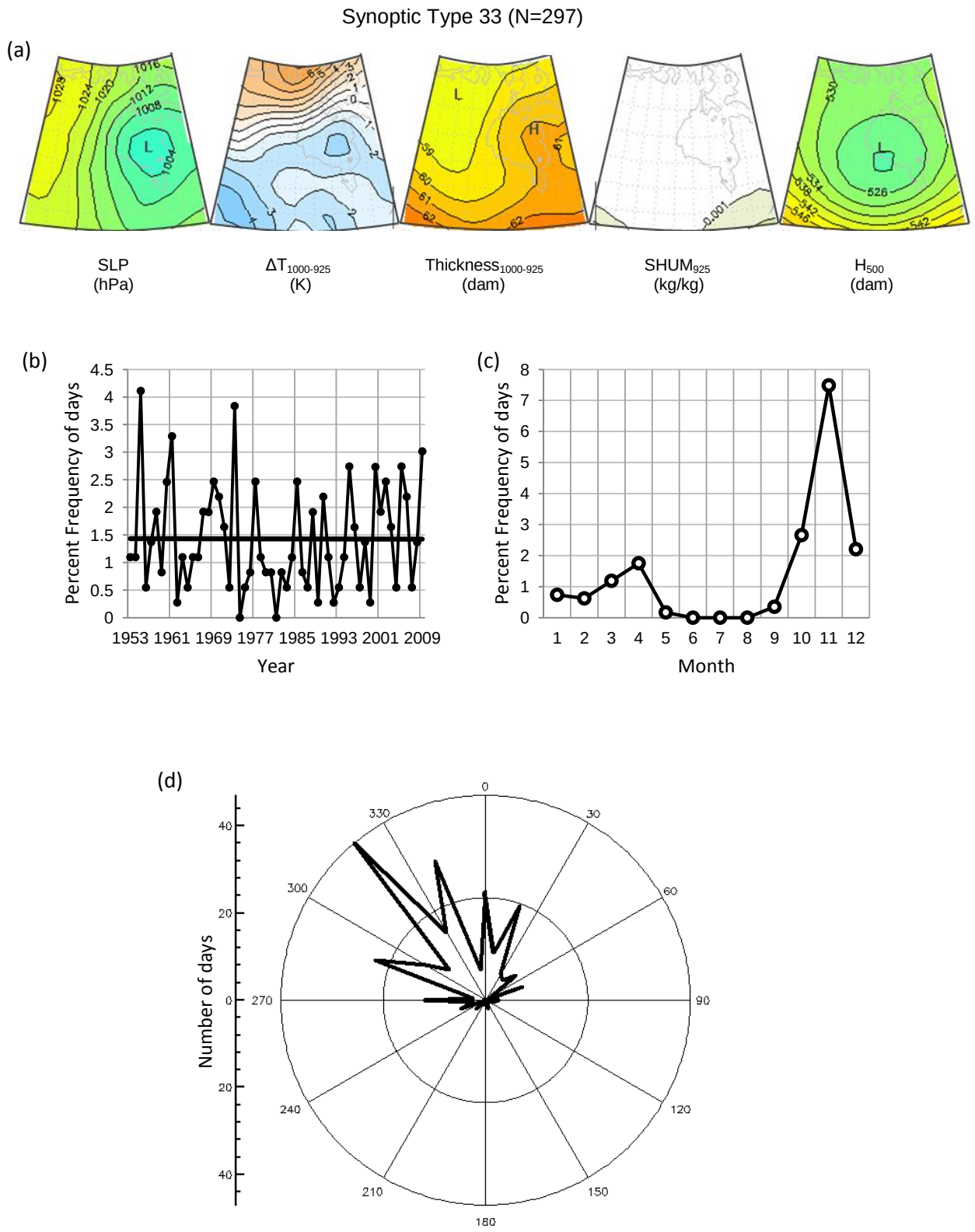

Figure 65: Synoptic Type 33 (a) composite maps, (b) annual percent type frequencies, (c) monthly percent type frequencies and (d) wind rose diagram displaying surface winds observed in Churchill at 12:00 GMT during this synoptic type

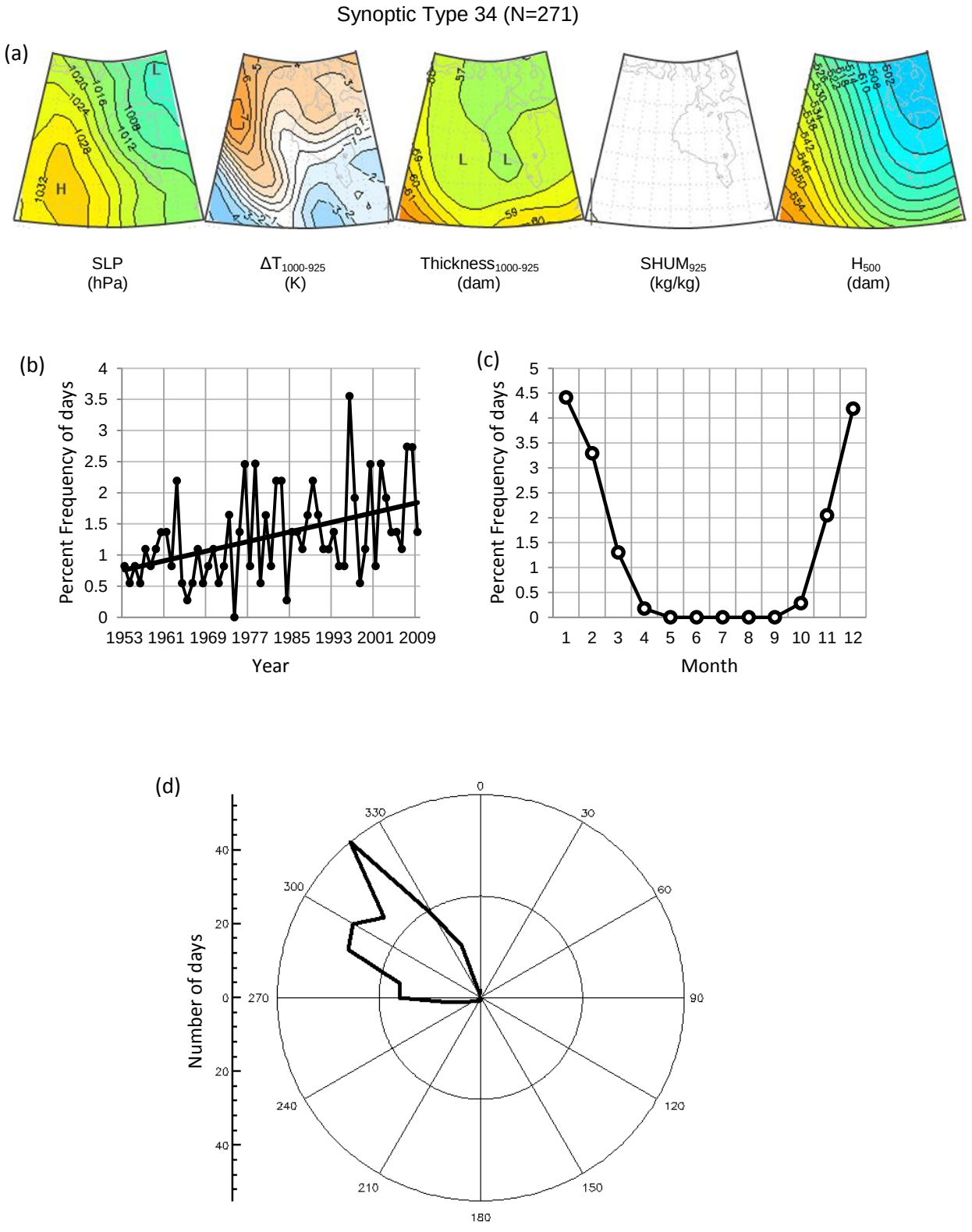

Figure 66: Synoptic Type 34 (a) composite maps, (b) annual percent type frequencies, (c) monthly percent type frequencies and (d) wind rose diagram displaying surface winds observed in Churchill at 12:00 GMT during this synoptic type

5.5 Synoptic Classification and Surface Temperature Anomalies

A comparison between each synoptic type and the average daily surface temperatures in Churchill was completed. For the sake of simplicity, no attempt was made to take into account any trend in daily temperature. Positive average daily temperature anomalies imply that the synoptic pattern generally resulted in warmer than average surface temperatures in Churchill. Negative average temperature anomalies imply the opposite (Figure 67).

As expected, it was found that synoptic types associated with southerly winds (and therefore presumably warmer air) were also associated with higher daily temperature anomalies. Similarly, synoptic types associated with northerly winds resulted in cooler air temperatures and lower temperature anomalies. The result also demonstrates that the expected surface winds, based on the orientation of the SLP isobars, closely match the observed surface winds for many of the types.

This result is important for two main reasons. First, since freezing rain forms when above-freezing air advects over below-freezing air, and such conditions are known to occur during the passage of a warm front, it was expected that synoptic types conducive to freezing rain would also be associated with higher temperature anomalies. Second, this analysis is a very simple 'verification' of the synoptic typing procedure, for if the classification did not relate well with surface temperature anomalies then the entire classification strategy may fall into question.

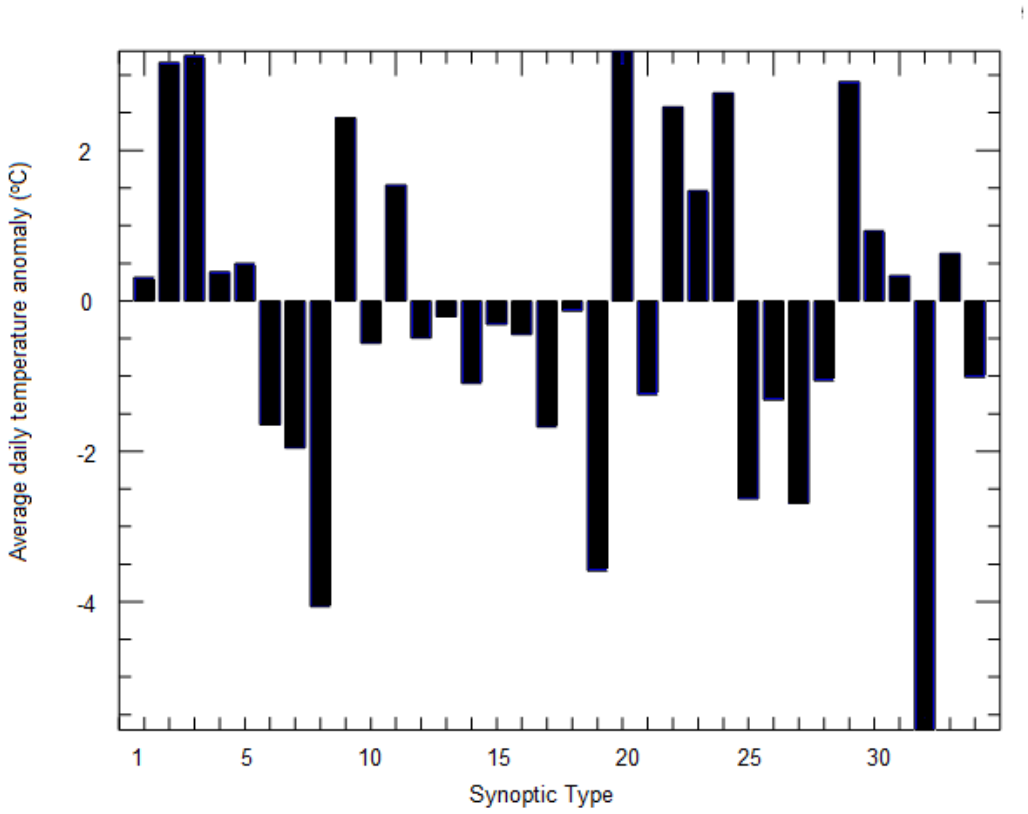

Figure 67: Average daily temperature anomaly in Churchill associated with each of the 34 synoptic types

5.6 Freezing Rain vs. Synoptic Classification

For each synoptic type, the number of freezing rain days and extreme freezing rain days (days with at least one freezing rain event with a duration at or above the 90th percentile) per type was counted (Figure 68). Type-20 was found to be the synoptic pattern most often associated with freezing rain (63 freezing rain days, including 21 extreme freezing rain events). Types 3, 9, 11, 13, 21, 22 and 24 each had between 10 and 19 freezing rain days associated with them. Seven synoptic types were associated with zero freezing rain days.

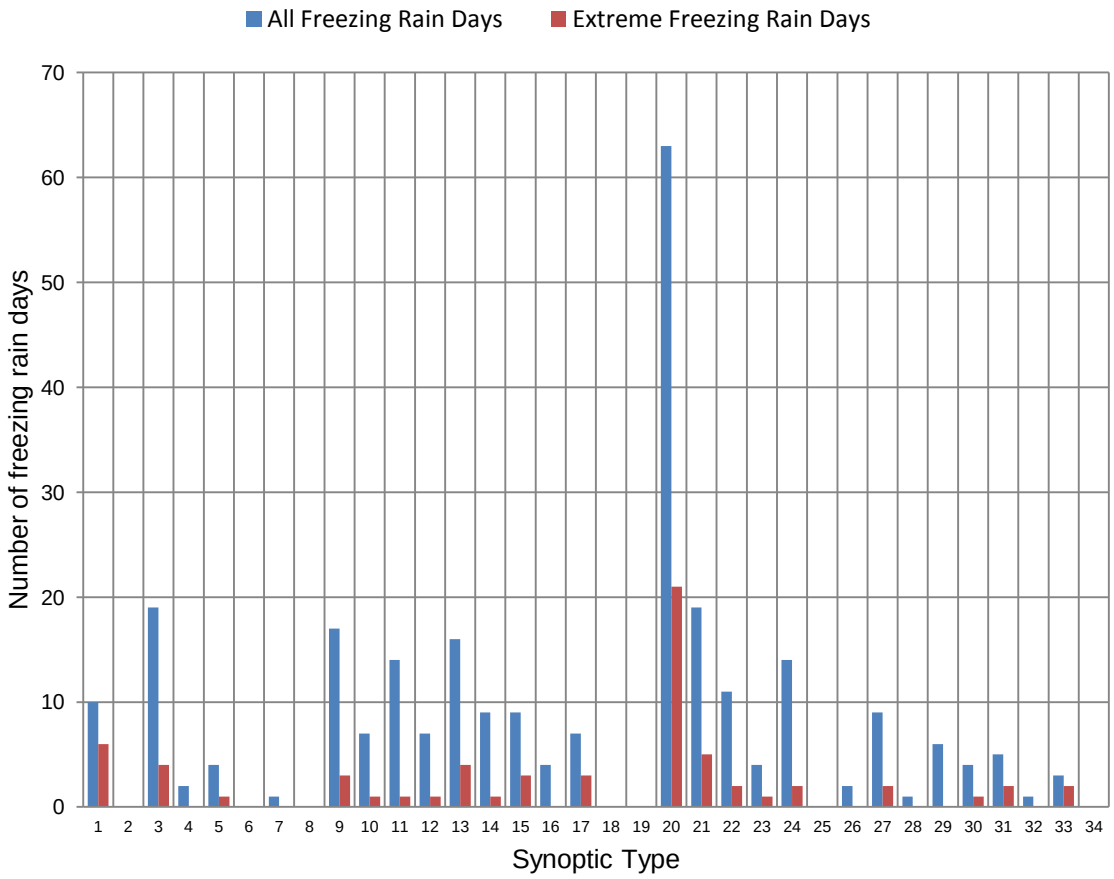

Figure 68: number of freezing rain days and extreme freezing rain days associated with each of the 34 synoptic types

Because some synoptic types occur so much more frequently throughout the year compared to other synoptic types, the relative percent frequencies of freezing rain days and extreme freezing rain days per synoptic type were also calculated (Figure 69). Again, Type-20 stands out from the rest of the types with 10.8 percent of all Type-20 events associated with at least one freezing rain event per day and 3.6 percent associated with at least one extreme freezing rain event per day.

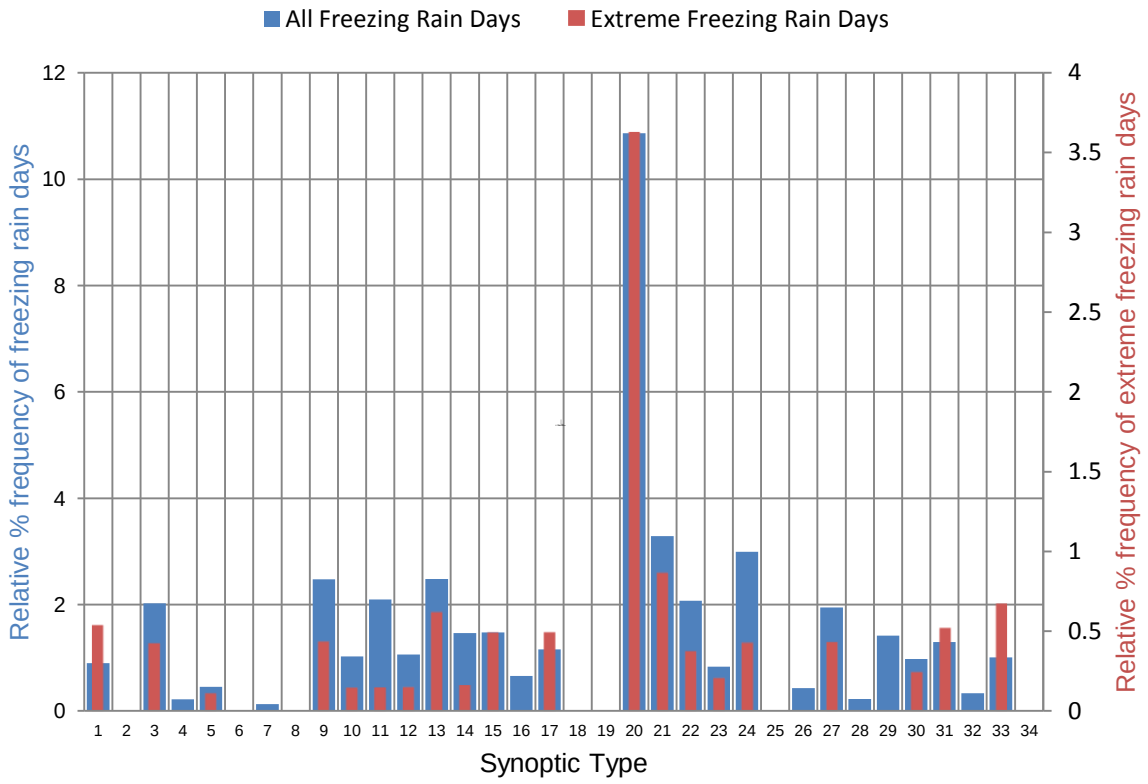

Figure 69: Relative percent frequencies of freezing rain days (blue) and extreme freezing rain days (red) per synoptic type

For each of the top eight freezing rain types identified above, the number of freezing rain events by month was counted (Figure 70). Type-3 freezing rain events occurred during the winter and early spring months (November to April), whereas types 13 and 24 were responsible for many of the fall freezing rain events (October November). Type 20 was responsible for most of the freezing rain events that occurred during April and May. Type-21 was found to occur during late spring and early summer freezing rain events (May and June). Similarly, for each of the top eight freezing rain types, the number of extreme freezing rain events per month was counted (Figure 71).

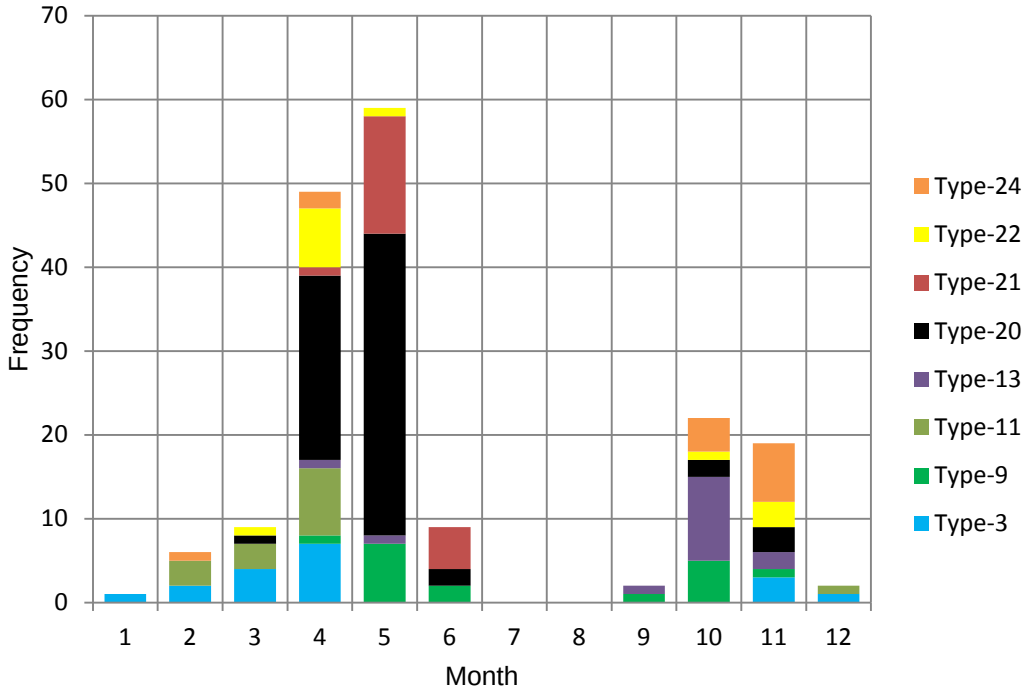

Figure 70: Number of freezing rain events counted per month for each of the top eight synoptic types associated with freezing rain events

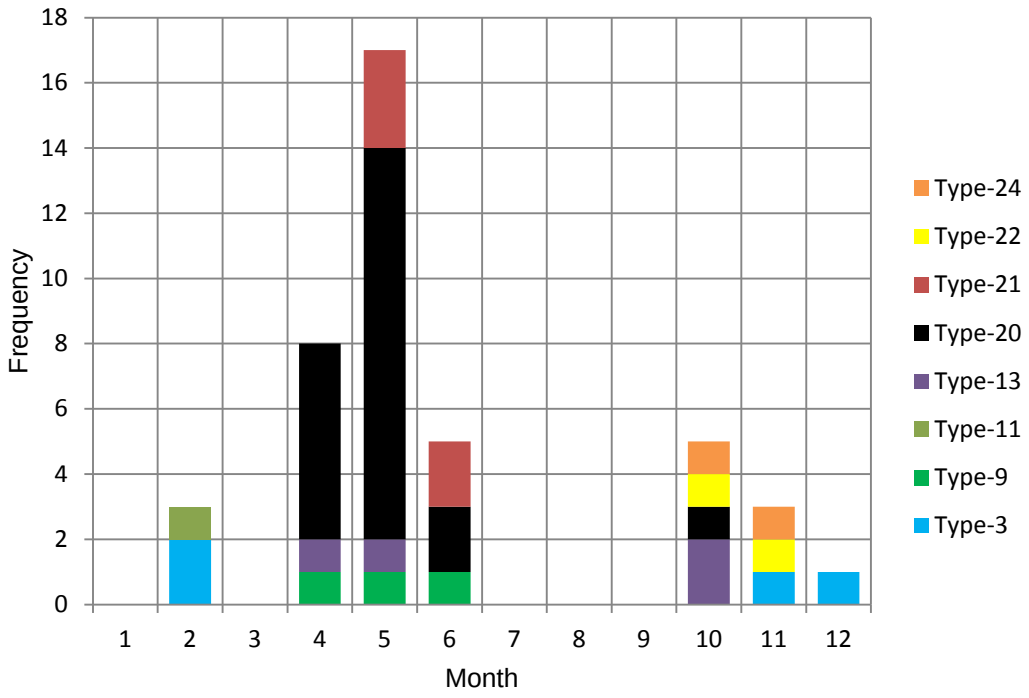

Figure 71: Number of extreme freezing rain events counted per month for each of the top eight synoptic types associated with freezing rain events

For comparison, the number of days associated with rain and snow during each synoptic type (and the relative percent frequency of rain and snow days per synoptic type) was counted (Figure 72 and Figure 73). Of all days classified as Type-20, 31.2 percent experienced at least one snow event and 27.4 percent experienced at least one rain event.

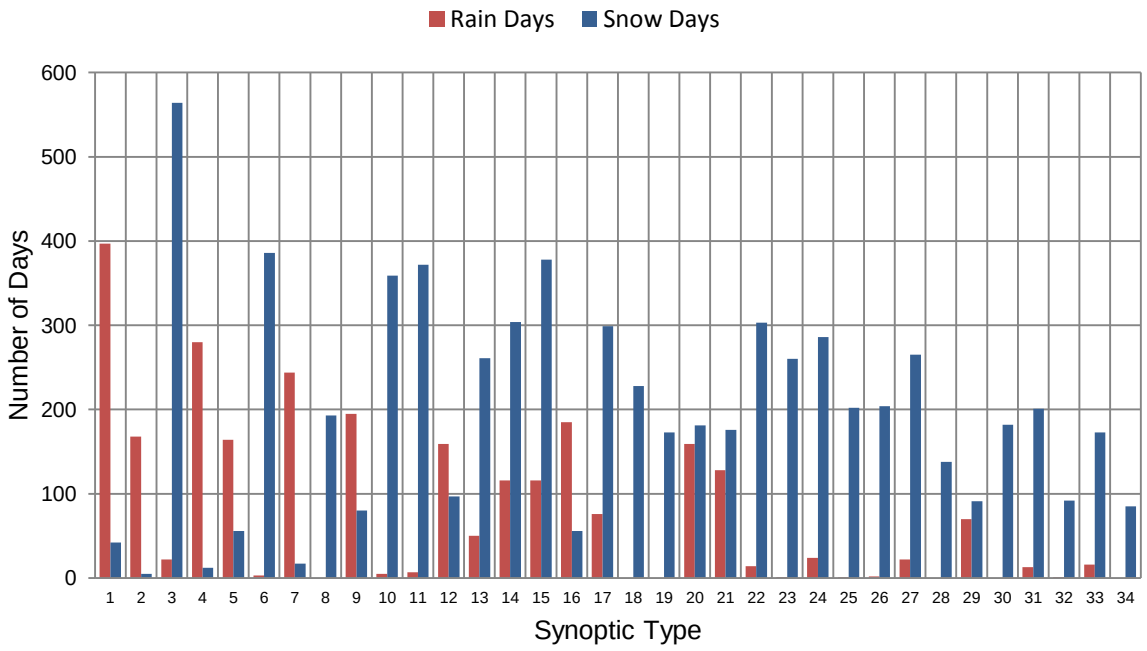

Figure 72: Number of days rain (red) and snow (blue) were observed during each synoptic type

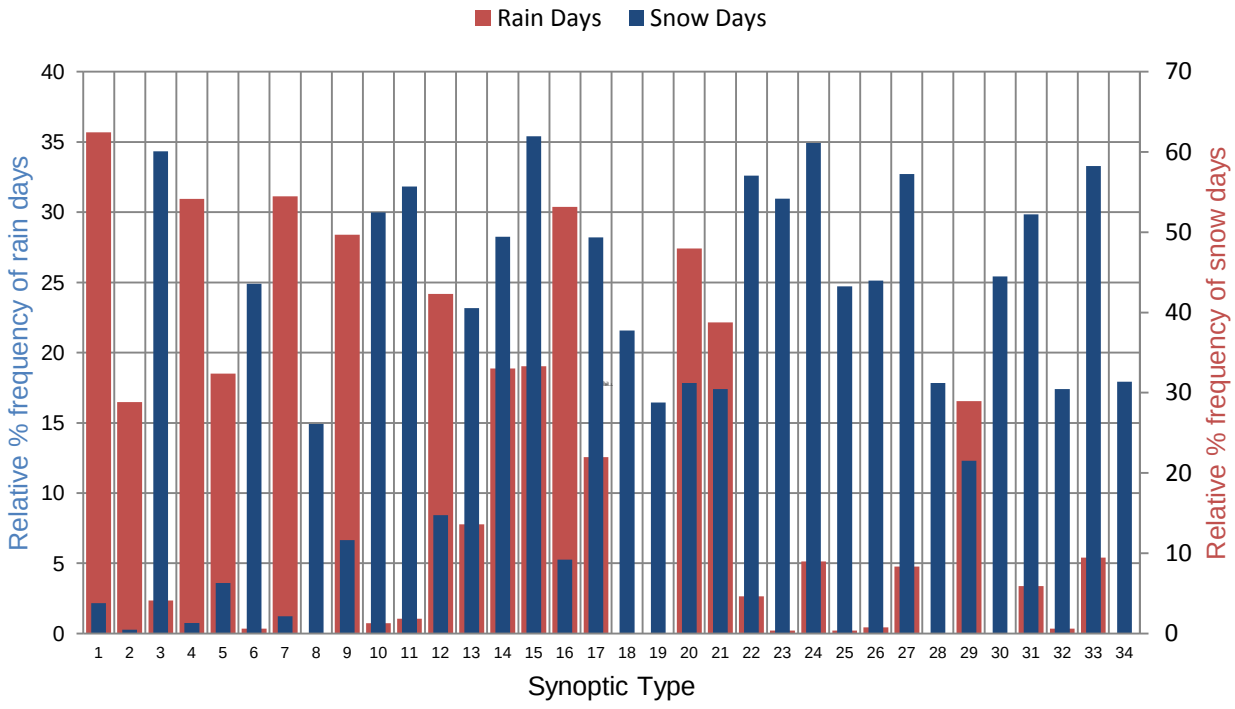

Figure 73: Relative percent frequency of rain days (red) and snow days (blue) per synoptic type

5.7 Freezing Rain Case Studies

The eight synoptic types which had the most freezing rain events associated with them were analyzed in more detail using case studies. In this case, the most recent freezing rain event associated with each of the eight synoptic types was selected for each case study.

5.7.1 Case Study #1 – April 15, 2009 (Synoptic Type 20)

Freezing rain case study number one is an example of a freezing rain event observed during a day classified as Synoptic Type 20, the type that occurred during nearly half of all freezing rain events observed in Churchill. In the case of April 15, 2009, freezing rain was observed off and on for a total of thirteen hours from 18:00 GMT on April 14th to 19:00 GMT on April 15th. This event was also classified as extreme (its duration exceeded the 90th percentile of freezing rain durations).

Surface observations made in Churchill many hours prior to the event indicate that snow was falling during the morning of April 14th. Temperatures rose throughout the day (and continued to rise overnight) and eventually the precipitation transformed from snow to freezing rain. The dew point temperatures rose alongside air temperature, at times indicating that the surface air was at saturation. During this same time period, station barometric pressure fell (Figure 74).

At 00:00 GMT and 12:00 GMT the soundings made in Churchill on April 15th, steep temperature inversions with maximum temperatures of nearly 8°C were recorded. The noses of these inversions were between the 1000 mb and 900 mb pressure surfaces.

Furthermore, dew point depressions throughout the first three to five kilometers above the surface indicate that this air was also at or very near saturation.

Forty-eight hours prior to April 15th, at the synoptic scale, a trough of low SLP, which at times appears to be a closed cyclone, was moving into the study region from the southwest. Ahead of this low pressure, relatively strong on-shore winds (winds from the east) were visible near the Churchill area. It is likely that these on-shore winds were suppressing surface air temperatures along the west coast of Hudson Bay. At 925 mb, winds throughout the lower portion of the study region were from the south, creating a ridge of relatively high temperatures that begins to propagate north towards Churchill. By 12:00 GMT on April 15th, temperatures at 925 mb over the Churchill were significantly warmer than those at the surface. At 500 mb a ridge of higher geopotential height can be seen moving into the study region. By the time freezing rain was observed at the surface, this ridge starts to move off to the east. West of the 500 mb ridge (and east of the 500 mb trough) a southwest and diverging flow high over the southwest portion of the study region exists, and possibly explains the source of the cyclonic circulation observed at the surface as well as the general southwest to northeast track of this cyclone (Figure 75).

Overall, this case study very clearly shows how freezing rain can develop when warm, moist air advects overtop cold surface air. The presence of warm, moist air aloft is most likely explained by the presence of a warm front. It is also likely that the strong, easterly surface winds present over Churchill helped depress the surface temperatures below the freezing point.

Case Study #1 - April 15, 2009

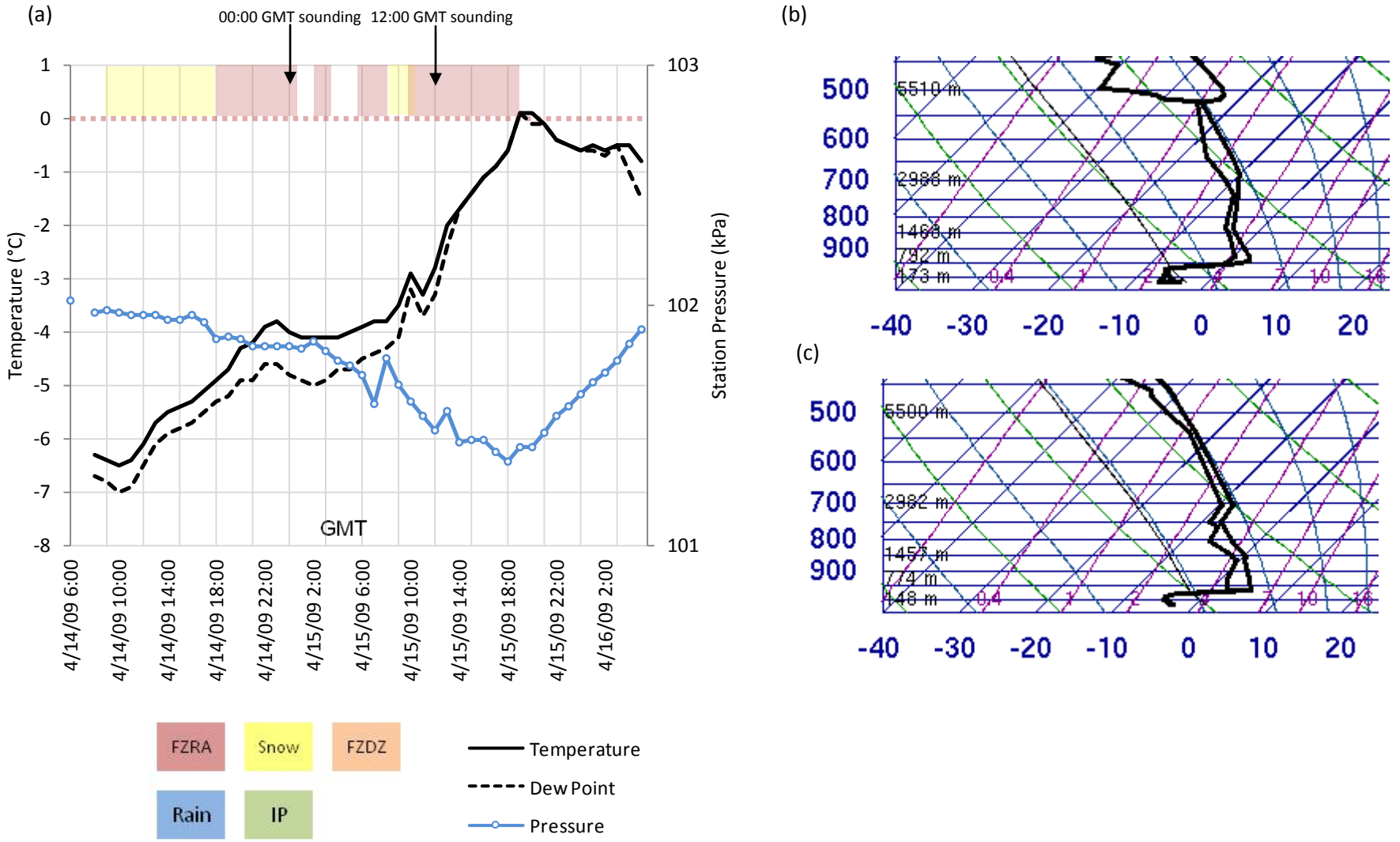

Figure 74: Case study #1 - April 15th, 2009 (a) hourly meteorological observations made in Churchill (b) 00:00 GMT Skew-T diagram (c) 12:00 GMT Skew-T diagram (source: Environment Canada, 2011 and University of Wyoming, 2012)

	04/15/2009 00:00 GMT	04/15/2009 12:00 GMT	04/15/2009 00:00 GMT	04/15/2009 12:00 GMT
SLP	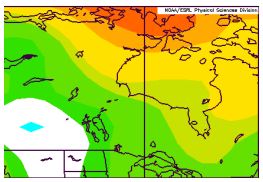	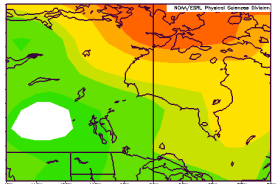	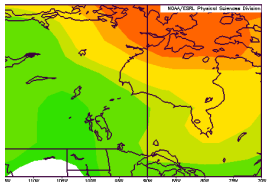	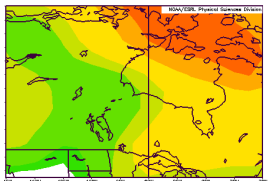
Surface Wind	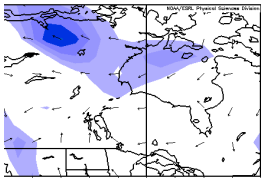	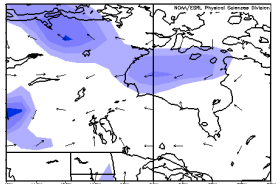	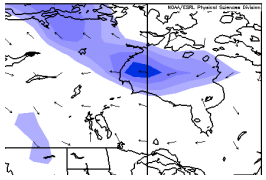	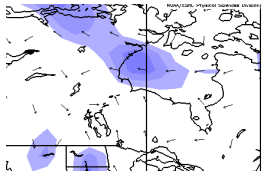
Surface Air Temp	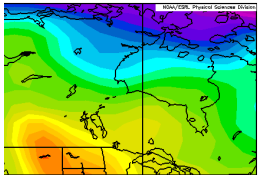	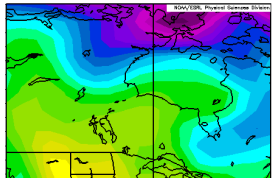	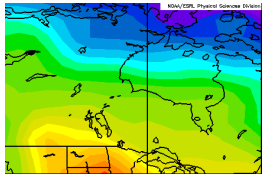	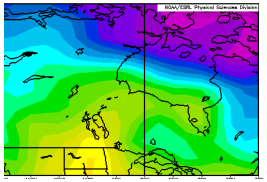
925 mb Air Temp	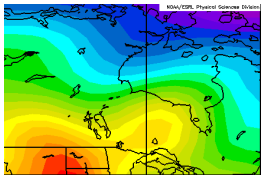	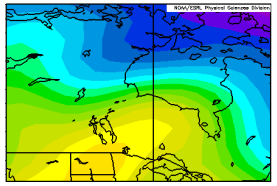	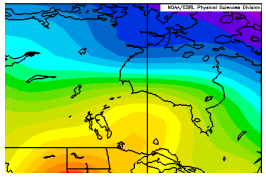	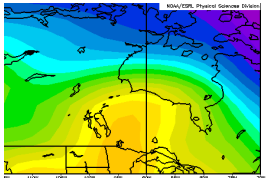
500 mb Height	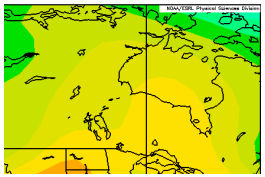	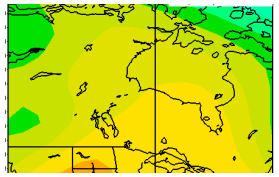	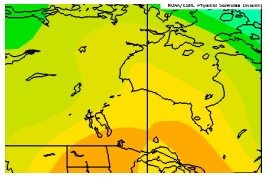	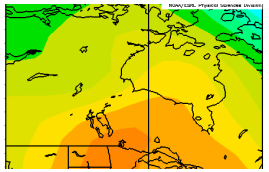

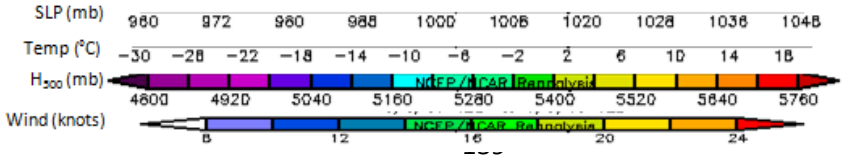

source: NCEP/NCAR re-analysis (2012)

Figure 75: SLP, surface winds, surface air temperature, 925mb air temperature and 500mb geopotential height maps 48-hours prior the freezing rain event on April 15th, 2009

5.7.2 Case Study #2 – January 2, 2007 (Synoptic Type 3)

Based on the average freezing rain monthly frequencies, observing freezing rain in early January is relatively rare. This is most likely because air temperatures at the surface and with height are generally too cold to support liquid water. However, it is common for very steep temperatures inversions to form during winter, when low cloud cover can trap heat that escapes readily from the snow covered surface (Wu et al., 2004). In the case of January 2nd, 2007, categorized as a Type-3, an especially steep temperature inversion allowed air temperatures above the surface to rise above zero for a small period of time, therefore facilitating the development of freezing rain.

Forty-eight hours prior to the freezing rain event, barometric pressure in Churchill began to fall. The evening before the event, surface temperatures rose and reached a maximum daytime temperature of -2°C. As temperatures began to rise, snow was observed in Churchill. During one hour, freezing rain was observed intermixed with snow. The 00:00 GMT and 12:00 GMT soundings on January 2nd clearly show a very steep temperature inversion had formed in the early hours of the day (Figure 76).

The synoptic maps leading up to the freezing rain event show that a trough of low pressure was moving into the study region from the west/northwest. Forty-eight hours prior to the freezing rain event, surface winds in the Churchill area were fairly strong and from the west as the cyclonic system passed north of Hudson Bay. This surface flow most likely supported mild winter daytime temperatures throughout the Hudson Bay region at this time. However, surface temperatures quickly fell over Hudson Bay as these winds began to weaken and the warm air supply from the west was cut-off. At 925 mb

the southwesterly flow was sufficient to maintain mild temperatures. Hudson Bay remained under the influence of very low surface temperatures, such that temperatures in Churchill reached -17°C the night prior to the freezing rain event. By 00:00 GMT January 2nd, a new trough of low pressure was beginning to manifest itself over the northwest portion of the study region. This cyclonic system facilitated a southwesterly flow over the region, again resulting in more mild temperatures (Figure 77).

It is difficult to determine how severe this freezing rain event was, mainly because it is unclear, based on the Environment Canada records, how much freezing rain fell compared to snowfall also observed during the same hour. Nevertheless, this case study is a good example of how quickly temperatures can become depressed over Churchill when easterly winds blow cold air off of Hudson Bay.

Case Study #2 – January 2, 2007

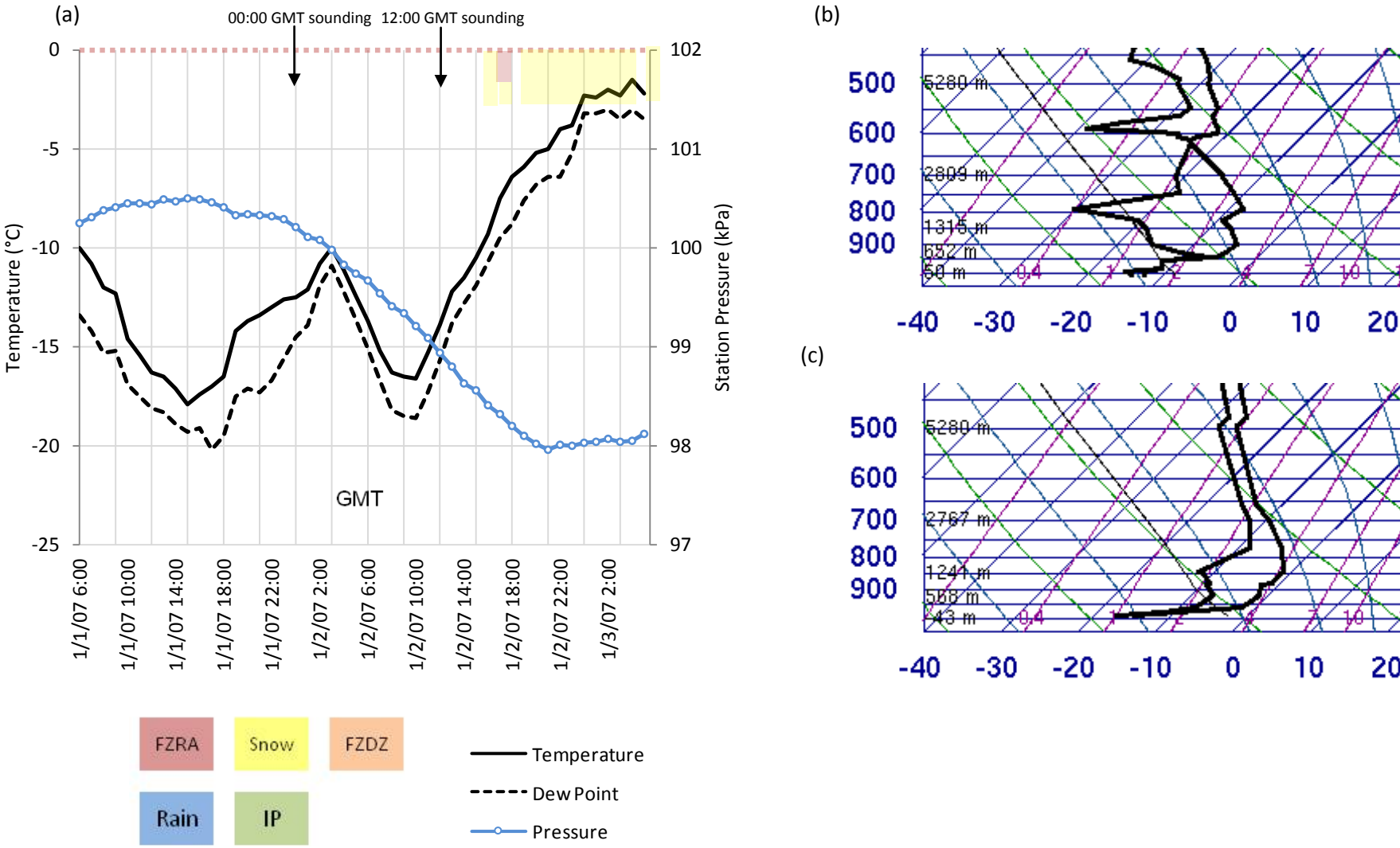

Figure 76: Case study #2 – January 2nd, 2007 (a) hourly meteorological observations made in Churchill (b) 00:00 GMT Skew-T diagram (c) 12:00 GMT Skew-T diagram (source: Environment Canada, 2011 and University of Wyoming, 2012)

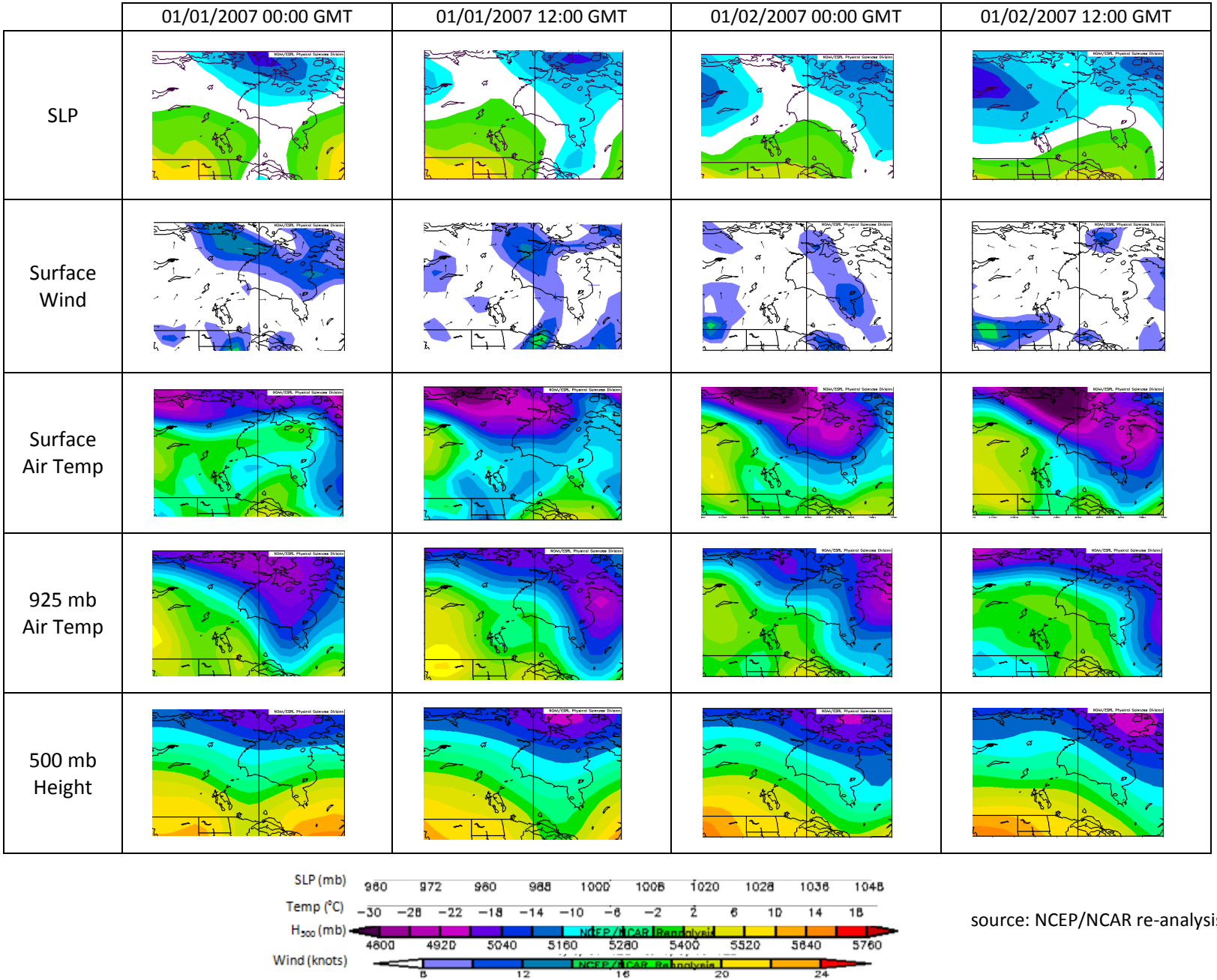

source: NCEP/NCAR re-analysis (2012)

Figure 77: SLP, surface winds, surface air temperature, 925mb air temperature and 500mb geopotential height maps 48-hours prior the freezing rain event on January 2nd, 2007

5.7.3 Case study #3 – April 25, 2007 (Synoptic Type 9)

Synoptic Type 9 was found to occur frequently during the spring and early summer as well as during late summer and fall. However, compared to Type-20 events, very few (18) Type-9 events were associated with freezing rain events. This is likely because surface winds observed in Churchill tended to be out of the south during a Type-9 event rather than from the north or east, and therefore there was a lack of cold surface air moving on-shore from over Hudson Bay. Also, the position of low SLP on the Type-9 composite map relative to Churchill may mean that relatively few warm fronts pass directly over Churchill.

Prior to the freezing rain event on April 25th, 2007, surface temperatures were consistently below zero. Then, on the day of the event, the temperature rose to nearly 5°C. Many hours after the freezing rain was reported, rain was observed in Churchill. A full day before the freezing rain event and for many hours after, station barometric pressure fell (Figure 78).

At the synoptic scale on April 24th at 00:00 GMT, low SLP to the east of Hudson Bay and high sea level pressure to the west generated strong northwest surface winds over much of the Hudson Bay area (Figure 79). This low level flow was supported by a large trough at the 500 mb level over the Bay. These strong winds helped lower the surface and 925 mb temperatures over the Bay prior to the April 25th freezing rain event. Twelve hours prior to the event, a new cyclonic system can be seen developing in the central-west portion of the SLP map. Surface winds started to change from northwest to south. At 925 mb, a region of very warm air southwest of Hudson Bay started to move

northward towards the Churchill region. By this time, the trough at the 500 mb was beginning to weaken, being replaced a ridge (to the west of Churchill). By 12:00 GMT on April 25th, much of the cold air over Churchill was replaced by this warm air. The freezing rain event occurred at 02:00 on April 25th, during this transition from cold to warm air.

Overall, this case study is an example of how freezing rain can form during a transition from cold to warm synoptic patterns, even when a well defined warm front may not be present. In place of a warm front, a temperature inversion produced the right thermal conditions during the early morning hours of April 25th to facilitate the production of freezing rain before the surface temperature rose very quickly above the freezing point.

Case Study #3 – April 25, 2007

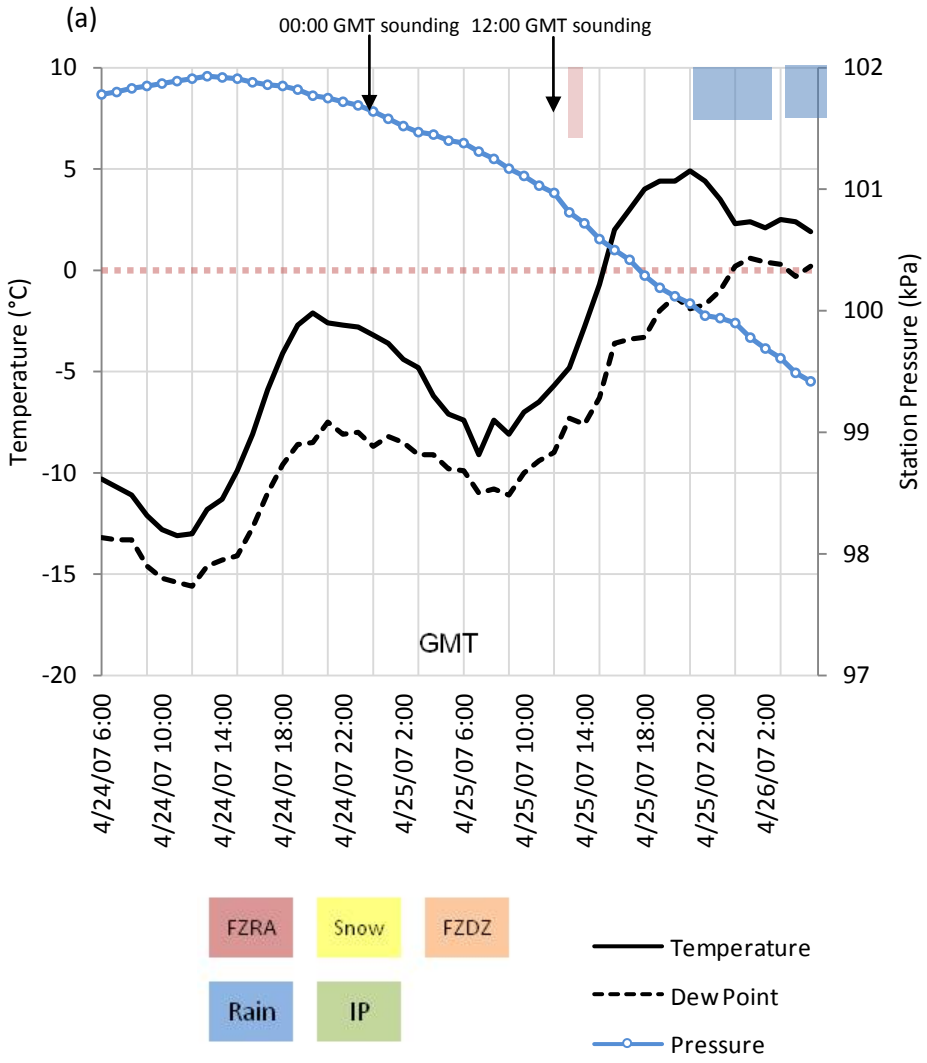

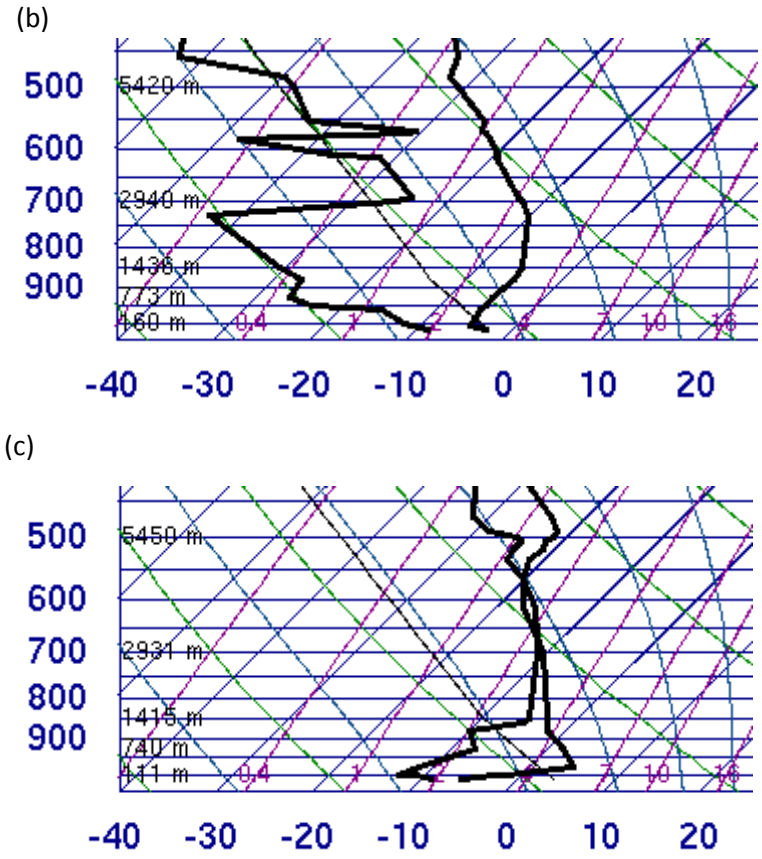

Figure 78: Case study #3 - April 25th, 2007 (a) hourly meteorological observations made in Churchill (b) 00:00 GMT Skew-T diagram (c) 12:00 GMT Skew-T diagram (source: Environment Canada, 2011 and University of Wyoming, 2012)

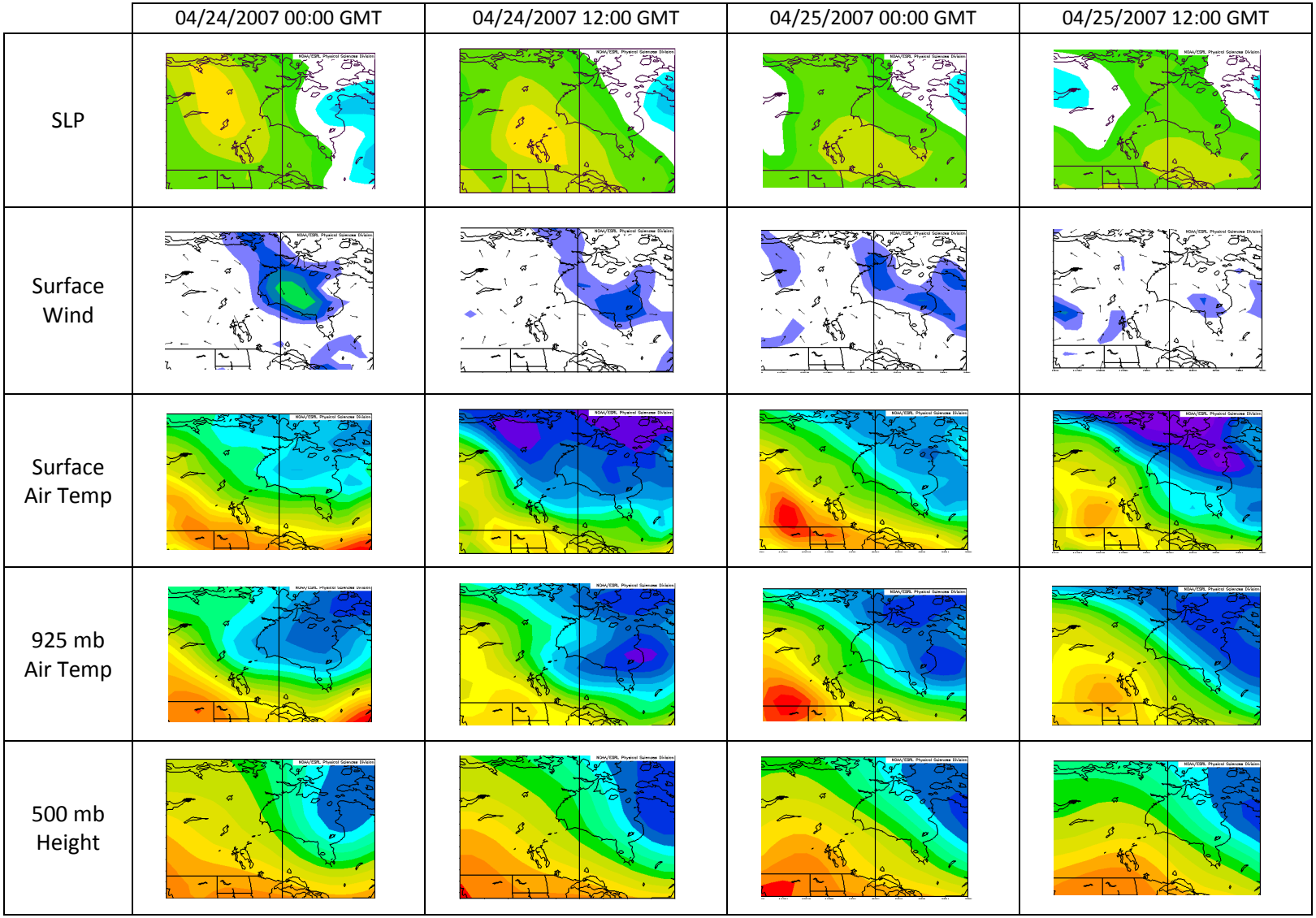

source: NCEP/NCAR re-analysis (2012)

Figure 79: SLP, surface winds, surface air temperature, 925mb air temperature and 500mb geopotential height maps 48-hours prior the freezing rain event on April 25th, 2007

5.7.4 Case Study #4 – March 30, 2005 (Synoptic Type 11)

In contrast to days categorized as Type-9, it seems likely that Type-11 days are generally too cool to support the frequent development of freezing rain over Churchill. This type most frequently occurs in March, when daytime temperatures can often remain well below zero at the surface and at height. Most of the precipitation associated with Type-11 events is in the form of snow (Figure 73).

Freezing rain was observed intermittently between 02:00 GMT and 19:00 GMT on March 30th, and was accompanied by and intermixed with snow, freezing drizzle and ice pellets. During this extended period of mixed precipitation, temperatures rose in Churchill and station barometric pressure fell. On both the 00:00 GMT and 12:00 GMT soundings for March 30th, a very steep temperature inversion is visible at times, with temperatures at about 850 mb nearly 15°C warmer than at the surface. It is interesting to note that the nose of the inversion is slightly higher compared to the previous freezing rain case studies. This also means that the depth of the freezing layer is thicker and this may be one of the reasons why much of the precipitation that fell on this day was recorded as snow and ice pellets (Figure 80).

At the synoptic scale, many of the maps leading up to the March 30th freezing rain event look very similar to those recorded during the Type-20 freezing rain case study (Figure 81). A trough of low pressure at the surface moved into the study region from the southwest, drawn towards the Hudson Bay region by a ridging pattern at the 500 mb level. As the cyclonic system moved northeast, winds became very strong across most of Hudson Bay. In Churchill a strong east wind was recorded, drawing the cold Hudson Bay

air over the Churchill region. At 925 mb, a southerly wind advected more mild air from the south, generating a steep temperature inversion over much of the region. However, the ridge of warmer temperatures at 925 mb was located further east compared to some of the previous case studies. This means that the greatest potential for steep temperature inversions fell east of Churchill. Furthermore, by 12:00 GMT on March 30th, low-level wind flow in Churchill already was starting to blow out of the northwest, as the surface cyclone passes just south of Churchill.

Overall, this case study shows how a synoptic type frequently associated with snowfall in Churchill can also occasionally result in intermittent freezing rain by supporting very steep temperature inversions in the lower part of the atmosphere. The temperature inversion is most likely due to a passing warm front associated with a cyclonic system moving into the region from the southwest.

Case Study #4 – March 30, 2005

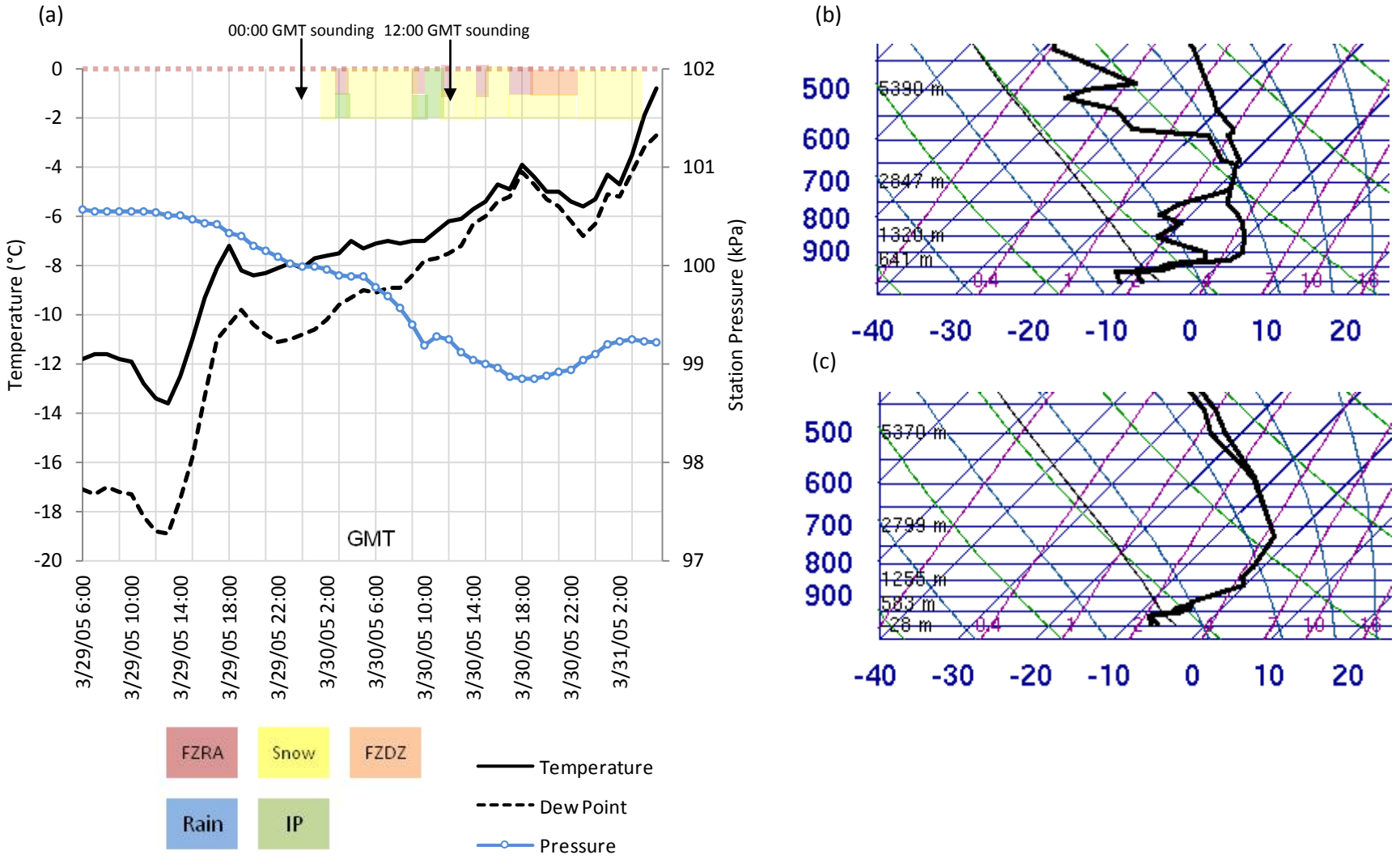

Figure 80: Case study #4 – March 30th, 2005 (a) hourly meteorological observations made in Churchill (b) 00:00 GMT Skew-T diagram (c) 12:00 GMT Skew-T diagram (source: Environment Canada, 2011 and University of Wyoming, 2012)

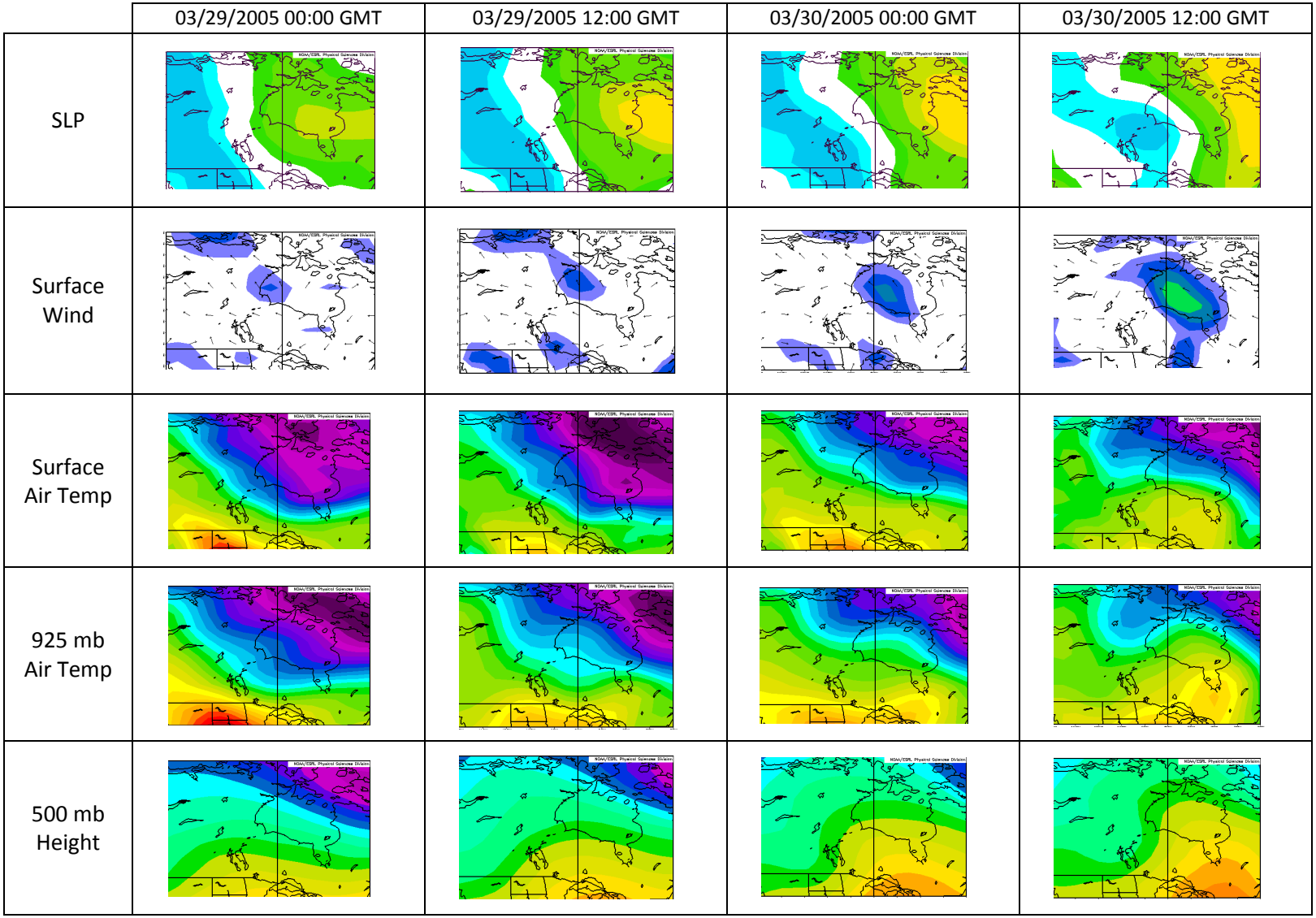

source: NCEP/NCAR re-analysis (2012)

Figure 81: SLP, surface winds, surface air temperature, 925mb air temperature and 500mb geopotential height maps 48-hours prior the freezing rain event on March 30th, 2005

5.7.5 Case Study #5 – May 11, 2009 (Synoptic Type 13)

This freezing rain case is interesting for several reasons. First, the two consecutive hours during which freezing rain was reported in Churchill, surface temperatures started out at -2°C but quickly increased to nearly 2°C. The event coincided with a small dip in barometric pressure. Then, a few hours after the pressure dipped, it rose again and temperatures fell quickly. Snow was observed once temperatures passed well below freezing (Figure 82). This case is also interesting because of the synoptic type associated with it. Type-11 is, in many ways, opposite to Type-20. During a Type-11, high pressure dominates at the surface and westerly winds are typically observed in Churchill. Furthermore, temperature lapse rates are often negative over much of Hudson Bay. However, in this case, a very small and weak centre of low pressure developed west of Churchill. This rapid drop in pressure shifted surface winds from the west to the south, drawing in warm air, causing a sudden increase in temperatures in the Churchill area.

The 12:00 GMT synoptic pattern on May 11th (Figure 83) does not fit very well (visually) with the Type-13 composite map (Figure 45). Specifically, the small centre of low pressure to the west of Churchill and the shallow ridge at the 500 mb level do not match the Type-13 composite patterns. Therefore, this case study may represent an instance where a freezing rain event was associated with the inappropriate synoptic type. Nonetheless, this case shows that mixed precipitation in Churchill occurs when surface temperatures hover close to the freezing point. Furthermore, this case study shows that even relatively small centres of low pressure have the potential develop quickly and draw in warm and moist air from the south.

Case Study #5 – May 11, 2009

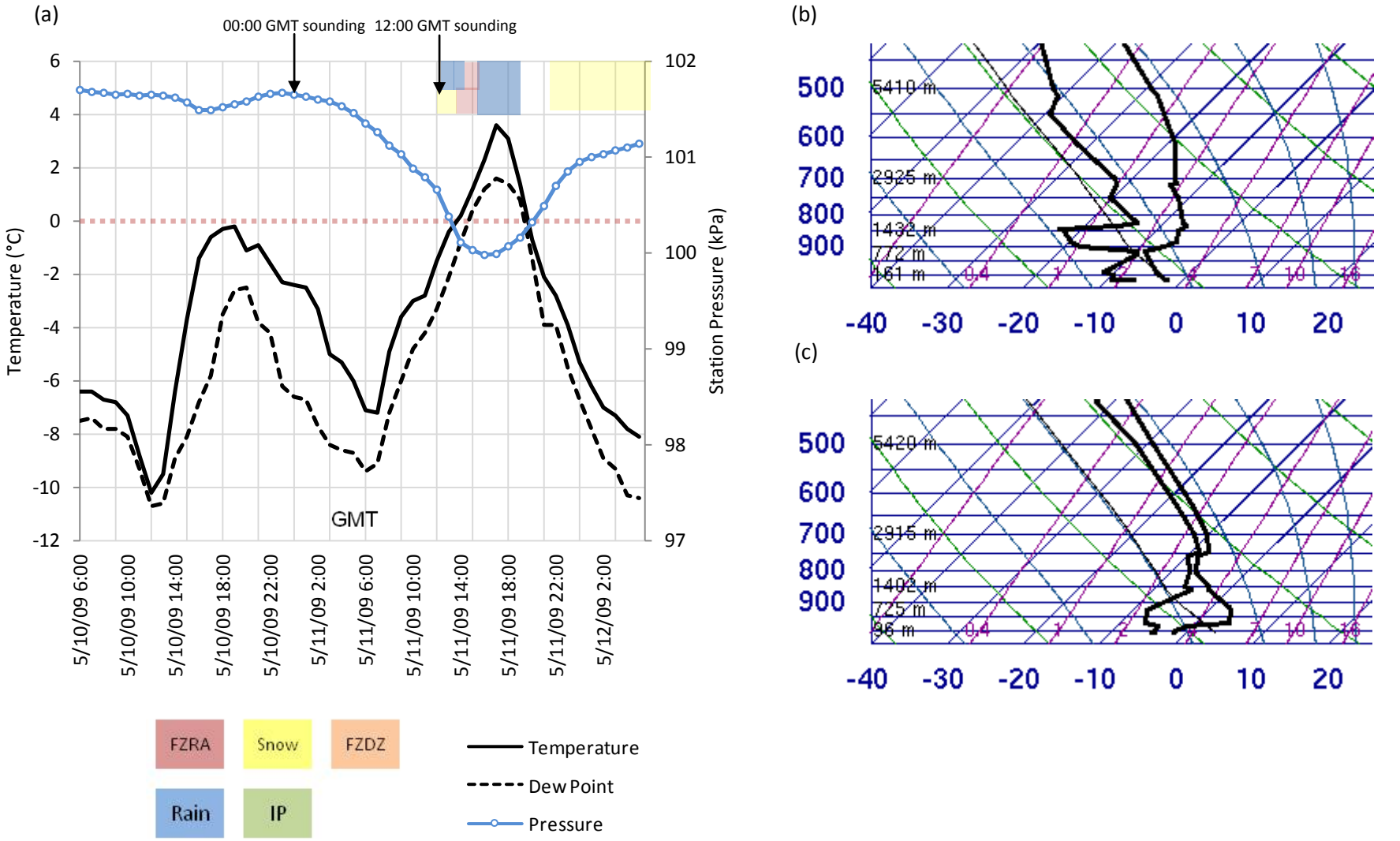

Figure 82: Case study #5 –April 11th, 2009 (a) hourly meteorological observations made in Churchill (b) 00:00 GMT Skew-T diagram (c) 12:00 GMT Skew-T diagram (source: Environment Canada, 2011 and University of Wyoming, 2012)

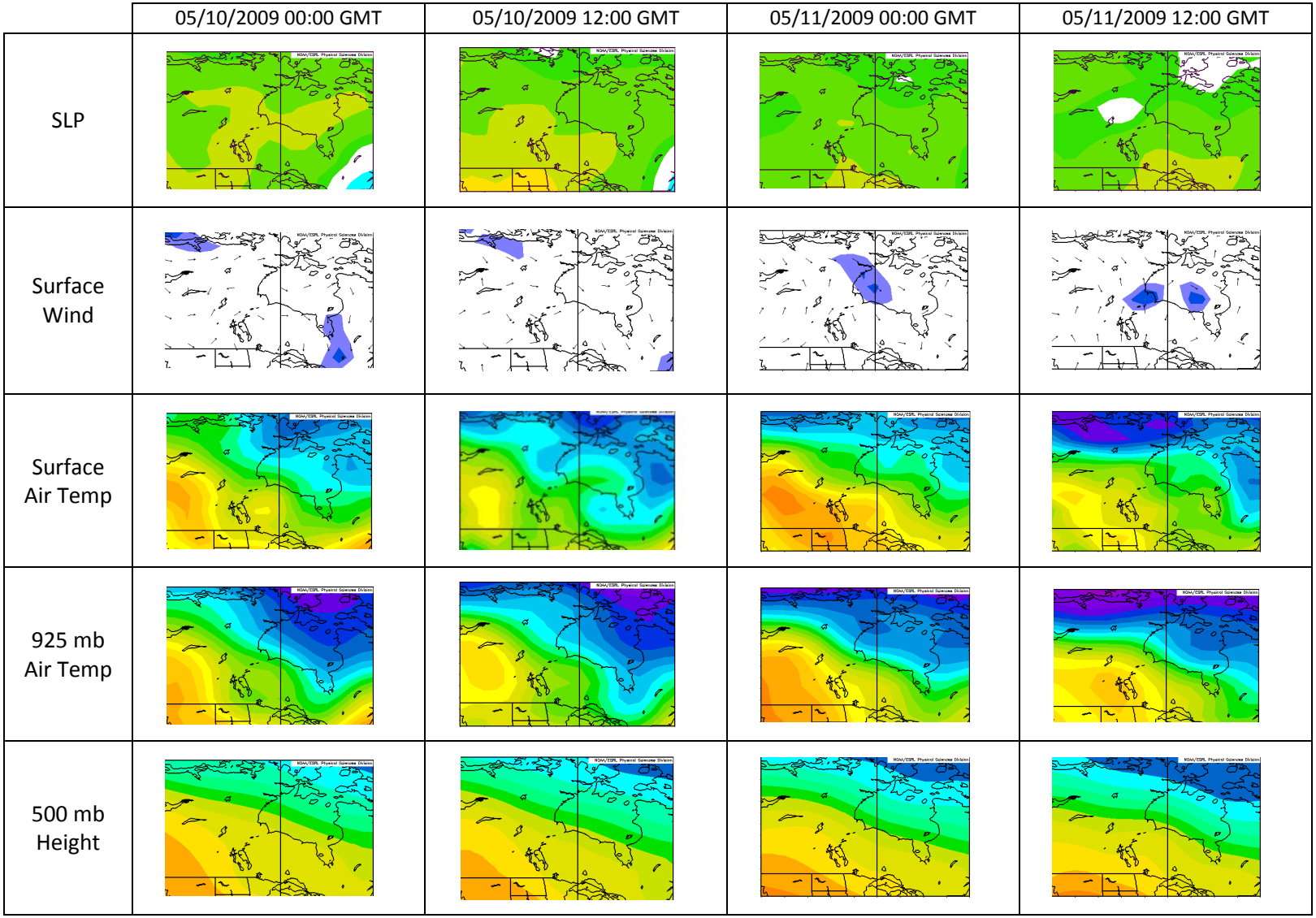

source: NCEP/NCAR re-analysis (2012)

Figure 83: SLP, surface winds, surface air temperature, 925mb air temperature and 500mb geopotential height maps 48-hours prior the freezing rain event on May 11th, 2009

5.7.6 Case Study #6 – June 5, 2009 (Synoptic Type 21)

This freezing rain case is quite different from the previous case studies, mainly because barometric pressure did not fall prior to or during the freezing rain event. Freezing rain was observed during the middle of the night of June 5th, and was preceded by both snow and ice pellets. The surface temperatures in Churchill hovered just below the freezing point. On the 00:00 GMT and 12:00 GMT Skew-T diagrams, temperature inversions are not evident. In fact, temperature lapse rates above Churchill on this day were slightly negative throughout most of the soundings. This makes it difficult to assess whether or not the freezing rain observation was indeed accurate, or whether other types of precipitation were falling. The fact that the observation was made while it was still dark may have further complicated the issue (Figure 84).

On the 12:00 GMT June 4th and 00:00 GMT June 5th synoptic maps, a cyclonic system can be seen developing at the surface south of Hudson Bay. This generated northeasterly surface winds in Churchill that suppressed daytime temperature gains at the surface and at 925 mb. This northeasterly flow may have brought with it moisture from over Hudson Bay, which is often beginning to melt during this time of year, and therefore may explain the rain/snow/freezing rain mix that fell in Churchill (Figure 85).

This case study illustrates the maritime influence that a (presumably) ice free Hudson Bay can have on the weather over Churchill in early June. Northeasterly surface winds over Churchill, supported by a low pressure system south of Hudson Bay, advects moist air that has a temperature very near the freezing point over Churchill. This cool and moist air facilitates the development of snow, ice pellets and some freezing rain.

Case Study #6 – June 5, 2009

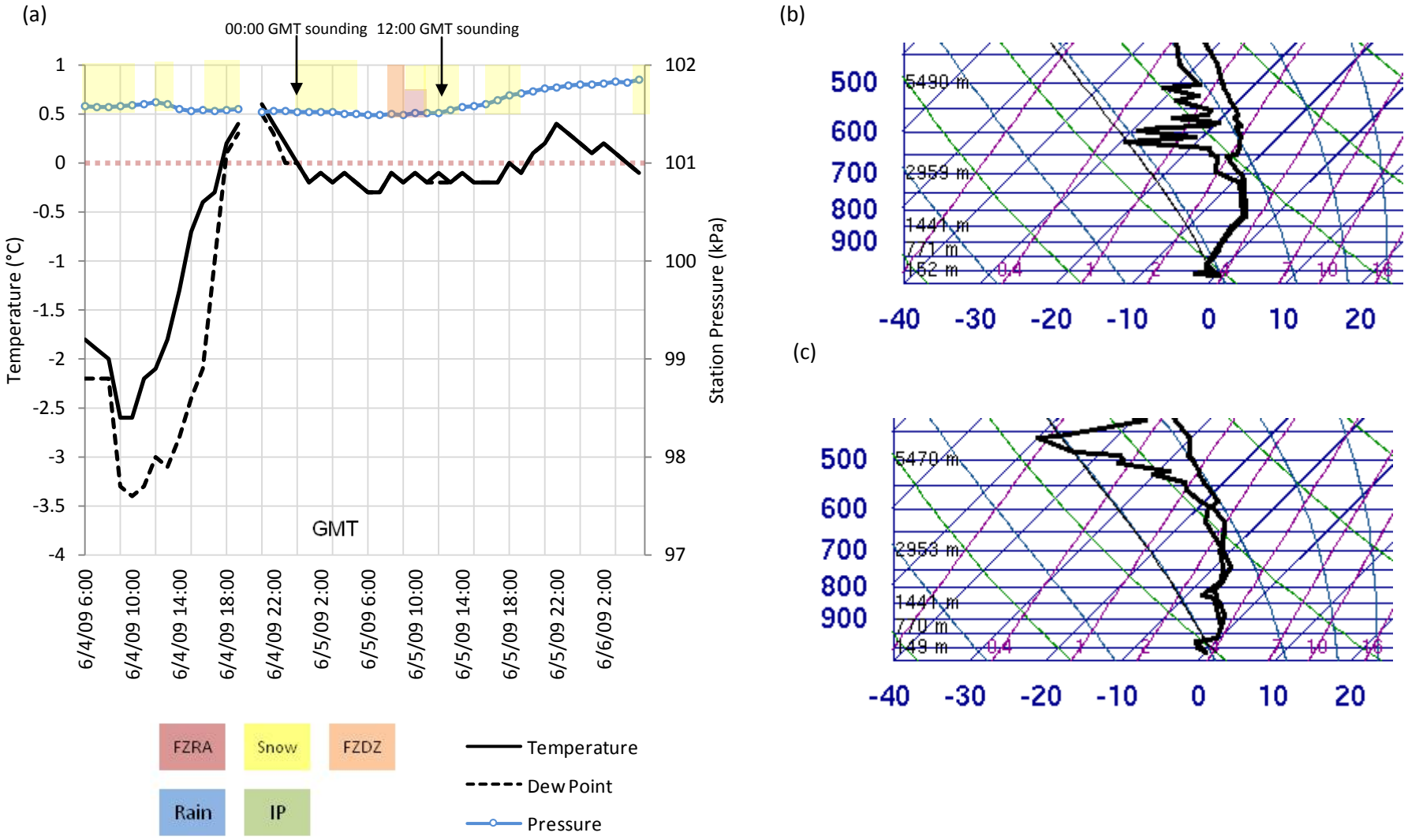

Figure 84: Case study #6- June 5th, 2009 (a) hourly meteorological observations made in Churchill (b) 00:00 GMT Skew-T diagram (c) 12:00 GMT Skew-T diagram (source: Environment Canada, 2011 and University of Wyoming, 2012)

	06/04/2009 00:00 GMT	06/04/2009 12:00 GMT	06/05/2009 00:00 GMT	06/05/2009 12:00 GMT
SLP	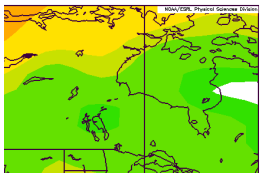	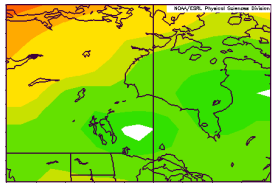	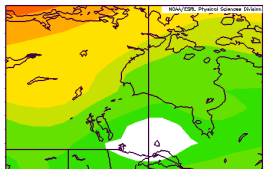	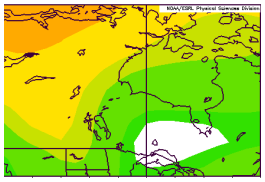
Surface Wind	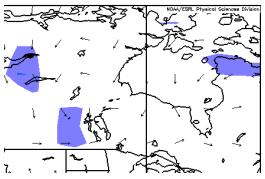	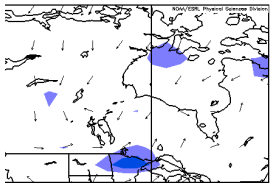	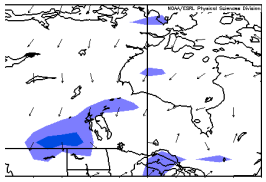	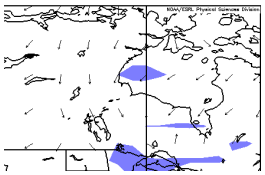
Surface Air Temp	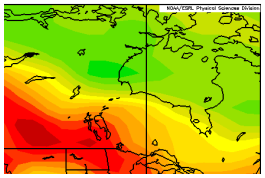	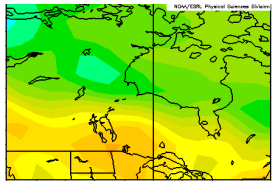	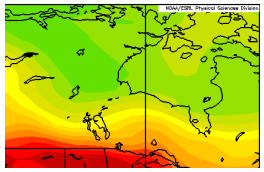	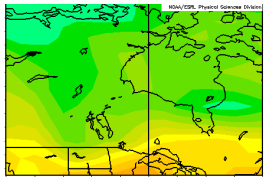
925 mb Air Temp	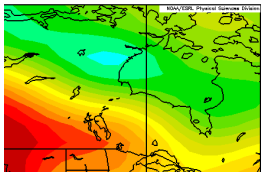	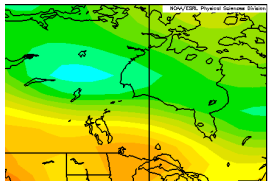	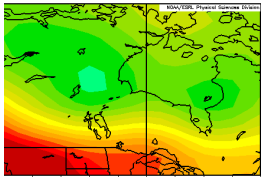	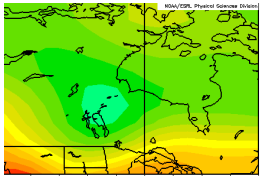
500 mb Height	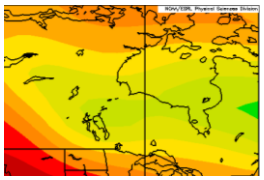	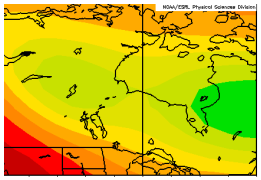	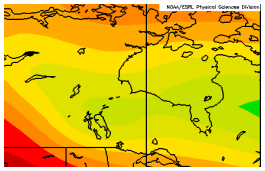	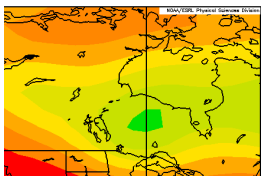

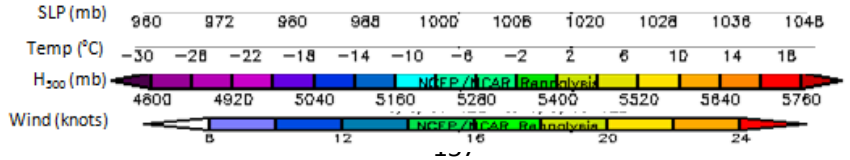

source: NCEP/NCAR re-analysis (2012)

Figure 85: SLP, surface winds, surface air temperature, 925mb air temperature and 500mb geopotential height maps 48-hours prior the freezing rain event on June 5th, 2009

5.7.7 Case Study #7 – April 26, 2003 (Synoptic Type 22)

Freezing rain was observed during a single hour on April 26th, 2003. This event was accompanied by Type-22. Typically, during a Type-22 event, a ridge of high surface pressure over the Churchill area drives northerly surface winds and cold surface temperatures into the region. Indeed, this is exactly what happened in the hours leading up to the freezing rain event. However, a fairly well defined closed low south of Hudson Bay at the 500 mb level and, to a lesser extent, at the surface, wrapped relatively warm air around to the east coast of Hudson Bay. Therefore, unlike any of the other case studies examined so far, the source of the warm air above the surface was actually from the east instead of from the south (Figure 86 and Figure 87).

The reason this freezing rain event was comparatively minor (there was only one hour during which freezing rain was reported) may be because temperatures in Churchill were still too cold to trigger a more persistent event. On the both the 00:00 and 12:00 GMT soundings for April 26th, temperatures throughout the atmosphere were below zero. Furthermore, the nose of the temperature inversion (not well defined) was very high above the surface, meaning that the depth of the freezing layer was also very large. Therefore, it is not surprising that snow was the dominant form of precipitation observed falling on this day, and not freezing rain. Nonetheless, this case study illustrates the importance of cyclonic circulation south of Churchill and the advection of warm air aloft in the formation of freezing rain.

Case Study #7 – April 26, 2003

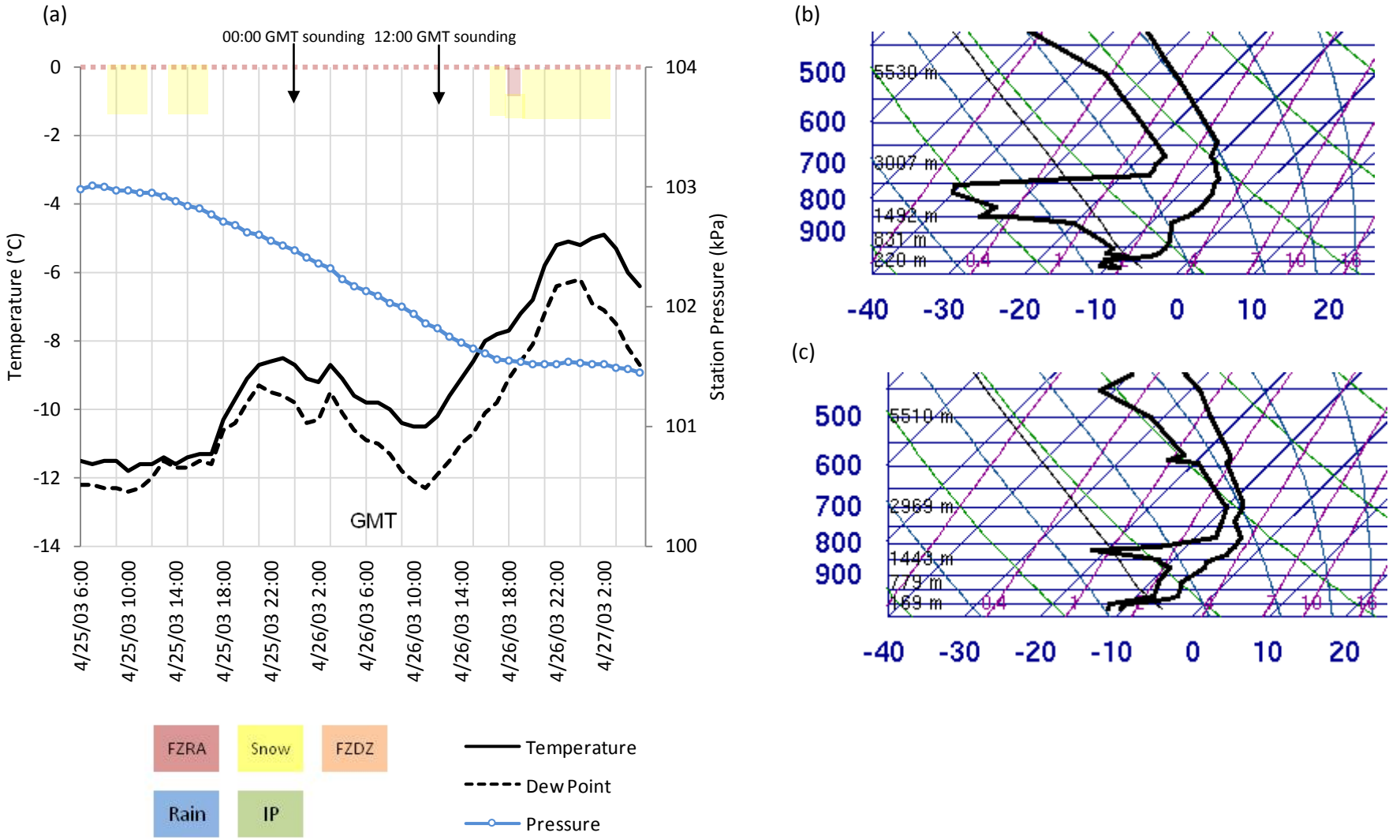

Figure 86: Case study #7 – April 26th, 2003 (a) hourly meteorological observations made in Churchill (b) 00:00 GMT Skew-T diagram (c) 12:00 GMT Skew-T diagram (source: Environment Canada, 2011 and University of Wyoming, 2012)

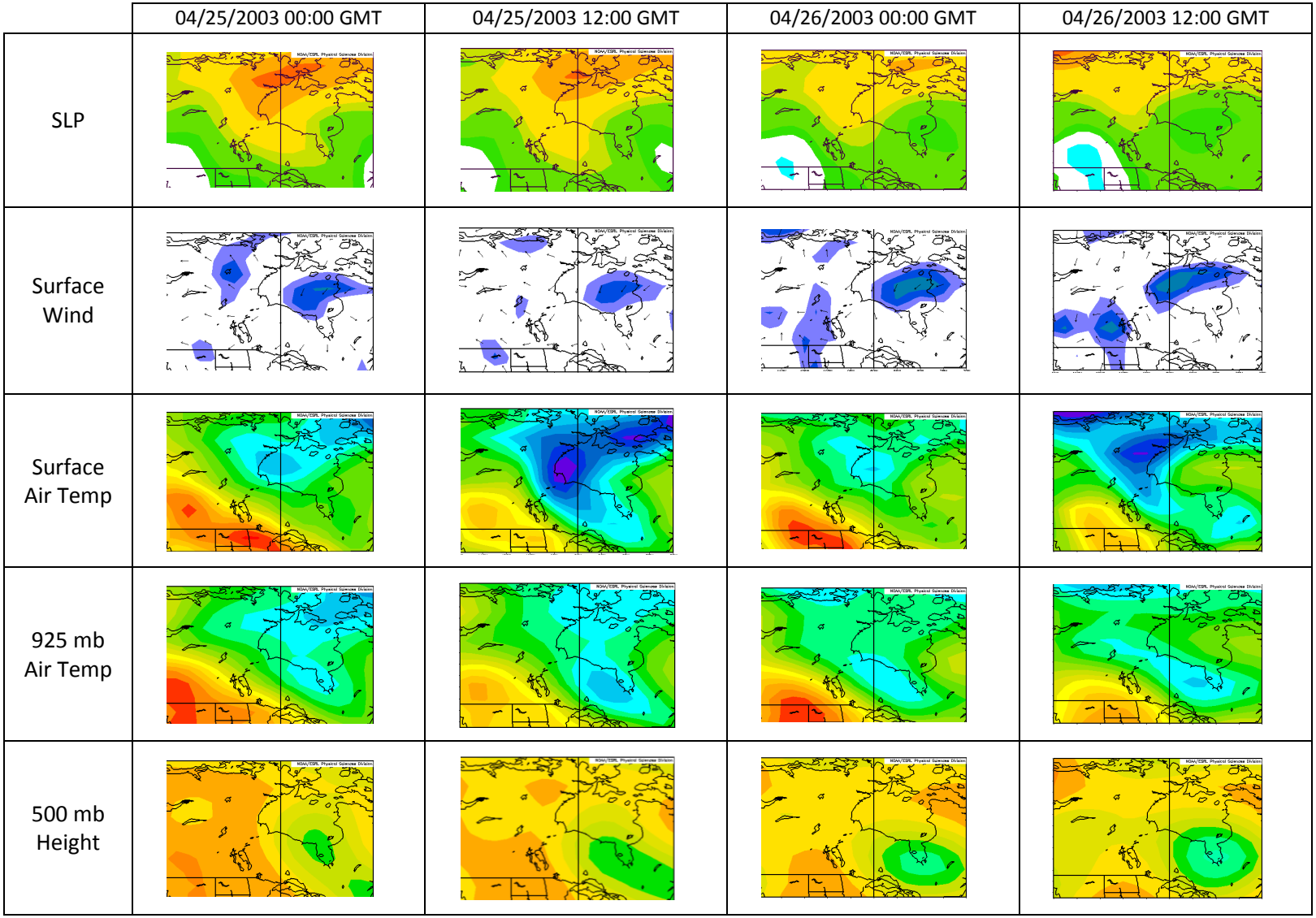

source: NCEP/NCAR re-analysis (2012)

Figure 87: SLP, surface winds, surface air temperature, 925mb air temperature and 500mb geopotential height maps 48-hours prior the freezing rain event on April 26th, 2003

5.7.8 Case Study #8 – November 13th, 2001 (Synoptic Type 24)

This freezing rain case occurred during November, when much of Hudson Bay is still free of ice. Freezing rain was observed during two hours in the morning on November 13th, 2001. Prior to the freezing rain event, the temperature in Churchill was rising and the pressure was falling. Some snow was also reported prior to and again after the freezing rain. Unfortunately, weather balloon soundings were not available for this date, presumably due to high winds in the area (Figure 88).

Forty-eight hours prior to the freezing rain event, at the synoptic scale, a ridge of high surface pressure with strong winds over the western portion of Hudson Bay was facilitating very cold surface temperatures in the Churchill area (Figure 89). By 00:00 GMT on November 13th, this ridge of high pressure and the strong northerly flow it was supporting was replaced by a trough of low pressure moving in from the west. A more southerly flow started to raise temperatures in the region. The air over Hudson Bay in particular warmed up quickly once the northerly surface winds abated. By 12:00 GMT on November 13th, the temperature at the surface was now close to 0°C. In Churchill, a light southwesterly flow was observed, drawing some of this milder (and presumably more humid) Hudson Bay air into the Churchill area. The freezing rain event coincided with the daytime maximum temperature in Churchill, and was replaced quickly by snow once temperatures started to drop again in the afternoon.

This case study illustrates the influence an ice-free Hudson Bay can have on Churchill's weather in late fall, when air over the bay can often be much warmer than air over land. Specifically, on-shore winds observed in Churchill twelve hours prior to the

November 13th freezing rain event likely explain why the air temperature and the dew point temperature rose to just below the freezing point. The transition from snow to freezing rain and then back to snow illustrates the very sensitive relationships between the type of precipitation observed at the surface, the surface air temperature and the depth of the freezing layer.

Case Study #8 – November 13, 2001

(a)

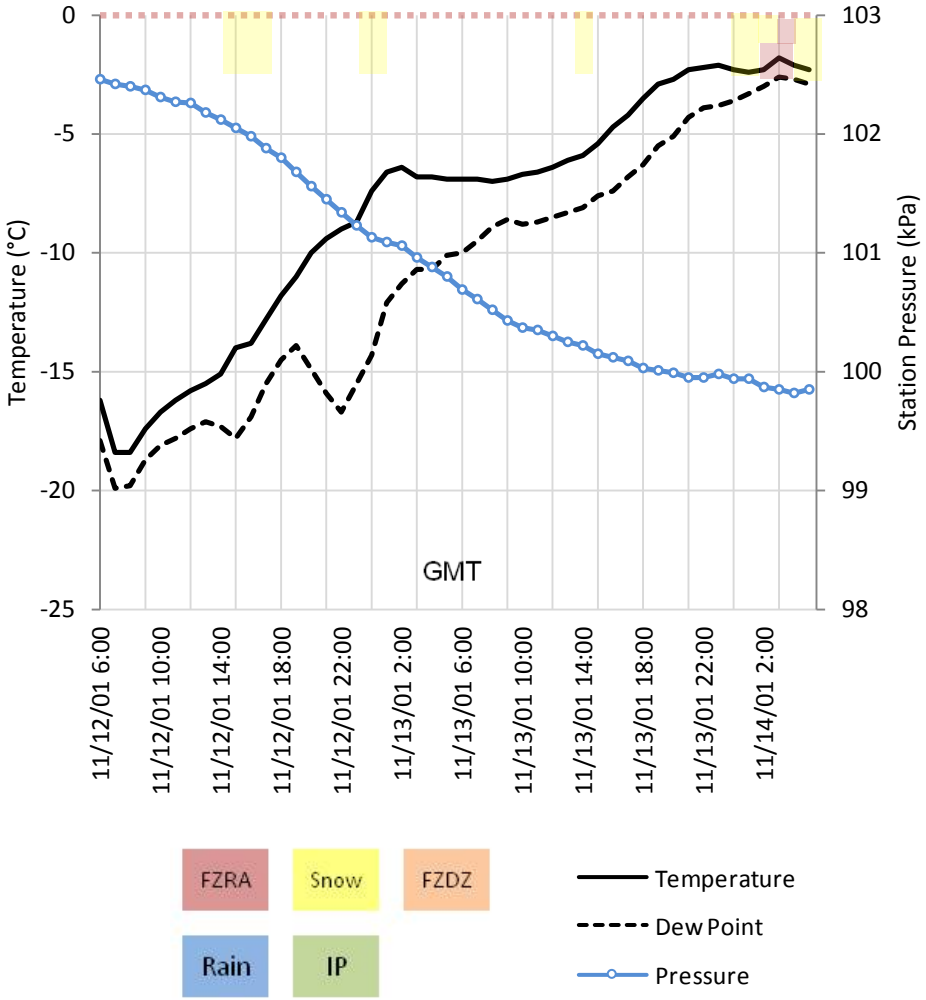

(b) No sounding available

(c) No sounding available

Figure 88: Case study #8 – November 13th, 2001 (a) hourly meteorological observations made in Churchill (b) 00:00 GMT Skew-T diagram (c) 12:00 GMT Skew-T diagram (source: Environment Canada, 2011)

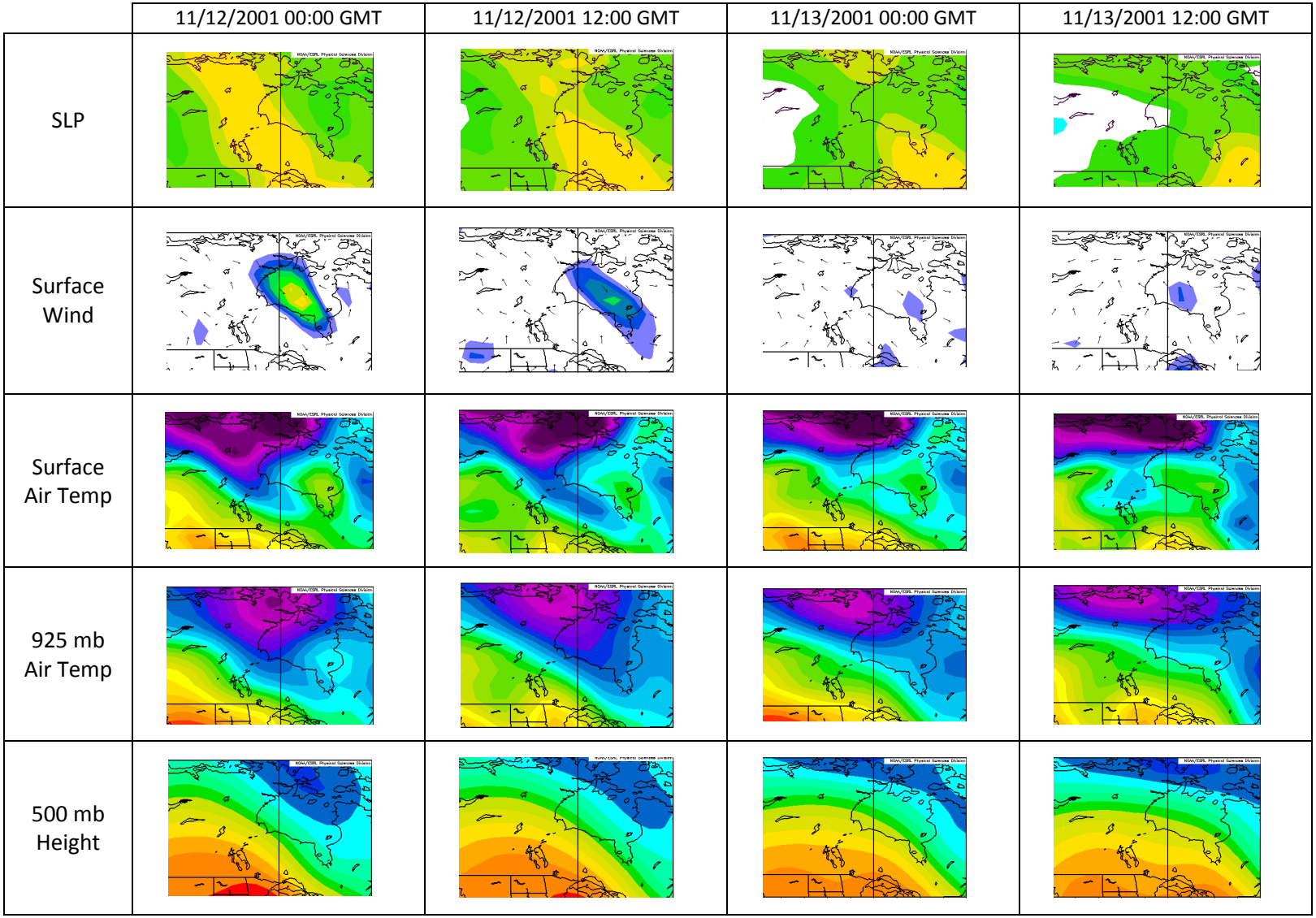

source: NCEP/NCAR re-analysis (2012)

Figure 89: SLP, surface winds, surface air temperature, 925mb air temperature and 500mb geopotential height maps 48-hours prior the freezing rain event on November 13th, 2001

5.8 Discussion of Case Study Results

Not surprisingly, the eight case study events demonstrated that freezing rain can form under a wide range of synoptic patterns and meteorological conditions. This is not surprising given the large seasonal variation within the climate of Hudson Bay and the fact that the bay undergoes a complete cryogenic cycle each year. Additionally, as discussed by Stewart (1992), synoptic scale data alone can never fully explain how complex micro-processes within winter storms will interact to form or not form freezing precipitation. This can especially true when freezing rain is witnessed during a transition between rain and snow. Within the so-called 'transition zone', the temperature and depth of the melting and freezing layers can change very quickly and over a small area, and therefore the extent and duration of freezing rain events can be very small and short lived (Stewart, 1992).

The Type-20 case study demonstrates how a warm front over Churchill can result in freezing rain, especially in spring. The warm front is generated by cyclonic circulation southwest of Churchill, advected into the region by a prominent ridge over Hudson Bay at the 500 mb level. North of the warm front, winds blow from the east or northeast as they wrap counter-clockwise around the centre of low pressure. During the early spring Hudson Bay is completely frozen, and therefore these easterly winds advect very cold and dry Arctic air along the west coast of the bay. The combination of relatively warm and moist air aloft and very cold and dry air at the surface form a vertical structure in the lower part of the atmosphere primed for freezing precipitation. It was expected that many of the freezing rain cases would be associated with warm fronts, based on freezing

rain research conducted in other parts of Canada (*see* Cheng et al., 2004; Roberts and Stewart, 2008).

Case studies six and eight demonstrated how freezing rain formed during in the early summer and later fall, respectfully, when Hudson Bay has a larger influence on the climate of Churchill. During these times of the year, the local effects of Hudson Bay are arguably just as important as the synoptic when it comes to the formation of freezing rain. In Atlantic Canada, research has shown that freezing rain can be enhanced along sub-arctic coastal areas. Specifically, Szeto et al. (1999) modeled an Atlantic Canadian freezing rain storm and discovered that warm fronts can become enhanced in this type of climate (larger above freezing layers aloft and colder temperatures at the surface).

The remaining case studies highlighted some but not all the complexity within freezing rain storms, especially when precipitation was intermittent or when precipitation types transitioned quickly between snow, rain, ice pellets, freezing drizzle and freezing rain. Clearly, the synoptic classification was unable to resolve all of this complexity and more detailed case studies are still needed to understand the details. However, the importance of cyclonic circulation, warm fronts and on-shore surface winds to freezing rain production was captured very well by the synoptic classification.

5.9 Preliminary Assessment of Long-term Trends in Synoptic Type Frequencies

The long-term change in synoptic type annual frequencies was calculated using a linear line of best fit. There is no expectation that any trend that might be present would

be linear. A summary of the results is shown in Table 1. Most of the types show small positive or negative trends during 1953-2009; however, most of these trends are not statistically significant at a confidence interval of 95 percent. Trends that are statistically significant are highlighted in blue if the trend was negative (decreasing frequency over time) or red if the trend was positive (increasing frequency over time). Additionally, the season in which each type tended to occur was noted as was the average temperature anomaly (warm or cool).

Eight of the nine types that were found to have significant linear trends are types that are mostly associated with winter. Out of these eight winter types which show significant changes in their annual frequencies, only two types were associated with 'warm' daily temperature anomalies in Churchill (Type-11 and Type-25). This result may indicate that the number of winter types responsible for producing cooler than average daily air temperatures in Churchill has been decreasing over this time period. However, there is still much variability within the annual frequencies and therefore these trends should not be overstated. Furthermore, since temperature is part of the multi-level synoptic classification and it is known that the temperature of the Arctic and sub-arctic, especially in winter, is rising, it may be inappropriate to conclude that these trends are indicative of more warm or fewer cold types. A classification without temperature would be better for assessing changes in the synoptic patterns.

Synoptic types frequently observed during spring and fall, the time of year when most freezing rain events were observed, witnessed little changes in their annual type frequencies since 1953. Type-11 was the only synoptic type found to relate to freezing rain that had a statistically significant negative trend associated with it. Type-11 is

generally considered a winter pattern, but was also observed relatively frequently during the month of March. Type-20, the type found to be most commonly observed with freezing rain, had a slight positive trend of 1.7 percent per century; however this trend is not significant. Therefore, a more elaborate technique is necessary to evaluate whether synoptic scale conditions associated with freezing rain events in Churchill are becoming more or less common over the Hudson Bay region.

Table 1: Long-term linear trends in synoptic type annual frequencies (1953-2009). Blue shading indicates the linear trend is negative and statistically significant. Red shading indicates that the linear trend is positive and statistically significant.

Synoptic Type	Month(s)with Greatest Frequency of this Type	Daily Temperature Anomaly in Churchill Associated with Each Type (warm/cool)	Linear Trend (percent change per year)	Linear Trend (percent change per century)	r^2	p
1	Summer	Warm	0.007	0.7	0.01	0.38
2	Summer	Warm	-0.015	-1.5	0.02	0.30
3	Winter	Warm	0.000	0.0	0.00	0.68
4	Summer	Warm	-0.003	-0.3	0.00	0.73
5	Summer	Warm	-0.001	-0.1	0.00	0.98
6	Winter	Cool	-0.036	-3.6	0.15	0.00
7	Summer	Cool	0.013	1.3	0.02	0.46
8	Winter	Cool	0.044	4.4	0.18	0.00
9	Spring and Fall	Warm	-0.001	-0.1	0.01	0.75
10	Winter	Cool	0.007	0.7	0.00	0.78
11	Winter	Warm	-0.023	-2.3	0.09	0.02
12	Fall	Cool	0.010	1.0	0.02	0.15
13	Spring and Fall	Cool	0.003	0.3	0.00	0.72
14	Spring and Fall	Cool	0.003	0.3	0.00	0.79
15	Spring and Fall	Cool	0.000	0.0	0.00	0.74
16	Summer and Fall	Cool	0.018	1.8	0.08	0.03
17	Spring and Fall	Cool	0.005	0.5	0.01	0.98
18	Winter	Cool	-0.035	-3.5	0.12	0.02
19	Winter	Cool	-0.020	-2.0	0.08	0.02
20	Spring	Warm	0.017	1.7	0.04	0.39
21	Spring	Cool	0.002	0.2	0.00	0.64
22	Spring and Fall	Warm	-0.004	-0.4	0.00	0.72
23	Winter	Warm	0.000	0.0	0.00	0.95
24	Fall	Warm	0.012	1.2	0.03	0.50
25	Winter	Cool	-0.006	-0.6	0.01	0.68
26	Winter	Cool	0.013	1.3	0.06	0.02
27	Fall	Cool	-0.006	-0.6	0.01	0.29
28	Winter	Cool	-0.020	-2.0	0.07	0.03
29	Spring and Fall	Warm	-0.003	-0.3	0.00	0.56
30	Spring and Fall	Warm	-0.008	-0.8	0.02	0.22
31	Winter	Warm	0.001	0.1	0.00	0.89
32	Winter	Cool	0.013	1.3	0.07	0.06
33	Fall	Cool	0.000	0.0	0.00	0.83
34	Winter	Cool	0.019	1.9	0.19	0.00

Chapter 6

Concluding Remarks

The climate of the Hudson Bay region and the Arctic as a whole is warming. This warming is due, in part, to global climate/atmospheric circulation changes as well as positive feedbacks between ice in Hudson Bay and the atmosphere. The warming of Hudson Bay will have large impacts on the local climate of Churchill, Manitoba. In particular, the timing, frequency and intensity of severe weather is expected to change as the climate warms (Anisimov et al., 2007). Freezing rain is an especially hazardous type of severe weather and is frequently observed in Churchill. Studies have shown that freezing rain is enhanced along the western coast of Hudson Bay (Stuart and Isaac, 1999). Similar enhancement occurs adjacent to the Atlantic Ocean in northern Canada and along the shores of the Great Lakes (Stewart and King, 1987; Bernstein, 2000; Cortinas et al., 2004; Cheng et al., 2004); however, unlike these bodies of water, Hudson Bay remains completely frozen during the time of year most of the freezing rain is observed (Stuart and Isaac, 1999). Clearly, Hudson Bay and its annual cycle of sea ice formation and

thaw have an influence on the timing of freezing rain events. This study was undertaken to better understand the climatology of freezing rain events in Churchill by focusing on four main objectives, detailed below.

The first objective of this study was to assess the climatology of freezing rain events in Churchill, Manitoba. Using Environment Canada archived hourly weather data from Churchill, the climatology of freezing rain events was analyzed. The resulting climatology agrees very well with the one developed by Hanesiak et al. (2003), who studied freezing rain in Churchill for the years 1953-2004. One very interesting result from the analysis of these data was the apparent role that Hudson Bay plays in determining the timing of freezing rain events along its western shore throughout the year. Specifically, many more freezing rain cases were observed during spring compared to fall. Based on previous research related to sea ice and freezing precipitation, it is very likely that an ice-covered Hudson Bay leads to more spring days when the surface air temperature is much lower than the temperature of the air aloft (Hanesiak and Stewart, 1995). The combination of relatively warm, above freezing air aloft and cold, below freezing air at the surface is necessary to have freezing rain (Cheng et al., 2004). The cooling effect at the surface is enhanced by on-shore winds, which are typically witnessed during freezing rain events in Churchill (Stuart and Isaac, 1999). In the fall, the ice-free bay keeps surface air temperatures warmer than upper air temperatures and therefore freezing rain is less common; however, the bay becomes an important source of heat and moisture during this time of year and may therefore enhance some types of precipitation.

Surface air temperatures can only explain part of why Churchill receives so much more freezing rain during spring compared to fall. It has been shown many times in various locations across Canada and the United States that warm fronts produce the vast majority of freezing rain events (Cheng et al., 2004). Therefore, the location of Churchill with respect to the position of cyclones passing over the region was an important aspect to consider for this study, as outlined below.

The second objective of this study was to assess the synoptic climatology of the Hudson Bay region in order to better understand how the synoptic climate of Hudson Bay affects the frequency and intensity of freezing rain in Churchill. Five synoptic scale variables were analyzed over a large study region encompassing the bay: SLP, the change in air temperature between the 1000-925 mb pressure surface, the atmospheric thickness between the 1000 and 925 mb pressure surfaces, the specific humidity at 925 mb and the geopotential height of the 500 mb pressure surface. A new synoptic classification strategy using these five variables was developed to classify each day during 1953-2009 into one of 34 synoptic types. One of the goals of synoptic classification is to try to calculate as few types as needed to summarize or explain specific aspects of the synoptic climate; however, it was necessary to calculate such a large number of synoptic types in this case because the multi-level classification strategy used introduced a much wider range of synoptic patterns compared to a standard 'single-level' classification strategy. Furthermore, the climate of Hudson Bay undergoes extreme seasonal changes that require many synoptic types to adequately showcase.

One of the major challenges of constructing any synoptic classification is assessing how well the classification explained the surface phenomenon being studied.

The lack of control over how types are computed in objective and semi-objective classification strategies, including PCA and K-means cluster analysis, will always result in non-perfect relationships which make it impossible to determine which classification strategy is to use is best (Yarnal et al., 1988). In this study, the number of clusters calculated was primarily based on how many freezing rain cases were associated with each type. In particular, the 'best' number of types was determined when the number of freezing rain cases per type and the relative percent frequency of freezing rain cases per type were both high. However, the usefulness of the synoptic classification would be very limited if the types also failed to adequately explain other important aspects of the synoptic climate of Hudson Bay and the local climate of Churchill, including seasonality, surface wind direction, temperature and other forms of precipitation (rain and snow).

Clearly, the synoptic types captured the seasonality of the Hudson Bay region very well. In almost all cases, the synoptic types were associated with very specific months and seasons, demonstrating the synoptic typing strategy's ability to distinguish between unique synoptic patterns. Similarly, many of the synoptic types were associated with a very specific range of surface wind directions in Churchill, further demonstrating how well synoptic patterns were sorted. As many synoptic climatologists have found, relationships between synoptic types and temperature are generally less sensitive to the classification strategy used compared to relationships between synoptic classifications and precipitation (*see* Yarnal et al., 1988). As expected, this study demonstrated that the synoptic types were related to average daily temperature anomalies, specifically when determining which synoptic types were, on average, associated with warm or cool temperature anomalies in Churchill. The synoptic types appeared to also distinguish well

between precipitation that fell as rain or snow in Churchill, further demonstrating classification's ability to sort the synoptic patterns into unique classes.

The third objective of this study was to assess the relationship between synoptic scale circulation and freezing rain events in Churchill. Not surprisingly, very few of the synoptic types were associated with freezing rain events in Churchill. The classification produced one synoptic type (Type-20) that was associated with more than half of all freezing rain days observed in Churchill. Type-20 was also associated with the most 'extreme' freezing rain cases, when freezing rain event durations exceeded the 90th percentile.

During a Type-20 event, lower SLP is observed southwest of Churchill. There is a much greater chance that Churchill will experience the passage of a warm front aloft when cyclones are in this position compared to many of the other synoptic types. However, what makes the Type-20 SLP composite map especially conducive to freezing rain in Churchill compared to most other types is the presence of high SLP along the eastern portion of the study region. The orientation of high and low pressure during a Type-20 event facilitates easterly surface winds in Churchill. In fact, Type-20 events accounts for almost all easterly surface wind observations in Churchill (an easterly wind is relatively rare in Churchill to begin with) (Figure 24). As previously stated, the easterly wind seems to be an important mechanism for depressing surface temperatures during times of heavy sea ice cover over Hudson Bay (Stuart and Isaac, 1999).

Another very important characteristic of Type-20 events which may help explain why it was found to correlate with so many freezing rain cases in Churchill is the ridging

pattern in the 500 mb height contours. Throughout the year, it was shown that the average 500 mb height surface forms a trough over the study region (the so-called "North American" trough). A ridge moving east (out of the study region) indicates that geostropic winds at the 500 mb level are most likely out of the southwest, which can help advect cyclonic systems located in lower latitudes into the study region. Furthermore, the advection of positive vorticity west of the ridge at 500 mb can lead to upper-level divergence and low pressure at the surface west of the ridge.

In addition to promoting low SLP values in the southwest quadrant of the study region, Type-20 events also appear to have the right combination of temperature and humidity to facilitate freezing rain in Churchill. The average 1000-925 mb thickness values over Churchill during a Type-20 event are between 62 and 63 dam, and this may prove to be a useful range for forecasters considering issuing freezing rain warnings in the region. Temperatures at 925 mb are warmer on average than at 1000 mb, a good indication that a warm front is moving through the region. Finally, a plume of moisture at 925 mb up the west coast of Hudson Bay is another good indication that southerly winds are blowing at this level, bringing warmer temperatures and the water vapour needed to generate freezing rain.

While Type-20 events definitely captured the majority of freezing rain cases in Churchill, many freezing rain cases were observed when a Type-20 event was not present. In order to understand whether these particular freezing rain cases were either (a) assigned to the wrong synoptic type, (b) erroneously observed as freezing rain or (c) due to different synoptic patterns and meteorological circumstances, eight detailed case

studies were constructed using one freezing rain event from each of the eight synoptic types most commonly associated with freezing rain (including Type-20).

It was found, not surprisingly, that a variety of synoptic patterns could lead to the development of freezing rain in Churchill. However, all of the non-Type-20 freezing rain cases that were examined were very short lived (one hour or less) and occurred when precipitation was transitioning between rain and snow. There is also the chance that several of the short-lived freezing rain events were actually freezing drizzle or ice pellet events and were misidentified due to observer error, during poor visibility or at night. However, long-lived and (presumably) more severe freezing rain events tend to be continuous in nature.

The case studies also highlighted some of the problems and challenges associated with studying freezing rain. First, the potential for human observation error was noted several times, especially when freezing rain was observed while the sounding data showed temperatures throughout the atmosphere were below zero. This also highlights the need for more frequent sounding data and surface observations. Similarly, hourly precipitation measurements would be useful for estimating how much precipitation fell as freezing rain opposed to other forms of precipitation throughout the day.

Given the propensity for observer errors, the coarse temporal and spatial resolution of the surface and synoptic data and the large amount of subjectivity inherent within PCA-based synoptic classification, the relationships found between the synoptic climate of the Hudson Bay region and freezing rain events in Churchill are surprisingly

robust. This again highlights that synoptic classifications can be very useful tools for explaining surface phenomena.

The fourth, and final, objective of this study was to assess the trends in synoptic types and to discuss the implications of climate change in relation to the expected changes in freezing rain frequency and intensity in Churchill. A brief analysis of the long-term changes in the annual synoptic type frequencies was conducted. It was found that many of the synoptic types that occurred during winter and were associated with negative daily temperature anomalies were occurring less frequently between 1953 and 2009. However, because temperature was included in the synoptic classification, and temperatures in the Arctic and sub-arctic are warming, these trend results may be contaminated. Therefore, it is difficult to state with any certainty based on these trend results alone how the synoptic climate may change in the future and what impact any changes may have on the frequency and intensity of freezing rain.

None of the synoptic types associated with freezing rain events showed statistically significant trends (with 95 percent confidence) between 1953-2009. Although synoptic type 20 showed a slight positive trend, it was not statistically significant at 95 percent confidence; the p-value was found to be 0.39. Hanesiak and Wang (2005) found a very weak positive statistically significant rend in Churchill freezing rain/drizzle events between 1953-2004; however, this study included freezing rain and freezing drizzle event combined. In any case, a more elaborate methodology is necessary to assess trends in freezing rain.

It is difficult to know for certain based on these analyses how the timing, frequency and intensity of freezing rain events in Churchill may change in the coming years. Warmer winters will certainly result in lower sea ice concentration over Hudson Bay. Lower sea ice concentration in spring will certainly result in increased surface temperatures over much of the bay. In Churchill, this will almost certainly result in fewer days below freezing during the spring months and therefore less freezing rain. However, freezing rain may then simply occur earlier in the year or later in the year.

The applicability and utility of the methods and results presented in this study to forecasters must also be discussed, although this was not an official objective of this study. Typically, forecasters use atmospheric thickness to infer temperatures within the above-freezing layer and the surface-freezing layer to then determine the likelihood of freezing rain (*see* Stewart and King, 1987). A typical set of partial thicknesses may be 1000-850 mb and 850-700 mb for the freezing layer and above-freezing layer, respectfully (Stewart and King, 1987). Based on sounding data collected for several freezing rain cases in Churchill, the depth of the freezing layer may be much lower than 850 mb (closer to 925 mb) and therefore these thickness calculations may not be adequate for predicting freezing rain in Churchill. Typical 1000-925 mb thicknesses associated with freezing rain events is between 62-63 dam. Furthermore, additional synoptic scale variables were clearly shown to be associated with freezing rain. Forecasters could visually or objectively classify real-time synoptic data into one of the 34 synoptic types presented in this study to help identify potentially hazardous conditions.

It is clear that much work is still needed to understand freezing rain events in the current climate, let alone how climate change will impact Hudson Bay and associated

freezing rain events. Furthermore, our understanding of other complex relationships and feedbacks between sea ice, air temperature, precipitation, cyclones and adverse weather events is still very limited. This study has shown that at least some of these relationships can be explained by analyzing the synoptic climate. Through continued innovation, experimentation and data collection, it is the authour's hope that the synoptic classification program, Synoptic Typer Tools, can be used to improve our understanding of how the climate system operates.

References

Anisimov, O., D.G. Vaughan, T.V. Callaghan, C. Furgal, H. Marchant, T.D. Prowse, H. Araneo, D. C. and Compagnucci, R. H., 2007. Removal of systematic biases in S-mode principal components arising from unequal grid spacing. Journal of Climate, 17, 394-400.

Asplin, M., Lukovich, J. and Barber, D., 2009. Atmospheric forcing of the Beaufort Sea ice gyre: surface pressure climatology and sea ice motion. Journal of Geophysical Research, 114, 1-13.

Barry R. G. and Perry, A.H., 1973. *Synoptic climatology: methods and applications*. Methuen & Co Ltd, London.

Bengtsson, L., Semenov, V. and Johannessen, O., 2004. The early twentieth-century warming in the Arctic: a possible mechanism. Journal of Climate, 17, 4045-4057.

Bernstein, B.C., 2000. Regional and local influences on freezing drizzle, freezing rain, and ice pellets. Weather and Forecasting, 15, 485-508.

Bettolli, L., Penalba, O. and Vargas, W., 2010. Synoptic weathe types in the south of South America and their relationship to daily rainfall in the core crop-producing region in Argentina. Australian Meteorological and Oceanographic Journal, 60, 37-48.

Blair, D., Smith, R. and Dahni, R., 2011. Synoptic Typer Tools. Available online: http://stt.uwinnipeg.ca/.

Buell, C.E., 1979. On the physical interpretation of empirical orthogonal functions. American Meteorological Society, 6th conference on probablity and statistics in the atmospheric sciences, 112-117.

Cattell, R.B., 1966. The scree test for the number of factors. Multivariate Behavior Research, 1, 245-276.

CCEA, 2007. *Ecozones of Canada*. Accessed online, July 2011 <http://www.ccea.org/ecozones/>

Cheng, C. S., Auld, H., Li, G., Klaasen, J., Tugwood, B. and Li, Q., 2004. An automated synoptic typing procedure to predict freezing rain: an application to Ottawa, Ontario, Canada. Weather and Forecasting, 19, 751-768.

Cortinas, J. V., Bernstein, B. C., Robbins, C. C. and Strapp, J. W., 2004. An analysis of freezing rain, freezing drizzle, and ice pellets across the United States and Canada: 1976-90. Weather Forecasting, 19, 377-390.

Cuell, C. and Bonsal, B., 2009. An assessment of climatological synoptic typing by principal component analysis and kmeans clustering. Theoretical Applied Climatology, 98, 361-373.

Dahni, R., 2003. An automated synoptic typing system using archived and real-time NWP model output. 19th International Conference on Interactive Information and Processing Systems for Meteorology, Oceanography, and Hydrology, American Meteorological Society, Long Beach, California.

Dahni, R., 2004. Synoptic Typer Reference Manual Version 2.2. Bureau of Meteorology, Melbourne, Australia.

Dahni, R., and Ebert, E., 1998. Automated objective synoptic typing to characterize errors in NWP model QPFs. *12th Conference on Numerical Weather Prediction*, Pheonix, Arizona, Jan 11-16, 1998.

Déry, S. Stieglitz, M., McKenna, E. and Wood, E., 2005. Characteristics and trends of river discharge into Hudson, James and Ungava Bays, 1964-2000. Journal of Climate, 2540-2557.

Deser, C., Walsh, J. and Timlin, M., 2000. Arctic sea ice variability in the context of recent atmospheric circulation trends. Journal of Climate, 13, 617-633.

Else, B., Papakyriakou, T., granskog, M. and Yackel, J., 2008. Observations of sea surface fCO2 distributions and estimated air-sea CO2 fluxes in the Hudson Bay region (Canada) during the open water season. Journal of Geophysical Research, 113.

Environment Canada, 1990. Manual of Surface Weather Observations (MANOBS). User's manual. [Available from Meteorological Service of Canada, 4905 Dufferin St., Downsview, ON, M3H 574, Canada].

Environment Canada, 2011. National Climate and Information Data Archive. Accessed online <http://climate.weatheroffice.gc.ca/climateData/canada_e.html>, November, 2011.

Environment Canada, 2012. Canadian Centre for Climate Modeling and Analysis. Accessed online < http://www.cccma.ec.gc.ca/data/cgcm4/CanCM4/index.shtml>, March, 2012.

Frank, K. L, Kalkstein, L. S., Geils, B. W. and Thistle, H. W. Jr., 2008a. Synoptic climatology of the long-distance dispersal of white pine blister rust. I. Development of an upper level synoptic classification. International Journal of Biometeorolgy, 52, 641-652.

Frank, K. L, Kalkstein, L. S., Geils, B. W. and Thistle, H. W. Jr., 2008b. Synoptic climatology of the long-distance dispersal of white pine blister rust. II. Combination of surface and upper-level conditions. International Journal of Biometeorology, 52.

Gibson, S. R. and Stewart, R.E., 2007. Observations of ice pellets during a winter storm. Atmospheric Research, 85, 64-76.

Hanesiak, J. M. and Stewart, R. E., 1995. The mesoscale and microscale structure of a severe ice pellet storm. Monthly Weather Review, 123, 3144-3162.

Hanesiak, J. M. and Wang, X. L., 2005. Adverse-weather trends in the Canadian Arctic. Journal of Climate, 18, 3140-3156.

Hanesiak, J. M., Fisico, T., Rindahl, C. and Carriere, E., 2003. Climatology of adverse-weather events in the Canadian Arctic. Faculty of Geography and the Environment, University of Manitoba, Centre for Earth Observation Science Tech. Report. CEOS-Tech-2003-2, 3540 pp.

Hochheim, K. and Barber, D., 2010. Atmospheric forcing of sea ice in Hudson Bay during the fall period, 1980-2005. Journal of Geophysical Research, 115-120.

Hochheim, K., Barber, D. and Lukovich, J., 2010. Changing sea ice conditions in Hudson Bay, 1980-2005. Appearing in: *A little less Arctic: top predatos in the world's largest northern inland sea, Hudson Bay*. Ferguson, S., Loseto, L. and Mallory, M. (editors). Springer, New York, pp.308.

Hochheim, K., Lukovich, J. and Barber, D., 2011. Atmospheric forcing of sea ice in Hudson Bay during the spring period, 1980-2005. Journal of Marine Systems, 88(3), 476-487.

Iseri, Y., Matsuura, T., Iizuka, S., Nishiyama, K. and Jinno, K., 2009. Comparison of pattern extraction capability between self-organizing maps and principal component analysis. Memoirs of the Faculty of Engineering, Kyushu University, 69(2).

Jolliffe, I. T., 2002. *Principal Component Analysis, Second Edition*. Springer.

Joly, S., Senneville, S., Caya, D. and Saucier, F., 2011. Sensitivity of Hudson Bay sea ice and ocean climate to atmospheric temperature forcing. Climate Dynamics, 36, 1835-1849.

Kaiser, H.F., 1958. The varimax criterion for analytic rotation in factor analysis. Psychometrika, 23, 187-200.

Kaiser, H.F., 1960. The application of electronic computers to factor analysis. Educational and Psychological Measurement, 20, 141-151.

Kalnay, E. et al., 1996. The NCEP/NCAR 40-year reanalysis project. Bulletin of the American Meteorological Society, 77, 437-471.

Kohonen, T., 1991. Self-organizing maps: optimization approaches. *Artificial Neural Networks. Proceedings of ICANN'91, International Conference on Artificial Neural Networks*, volume II, 981-990, North-Holland, Amsterdam.

Kuzyk, Z., Macdonald, R., Granskog, M., Scharien, R., Galley, R., Michel, C., Barber, D. and Stern, G., 2007. Sea ice, hydrological, and biological processes in the Churchill River estuary region, Hudson Bay. Estuarine, Coastal and Shelf Sciences, 77(3), 369-384.

Lamb, H., 1972. British Isles weather types and a register of the daily sequences of circulation patterns 1861-1971. Geophysical Memoirs, 116(85).

Lecomte, E., Pang, A.W. and Russell, J.W., 1998. Ice storm ’98. Institute for Catastropic Loss Reduction and Institute for Business and Home Safety, December 1998.

Lindsay, R. and Zhang, J., 2005. The thinning of sea ice, 1988-2003: have we passed a tipping point? Journal of Climate, 18, 4879-4894.

Lund, I., 1962. Map-pattern classification by statistical methods. Journal of Applied Meteorology, 2, 56-65.

Martínez, C., Campins, J., Jansà, A. and Genovés, A., 2008. Heavy rain events in the Western Mediterranean: an atmospheric pattern classification. Advances in Science and Research, 2, 61-64.

McClelland, J., Déry, S., Peterson, B., Holmes, R. and Wood, E., 2006. A pan-arctic evaluation of changes in river discharge during the latter half of the 20th century. Geophysical Research Letters, 33.

McKendry, I. G., Stahl, K. and Moore, R. D., 2006. Synoptic sea-level pressure patterns generated by a general circulation model: comparison with types derived from NCEP/NCAR Re-analysis and implications for downscaling. International Journal of Climatology, 26, 1727-1736.

Mundy, C. Gosselin, M., Starr, M. and Michel, C., 2010. Rivering export and the effects of circulation on dissolved organic carbon in the Hudson Bay system, Canada. Limnology and Oceanography, 315-323.

NAV CANADA, 2011. The weather of Nunavut and the Arctic: graphic area forecast 36 and 37.

Pickett-Heaps, C., Jacob, D., Wecht, K., Kort, E., Wofsy, S., Diskin, G., Worthy, D., Kaplan, J., Bey, I. and Drevet, J., 2011. Magnitude and seasonality of wetland methane emissions from the Hudson Bay Lowlands (Canada). Atmospheric Chemistry and Physics, 11, 3773-3779.

Qian, M., Jones, C., Laprise, R. and Caya, D., 2008. The influences of NAO and the Hudson Bay sea-ice on the climate of eastern Canada. Climate Dynamics, 31, 169-182.

Rauber, R.M., Olthoff, L.S., Ramamurthy, M.K. and Kunkel, K.E., 2000. The relative importance of warm rain and melting processes in freezing precipitation events. Journal of Applied Meteorology, 39, 1185-1195.

Reusch, D. B. and Alley, R. B., 2007. Antarctic sea ice: a self-organizing map-based perspective. Annals of Glaciology, 46.

Roberts, E. and R.E. Stewart, 2008. On the occurrence of freezing rain and ice pellets over the eastern Canadian Arctic. Atmospheric Research, 93, 10.

Rouse, W., 1991. Impacts of Hudson Bay on the terrestrial climate of the Hudson Bay lowlands. Arctic and Alpine Research, 23(1), 24-30.

Saucier, F., Senneville, S., Prinsenberg, S., Rog, F., Smith, G., Cachon, P., Caya, D. and Laprise, R., 2004. Modelling the sea ice-ocean seasonal cycle in Hudson Bay, Foxe Basin and Hudson Strait, Canada. Climate Dynamics, 23, 303-326.

Screen, J. and Simmonds, I., 2010. The central role of diminishing sea ice in recent Arctic temperature amplification. Nature, 464, 1334-1337.

Serreze, M., 1994. Climatological aspects of cyclone development and decay in the Arctic. Atmosphere-Ocean, 33(1), 1-23.

Sheridan, S., Power, H. and Senkbeil, J., 2008. A further analysis of the spatio-temporal variability in aerosols across North America: incorporation of lower troposphere (850-hPa) flow. International Journal of Climatology, 28, 1189-1199.

Simmonds, I. and Keay, K, 2009. Extraordinary September Arctic sea ice reductions and their relationship with storm behaviour over 1979-2008. Geophysical Research Letters,36.

Skinner, W. R., Flannigan, M. D., Stocks, B. J., Martell, D. L., Wotton, B. M., Todd, J. B., Mason, J. A., Logan, K. A. and Bosch, E. M., 2002. A 500 hPa synoptic wildland fire climatology for large Canadian forest fires, 1959-1996. Theoretical and Applied Climatology, 71, 157-169.

Smith, L., 2002. A *tutorial on Principal Components Analysis*. Accessed online: <http://www.cs.otago.ac.nz/cosc453/student_tutorials/principal_components.pdf> *January 21, 2010*.

Smith, R., 2008. Synoptic Typer Tools: designing and testing an automated synoptic classification program. Submitted in partial fulfilment of the degree of Bachelor of Science with Honours, University of Winnipeg, Canada, April.

Sorteberg, A. and Walsh, J., 2008. Seasonal cyclone variability at 70ºN and its impact on moisture transport into the Arctic. Tellus, 60, 570-586.

Stahl, K., Moore R. D. and McKendry, I. G., 2006. The role of synoptic-scale circulation in the linkage between large-scale ocean-atmosphere indices and winter surface climate in British Columbia, Canada. International Journal of Climatology, 26, 541-560.

Stewart, D. and Barber, D., 2010. The ocean-sea ice-atmosphere system of the Hudson Bay complex. Appearing in: *A little less Arctic: top predatos in the world's largest northern inland sea, Hudson Bay*. Ferguson, S., Loseto, L. and Mallory, M. (editors). Springer, New York, pp.308.

Stewart, D. and Lockhart, W., 2005. An overview of the Hudson Bay marine ecosystem. Can. Tech. Rep. Fish. Aquat. Sci. 2586: 487 pp.

Stewart, R. E. and King, P., 1987. Freezing Precipitation in Winter Storms. Monthly Weather Review, 115, 1270–1280.

Stewart, R. E., 1992. Precipitation Types in the Transition Region of Winter Storms. Bulletin from the American Meteorological Society,73, 287–296.

Stewart, R., Bachand, D., Dunkley, R., Giles, A., Lawson, B., Legal, L., Miller, S., Murphy, B., Parker, M., Paruk, B. and Yau, M., 1995. Winter storms over Canada. Atmospheric-Ocean, 33(2), 223-247.

Stuart, R. A. and Isaac, G. A., 1999. Freezing precipitation in Canada. Atmosphere-Ocean, 37(1), 87-102.

Stuart, R. A., 1994. Freezing precipitation in Canada: 1961-1990 – maps of occurrence frequency and duration. Weather Research House, 306 pp.

Szeto, K. K., Tremblay, A., Guan, H., Hudak, D.R., Stewart, R. E. and Cao, Z., 1999. The mesocale dynamics of freezing rain storms over Eastern Canada. Journal of the Atmospheric Sciences, 56(10), 1261-1281.

Thériault, J.M. and Stewart, R.E., 2010. A parameterization of the microphysical processes forming many types of winter precipitation. Journal of the Atmospheric Sciences, 67, 1492-1508.

Tivy, A., Alt, B., Howell, S., Wilson, K. and Yackel, J., 2006. A statistical model for long-range forecasting of the opening of the shipping route in Hudson Bay. Weather and Forecasting, 22(5), 1063-1075.

Vavrus, S., Holland, M. and Bailey, D., 2010. Changes in Arctic clouds during intervals of rapid sea ice loss. Climate Dynamics.

Wang, J., Mysak, L. and Ingram, R., 1994. Interannual variability of sea-ice dover in the Hudson Bay, Baffin Bay and the Labrador Sea. Atmosphere and Ocean, 32, 421-447.

Ward, J., 1963. Hierarchical grouping to optimize an objective function. Journal of the American Statistical Association, 58, 236-244.

Wilks, D.S., 2006. *Statistical methods in the atmospheric sciences, second edition*. International Geophysics series, vol. 91.

Wu, B., Wang, J. and Walsh, J., 2004. Possible feedback of winter sea ice in the Greenland and Barents Seas on the local atmosphere. Monthly Weather Review, 132, 1868-1876.

Yarnal, B. and Draves, J.D., 1993. A synoptic climatology of stream flow and acidity. Climate Research, 2, 193–202.

Yarnal, B., 1993. Synoptic climatology in environmental analysis. Belhaven Press: London.

Yarnal, B., Comrie, A., Frakes, B. and Brown, D., 2001. Developments and prospects in synoptic climatology. International Journal of Climatology, 21, 1923-1950.

Yarnal, B., White, D. A. and Leathers, D. J., 1988. Subjectivity in a computer-assisted synoptic climatology II: Relationships to surface climate. Journal of Climatology, 8, 227–239.